Local adaptation and intraspecific variation of the dominant prairie grass: Identifying populations for restoration in future droughts

by

Jack Sytsma

B.A., Central College, 2019

AN ABSTRACT OF A DISSERTATION

submitted in partial fulfillment of the requirements for the degree

DOCTOR OF PHILOSOPHY

Division of Biology
College of Arts and Sciences

KANSAS STATE UNIVERSITY
Manhattan, Kansas

2026

Abstract

Understanding how climate, genetic differentiation, and trait variation interact to shape adaptation, abundance, and drought tolerance is critical for predicting ecosystem responses to global change. This dissertation investigates these processes in *Andropogon gerardi* (big bluestem), a dominant North American tallgrass prairie species, using an integrated approach combining reciprocal garden experiments, ecological genomics, trait-based analyses, and range-wide surveys. The overarching goal was to understand how environmental gradients and genetic variation interact to determine local adaptation, population performance, and resilience under drought.

Four complementary objectives guided this research: (1) quantify local adaptation across precipitation gradients; (2) identify molecular and trait-based mechanisms of local adaptation and drought response; (3) evaluate range-wide patterns of abundance, diversity, and trait variation, and (4) assess the relative contributions of genetic differentiation and phenotypic plasticity to intraspecific trait variation (ITV). We hypothesized (1) that local ecotypes would exhibit higher fitness and performance than non-local ecotypes when grown in their home sites (local adaptation) and would be competitively dominant over the surrounding plant community. We expected (2) that drought-adaptive trait assemblages and gene expression profiles will be more pronounced in the dry ecotype compared to the wet ecotype, reflecting genomic and trait-based mechanisms of local adaptation. We hypothesized (3) that population abundance and genetic diversity would peak at the range core, consistent with the Abundant Center Hypothesis (ACH), and trait variation will correspond to linear clines according to climatic gradients, in support of a clinal patterns model (CPM). Finally, we expected (4) that ITV will result primarily

from genetic differentiation among populations rather than phenotypic plasticity or short-term environmental acclimation.

To test these hypotheses, we first leveraged long-term reciprocal gardens established in 2009 across broad rainfall gradients (500–1200 mm yr^{-1}) and measured cover and biomass of ecotypes and their surrounding plant community. Second, within these gardens, we measured functional traits—including leaf morphology, biomass allocation, phenology, and water-use efficiency among others— and used RNA sequencing to provide transcriptomic data to link gene expression with phenotypic responses. Third, we conducted range-wide measurements of abundance, traits, and genetic diversity across broad environmental gradients in populations spanning sharp temperature (4-21ºC, TX-MN USA) and precipitation (350-1400 mm yr^{-1}, CO-NC) gradients. Finally, we used controlled greenhouse experiments to disentangle environmental versus genetic contributions to trait variation of the same populations used in our range-wide demographic study.

Our results demonstrate strong local adaptation: *A. gerardi* ecotypes consistently exhibited higher fitness in home environments with this trend becoming more pronounced at decadal scales. The strength of local adaptation extended to the community level where local ecotypes were competitively dominant over the surround plant community whereas non-local ecotypes allowed for competitive release. Trait-based analyses of ecotypes showed the dry ecotype demonstrated trait assemblages consistent with stress tolerance (increased water-use efficiency, shorter stature) where the wet ecotype showed traits associated with increased light competition (greater height, biomass, and leaf width). At the transcriptome level, differential gene expression revealed drought-responsive genes (e.g., *ABA signaling, Drought Induced 19*) were upregulated in the dry ecotype, with growth-promoting genes (e.g., *Gibberellins*, *Auxin*

Response Factors) were upregulated in the wet ecotype. Range-wide analyses showed that abundance and genetic diversity aligned with the ACH, peaking near range centers. In contrast, functional trait variation increased linearly along climatic gradients, supporting the CPM. Finally, ITV was shaped by both climate and underlying genetic differentiation, indicating that precipitation regimes have imposed persistent selective pressures on trait variation. Together, these findings reveal a multi-scalar interplay between environmental selection, evolutionary processes, and functional trait differentiation.

This research advances both ecological theory and applied restoration science. Theoretically, it integrates frameworks of local adaptation, ecological genomics, and ITV, providing mechanistic insight into how genotype, phenotype, and environment interact across spatial and temporal scales. Practically, it informs climate-adjusted seed sourcing, ecotype selection, and restoration strategies aimed at enhancing ecosystem resilience under increasing drought and changing rainfall patterns. By combining long-term field experiments, genomic data, and trait-based approaches, this dissertation provides a mechanistic understanding of adaptation in a dominant prairie grass and offers actionable recommendations for land managers. These include identifying drought-tolerant genotypes that can enhance restoration outcomes, such as informing species and genotype selection for large-scale programs such as the Conservation Reserve Program, which manages millions of acres of conservation land.

Local adaptation and intraspecific variation of the dominant prairie grass: Identifying populations for restoration in future droughts

by

Jack Sytsma

B.A., Central College, 2019

A DISSERTATION

submitted in partial fulfillment of the requirements for the degree

DOCTOR OF PHILOSOPHY

Division of Biology
College of Arts and Sciences

KANSAS STATE UNIVERSITY
Manhattan, Kansas

2026

Approved by:

Major Professor
Dr. Loretta Johnson

Copyright

Abstract

Understanding how climate, genetic differentiation, and trait variation interact to shape adaptation, abundance, and drought tolerance is critical for predicting ecosystem responses to global change. This dissertation investigates these processes in *Andropogon gerardi* (big bluestem), a dominant North American tallgrass prairie species, using an integrated approach combining reciprocal garden experiments, ecological genomics, trait-based analyses, and range-wide surveys. The overarching goal was to understand how environmental gradients and genetic variation interact to determine local adaptation, population performance, and resilience under drought.

Four complementary objectives guided this research: (1) quantify local adaptation across precipitation gradients; (2) identify molecular and trait-based mechanisms of local adaptation and drought response; (3) evaluate range-wide patterns of abundance, diversity, and trait variation, and (4) assess the relative contributions of genetic differentiation and phenotypic plasticity to intraspecific trait variation (ITV). We hypothesized (1) that local ecotypes would exhibit higher fitness and performance than non-local ecotypes when grown in their home sites (local adaptation) and would be competitively dominant over the surrounding plant community. We expected (2) that drought-adaptive trait assemblages and gene expression profiles will be more pronounced in the dry ecotype compared to the wet ecotype, reflecting genomic and trait-based mechanisms of local adaptation. We hypothesized (3) that population abundance and genetic diversity would peak at the range core, consistent with the Abundant Center Hypothesis (ACH), and trait variation will correspond to linear clines according to climatic gradients, in support of a clinal patterns model (CPM). Finally, we expected (4) that ITV will result primarily

from genetic differentiation among populations rather than phenotypic plasticity or short-term environmental acclimation.

To test these hypotheses, we first leveraged long-term reciprocal gardens established in 2009 across broad rainfall gradients (500–1200 mm yr^{-1}) and measured cover and biomass of ecotypes and their surrounding plant community. Second, within these gardens, we measured functional traits—including leaf morphology, biomass allocation, phenology, and water-use efficiency among others— and used RNA sequencing to provide transcriptomic data to link gene expression with phenotypic responses. Third, we conducted range-wide measurements of abundance, traits, and genetic diversity across broad environmental gradients in populations spanning sharp temperature (4-21ºC, TX-MN USA) and precipitation (350-1400 mm yr^{-1}, CO-NC) gradients. Finally, we used controlled greenhouse experiments to disentangle environmental versus genetic contributions to trait variation of the same populations used in our range-wide demographic study.

Our results demonstrate strong local adaptation: *A. gerardi* ecotypes consistently exhibited higher fitness in home environments with this trend becoming more pronounced at decadal scales. The strength of local adaptation extended to the community level where local ecotypes were competitively dominant over the surround plant community whereas non-local ecotypes allowed for competitive release. Trait-based analyses of ecotypes showed the dry ecotype demonstrated trait assemblages consistent with stress tolerance (increased water-use efficiency, shorter stature) where the wet ecotype showed traits associated with increased light competition (greater height, biomass, and leaf width). At the transcriptome level, differential gene expression revealed drought-responsive genes (e.g., *ABA signaling, Drought Induced 19*) were upregulated in the dry ecotype, with growth-promoting genes (e.g., *Gibberellins*, *Auxin*

Response Factors) were upregulated in the wet ecotype. Range-wide analyses showed that abundance and genetic diversity aligned with the ACH, peaking near range centers. In contrast, functional trait variation increased linearly along climatic gradients, supporting the CPM. Finally, ITV was shaped by both climate and underlying genetic differentiation, indicating that precipitation regimes have imposed persistent selective pressures on trait variation. Together, these findings reveal a multi-scalar interplay between environmental selection, evolutionary processes, and functional trait differentiation.

This research advances both ecological theory and applied restoration science. Theoretically, it integrates frameworks of local adaptation, ecological genomics, and ITV, providing mechanistic insight into how genotype, phenotype, and environment interact across spatial and temporal scales. Practically, it informs climate-adjusted seed sourcing, ecotype selection, and restoration strategies aimed at enhancing ecosystem resilience under increasing drought and changing rainfall patterns. By combining long-term field experiments, genomic data, and trait-based approaches, this dissertation provides a mechanistic understanding of adaptation in a dominant prairie grass and offers actionable recommendations for land managers. These include identifying drought-tolerant genotypes that can enhance restoration outcomes, such as informing species and genotype selection for large-scale programs such as the Conservation Reserve Program, which manages millions of acres of conservation land.

Table of Contents

List of Figures

List of Tables

Acknowledgements

I am deeply grateful to the many individuals and organizations who supported this research. I am especially grateful to my dissertation committee—Dr. Allison Louthan, Dr. Zak Ratajzak, Dr. Chris Toomajian, and my PI Dr. Loretta Johnson—for their guidance, mentorship, and encouragement throughout this project. Their expertise and support were invaluable at every stage of the research and writing process.

I am grateful to my coauthors—Dr. Matthew Galliart, Kian Fogarty, Kori Howe, Dr. Bradley Olson, Dr. Sara Baer, Dr. David Gibson, Dr. Brian Maricle, Eli Hartung, Dr. Trevor Hefley, Dr. Adam Smith, Hannah Tetreault, Dr. Allison Louthan, Helen Winters, Dr. Erica Newman, Dr. Sonny Lee, Dr. Ari Jumpponen, Brooke Vogt, Dr. Anna Kazarina, Allison Ricker, and others—for their contributions to experimental design, data collection, analysis, and manuscript preparation. Their expertise and dedication were essential in producing the collaborative studies that underpin this dissertation.

I sincerely thank Dr. Zhe Ren, Dr. David Barfknecht, Saroj Thapa, Nora Bishop, and Dasik Clouse for their invaluable assistance in the field, including biomass collection, sample processing, and experimental planning. Additional thanks to Jared Craine, Paul St. Amand, Jesse Polland, Ethan Faryna, and Shuywe Wu for help with DNA extraction and library preparation. I am also grateful to the National Center for Genome Resources and New Mexico State University INBRE for assistance with analyses and access to computational resources.

I extend my deepest appreciation to the landowners, property managers, and site coordinators who permitted access to their properties and facilitated fieldwork. In particular, I thank T. Smetzer, G. Hanks, S. Pennings, T. Beckert, D. Crowley, K. Shannon, C. Osborne, M. Bell, D. Testerman, J. Gruchy, J. Hill, K. R. Heidorn, M. Kroll, L. Rowley, L. Reidel, K. Viste-

Sparkman, W. Williams, P. Duekrop, K. Menard, S. Wessel, A. Jarding, T. Richardson, S. Digiacomo, N. Ellingson, A. Eigirdas, and M. Ahlering for their support in the field.

Funding for this work was generously provided by USDA Grant #2020-03665 and the US Department of Education GAANN Grant P200A240009. Additional support was provided by the Kansas Academy of Science 2023 Graduate Student Research Grant, the 2023 Kansas Native Plant Society Bancroft Grant, the Love of Learning Phi Kappa Phi Grant, the 2024 Grassland Heritage Foundation Research Grant, the 2024 Ecumenical Ministry Grant, the Kansas Academy of Science 2025 Graduate Student Research Grant, and the 2025 Biology Graduate Student Association Research Grant.

Finally, I am grateful for the guidance, camaraderie, and encouragement from my colleagues, peers, and family throughout this project. Their collaboration and support were essential in making this research possible.

Preface

This dissertation represents the culmination of several years of research investigating how climate, genetic differentiation, and trait variation shape adaptation, abundance, and drought tolerance in *Andropogon gerardii*, a dominant grass of the North American tallgrass prairie. This work integrates long-term reciprocal transplant experiments, ecological genomics, trait-based analyses, and range-wide surveys to examine these processes across multiple spatial and temporal scales.

The concepts and approaches developed herein emerged from early discussions with my advisor, Dr. Loretta Johnson, and were refined through extensive collaboration and intellectual exchange within a dynamic research community. I am deeply appreciative of the scientists, students, and colleagues whose insight, enthusiasm, and constructive feedback informed this work at every stage. Members of the Johnson Lab provided an engaging and supportive environment in which to develop ideas, troubleshoot challenges, and cultivate a deeper understanding of ecological systems. Conversations in the laboratory, during fieldwork, and at professional meetings continually advanced the scientific and conceptual framework that underpins this dissertation.

This research also benefited from the generosity and expertise of the broader grassland ecology community. Collaborations across institutions and research networks provided access to diverse datasets, methodological innovations, and critical perspectives that enriched both the scope and rigor of this work. The collective efforts of these colleagues reflect the cooperative spirit that defines ecological science and underscore the value of sustained collaboration in addressing complex environmental questions.

I am especially grateful to my dissertation committee—Dr. Allison Louthan, Dr. Zak Ratajczak, Dr. Chris Toomajian, and my advisor, Dr. Loretta Johnson—for their mentorship, guidance, and encouragement throughout this process. Each has contributed distinct expertise and thoughtful critique that strengthened this research and fostered my growth as a scientist. I also extend my sincere appreciation to my coauthors, collaborators, and many field and laboratory assistants whose careful work and persistence were essential for the successful completion of this project.

Financial support from the United States Department of Agriculture (USDA), the U.S. Department of Education, and additional grants provided critical resources for both the research and the professional development that made this dissertation possible. Beyond its scientific contributions, this work reflects an ongoing commitment to understanding and sustaining grassland ecosystems under changing climatic conditions, with the aspiration that its findings advance both ecological theory and applied conservation practice.

Finally, I dedicate this work to the teachers, mentors, colleagues, friends, and family members who have supported and inspired me throughout this endeavor. Their guidance, encouragement, and confidence in my abilities have been integral to my academic and personal development. The knowledge, skills, and perspectives gained through these experiences have shaped not only this dissertation but also my continuing growth as a researcher and member of the broader scientific community.

Chapter 1 - Introduction

Overview and Rationale

Grasslands are among the most extensive biomes on Earth, covering ~40% of terrestrial surfaces (White, 2000), and provide critical ecosystem services including carbon storage, forage production, and support high levels of plant biodiversity (Hungate et al., 2017; Moore et al., 2020; Petermann & Buzhdygan, 2021; Bai & Cotrufo, 2022). Grasslands also exert a strong influence on global climate regulation (Petermann & Buzhdygan, 2021), stabilize soils, filter water, and sustain diverse animal communities (Werling et al., 2014). Despite their ecological importance, grasslands are among the most threatened ecosystems globally, with North American tallgrass prairie reduced to less than 5% of its historical extent due to agricultural conversion (Samson & Knopf, 1994; Wright & Wimberly, 2013; Baer et al., 2019). Additional pressures—including habitat fragmentation, invasive species, and climate change—further threaten grasslands (Hoekstra et al., 2005; Gaskin et al., 2021; Smith et al., 2024). Grasslands are particularly vulnerable to drought and precipitation variability (Nippert et al., 2006; Cherwin & Knapp, 2012; Knapp et al., 2001, 2008; Smith et al., 2024), stressors that are projected to intensify in the future (IPCC, 2023; King et al., 2024). Understanding mechanisms of drought tolerance in dominant grass species is therefore critical for sustaining grassland resilience, biodiversity, and ecosystem services into the future (Craine et al., 2012; Smith et al., 2024).

Andropogon gerardi (Nash, big bluestem, Poaceae; Figure 1) is a foundational grass species in the North American tallgrass prairies, contributing up to 70% of aboveground biomass (Knapp et al., 1998) and exerting strong influence on community composition and ecosystem processes (Swemming et al., 2006). Its broad distribution across precipitation and temperature gradients (Wang et al., 2014; USDA Plants Database, 2023; Figure 1.1) makes it a valuable

model for understanding plant responses to climate. Furthermore, *A. gerardi* demonstrates tolerance to various stressors such as variation in rainfall (Swemmer et al., 2006), temperature (Fay et al., 2011), and elevated CO_2 (Knapp et al., 1999). Studying this species therefore offers insight into key mechanisms shaping population responses to environmental stress.

Although *A. gerardi* has been widely studied for its physiological responses (Knapp et al., 1999; Swemming et al., 2006; Fay et al., 2011) and dominance in prairie ecosystems (Knapp et al., 1998; Epstein et al., 1998; Swemming et al., 2006), important questions remain about how ecological and evolutionary processes interact to shape its performance across environmental gradients. In particular, the role of intraspecific trait variation (ITV; Anderson et al., 2021), and local adaptation, where populations perform best in their home environments (Savolainen et al., 2007, 2013) remain poorly understood. Integrating the concepts of local adaptation and ITV across the species range provides a framework for linking population-level ecological responses to broader ecosystem outcomes.

This dissertation highlights how genetic and phenotypic differences together influence productivity, competition, and drought tolerance in *A. gerardi*. By grounding this research in ecological context, such an approach not only advances theory on adaptation and functional diversity but also supports practical applications in restoration (Vitt et al., 2022) by identifying how adaptive variation can enhance ecosystem function (Shaw et al., 2025) and persistence in variable climates. This work also integrates ecological genomics (Ungerer et al., 2008) to link genetic variation directly to ecological outcomes. Both processes influence how *A. gerardi* mediates grassland resilience and provides a framework for predicting ecosystem trajectories under future climate scenarios (Aitken & Whitlock, 2013).

To address how the phenotypic and genotypic mechanisms contribute to productivity and drought tolerance in *A. gerardi*, this research is grounded in several complementary theoretical frameworks. These include local adaptation, intraspecific trait variation, and biogeographic models, each offering a lens for understanding how genetic and functional diversity shape grassland resilience across environmental gradients.

Theoretical Frameworks

Local Adaptation. Local adaptation occurs when populations of a species exhibit highest fitness in their home environments than non-local conditions (Savolainen et al., 2007; 2013). This process is critical because it underpins how species respond to environmental heterogeneity, shaping biodiversity and ecosystem resilience across landscapes. Understanding local adaptation is especially important for ecological restoration, as mismatches between seed source and planting sites can reduce survival and long-term persistence. An ecotype is a genetically distinct population within a species that is adapted to specific local environmental conditions (Clausen et al., 1944; McMillian, 1968; Lowry et al., 2012), making them valuable units for conservation and restoration planning. Genomic tools now allow researchers to detect adaptive loci, allele frequency shifts, and gene expression patterns linked to environmental gradients (Ungerer et al., 2008). Reciprocal gardens are the "gold standard" for studying local adaptation of a species (Johnson et al., 2022) and combining reciprocal gardens with genomic analyses (Ungerer et al., 2008; Savolainen et al., 2013) can reveal the strength of local adaptation at both phenotypic and genetic levels (Schwinning et al., 2022; Johnson et al., 2022).

Intraspecific Trait Variation. Intraspecific trait variation (ITV) refers to functional trait differences within species or among populations (Moran et al., 2016; Westerband et al., 2021). It buffers populations against environmental stress and helps maintain ecosystem function (Moran

et al., 2016), particularly in climatically variable systems like grasslands. Specifically, traits such as water-use efficiency, root allocation, and phenology often mediate responses to drought and disturbance (Grime, 1988). These trait differences can arise from both genetic differentiation (Mitchell-Olds et al., 2007) and phenotypic plasticity (Ahrens et al., 2021), allowing populations to persist under fluctuating or novel climatic conditions. High levels of ITV may enhance community stability (Moran et al., 2016) and in restoration contexts, accounting for ITV can improve the adaptive capacity of plantings (Siefert et al.., 2015) and increase the likelihood of long-term ecosystem resilience (Moran et al., 2016). Genomic approaches can link ITV to its genetic basis (Mitchell-Olds et al., 2007), clarifying whether ITV arises from plasticity, standing genetic diversity, or local adaptation (Savolainen et al., 2013). Studying ITV in *A. gerardi* across climatic gradients therefore provides insight into how genetic differentiation and plasticity contribute to morphological differences between populations and its drought tolerance.

Abundant Center Hypothesis vs. Clinal Pattern Model. While ITV highlights the mechanisms driving variation within species, broader biogeographic frameworks such as the Abundant Center Hypothesis (ACH) and Clinal Pattern Model (CPM) provide context for how these patterns manifest across species' ranges. The ACH predicts that abundance, performance, and genetic diversity peak at range centers and decline toward margins due to suboptimal conditions for the species (Brown, 1984). The CPM instead attributes variation to environmental gradients (Estarangue et al., 2023), independent of range position. While both frameworks offer valuable perspectives, empirical tests show mixed support (Dallas et al., 2020; Panter et al., 2025), highlighting species-specific dynamics. In addition to trait-based analyses and abundance estimates, genomic data provide new opportunities to evaluate these models by measuring genome-wide diversity and detecting selection along climatic and geographic gradients. Testing

models of the ACH and CPM helps to disentangle the roles of selection due to climate, range position, and adaptation in shaping range-wide patterns of a species.

Literature Review of Ecological Genomics

Ecological genomics offers a powerful framework for investigating these mechanisms by linking genetic variation with phenotypic traits and environmental responses in natural populations. To contextualize the current state of this field, we conducted a systematic literature review of ecological genomics studies in grasses. Using the Web of Science, we surveyed peer-reviewed publications from July 2014 to July 2023 with the search terms "grassland AND genetics NOT animal AND plant NOT micro*." After excluding reviews and studies on animals and microbes, our final dataset included 190 papers. For each study, we recorded key characteristics including species, phenotypes measured, experimental setting, plot design, sequencing techniques, and study duration. This synthesis provides a framework for evaluating how genomic tools have been applied to grassland systems and identifies opportunities for advancing our understanding of adaptation and resilience across broad spatial and temporal scales.

A large proportion of studies (42%) examined tallgrass prairie grasses, followed by Mediterranean grasslands (17%) and shortgrass steppe ecosystems (16%; Figure 1.2A). Very few focused on savanna or deciduous forest grasses (2%). Geographically, roughly half of all studies were conducted in North America, with Europe contributing 25%, Asia 17.2%, South America 5.6%, and Africa 2.2%. Most studies concentrated on one (16%) or two (50%) phenotypic traits, with only a small fraction assessing three or more (8%; Figure 1.2B). Morphological traits dominated (68%), while physiological traits were less frequently measured (28%). Field-based research represented nearly two-thirds of the literature (63%), compared to greenhouse studies

(34%), and most experiments evaluated individual plants without competitors (66%) rather than in community contexts (36%; Figure 1.2C).

Taxonomic coverage spanned 85 grass species across 18 tribes (Figure 1.2E). Paniceae (36%), Triticeae (14%), and Andropogoneae (17%) were most frequently represented, with *Panicum virgatum* (24%), *Andropogon gerardi* (10%), and *Lolium perenne* (7%) serving as the primary focal species (Figure 1.2F). However, 66 species appeared in only one or two studies, highlighting limited breadth across taxa. Perennial grasses were overwhelmingly represented (85%) compared to annuals (16%), and wild taxa (92%) were studied far more often than cultivated varieties (5%).

Most studies (76%) employed experimental designs, though durations were typically short: 61% lasted less than one year, and only 4% extended beyond five years (Figure 1.2G). Abiotic manipulations were common (54%; Figure 1.2H), especially drought (20%) and temperature (18%), while other variables such as watering, light, CO_2, or soil type were rarely tested (<5%). Biotic manipulations occurred in 24% of studies, primarily involving microbial communities (17%) and competition (12%), with herbivory addressed in just 1% (Figure 1.2I). Genomic approaches varied: 29% of studies relied solely on phenotypes without genetic data, while others incorporated candidate-gene analyses, older marker systems (AFLPs, RAPDs, microsatellites), or modern methods such as GBS, DDrad54, and SNP arrays (Figure 1.2J). Whole-genome sequencing (2 studies) and exome sequencing (4) were rare, and transcriptomic work was mostly limited to RNAseq (10). Other “omics” approaches—including methylome (3), metabolic (1), and proteomic (1) studies—were scarcely applied, with chloroplast genome sequencing appearing in only two phylogenetic studies.

Key insights and gaps. Our survey reveals strong research emphasis on dominant prairie grasses in North America, especially *P. virgatum*, which alone accounted for nearly a quarter of all studies. While this provides depth in model species, it leaves the broader diversity of grasses underexplored. Major gaps include limited work in natural ecological contexts, minimal attention to biotic stressors, and narrow coverage of phenotypic traits.

Accessibility of advanced genomic tools remains a limiting factor. Roughly one in four studies did not incorporate genetics at all, implicitly attributing phenotypic variation to genetic differences without testing that assumption. Reduced-representation sequencing methods show promise for extending genomic resources to non-model grasses (e.g.., GBS; Poland & Rife, 2012). However, the heavy reliance on a few well-studied cultivars risks overlooking valuable diversity in wild grasses and landraces, which may harbor traits crucial for stress tolerance and disease resistance. Furthermore, functional genomic approaches—including transcriptomic (RNAseq), methylome, proteome, and metabolome profiling—remain rare (less than 5% of studies) but offer exciting opportunities for future research, provided adequate sequencing infrastructure and bioinformatic resources are available.

Overall progress. Despite these limitations, the past decade has seen steady growth in ecological genomics of grasses. Annual publications rose from 18 in 2014 to 20–30 between 2020 and 2023, reaching a total of 190 by mid-2023 (Figure 1.2K). Considerable progress has been made in genotyping, but substantial opportunities remain for broadening taxonomic coverage, incorporating underused genomic tools, and expanding research into ecological and evolutionary dimensions of grass diversity.

Literature Review of Range Wide Patterns of Abundance, Traits, and Genetic Diversity Across Plant Species

While our synthesis of genomic studies in grasses highlights how researchers have explored genetic and functional diversity within species, a complementary perspective comes from examining how these patterns scale across geographic ranges. Therefore, to complement our review of ecological genomics in grasses, we also reviewed empirical tests of range-wide patterns in plant abundance, traits, and genetic diversity. This second review focused on two conceptual frameworks—the ACH (Brown, 1984) and the CPM (Estarangue et al., 2023)—which generate contrasting predictions about how populations vary across species' ranges. We conducted a systematic literature review to assess empirical support for two frameworks describing plant range dynamics: the ACH and CPM. These models make different predictions about abundance, traits, and genetic diversity across ranges, yet their relative support remains unclear. By systematically surveying studies that explicitly addressed these models, we aimed to evaluate the extent to which empirical evidence supports ACH or CPM and to identify conditions under which each framework is most applicable.

Using Web of Science, we searched studies published between January 1, 1985, and July 7, 2025, with the string: ("Abundant Center" OR "Center Periphery" OR "Center Margin" OR "Center Edge" OR "Central Marginal Hypothesis") AND plant* AND (trait OR genetic) NOT animal*. This yielded 152 peer-reviewed papers, and we included studies that (1) focused on plants, (2) measured empirical trait or genetic data across geographic ranges, and (3) addressed ACH or CPM. We excluded reviews, meta-analyses, and experimental manipulations.

Each eligible study was categorized by: Data type: Abundance (A), Trait (T), Genetic (G), ACH support: yes/no/mixed, and CPM support: yes/no/mixed. This structured framework enabled consistent study of classification and comparison across data types and range patterns.

Our systematic review of 152 studies provides insight into how well empirical evidence supports the ACH and the CPM in plants. For abundance and genetic diversity, results largely aligned with the predictions of the ACH: more than half of the studies reported peak abundance at the range center (56.5%, 35 of 62 papers; Figure 1.3), and a majority observed the highest levels of genetic diversity in core populations with declines toward range margins (62%, 31 of 50 papers; Figure 1.3A). These findings suggest that demographic and genetic processes often follow expectations of reduced population size and diversity in peripheral habitats.

In contrast, studies of trait variation provided stronger support for the CPM. While roughly one-third of trait-focused studies were consistent with the ACH (33.8%, 23 of 68 papers), most instead documented linear or curvilinear clines associated with environmental gradients (66.2%, 45 of 68 papers; Figure 1.3B). These literature survey results indicate that functional traits are more strongly structured by underlying ecological gradients than by simple spatial position within a species' range. Importantly, only a small fraction of studies (3%, 5 of 152 papers) simultaneously examined abundance, genetic diversity, and traits, limiting the ability to evaluate how these dimensions of variation interact. Addressing this gap will require integrative, multi-dimensional approaches that explicitly connect demographic, genetic, and trait-based perspectives to better understand the mechanisms shaping range-wide patterns in plants.

Knowledge Gaps. Despite decades of research, several critical gaps remain which are highlighted by both literature reviews. First, the extent and patterns of ecotypic variation across broad climatic gradients are poorly characterized. While greenhouse experiments have provided

insight into trait variation, they often fail to capture long-term responses within natural communities. Second, the integration of genetic variation, phenotypic traits, and environmental responses is incomplete. Linking these components is essential for understanding the mechanisms underlying adaptation and predicting population performance under future climates. Third, range-wide patterns in abundance, trait distribution, and genetic diversity remain largely unexplored, as most studies focus on local populations. Finally, long-term, field-based studies are scarce, yet such studies are crucial for revealing adaptive patterns and community dynamics over decadal timescales.

Taken together, our literature surveys highlight both the progress and the persistent limitations in ecological genomics and range dynamics of plants. While there has been a clear expansion in genetic tools and an increase in the number of studies, research has been disproportionately concentrated on a handful of model species, short-term experiments, and a narrow range of phenotypic traits. Gaps remain particularly evident in the integration of ecological, phenotypic, and genomic perspectives across species and climates. Addressing these gaps is especially important for dominant prairie grasses, which function as foundation species in North American grasslands. To move beyond these limitations, this dissertation focuses on *A. gerardi*, a dominant species in the tallgrass prairie (Knapp et al., 1998). By situating our study within established ecological and evolutionary theory, we aim to connect patterns of intraspecific variation with underlying genomic mechanisms and ecological outcomes. In particular, we use frameworks such as ITV, local adaptation (Savolainen et al., 2007; 2013) and competing models of species' range dynamics (ACH vs CPM) to interpret how genetic and phenotypic diversity are distributed across climatic gradients.

Research Questions

Our theoretical grounding enables us to address several unresolved questions raised by the literature review:

1. How strongly does local adaptation structure performance across climate gradients?
2. What are the mechanisms of local adaptation to rainfall and drought tolerance in *A. gerardi?*
3. Do patterns of abundance, diversity, and adaptation align more closely with ACH predictions or with clinal gradients (CPM)?
4. To what extent does trait variation in *A. gerardi* reflect plasticity versus genetic differentiation?

By integrating ecological genomics with these frameworks, this dissertation advances our understanding of how a foundation grass species responds to environmental variation, providing insight into both basic evolutionary processes and applied conservation strategies under global change.

Objectives and Hypotheses

The overarching goal of this dissertation is to understand how climate, genetic differentiation, and trait variation interact to shape adaptation, abundance, and drought tolerance in the dominant grass *A. gerardi*. Since *A. gerardi* plays a critical role in ecosystem functioning (Knapp et al., 1998; Silleti & Knapp, 2002), its responses to environmental gradients provide both theoretical insights into the mechanisms of adaptation and applied guidance for grassland management under global change. To address this goal, this research integrates field

experiments, controlled common gardens, trait-based ecology, and ecological genomics (Figure 1.4) across multiple spatial and temporal scales.

Objective 1: Local adaptation across rainfall gradients. In Chapters 2 and 3, we use reciprocal garden experiments across a broad precipitation gradient (MAP 500-1200 mm yr^{-1}) to test whether *A. gerardi* ecotypes show higher fitness in their home environment compared to foreign sites. This directly evaluates local adaptation and the selective pressures imposed by water availability, a major selection force across ecosystems (Siepielski et al., 2017; Feldman et al., 2024). We hypothesized that local ecotypes (e.g., a dry ecotype in the home dry site) would perform best with survival, growth, and reproduction maximized in home environments. A non-local ecotype (e.g., a wet ecotype in the dry site), by contrast, would exhibit reduced fitness which would result in decreased abundance and biomass of the non-local ecotype.

Objective 2: Gene expression, traits, and drought response. Building on the reciprocal gardens, Chapter 3 integrates transcriptomic data and trait-based analyses to provide possible mechanisms for local adaptation in *A. gerardi*. By linking differential gene expression to functional traits such as water-use efficiency, biomass, and phenology, this objective identifies molecular and physiological mechanisms underlying resilience. We hypothesized that drought-adaptive traits (e.g., increased water use efficiency, thicker leaves, shorter stature) and drought-responsive genes (e.g., ABA Signaling, *LEA;* Gupta et al., 2020) will align with the dry ecotype at its home, dry site. In contrast, we expected that the wet ecotype would show growth-promoting traits (e.g., increased height and biomass, greater leaf area) and genes (e.g., Gibberellins, *Vascular Tissue Generation*; Gupta et al., 2020).

Objective 3: Range-wide patterns of abundance, traits, and genetic diversity. Next, Chapter 4 evaluates whether *A. gerardi* populations conform more closely to the ACH (Brown,

1984) or the CPM. Using range-wide data, this objective examines how abundance, genetic diversity, and trait variation are structured across geography and climate (Figure 1.4). We hypothesized that abundance and genetic diversity will peak in range core populations, consistent with the ACH, while variation in traits will align primarily with climatic gradients, consistent with the CPM (Estarague et al., 2023). Together, these patterns provide a framework for understanding how range position and environmental gradients jointly shape species distributions and adaptive potential.

Objective 4: Drivers of trait variation. Finally, Chapter 5 addresses the extent to which ITV in *A. gerardi* is driven by genetic differentiation among populations versus plastic, short-term acclimation to environmental conditions. Since ITV is a key determinant of resilience in variable climates (Westerband et al., 2021), this objective combines trait, genetic, and climatic data (Figure 1.4) to parse these contributions. We hypothesized that genetic differentiation underlies much of the observed ITV and modulates drought responses. Specifically, if ITV had a strong genetic basis, trait variation would align between the same populations from the field sampling in Obj. 3 planted in a controlled common garden. Confirming this hypothesis would demonstrate the evolutionary basis of ITV and highlight its role in buffering populations against climate change, with direct implications for designing restoration strategies that leverage functional diversity.

Together, these objectives are guided by the central research question**: How do climate gradients, genetic differentiation, and trait variation interact to shape adaptation, abundance, and drought tolerance in *A. gerardi*?** Addressing this question contributes to both ecological theory—by integrating frameworks of local adaptation, species distribution models,

and ITV—and applied management, by identifying ecotypes and trait syndromes most likely to sustain ecosystem function under future climate scenarios.

Significance and Implications

This research contributes meaningfully to both applied and theoretical ecology. From an applied perspective, clarifying the extent of local adaptation and ITV provides actionable knowledge for ecological restoration. Identifying climate-appropriate ecotypes (Hufford & Mazer, 2003; Leimu & Fischer, 2008) enables practitioners to select plant populations that are more likely to establish, persist, and maintain ecosystem function. This is particularly important given the increasing frequency of droughts and altered precipitation regimes (Franks et al., 2007; Knapp et al., 2008; Wilcox et al., 2017). Seed sourcing strategies that integrate genetic and trait-based information (Breed et al., 2013; Bucharova et al., 2019) can help ensure that restoration projects preserve genetic diversity while maximizing performance. Approaches such as climate-adjusted provenancing (Prober et al., 2015) demonstrate how incorporating genomic and climatic data can guide seed sources in ways that promote long-term persistence under future droughts.

The theoretical contributions of this work are equally significant. By integrating ecological genomics with frameworks of intraspecific trait variation, local adaptation, and species distribution models such as the ACH and CPM, this study provides a multidimensional approach to understanding how evolutionary and ecological processes interact across spatial and environmental gradients. This integration moves beyond descriptive patterns, allowing for a mechanistic understanding of how genetic differentiation drives trait variation (Savolainen et al., 2013; Hoban et al., 2016) and ultimately shapes population performance. It also bridges the gap between classical ecological research and contemporary genomic tools (Ungerer et al., 2008;

Sytsma et al., in press), demonstrating how molecular approaches can uncover signatures of adaptation that are often hidden at the phenotypic level.

Finally, linking gene expression, phenotypic traits, and environmental gradients offers a predictive framework for both conservation and management. Species distribution models can anticipate how populations are likely to respond to future climate scenarios, helping forecast vulnerabilities and adaptive potential (Aitken & Whitlock, 2013; Fitzpatrick & Keller, 2015). These insights enable proactive management strategies, such as assisted gene flow, targeted seed transfers, and the design of restoration projects that anticipate future environments rather than replicate past ones. In doing so, this work contributes to the practical goal of sustaining grassland ecosystems under rapid global change while also advancing ecological and evolutionary theory.

Figure 1.1. A. Range of *A. gerardi* (green) across North America. B. Photograph of *A. gerardi,* the focal species of this dissertation.

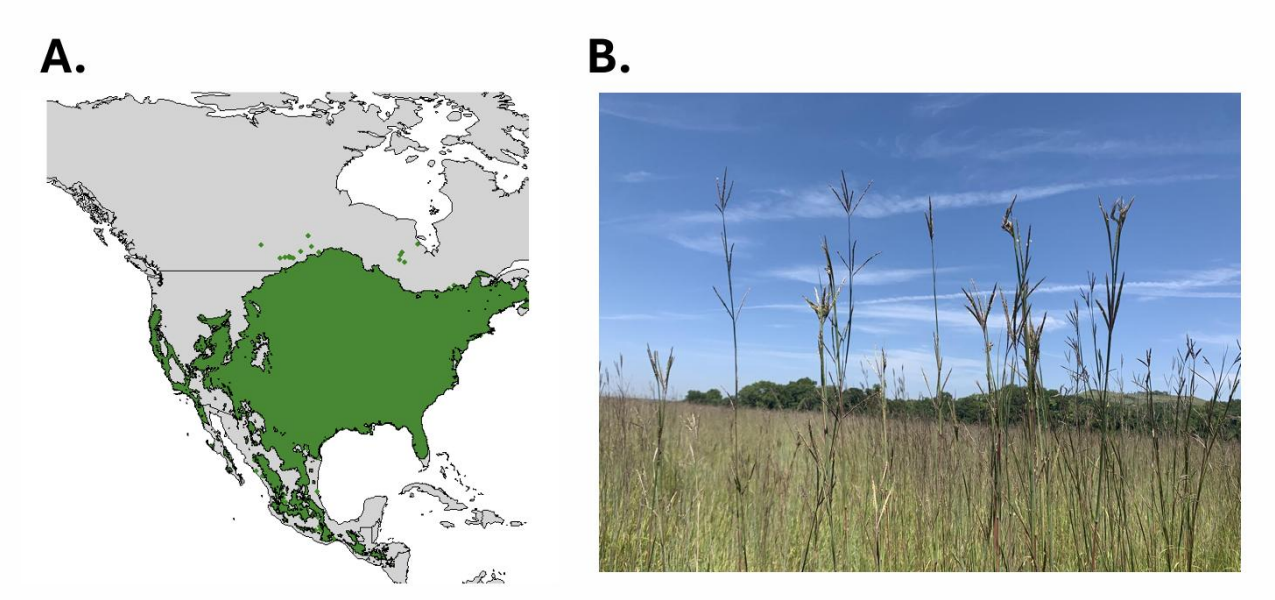

Figure 1.2. Summary of ecological genomics literature survey results (2014–2023): (A) habitat, (B) phenotypes studied, (C) research setting, (D) plot design, (E) tribe, (F) focal species, (G) study duration in years, (H) abiotic manipulations, (I) biotic manipulations, (J) sequencing methods, and (K) cumulative publications per year in grassland ecological genomics.

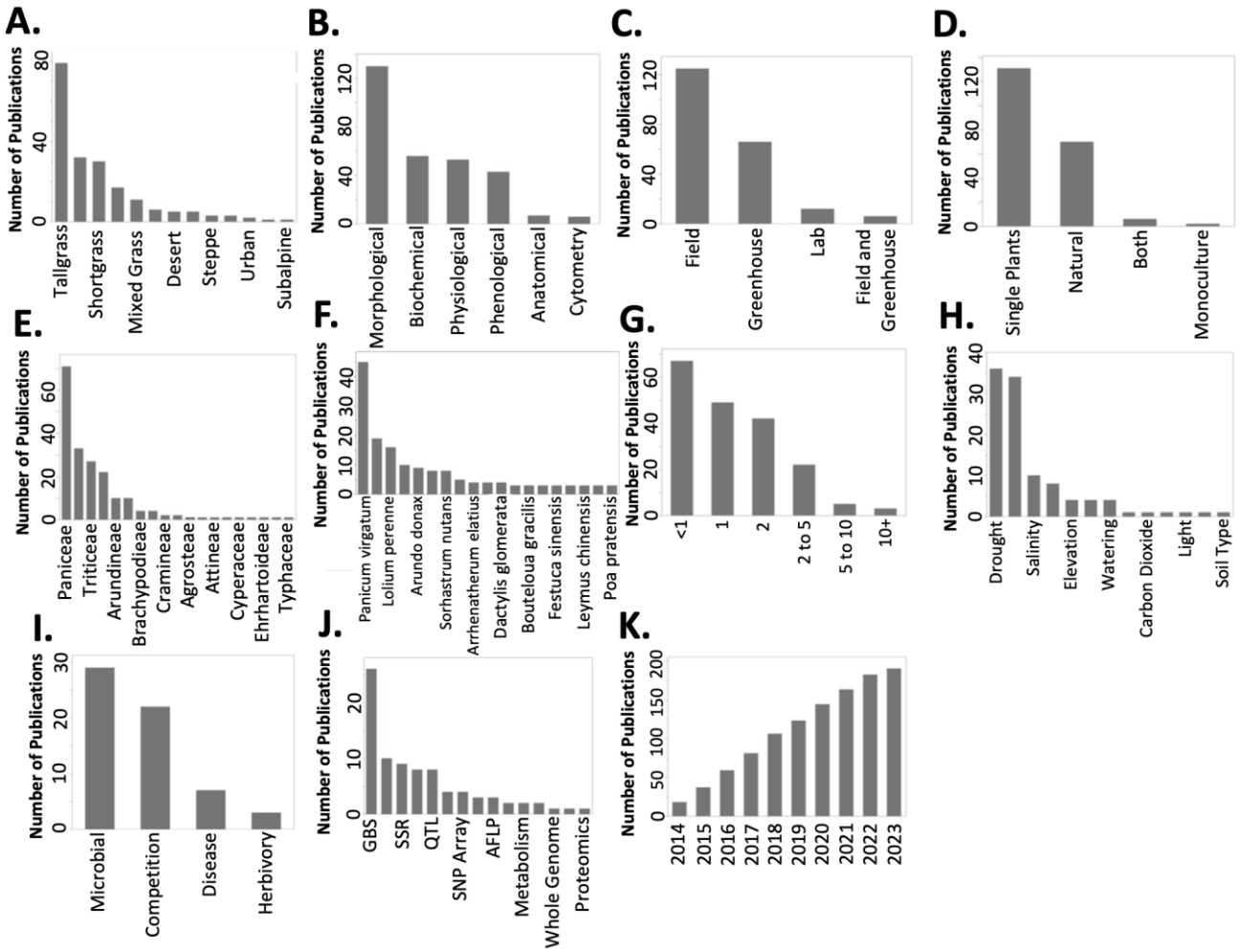

Figure 1.3. Summary of plant range patterns literature survey results (1984–2025): support of either (A) the ACH or (B) the CPM. Data used in each study (abundance, trait, or genetic data).

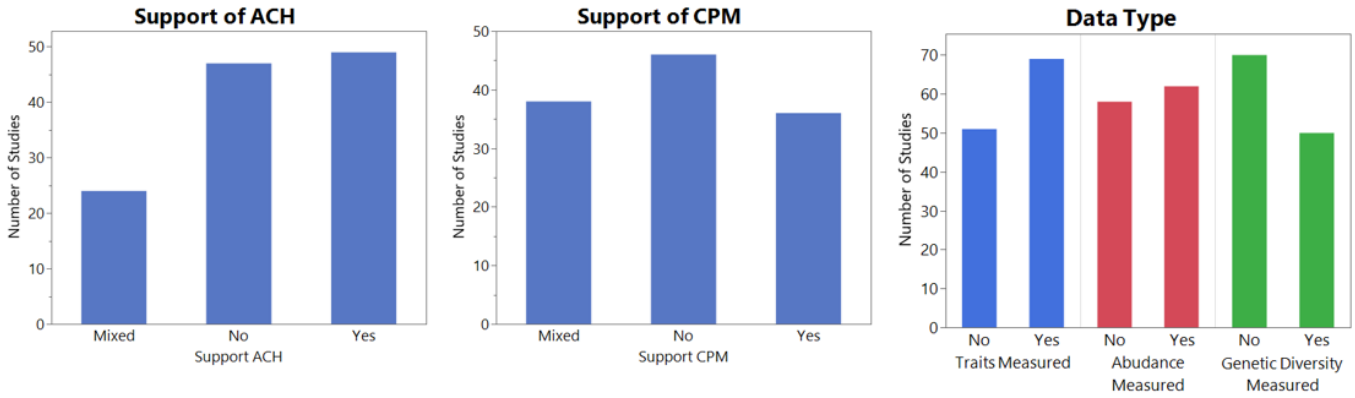

Figure 1.4. Conceptual framework linking climate gradients, genetic response, and plant form and function in *A. gerardi*. Climate gradients (e.g., precipitation, temperature) act as selective pressures shaping genetic responses and plant form and function. These processes influence ecological outcomes at multiple scales, including local adaptation (Obj. 1 & 2), range-wide abundance and diversity patterns (ACH vs. CPM; Obj. 3), and plant intraspecific trait variation (ITV; Obj. 4). *Andropogon gerardi* serves as the focal species connecting gradients, genetic responses, and plant form and function, with four objectives linking reciprocal gardens, transcriptomics, trait analyses, and diversity patterns to test mechanisms of drought tolerance and resilience.

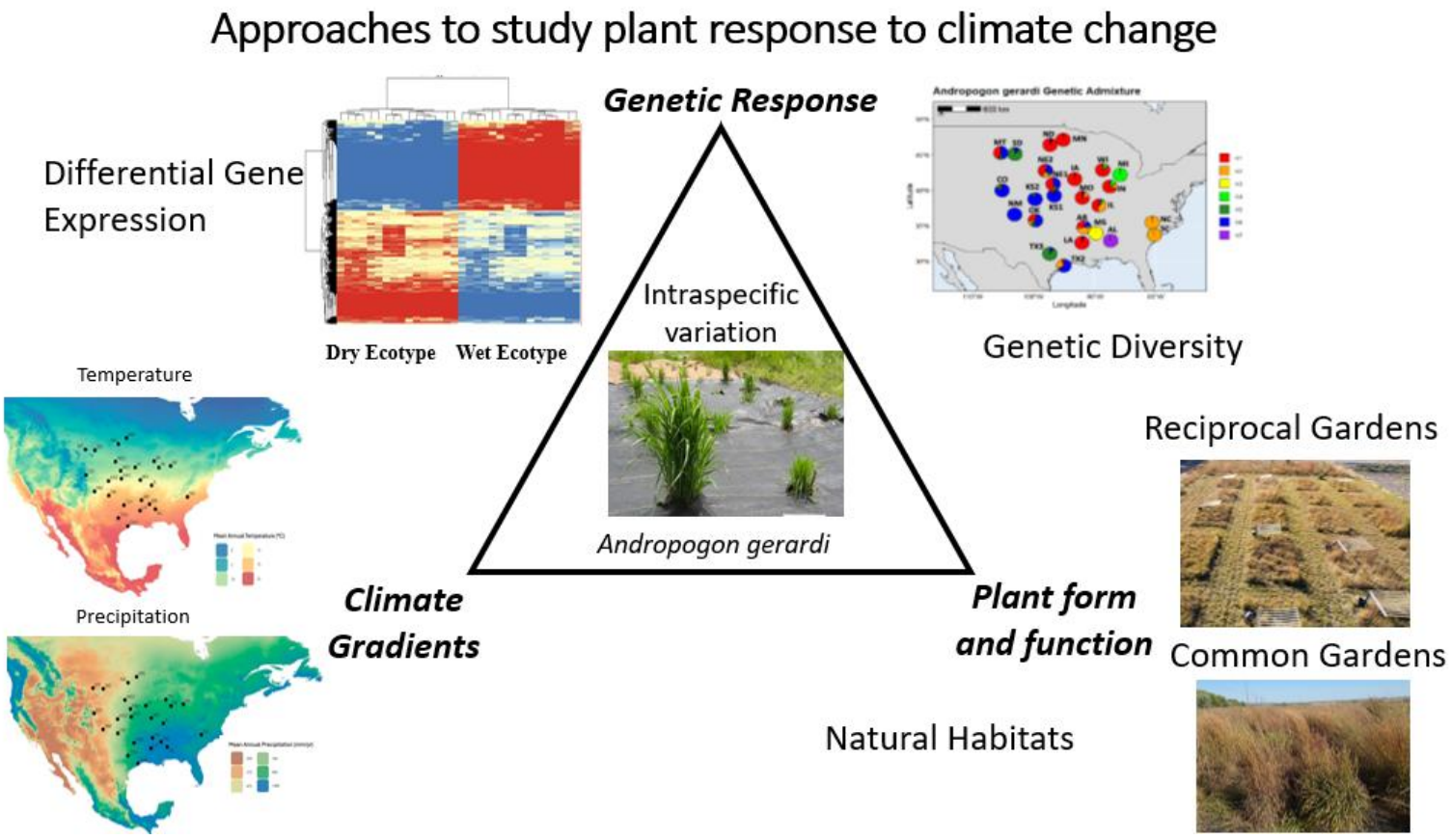

Chapter 2 - Prairie Grass Ecotypes Across the Rainfall Gradient of the US Great Plains Show Decadal Evidence of Local Adaptation and Shifts in Community Composition

Running title: Decadal Study of Local Adaptation

Authors: Jack Sytsma[1] and Matthew Galliart[2], Trevor Hefley[3], Sara G. Baer[4], David Gibson[5], Hannah Tetreault[6], Eli Hartung[1], Brian Maricle[7], and Loretta Johnson[1]

[1]Department of Biology, Kansas State University; [2]Department of Biological Sciences, Fort Hays State University;[3] Department of Statistics, Kansas State University; [4]Kansas Biological Survey & Center for Ecological Research and Department of Ecology & Evolutionary Biology, University of Kansas; [5]School of Biological Sciences, Southern Illinois University Carbondale, Illinois; [6]USDA REE-ARS, Fort Collins, CO; [7]Department of Biology, Saginaw Valley University

Keywords: *Andropogon gerardi,* drought, ecological genomics, gene expression, grassland, reciprocal gardens, RNAseq

Abstract

Understanding ecotypic variation is critical for ecosystem restoration and management, especially across vast ecosystems spanning sharp environmental gradients, such as the North American Great Plains. We report here the use of long-term reciprocal gardens with natural grassland communities to test for local adaptation of the dominant grass big bluestem (*Andropogon gerardi*; Poaceae) across an annual precipitation gradient of ~480-1256 mm yr^{-1} spanning 723 km. This decadal study represents one of the longest running test of local adaptation in realistic communities. First, local adaptation of wet and dry ecotypes strengthened over time as community development progressed. A severe drought in 2012 further tested adaptation, which placed extreme stress on wet ecotypes in dry regions. Second, rainout shelters that experimentally reduced rainfall corroborated that rainfall is a key selection pressure. Across sites, local ecotypes suppressed neighboring plant functional groups, confirming the "extended phenotype" concept and demonstrates the strength of local adaptation. Finally, phenotypic variation among ecotypes was reflected in genetic differences, where wet and dry ecotypes showed strong divergence in SNP variation and gene expression. Together, results show expansive ecosystems across climate gradients foster local adaptation detectable only over long timescales and under natural environmental variability. Restorations of this ecosystem should use climate-matched ecotypes.

Main Text

Grasslands cover about 40% of Earth's land surface (White et al., 2000) and provide essential ecosystem services, including carbon storage, forage, and biodiversity support (Hungate et al., 2017; Moore et al., 2020; Petermann & Buzhdygan, 2021; Bai & Cotrufo, 2022).

Grasslands also face the highest extinction risk of any biome (Hoekstra et al., 2005), with North American tallgrass prairie ecosystem reduced to <5% of its original extent (Samson & Knopf, 1994; Wright et al., 2013), primarily due to conversion to row crop agriculture (Baer et al., 2019). Ongoing conversion of tallgrass prairie to agriculture makes restoration and conservation particularly urgent (Bargett et al., 2021), and with this, an escalating need to better understand prairie response drought frequency and intensity as climate changes (Cook et al., 2015; IPCC, 2023; King et al., 2024; Smith et al., 2024). Because tallgrass prairie is highly sensitive to rainfall amount and variability (Nippert et al., 2006; Knapp et al., 2008), understanding local adaptation to climate, particularly precipitation, will be key to restoring resilient grasslands (Smith et al., 2024).

Rainfall strongly influences plant performance, community structure, and ecosystem functioning (Fay et al., 2000; 2008; Knapp et al., 2001; 2008; Cherwin & Knapp, 2012; Cleland et al., 2013; Smith et al., 2024), making it a key driver of grassland dynamics and a major selective force (Siepielski et al., 2017; Yang et al., 2022; Feldman et al., 2024). Although the effects of rainfall variability and drought on grassland diversity and productivity are well established (Tilman & El Haddi, 1992; Knapp et al., 2001; 2008; Felton et al., 2020), far less is known about intraspecific responses, particularly in long-lived perennial grasses (Kitchenin et al., 2013; Sytsma et al., in press) that dominate these ecosystems. This gap is especially critical in the U.S. Great Plains, where increasingly frequent droughts and extreme rainfall events strongly shape grassland composition and resilience (Smith et al., 2024). Populations of widespread species often diverge along environmental gradients (Clausen et al., 1941; McMillan, 1969; Munzbergova et al., 2017; Lopez et al., 2020), giving rise to ecotypes (Turesson, 1925) that exhibit local adaptation (Savolainen et al., 2007; 2013) to climatic conditions such as rainfall

variability and drought frequency. Characterizing the climate-adaptive capacity of these ecotypes (Linhart & Grant, 1996; Joshi et al., 2001; Savolainen et al., 2013)—particularly in dominant grasses—is therefore essential for predicting drought resilience and guiding restoration strategies (Baer et al., 2019; VanWallendael et al., 2022).

To evaluate the adaptive capacity of a dominant US Great Plains grass, we examined how regional ecotypes of *Andropogon gerardi* (Vitman) respond to large rainfall gradients across the region. As a dominant C_4 perennial grass, *A. gerardi* can comprise up to 70% of tallgrass prairie aboveground biomass (Knapp et al., 1998) and strongly shapes diversity, productivity, and ecosystem functioning (Wilson et al., 2016; Ren et al., 2024). *Andropogon gerardi* also supports a major rangeland economy, including over $8 billion for cattle production in Kansas alone USD (Rogler, 1944; USDA NASS 2024) and 3.2 million ha of restoration plantings (CRP, 2024). Therefore, understanding the adaptation of *A. gerardi* to precipitation is critical for restoration, conservation, and rangeland economies.

Using one of the longest-running reciprocal garden experiments in natural grasslands (Johnson et al., 2022; Sytsma et al., in press), we quantified decadal patterns of local adaptation among dry, mesic, and wet ecotypes across a precipitation gradient spanning 480 to 1256 mm yr^{-1} (Colby, KS to Carbondale, IL, USA; Figure 1). Over 12 years (2010–2022), we tracked cover and biomass of *A. gerardi* ecotypes under natural climatic variation, including the extreme 2012 drought—the most severe since the 1930s Dust Bowl era (Rippey, 2015). Unlike most reciprocal transplant experiments, which on average last two years or less (Sytsma et al., in press) and involve limited source populations without experimental manipulation (Johnson et al., 2022), this platform provides a rare opportunity to evaluate adaptation and ecological dynamics

over more than a decade, capturing responses of long-lived grasses to both gradual and extreme climatic variation.

To independently test if rainfall is a key selective pressure, we incorporated experimental drought treatments using rainout shelters (Yahdjian & Sala, 2002) at three garden sites (Figure 1B, C). By imposing controlled reductions in precipitation, these shelters allow us to disentangle the role of water availability from other environmental variables that covary along natural gradients. We also leveraged NextGen sequencing to explore the genomic basis of local adaptation (Ungerer et al., 2008; Savolainen et al., 2013; Lasky et al., 2023), linking ecological performance with genotype and gene expression adaptation (Hufford & Mazer, 2003; Benfey & Michell-Olds, 2008; Bomblies & Peichel, 2022; Stronen et al., 2022). Specifically, we characterized genetic variation using genotyping-by-sequencing (Poland & Rife, 2012), and gene expression using RNAseq (Ferguson et al., 2025) in wet and dry ecotypes across sites. Finally, in addition to our focal species *A. gerardi*, we quantified cover and biomass of neighboring plant functional groups (Table 2.3) to assess whether locally adapted ecotypes influence the structure of surrounding plant community (Whitham et al., 2003; 2005; 2020; Woods et al., 2021).

Overall, this study integrates reciprocal gardens, experimental drought, and genomic analyses to test local adaptation in a dominant Great Plains grass. We hypothesized that (1) each ecotype would perform best in its home climate (local adaptation), with signatures of adaptation strengthening over time and during drought events (Grant et al., 2017; Aun et al., 2024); (2) experimental drought (rainouts) would confirm rainfall as a key selective force (Siepelski et al., 2017; Felman et al., 2024) by differentially affecting wet and dry ecotypes; (3) genomic and gene expression differences underlie observed patterns of ecotypic performance (Savolainen et

al., 2013); and (4) locally adapted, competitively dominant ecotypes (e.g., the dry ecotype at its home site) would suppress neighboring species, whereas non-local, less competitive ecotypes would permit greater cover and biomass of forbs and other grasses. By linking ecotypic performance to precipitation, drought, and community composition, we address a key knowledge gap with direct implications for restoration (Baer et al., 2019), rangeland management, and grassland resilience under future climate change (Huffard & Mazer, 2003; Chandanpurkar et al., 2025).

Results

Natural precipitation gradient reveals local adaptation in wet and dry ecotypes

Across the natural rainfall gradient, local adaptation of wet and dry ecotypes was evident in both canopy cover (Figure 2) and biomass (Figure S2). Starting with the dry ecotype in the driest sites, Colby KS (MAP 495 mm yr^{-1}) and Hays KS (MAP 550 mm yr^{-1}), *A. gerardi* cover was initially low (~20% cover) in the first years, but increased steadily over time to ~50%, (Figure 2A, B), but was always greater than the cover of the wet ecotype. Notably, the extreme in year three of the experiment (2012) caused a sharp decline in wet ecotype cover at the dry sites, with cover declining from 17% to less 6% after the drought at the driest site (Figure 2A) and from 21% to less than 5% after the drought at the dry site (Figure 2B). In contrast, the dry ecotype largely persisted at both the dry and driest sites (from 20-30% cover before drought to 25-30% after drought), highlighting drought as a strong selective pressure reinforcing local adaptation.

Comparing ecotypes, averaged over the length of the decadal experiment, cover of the dry ecotype in the driest site and dry site (Figure 2A, B) was greater by about four times than that of the wet ecotype transplanted in the same locations (driest site: dry ecotype 41% vs. wet

ecotype 11%, $p \leq 0.01$, dry site: dry ecotype 45% vs. wet ecotype 7%, $p \leq 0.01$). Similarly, by 2022, biomass of the dry ecotype was also significantly higher than the wet ecotype at both the driest and dry sites (driest site: dry ecotype 425 g m^{-2} vs. wet ecotype 120 g m^{-2}, $p \leq 0.01$, dry site: dry ecotype 470 g m^{-2} vs. wet ecotype 150 g m^{-2}, $p \leq 0.01$; Figure S2).

At the mesic site (Manhattan, KS; MAP 871 mm yr^{-1}), cover of all three ecotypes was similar throughout the course of the decadal experiment. By 2022, between the dry, mesic, and wet ecotypes, both cover (~58% cover; $p>0.05$; Figure 2C) and biomass (~300 g m^{-2}; Figure S2) remained not significantly different (all $p>0.05$).

In contrast, at the wet site 723 km eastward, Carbondale, IL (MAP 1167 mm yr^{-1}), the cover of all ecotypes was initially low (~10%) for several years into the experiment. However, as the experiment progressed, the dry ecotype stayed low in cover (~10%), while the wet ecotype increased cover to ~60% (Figure 2D). Averaged over the thirteen years of the experiment, cover of the wet ecotype was about 3.6 times greater than the dry ecotype transplanted into the wet site (wet ecotype 36% vs. dry ecotype 10%, $p<0.01$; Figure 2D). Furthermore, thirteen years after establishment, by 2022, wet and dry ecotypes had highest cover and biomass in their home sites (wet ecotype at the wet site and dry ecotype at the dry site, Figures 2, S2) demonstrating results congruent with local adaptation.

Over time, divergence of ecotypes was even greater compared to establishment years. For example, despite the 2012 drought, by 2022, cover of the dry ecotype in the westernmost, driest (49%) and dry (62%) sites were greater than that of the wet ecotype (9% and 11%; driest and dry sites, respectively, $p<0.01$). In contrast, by 2022, at the wet site, the cover of the wet ecotype (56%) was greater by about 9 times than that of the dry ecotype planted there (6%; $p<0.01$). Like

cover, by 2022, biomass of the wet ecotype was also significantly higher than the dry ecotype at the wet site (wet ecotype 1800 g m^{-2} vs. dry ecotype 225 g m^{-2}, $p \leq 0.01$).

In contrast with strong differences in cover between wet and dry ecotypes, the mesic ecotype showed intermediate cover regardless of site (Figure 2). Averaged over the length of the experiment, the cover of the mesic ecotype ranged from 25% in the wet site, to 37% in the mesic site, to 26% in both dry and driest sites (Figure 2). By 2022, biomass of the mesic ecotype also remained intermediate among sites, ranging from 460 g m^{-2} at the wet site to 380 g m^{-2} at the dry site (Figure S2).

The cover of each ecotype was also related to rainfall, regardless of the planting site (Figure 3). Wet and dry ecotypes showed a strong relationship with rainfall (Figure 3A, C). Consistent with local adaptation, the dry ecotype shows highest cover under low rainfall (Figure 3A) whereas the wet ecotype had the highest cover under high rainfall (Figure 3C). In contrast, the mesic ecotype (Figure 3B) had about the same cover regardless of rainfall, suggesting it can tolerate a wide range of rainfall.

Experimental rainouts independently corroborate rainfall as selective pressure

Experimental drought (rainouts) independently supported results from the natural rainfall gradient and demonstrated that reduced rainfall favored the dry ecotype over wet and mesic ecotypes (Figures 4, S3). Thirteen years after establishment, canopy cover of *A. gerardi* in the dry and mesic sites was significantly lower ($p < 0.01$) under the rainouts compared to ambient for all ecotypes (Figure 4A, B). By contrast, the dry ecotype in the wet site (Figure 4C) showed significantly higher cover under the rainouts (23%) compared to the ambient (6%), further corroborating the strong ecotype differences. Similarly, the dry ecotype demonstrated significantly increased biomass under the rainouts (460 g m^{-2}) compared to the ambient (195 g

m^{-2}; Figure S3). These results support strong local adaptation, with the dry ecotype showing a clear fitness advantage under reduced rainfall, consistent with its population origin in drier environments.

Genetic basis of ecotype differences driving local adaptation

The strong local adaptation to rainfall, especially of the dry and wet ecotypes, was reflected in genetic differences between these ecotypes. At the level of DNA, the ecotypes were clearly differentiated from each other based on DAPC analyses of SNPs in genomic DNA (Figure 5). This strong genetic divergence aligns with observations of local adaptation in the field, suggesting that adaptive divergence has a genomic basis.

At the level of the transcriptome (Figure 6), wet and dry ecotypes at their homesites showed diametrically opposed patterns of differential expression of genes. In their homesites (dry ecotype in dry site, wet ecotype in wet site) we found 195 differentially expressed genes between the two homesites (Figure 6). The genes expressed showed functional gene ontology differences between homesites (Figure S4). For example, *A. gerardi* growing in the dry homesite was significantly enriched in the following Gene Ontology (GO) terms: carbohydrate, lignin and lipid biosynthetic and metabolic processes, biotic and abiotic stress responses as well as root hair cell development and vernalization biological processes (Figure S4A). Specifically, at the dry homesite, *A. gerardi* showed upregulation of selected candidate genes (Table 2.4) involved in dehydration and stress response (*CASP1, aquaporin, RGA1, cytochrome P450 71A26, sphingolipid transporter spinster*), cuticle formation (*ABC transporter G family member 34*) and hydraulic conductivity (*bundle sheath cell specific protein 1*).

In contrast, at the wet homesite (Figure 6), *A. gerardi* was enriched in GO terms involving phospholipid metabolic process and carbohydrate catabolism, anatomical morphogenesis, methylation, organic substance biosynthetic process, salicylic acid process, and glutathione (Figure S4B). Specifically, the wet homesite showed selected candidate genes upregulated in growth and development (*MYB transcription factor, DUF3511, bHLH041, Cinnamoyl-CoA reductase 1*), several defense genes (*RPP13-like, RGA2*), and selective transport of nitrate (*S-type anion channel, SLLAH2-like;* Table 2.4). Together, the contrasting gene expression patterns between wet and dry ecotypes at their respective homesites indicate strong local adaptation, with each ecotype exhibiting transcriptional profiles specialized for the environmental conditions of its native habitat.

The RNAseq profiles of ecotypes in the driest site (Figure S5), putatively with the most water stress, showed 775 genes were differentially expressed between wet and dry ecotypes. The dry ecotype growing at the driest site showed enrichment in processes including response to salt stress, nitrogen-related metabolic processes, response to water deprivation, and oxidative phosphorylation (Figure S4C). In contrast, the wet ecotype, also at the driest site, showed enrichment in processes such as xenobiotic transport, response to oxidative stress, regulation of DNA damage checkpoint, and methylation (Figure S4D).

Considering selected candidate genes (Table 2.4), the dry ecotype in the driest site showed many genes related to coping with abiotic stress (*heat shock protein-like 23.2 kda*), especially drought (*LEA, r40c1*), seed maturation and development (*pectinesterase, embryonic flower 2, Bowman Birk*), negative regulation of GA (*1-hydroxy-2-methyl-2-(E)-butenyl 4-diphosphate reductase*), photosynthesis (*tic20-like protein*) and gas exchange (*photosystem 1 subunit o*). In contrast, the wet ecotype in the driest site, putatively more susceptible to abiotic

stress, had several transcription factors upregulated (*myb, BLH*), several genes in response to stress (*HSP90, elongation factor 1a, mitogen-activated*), regulation of plant growth and development (*FAR1, Embryo sac arrest*), regulation of gene expression through methylation (*Histone H2A.4*; Table 2.4). Taken together, the RNAseq data showed different strategies in coping with harsh abiotic conditions at the driest site. The stark gene expression differences between wet and dry ecotypes were already apparent in the first year and perhaps portend the differences in ecotypes that in some sites (e.g., wet site) did not become apparent until several years into the experiment.

Strong adaptation of local ecotype competitively suppresses the surrounding plant community

The strong phenotypic and genetic differentiation among wet and dry ecotypes had ecological consequences extending beyond the focal species by shaping the performance of the neighboring plant community. Specifically, the local ecotype at a site suppressed growth of other grasses and forbs (Figure 7). For example, at the dry site, other grass species growing with the highly competitive and locally adapted dry ecotype contributed only 5% cover (averaged over the experiment) and differed significantly ($p<0.01$) compared to other grass species growing with the poorly competitive non-local ecotype that comprised 24% of the cover (Figure 7A). Furthermore, at the dry and driest sites (Figure 7A, B), these differences continued over time. By 2022, other grasses reached cover of ~30% when growing with the non-local wet ecotype but only ~5% when growing with the local dry ecotype ($p<0.01$). A similar pattern was observed independently both in the driest and dry sites (Figure 7A, B).

The local ecotype of *A. gerardi* also strongly suppressed forb cover. For example, forbs growing with the locally adapted wet ecotype in the wet site averaged only 19% cover over the decade (Figure 7D). In contrast, forbs growing with the non-local dry ecotype at the wet site exhibited 45% cover for the same period ($p<0.01$; Figure 7D). Furthermore, in terms of temporal dynamics, by 2022 at the wet site, forb cover was ~60% when growing with the dry ecotype and significantly differed ($p<0.01$) from forb cover (~15%) growing with the wet ecotype.

Discussion

This study is one of the longest running tests of local adaptation of ecotypes using reciprocal gardens in a community context (Johnson et al., 2022). Here, we show unequivocal evidence for phenotypic and genetic differentiation of ecotypes across a rainfall gradient (Siepelski et al., 2017; Felman et al., 2024) and the community consequences of local adaptation in a dominant species. Four lines of evidence support our conclusion about the strength of local adaptation: 1) local adaptation was strongest for ecotypes at the extremes of the rainfall gradient and became more pronounced over time as communities develop. Local adaptation was further indicated by the reduced performance of wet ecotype during the 2012 drought compared to the dry ecotype, 2) experimental rainfall reduction favored the dry ecotype especially at the wet site, corroborating the importance of rainfall as a selective driver; 3) genetic divergence among ecotypes mirrored patterns of ecological performance, supporting a heritable genomic basis for local adaptation to rainfall; and 4) changes in the plant community resulting from the presence of local ecotypes being more competitive compared to those growing with a non-local ecotype. Finally, we explore our results and their implications for conservation, grassland restoration and anticipating future climate changes to this expansive, critical ecosystem.

Local adaptation to rainfall confirmed at decadal scales along the natural rainfall gradient

We found strong evidence of local adaptation in both the wet and dry ecotypes, with signals of adaptation strengthening over time and most pronounced at the range edges (dry and wet sites). The dry ecotype thrived in the arid (dry site MAP 550 mm yr^{-1}) high-light (85% light availability; Figure S6) conditions of the western Great Plains[63], while the wet ecotype performed best under shaded, high-moisture conditions in the east (wet site MAP 1256 mm yr^{-1}; 15% light availability; Figure S6). These patterns suggest that divergent abiotic and biotic pressures—water limitation in the west and light competition in the east—putatively maintain locally adapted ecotypes across the species' distribution (Sexton et al., 2009; Solarik et al., 2018), at least at the margins. Phenotypic differences reflect these selective pressures where the dry ecotype showed reduced leaf area, narrow blades, and dwarf stature (Galliart et al., 2020) (Figure S1), minimizing water loss and aligning with drought strategies (Baird et al., 2021). In contrast, the wet ecotype's taller stature enhanced light capture in dense, wetter environments (Moles et al., 2009; Hilty et al., 2021; Figure S1). These within-species trait differences indicate that intraspecific variation can equal or surpass interspecific differentiation (Siefert al., 2015) and sometimes exhibit trait divergence exceeding that of co-occurring grasses like *Sorghastrum nutans* (Silletti & Knapp, 2002; Swemmer et al., 2006).

Together, these findings highlight how local adaptation is structured across the dominant portion of a species range. Populations at range margins, though typically small and fragmented, may already be pre-adapted to climate extremes and thus valuable under future scenarios of rapid drying and heating (Nadeau & Urban, 2019). In contrast, mesic ecotypes in intermediate rainfall zones may function as generalists with broad adaptive capacity (Denelle et al., 2020). By

characterizing local adaptation, we provide guidance to which populations are most useful for restoration depending on management goals (Baer et al., 2019) where margin specialists may enhance resilience to extremes, while central generalists may provide stability across a wider range of environments.

This study provides a rare, long-term perspective on local adaptation in reciprocal garden experiments (Johnson et al., 2022). While fewer than 5% of studies in ecological genomics in grasslands last more than a decade (Sytsma et al., in press), our results demonstrate the critical value of long-term data (Cocciardi et al. 2024; Stroud & Ratcliff, 2025; Le et al., 2025) for understanding how ecotypic divergence unfolds in perennial plant communities (Figure 2). A short experiment would not have captured the strength of local adaptation where, at the wet site in our experiment, slow establishment and early competition with weedy species initially masked local adaptation, which only became evident after five years (Johnson et al., 2015; Galliart et al., 2019). By extending the experiment across 12 years of natural climate variability, including a severe drought (Rippey, 2015), we captured the ecological consequences of extreme selection pressures (Siepelski et al., 2017; Felman et al., 2024) that shorter, or single-year studies would have missed. Collectively, these findings underscore the necessity of long-term reciprocal garden studies for detecting adaptive processes and community responses in long-lived grasses increasingly exposed to climatic extremes (Smith et al., 2024).

Rainouts confirm rainfall as a selective force driving local adaptation

The rainout shelters provided independent secondary evidence for the strength of local adaptation, primarily in response to rainfall. Rainouts favored the growth of the dry ecotype at the wet site, thus independently corroborating the importance of rainfall. Based on both cover

and biomass, the dry ecotype is so adapted to its dry "home" conditions that it benefited from reduced rainfall when growing under rainout shelters at the wet site (Figures 4C, S3). Consistent with these abundance and biomass patterns, photosynthetic rates of the dry ecotype under rainouts at the wet site were even higher than under ambient conditions (Sytsma et al., in review), further demonstrating its physiological advantage under drought. These results unambiguously and independently identify rainfall as a strong selection pressure driving differentiation of wet and dry ecotypes. Since the wet ecotype was most negatively affected by rainouts based on cover in dry and mesic sites (Figure 4A, B), this suggests that *A. gerardi* populations adapted to high rainfall may be more negatively impacted by future decreases in rainfall (Soliani et al., 2021) than those dry ecotypes already adapted to dry conditions.

Results from the rainout treatment corroborate other grassland studies that manipulate rainfall (Knapp et al., 2008; Cherwin & Knapp, 2012; Xu et al., 2021; Zhang et al., 2022). Grassland ANPP is often reduced under rainfall reduction shelters (Knapp et al., 2008; Cherwin & Knapp, 2012; Zhang et al., 2022) confirming the role of rainfall in grassland productivity and extreme rainfall events shift ecosystem function (Smith et al., 2024) and carbon accumulation (Knapp et al., 2008). However, most previous studies do not consider the importance of ecotype variation in ecosystem response, and intraspecific variation is often overlooked in ecosystem and modeling studies. Our study highlights the importance of ecotypes in controlling and sustaining grassland productivity over environmental gradients, such as rainfall.

Genomic and transcriptomic divergence mirrors phenotypic evidence of local adaptation

Genetic and transcriptomic results demonstrate that wet and dry ecotypes of *A. gerardi* are not only morphologically distinct but also diverge at the molecular level. DAPC

analyses of SNPs revealed clear genomic differentiation between ecotypes (Figure 5), mirroring their divergent performance in cover and biomass across rainfall patterns (Figure 2) and confirming a strong genetic basis for local adaptation (Savolainen et al., 2013; Gray et al., 2014; Galliart et al., 2019). Our findings build upon other studies using genomic DNA in which SNP in GA1, a key gene in gibberellic acid synthesis, explained four-fold differences in ecotype height, consistent with selection for tall stature in shaded wet environments and reduced stature under arid, high-light conditions (Galliart et al., 2020; Figure S1). Precipitation explained more variation in genetic outliers than geographic distance, underscoring climate rather than neutral processes as the primary driver of divergence (Galliart et al., 2019). Similar adaptive divergence across rainfall gradients has been documented in other C_4 grasses including *Panicum hallii*, where genes tied to stress tolerance, photosynthesis, and growth regulation drive ecotypic differentiation (Lowry et al., 2015; Gould et al., 2018; Lovell et al., 2018; Bhaskara et al., 2023).

At the transcriptomic level, *A. gerardi* ecotypes exhibited distinct strategies across environments (Figures 6, S5). The dry ecotype upregulated genes tied to abiotic stress tolerance at the driest sites (Figures 6, S5), while the wet ecotype enhanced expression of genes related to light capture and carbon gain in its shaded homesite. Notably, home-site expression differences appeared in the first year, indicating that molecular divergence underlies long-term performance patterns. These results parallel findings in other prairie dominants such as *Panicum virgatum*, where ecotypic differentiation and rapid gene expression shifts drive local adaptation (Lowry et al., 2014; Meyer et al., 2014; Heckman et al., 2025).

Candidate genes further highlight ecotypic divergence: the dry ecotype emphasizes stress-response and dehydration genes (*CASP1*, *aquaporin*, *RGA1;* Trono & Pecchioni, 2022), as well as those for cuticle formation (*ABC transporter G34*) and hydraulic regulation (*bundle*

sheath cell-specific protein 1). In contrast, the wet ecotype prioritizes growth (*MYB*, *DUF3511*; Figueroa-Macias et al., 2021) and defense genes (*SAR DEFICIENT*, and *RPP13-like;* Figueroa-Macias et al., 2021). Under the most arid conditions in Colby, the dry ecotype further upregulated *LEA* and *HSP-like 23.2 kDa* genes associated with drought resilience (Trono & Pecchioni, 2022), whereas the wet ecotype activated broad regulators including *HSP90*, *elongation factor 1a*, *FAR1*, *MYB*, *BLH*, and *histone H2A.4*. Together, these findings show that genomic and transcriptomic divergence along rainfall gradients drives adaptive differentiation in a tallgrass prairie grass.

Local ecotypes exert strong competitive suppression on the surrounding plant community

Our long-term reciprocal garden experiment reveals how ecotypic variation in a dominant species influences not only its own performance (Figure 2) but also the surrounding plant community and competitive dynamics over time (Figure 7). Because the communities developed from seed for over a decade, we were able to detect how *A. gerardi* ecotypes altered plant functional group composition and interactions as both biotic and abiotic processes unfolded in realistic ecological settings (Johnson et al., 2022). By planting ecotypes with other species, as would be conducted to restore communities, our approach captures more natural ecological responses than typical single-species studies, highlighting the hierarchical effects of intraspecific variation (Des Roches et al., 2018) in a dominant species on structuring communities. Consistent with the "extended phenotype" framework (Whitham et al., 2003; 2005; 2020)—which posits that genetic variation in a species can influence not only its own traits but also the structure and function of its surrounding community—our results demonstrate that dominant grasses can shape their ecosystems through local adaptation. We found that locally adapted ecotypes of *A.*

gerardi suppressed neighboring species more strongly than nonlocal ecotypes, reinforcing their role as competitive foundation species whose effects intensify through succession (Wilson et al., 2016). Similar patterns in a functionally similar and often co-dominant C_4 grass, *Sorghastrum nutans,* show that genetic variation within dominant prairie species can drive community assembly and even influence higher trophic levels (Gustafson et al., 2014; Ren et al., 2023; 2024). Together, these findings underscore the novelty and importance of studying how ecotypic variation in dominant species shapes communities and ecosystems through long-term, community-integrated experiments.

Integrating ecotypic variation into restoration and climate predictions

This study has important implications for conservation, grassland restoration, and predicting climate change impacts on tallgrass prairie ecosystems. Climate warming and more frequent droughts (IPCC, 2023; King et al., 2024) are expected to alter grassland structure and function (Smith et al., 2024). These changes in climate are likely to favor dry-adapted species and ecotypes (Anderson, 2016) reduce *A. gerardi* abundance within its current range (Smith et al., 2017) and resulting in the potential for some populations to face local extinction. Because most predictive models overlook intraspecific responses to climate change (Rellstab et al., 2021), our results emphasize the need to incorporate ecotypic variation into forecasts and Earth system models (Song et al., 2023), particularly for dominant grasses that regulate ecosystem processes (Zhang et al., 2025). As the dominant species shapes tallgrass prairie structure and functioning (Knapp et al., 1998; Epstein et al., 1998), ecotypic variation in this species influences community composition, consistent with the "extended phenotype" concept (Whitham et al., 2005; 2020). Restoration strategies incorporating drought-resilient ecotypes and their ecological interactions

are thus more likely to support productive, biodiverse, and sustainable ecosystems (Zhang et al., 2025). Given projected losses of genetic diversity in the Anthropocene (Exposito-Alonso et al., 2022), leveraging local adaptation may be key to maintaining the long-term viability of the tallgrass prairie ecosystem.

Acknowledgements. Special thanks to Z. Ren, D. Barfneckdt, S. Thapa, K. Howe, H. Winters, and N. Bishop for biomass sample collection and processing.

Conflicts of Interest Statement. The authors declare no conflicts of interest related to the research, authorship, or publication of this manuscript.

Data Availability Statement. All data supporting the findings of this study are available in a publicly accessible Dryad repository (doi:xxxx).

CRediT Author Contributions. Jack Sytsma: Writing – original draft, supervision, conceptualization, investigation, data curation, formal analysis, methodology. **Matthew Galliart:** Investigation, formal analysis, writing- review and editing. **Sara Baer:** Conceptualization, resources, methodology writing- review and editing. **David Gibson:** Conceptualization, investigation, writing- review and editing, validation. **Trevor Hefley:** Formal analysis, writing – review and editing. **Hannah Tetreault:** Investigation, writing- review and editing, validation. **Brian Maricle:** Conceptualization, investigation, writing- review and editing, validation. **Loretta Johnson:** Conceptualization, methodology, project administration, resources, funding acquisition, writing – review and editing.

Funding Information. Funding was provided by USDA Grant #2020-03665, USDA #2008-35100-04545, NSF GRFP to Galliart, and the US Department of Education GAANN Grant P200A240009 to Sytsma. This study is also partially funded by the 2023 Kansas Academy of Science Research Grant awarded to Sytsma.

Methods

The long-term reciprocal gardens used here have been studied for over ten years since their establishment in 2009, including studies of genetics (Gray et al., 2014; Galliart et al., 2020), modeling phenotypes (Smith et al., 2017), early ecotype cover responses (Johnson et al., 2015; Galliart et al., 2019), and plant physiological response to drought (Kramer et al., 2018) among others. These other papers provide context and scope of the overall and long-term goals of the project.

Seed collection

Seed of *A. gerardi* was collected by hand in 2008 from three regions along a mean annual precipitation (MAP) gradient from central Kansas (MAP 550 mm y^{-1}), eastern Kansas (MAP 891 mm y^{-1}) and southern Illinois (MAP 1167 mm y^{-1}). Source locations of the 12 populations used in this study with relevant site information are found in Table 2.1 and visualized in Figure 1A. At each location, seeds were collected from four populations, which defined regional climate ecotypes. Populations originated from intact, remnant prairies within an 80 km radius of each reciprocal garden site. Seeds from four populations within each ecotype were mixed in equal quantities for the final seed mix used in plot establishment, and plots were planted in spring of

2009. Seeds were tested for viability (percent live seed) and mass of seed was adjusted for live seed before planting.

Plots along the natural rainfall gradient

Reciprocal garden field experiments were established in Colby, Kansas (driest site), Hays, Kansas (dry site), Manhattan, Kansas (mesic site), and Carbondale, Illinois (wet site), United States (Table 2.2). Note that the driest site had no local ecotype and was included to test the threshold of response to drier locations as might be experienced in the future.

At each planting site, the design consisted of four blocks, each containing three plots of sown communities. The plots were sown with seeds corresponding to the populations of each of the three regional ecotypes. At each planting site, ecotype treatments were assigned according to a randomized block design with four plots of each ecotype at each site (Figure 1B). Each ecotype was reciprocally sown into a newly plowed agricultural field at each site. Seeds were hand-broadcast and raked in by hand. We planted at seeding rates similar to those used in restoration (e.g., 160 seeds m^{-2} for *A. gerardi;* Baer et al., 2003*)*. In addition to the ecotypes of *A. gerardi*, we added seed of seven native forbs and other grasses (Table 2.3) as subordinate species that might be planted in a restoration (Baer et al., 2003). We allowed volunteer species from the regional source pool to establish over time. Species composition of the plots is reported elsewhere (Ren et al., 2023; 2024). Unseeded 5 m-wide borders and aisles separated the plots. Plots were burned annually in late winter or early spring for most years.

Soils were generally silty clay or silty loams across each of the garden sites. See soil details in Table 2.1 and complete soil description in Mendola et al. (2015). All reciprocal garden sites were former agricultural land.

Rainout shelter

To isolate the role of rainfall in plant and community responses, rainout shelters were established in three study locations: Hays Kansas, Manhattan Kansas, and Carbondale Illinois, USA. Rainout shelters were not established in Colby, Kansas as the rainfall is already reduced. Rainouts have been shown to be a well-suited design to alter ambient rainfall (Yahdijian & Sala, 2002). In 2011, rainout shelters were installed and designed to capture 50% of ambient rainfall over half of each plot in three garden sites using the rainout shelter design of Yahdjian & Sala (2002). The rainout shelters were placed on existing dry, mesic, and wet ecotype plots. Rainfall shed from the shelters ran into gutters and then collected in rain barrels and disposed of away from the plots. The roofs (2 m x 2 m) were installed in mid-June and taken down in mid-October each year. The polycarbonate roof material only reduced light by ~5%.

Response variables: testing for local adaptation

We tested local adaptation, and ecotypic differentiation with measurements of vegetative cover and plant biomass of *A. gerardi* ecotypes planted across the precipitation gradient, and to assess the local adaptation to their home site. Measurements of vegetative cover and aboveground biomass of *A. gerardi* were made to assess plant performance over the decade. Cover measurements were made on the surrounding plant community to assess how ecotypes affect other components of the communities.

Cover measurements

Vegetative cover was used as a proxy for abundance because it is a good predictor of success in long-lived perennial plants (Wilson, 2011). Vegetative cover was measured in 2010-2015, 2021 and 2022. We made cover measurements during peak season late July to early August within ten days of each other for all sites. To estimate percent cover, a 1.0 m^2 quadrat was used with one intersection every 10 cm for a total of 81 intersections. At every intersection, the occurrence of *A. gerardi*, other grass, forb, or bare ground was recorded. We used four non-overlapping quadrats per plot for a total of 324 intersections per plot (81 intersections per quadrat x 4 replications per plot x 3 ecotypes x 4 plots x 2 treatments (ambient vs rainout) per site=7,776 intersections per site x 4 sites=31,104 intersections each year). Quadrats were randomly placed at least 50 cm from the edge to minimize edge effect. Cover measurements were also made under rainouts in 2022 to quantify the impact of long-term drought.

Biomass harvest at end of season

Aboveground biomass was harvested during the late growing season (August-September) in 2010 and 2022. All plant biomass was clipped from 20 cm x 50 cm quadrats. We used four non-overlapping quadrats per plot for a total of 384 biomass samples per year (4 quadrats per plot x 2 rainfall treatments x 3 ecotypes x 4 blocks per site=96 samples per site x 4 sites=384 samples each year). Aboveground biomass of the communities was also harvested under rainouts in 2022 to quantify the impact of long-term drought compared to ambient conditions. Biomass of all plant material in the quadrat was harvested by cutting the aboveground plant material at soil level. Biomass was dried at 60^{o}C for at least one week, and weighed.

Statistical analysis

We used generalized additive models (GAMS; Wood, 2017) to assess each of our hypotheses. Briefly, generalized additive models are like other well-known regression-type modeling techniques such as linear models (i.e., regression and ANOVA), mixed models, and generalized linear models. The difference is that with GAMs, the effect of time, space, or other continuous variables of interest can be modeled with a so-called "smooth" effect which, in general, estimates a "curve" under limited assumptions (Wood, 2017; Hefley et al., 2017). The feature of GAMs is important for our study because the relationship between response variables like canopy cover and predictor variables like time (year) are generally unknown. The use of GAMs enables us to use a well-developed statistical framework to learn these types of relationships through the estimation of a "curve" or "function" while imposing minimal assumptions on the functional form of such relationships. In addition, GAMs can include simple linear and categorical predictors, random effects, and non-normal response variables. We used GAMs to analyze cover and biomass data, rainout effects, and effects of ecotypes on surrounding community functional groups. For those years when we could not measure cover, during the period 2016-2020, we used GAMs to predict what the % canopy cover from 2016 to 2020. In general, GAMs will appropriately inflate uncertainty measures (e.g., wider confidence intervals) for such prediction. See Methods S1 for full statistical analyses details.

DNA genotyping and genetic analyses.

We used genotyping-by-sequencing to identify SNPs (Poland & Rife, 2012). Leaf samples for DNA analysis were collected from the plants from the original populations used to originally seed the plots (REL, SAL, CDB, WEB for dry populations, TOW, KON, CAR, TAL for mesic populations and WAL, 12MI, DES, and FUL for wet populations; Table 2.1). Total

number of plants genotyped (289) included 96 from the dry ecotype, 95 from the mesic ecotype, and 98 from the wet ecotype. For collection, ~100 mg of leaf tissue was collected directly into 96-deep well matrix plates on ice. All samples were subsequently grounded to a fine powder and stored at -80°C until DNA isolation.

DNA was isolated using a modified CTAB protocol (Doyle & Dickson, 1987) to yield high quality DNA from *A. gerardi* leaves. We used 550 µl per sample of extraction buffer added to ground samples containing 100 mM Tris-HCl, pH 8.0, 100 mM EDTA, pH 8.0, 1.4 M NaCl, 2% CTAB, 12 mM TCEP (a non-toxic substitute for beta-mercaptanethanol), 16 mM Sodium Diethyldithiocarbamate Trihydrate, 4% PVPP. This was followed by 50 µl per sample of reducing buffer containing 100 mM Tris-HCl, pH 8.0, with 120 mM TCEP and 160 mM DIECA added separately. Quality was visually assessed on an 0.8% agrose gel and quantified for DNA concentration with PicoGreen (ThermoFisher.com) and normalized for library preparation. All samples were prepared for genotyping-by-sequencing (Poland & Rife, 2012) using a two restriction enzyme pair of PstI and MspI. For each plate, sequencing design included barcoding for each unique individual and each plate multiplexed (96-plexing) for 200 base paired-end sequencing in one lane per library on an Illumina HiSeq 2000. Ecotypes were split across plates and sequencing runs to avoid sequencing bias.

A SNP calling protocol was applied to genotype single-spaced plants of known ecotype. Individuals were genotyped and SNPs discovered using UNEAK pipeline implemented in TASSEL 3.0 Standalone Pipeline (Glaubitz et al., 2014; http://www.maizegenetics.net/tassel). Libraries were de-multiplexed from individual specific barcodes, and all reads were confirmed to contain PstI-MspI cut sites. Reads were trimmed to 64 base pairs long and combined into identical tags with five reads required to be retained. Tag pairs containing a single mismatch are

combined as putative SNPs with error tolerance of 0.03. Tags were combined across all individuals with minor allele frequency of 0.05. SNPs retained have 6x coverage and loci with <10% missing SNP calls were removed. The final genotype data set resulted in 4,641 high quality SNPs across 289 individuals.

Discriminant analysis of principal component (DAPC) was calculated from identified SNP markers from the 289 individuals and performed in the R package *Adgenet* (Jombart, 2008). To determine the number of principal components to retain, cross validation using 1,000 reps across PCs to identify the number associated with lowest mean squared error to retain in the DAPC. The final DAPC considered the three ecotypes (dry, mesic, and wet) and 80 principal components were retained for the final analysis.

RNA and gene expression

Leaf tissue was collected at the end of the first full year of growth 2010 in August in Colby Kansas, Hays Kansas and Carbondale, Illinois and at the same time of ecological measurements. We focus, for contrast, on the driest, dry and wet sites, and only wet and dry ecotypes as extremes. Roots were not collected due to the destructive nature of root sampling in long-term plots. Within each of the four replicated plots per ecotype, three plants were randomly flagged, for a total of twelve plants sampled per ecotype. For each plant collected, 2-3 mature leaves were taken. All collections were performed within a two-hour time frame in mid-afternoon. Leaves were flash frozen and put in liquid N in the field and transferred to -80C freezer at the laboratory.

Total RNA was isolated and purified using the QIAGEN RNeasy kit according to the manufacturer's recommended protocol for plants. Concentration and purity of total RNA was

evaluated on the Nanodrop Spectrophotometer (Thermo Scientific). The intactness of RNA samples was assessed using the Agilent Bioanalyzer 2100 (Agilent Technologies). To eliminate genomic DNA contamination of the RNA samples were treated with RNase-Free DNase I (Qiagen). cDNA libraries were constructed from messenger RNA and prepared for sequencing on the Illumina HiSeq2000. Briefly, messenger RNA was selected from 1ug of total RNA and converted to indexed RNA-seq paired-end libraries with the TruSeq RNA Sample Prep kit (Illumina, San Diego, CA). The final cDNA libraries were quantitated by qPCR with the Library Quantification kit Illumina compatible (Kapa Biosystems, Woburn, MA). The pooled libraries were then loaded onto HiSeq2000 at a concentration of 14 pM and sequenced for 100 cycles from each end of the fragments plus 7 cycles for the index read according to the manufacturer's instructions (Illumina, San Diego, CA). Raw files were converted to fastq files with Casava 1.8.2 (Illumina, San Diego, CA). Average quality scores were ≥30 across sequencing cycles. Reads were 100 bp in length with an average cDNA fragment length of 240 bp.

De novo transcriptome assembly, gene expression, and functional annotation

The next phase in the gene expression analysis was transcriptome assembly and mapping of reads. Quality of reads was assessed using *FastQC v0.11.9* (Andrews, 2010). *De novo* transcriptome assembly was conducted using *Trinity v2.8.5* (Grabherr et al., 2011). Using Trimmomatic (Bolger et al., 2014), extra Illumina adapters were removed, and reads were trimmed using a sliding window of 4 bases having removed reads with a phred score below 20. We assembled two transcriptomes. For the assembly of the transcriptome from the Carbondale (wet) and Hays (dry) plants, the assembly included reads from three individuals per ecotype per site sequenced on Illumina HiSeq and with one of those individuals also sequenced on Illumina

MiSeq to allow for longer read lengths to be incorporated for an improved *de novo* assembly. For the assembly of the Colby plants, we used the reads from three individuals per ecotype in Colby plus all of the reads from the Carbondale and Hays plants (mentioned above).

After each transcriptome assembly, statistics were assessed using the built-in perl script available with *Trinity*. Contigs from the *de novo* assembly were clustered using default similarity thresholds for CD HIT EST v4.8.1 (Li & Godzik, 2006). Following clustering, TransDecoder v5.5.0 (https://github.com/TransDecoder*)* was used to identify and predict coding regions from the clustered sequences. Finally, BUSCO v4.0.2 (Simao et al., 2015) was used to identify orthologs in the assembly. For alignment and mapping of transcripts, we used STAR v2.7.5 (Dobin et al., 2013). The clustered and filter transcriptome was used for alignment and mapping. First, the transcriptome was indexed using STAR v2.7.5. Each of the individual samples was mapped to the indexed reference transcriptome. Next, gene counts were obtained using the *rsem-calculate-expression* procedure as implemented in STAR v2.7.5.

The final phase of the gene expression study was to quantify differences in gene expression between site and ecotype and ecotypes in their home site and when abiotically stressed in Colby KS and to conduct annotations and functional analysis of the significantly expressed genes, and enrichment analyses. The ultimate goal was the identification of candidate genes related to functional differences between ecotypes and sites and in their homesites and genes that might confer abiotic stress tolerance as identified in the Colby (driest) site. To identify differentially expressed genes, we used DESeq2 v3.112 (Love et al., 2014). Data from the Hays (dry)-Carbondale(wet) transcriptome was analyzed using three separate approaches by 1) combining different ecotypes within a site to identify expression differences between sites, 2) combining the same ecotype from different sites to identify expression differences between

ecotypes and 3) ecotypes in their home site, the wet ecotype in Carbondale Illinois and the dry ecotype in Hays, KS. For the Colby (driest) site, we compared the wet and dry ecotypes within a site. Differentially expressed genes were then identified using BlastX. BLAST2GO (Gotz et al., 2008) was implemented to determine gene annotations and GO terms.

Significantly enriched GO terms from BLAST2GO were summarized using *rrvgo* (Sayols, 2023) in R to reduce redundancy and visualize functional patterns. GO terms were clustered and represented as tree maps for biological processes. This approach provided a concise overview of biological processes associated with differential gene expression across ecotypes and environments.

Environmental measurements

Climate data. Historical climate data, as well as climate data for study period (2010-2022), were obtained from weather stations (https://scacis.rcc-acis.org/; Table 2.2) closest to each site to characterize interannual variation in rainfall (shown graphically in Figure S7) and temperature.

Soil moisture. Volumetric soil water content (%) was measured to document the natural rainfall gradient and experimental rainfall reduction in 2022. Meter soil moisture probes (10HS-ECH20 Large Volume Soil Moisture Sensor) were used to monitor soil moisture in all site locations and treatment types (Figure S5). Soil moisture was measured with probes at 10 cm depth. One probe was used per block in ambient conditions and under rainout shelters (n=8), four readings were taken for each block.

Ground light availability. In 2022, light availability at the soil surface was measured using a LI-191R Line Quantum Sensor and a LI-250A Light Meter. Ten light readings per plot

were measured in both ambient and rainout conditions at soil level. The mean of each plot was divided by the above canopy light reading to estimate ground-level light availability (Figure S5B).

Figure 2.1. A. The location of the source populations, the garden sites along the US Great Plains rainfall gradient. Location of reciprocal gardens planting and collections sites across the US Great Plains. White circles are reciprocal garden locations and black triangles are the collection prairie for the seeds. Figure adapted from Galliart et al., 2020. B. Reciprocal Garden transplant design for research plots with rainout shelters Single colors are single ecotype plots (dry, mesic, or wet ecotypes). At each planting site, there are 4 replicate plots and ecotype plots at each site were randomized. Gray is experimental rainout shelter. Note: the Colby planting site had no local ecotype but was included to test the threshold of response to drier locations as might be experienced in the future. C. Aerial photograph of the reciprocal garden plots (photo taken at the mesic site, Manhattan KS) showing the spatial arrangement of ecotypes and rainout shelters. The image provides context for the research design and illustrates the community-scale layout of the experiment.

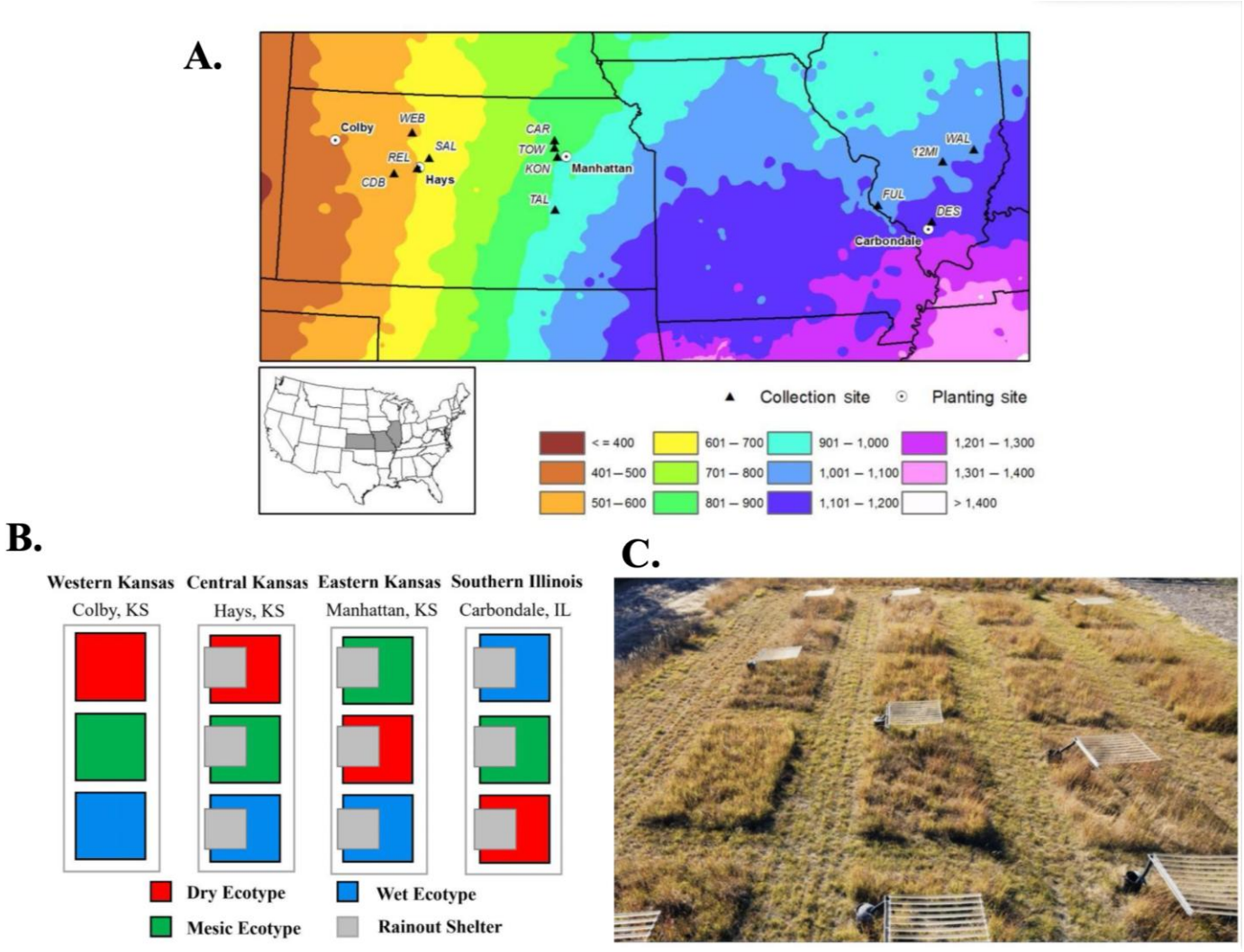

Figure 2.2. Vegetative cover of *A. gerardi* by planting sites (A. Colby, Kansas, B. Hays, Kansas, C. Manhattan Kansas, and D. Carbondale, Illinois) in ambient conditions for each ecotype from years 2010 to 2022 across the Great Plains precipitation gradient. Solid line indicates the mean and shaded area indicates 95% confidence intervals. Yellow tick marks on x axis indicates sampling years. The years without tick marks are modeled data. The black arrow indicates the year of the severe 2012 drought.

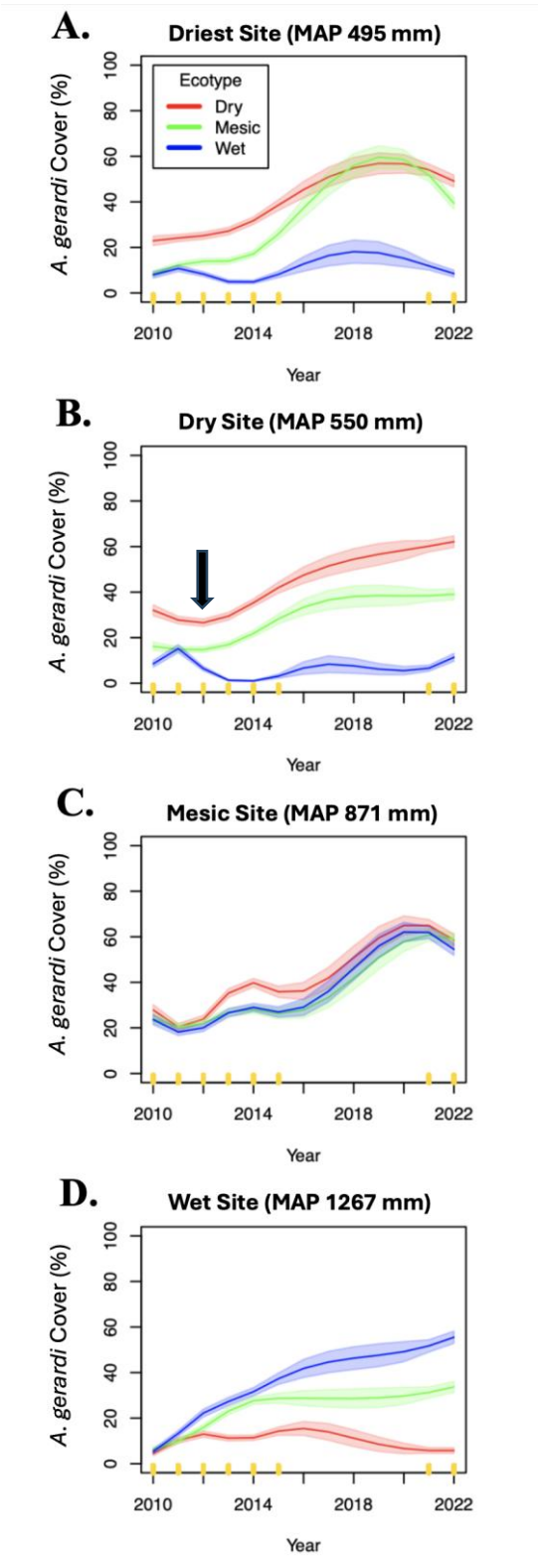

Figure 2.3**.** Vegetative cover of *A. gerardi* by ecotype (A. dry, B. mesic and C. wet) in ambient conditions versus rainfall. Data are presented for all sites and all years. Circles indicate data points; solid line is the regression line.

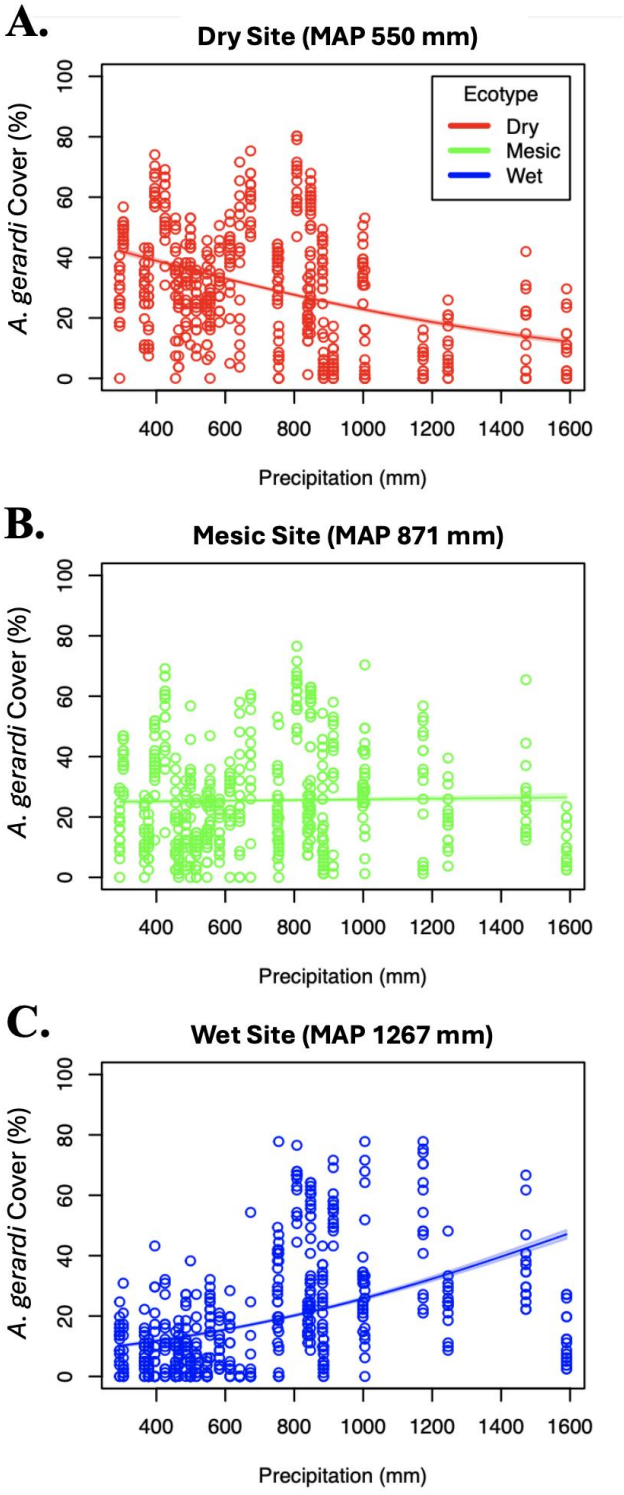

Figure 2.4. Vegetative cover in ambient and rainout plots for each ecotype in the ecotype plots by planting sites (A. Dry site-Hays, Kansas, B. Mesic site-Manhattan Kansas, and C. Wet site-Carbondale, Illinois). Data from 2022 is presented. Dots indicate the mean, bars indicate standard deviation, and different letters indicate significant ($p<0.05$) differences between control or rainout treatment.

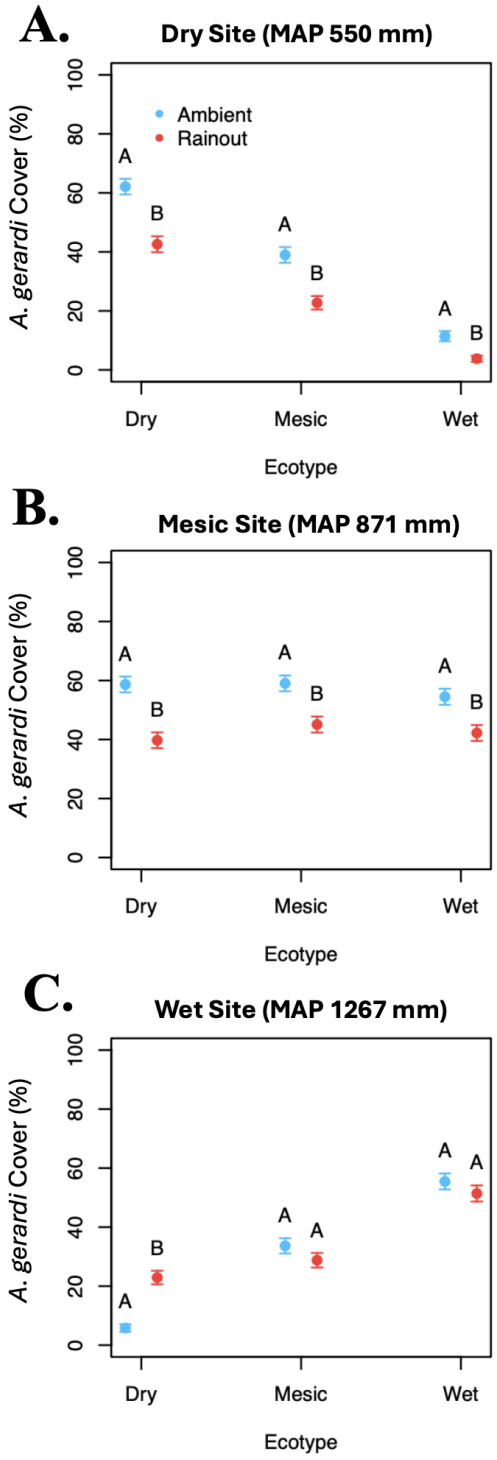

Figure 2.5. Discriminant Analysis of Principal Components (DAPC) of individuals grouped by ecotype (dry = red, mesic = green, wet = blue), showing distinct clustering by ecotype.

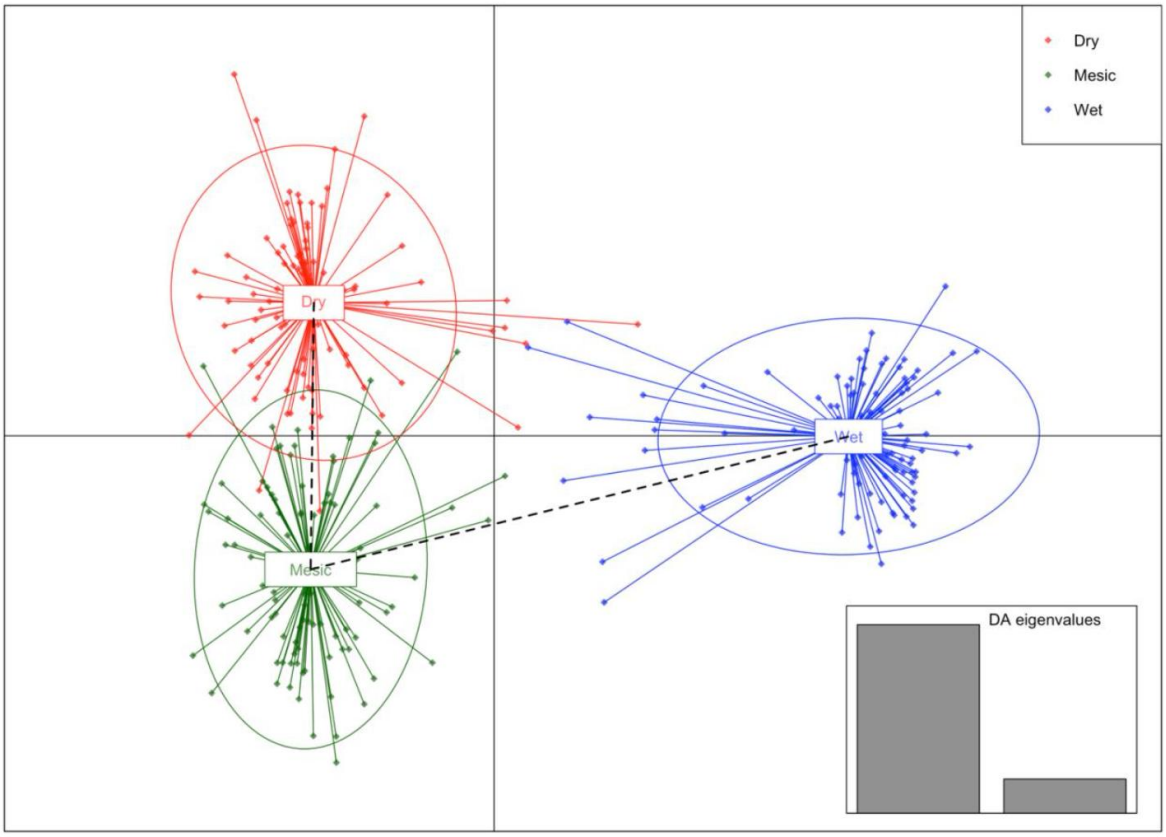

Figure 2.6. Heatmap and volcano plot of differentially expressed genes (adjusted $p < 0.05$) comparing the dry ecotype at the dry site (dry homesite) and the wet ecotype at the wet site (wet homesite).

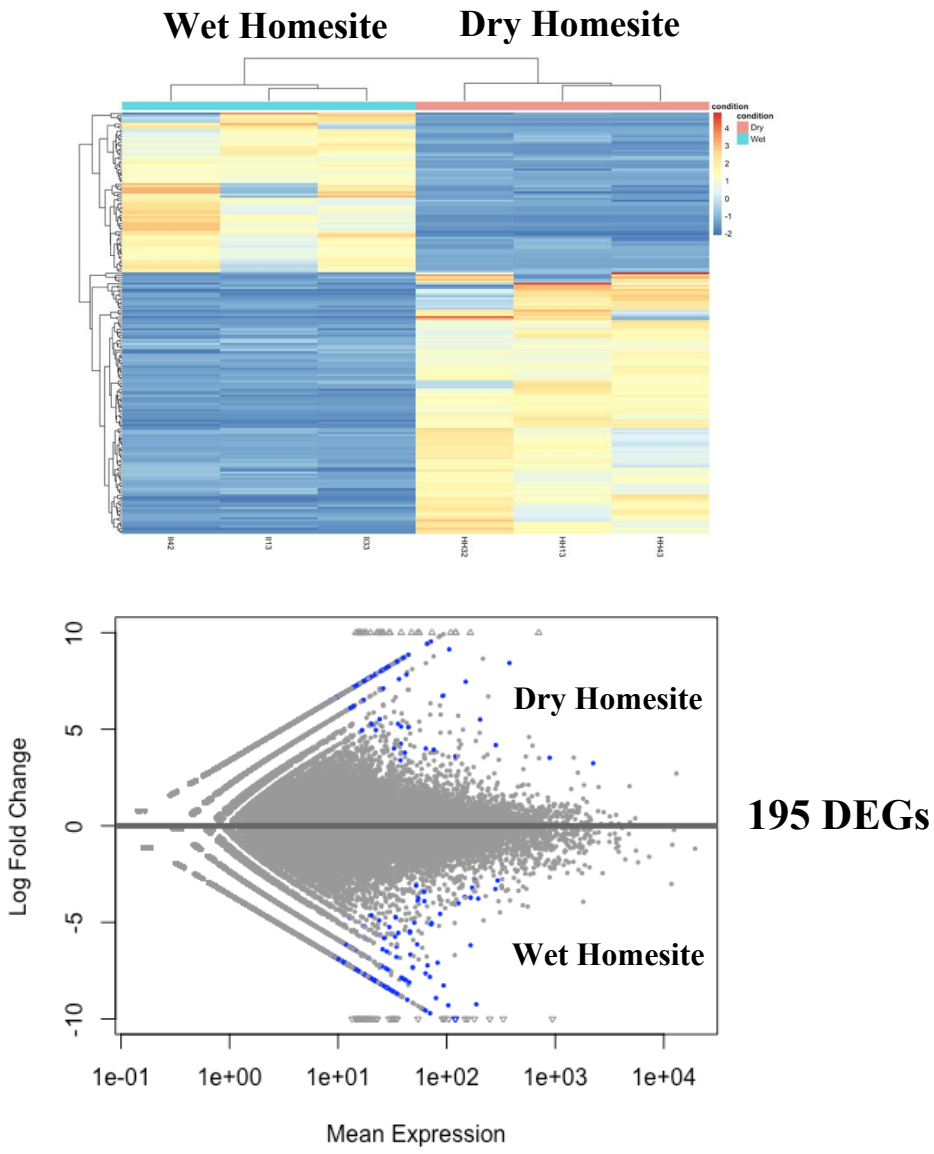

Figure 2.7**.** Vegetative cover of plant functional groups (Left: other grasses, right: forbs) by planting sites (A. Driest, B. Dry, C. Mesic, and D. Wet Sites) in ambient conditions for each ecotype from 2010 to 2022. Red indicates a functional group growing with dry ecotype, green indicates those growing with the mesic ecotype, and blue indicates those growing with the wet ecotype. Solid line indicates the mean and shaded area indicates 95% confidence intervals of the mean of a GAM model. Yellow tick marks on x axis indicate sampling years.

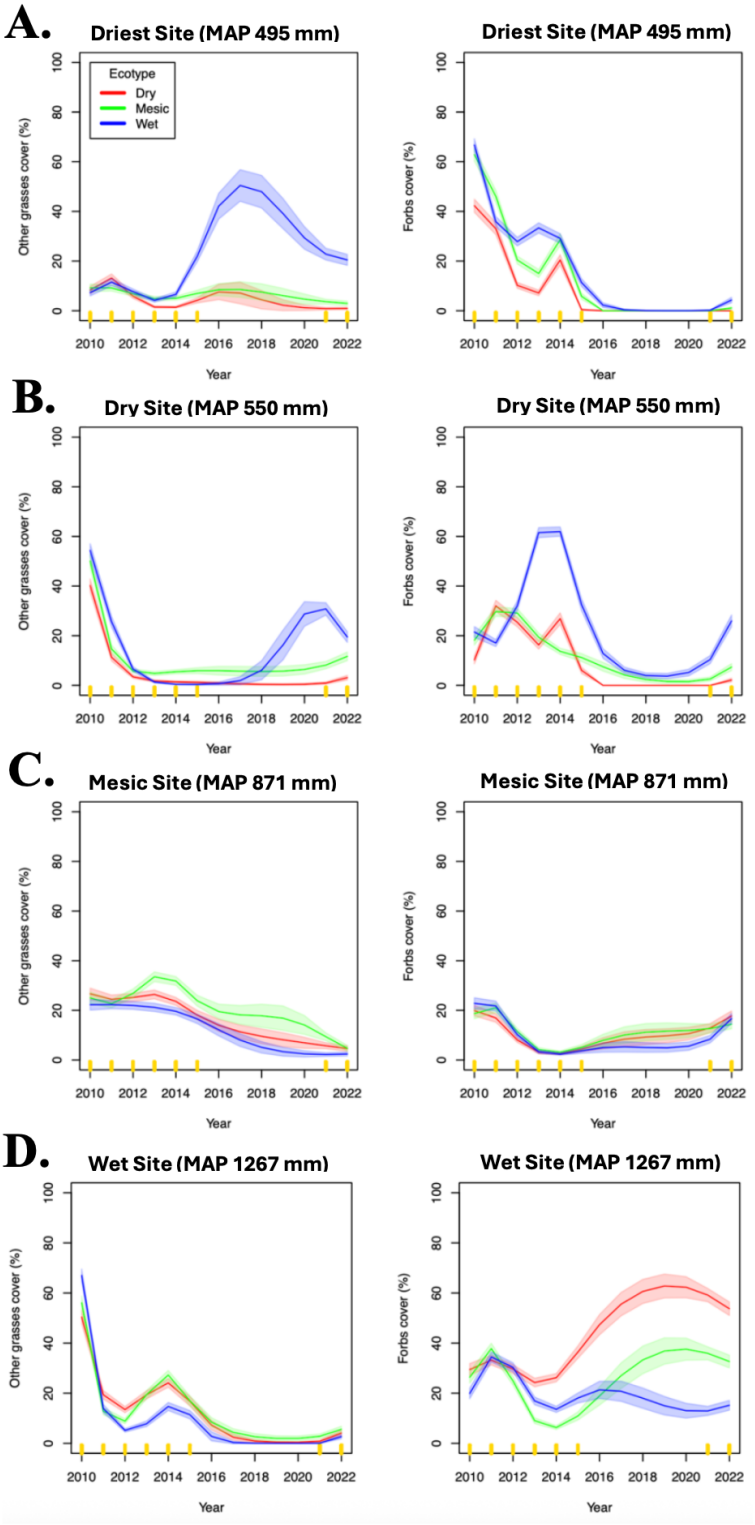

Supplemental Figure 1. Ecotypes of *A. gerardi* demonstrating morphological differences between the wet (left) and dry (right) ecotypes. Photo taken in the Carbondale, Illinois planting site.

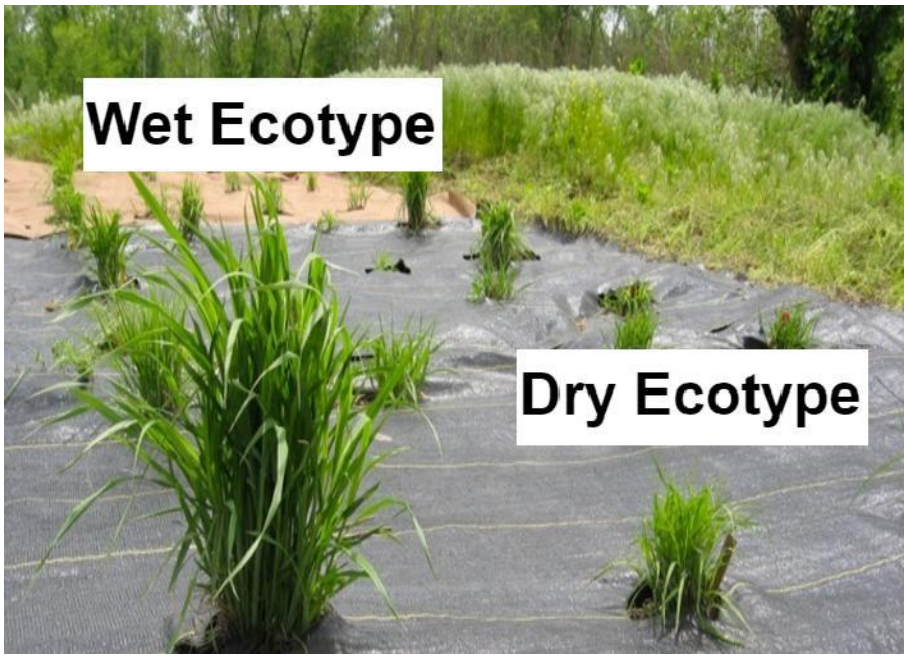

Supplemental Figure 2. Aboveground standing biomass of *A. gerardi* by planting sites (A. Colby, Kansas, B. Hays, Kansas, C. Manhattan Kansas, and D. Carbondale, Illinois) in ambient conditions for each ecotype in 2010 and 2022 across the Great Plains precipitation gradient. Bars indicate the mean (±standard deviation).

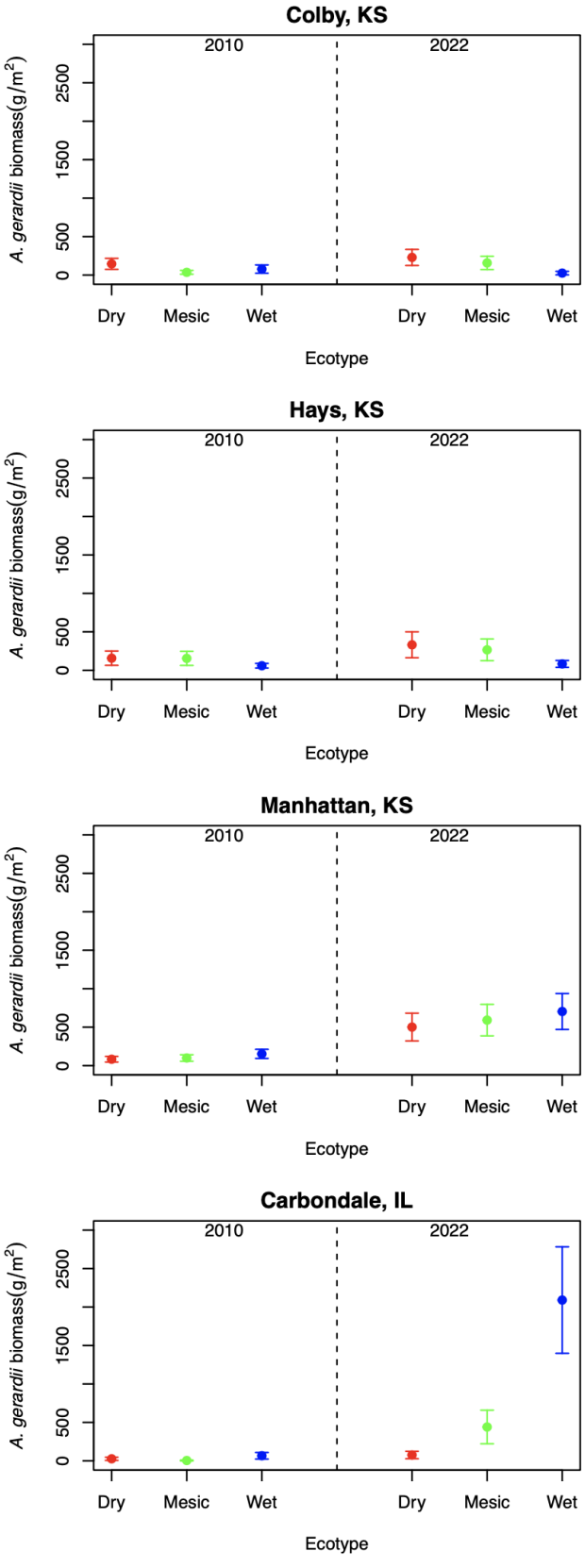

Supplemental Figure 3. Aboveground biomass for each ecotype in the single ecotype plots by planting sites (A. Hays, Kansas, B. Manhattan Kansas, and C. Carbondale, Illinois) in ambient and rainout conditions in 2022 across the Great Plains precipitation gradient. Dots indicate the mean, and the lines are the standard deviation.

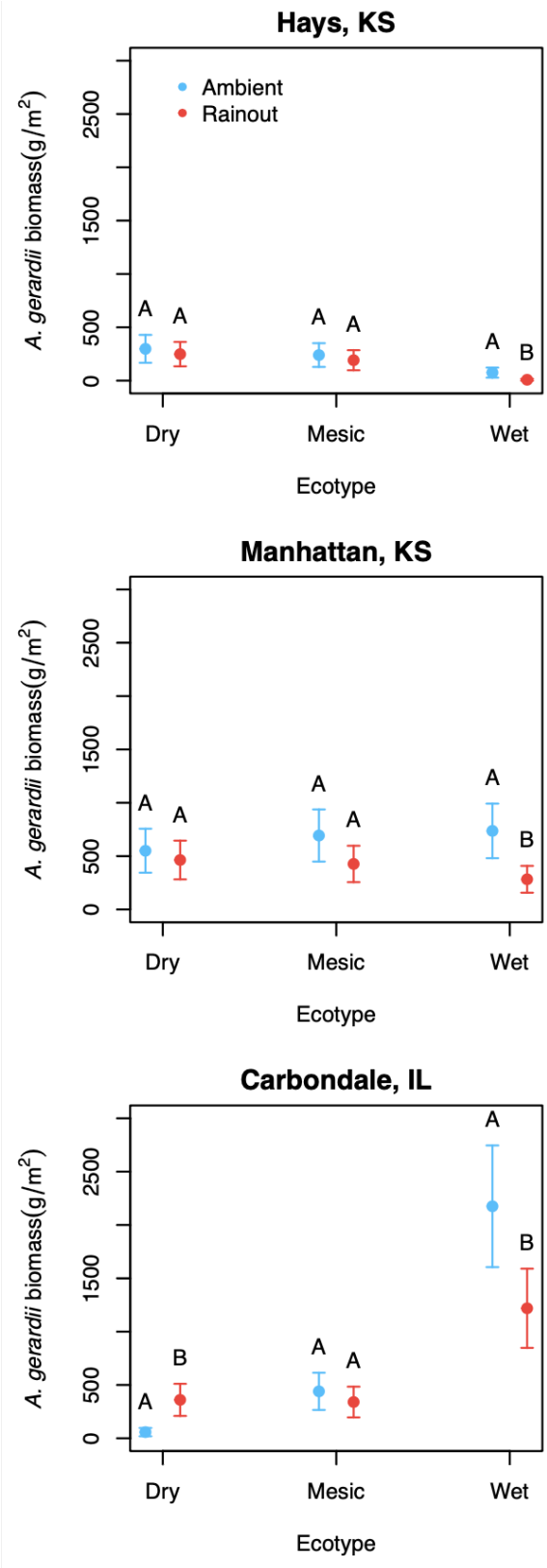

Supplemental Figure 4**.** *Rrivo* plots summarize Gene Ontology (GO) enrichment of differentially expressed genes between wet and dry ecotypes. A. Comparisons at the home sites show distinct functional enrichments, with the dry homesite emphasizing metabolic and stress-response processes and B. the wet homesite emphasizing growth, developmental, and signaling pathways. C. At the driest site (Colby, KS), the dry ecotype shows enrichment in abiotic stress-related processes, while D. the wet ecotype shows enrichment in processes linked to stress regulation and gene expression.

A.

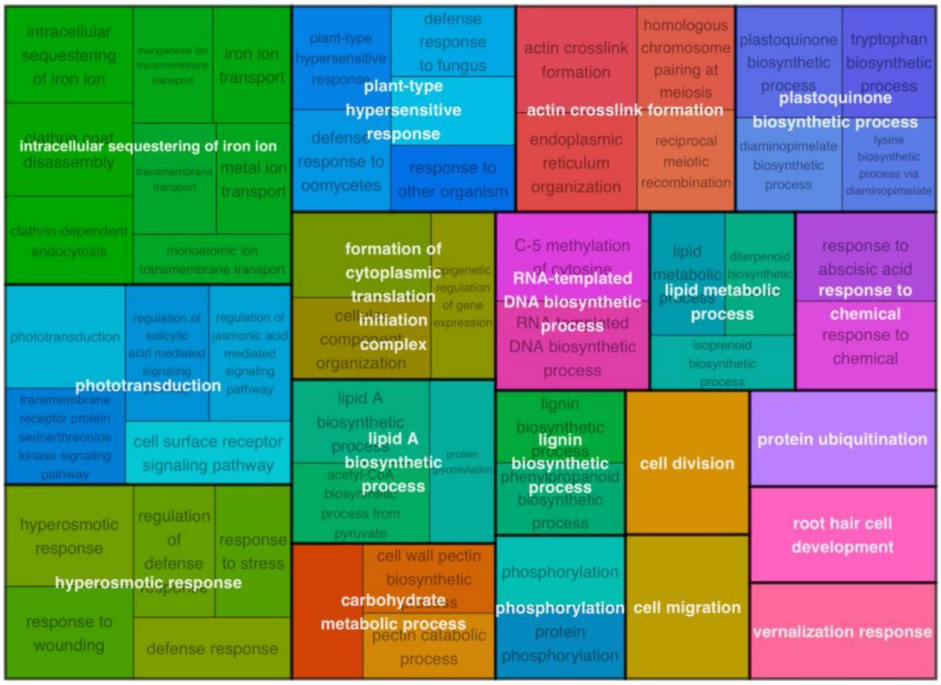

B.

C.

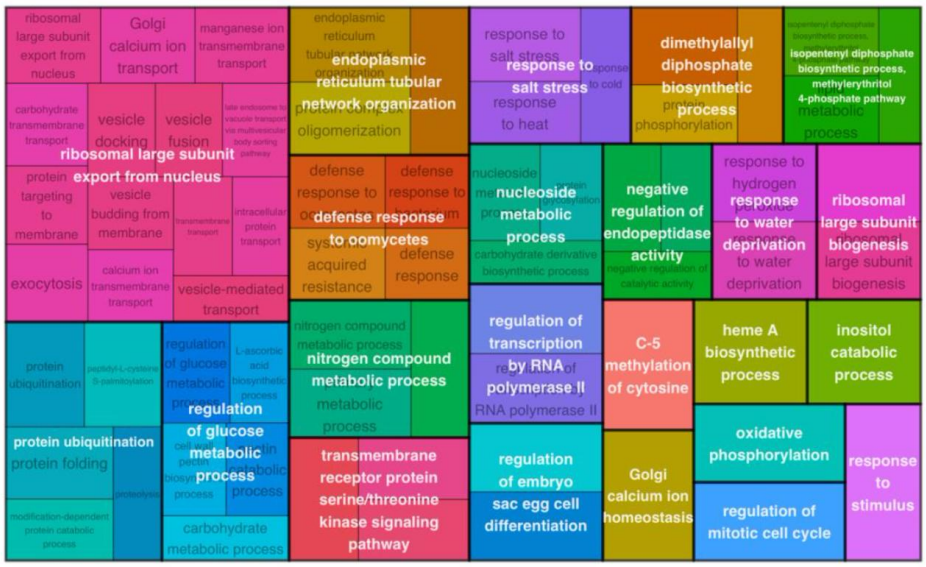
ribosomal large subunit export from nucleus
Golgi calcium ion transport
manganese ion transmembrane transport
endoplasmic reticulum tubular network organization
response to salt stress
dimethylallyl diphosphate biosynthetic process
isopentenyl diphosphate biosynthetic process, methylerythritol 4-phosphate pathway
carbohydrate transmembrane transport
vesicle docking
vesicle fusion
ribosomal large subunit export from nucleus
protein targeting to membrane
vesicle budding from membrane
intracellular protein transport
exocytosis
calcium ion transmembrane transport
vesicle-mediated transport
defense response to oomycetes
defense response
nucleoside metabolic process
negative regulation of endopeptidase activity
response to hydrogen peroxide
response to water deprivation
ribosomal large subunit biogenesis
protein ubiquitination
regulation of glucose metabolic process
nitrogen compound metabolic process
regulation of transcription by RNA polymerase II
C-5 methylation of cytosine
heme A biosynthetic process
inositol catabolic process
protein folding
transmembrane receptor protein serine/threonine kinase signaling pathway
regulation of embryo sac egg cell differentiation
Golgi calcium ion homeostasis
oxidative phosphorylation
response to stimulus
carbohydrate metabolic process
regulation of mitotic cell cycle

D.


xenobiotic transport
protein kinase C-activating G protein-coupled receptor signaling pathway
protein hexamerization
cell differentiation
response to oxidative stress
proteasomal ubiquitin-independent protein catabolic process
glycosaminoglycan metabolic process
peptide catabolic process
maturation of 5.8S rRNA
defense response to nematode
primary metabolic process
regulation of DNA damage checkpoint
plastid transcription
tricarboxylic acid cycle
regulation of transcription by RNA polymerase II
cell redox homeostasis
positive regulation of camalexin biosynthetic process
protein dephosphorylation
UDP-glucose metabolic process
protein deacetylation
[2Fe-2S] cluster assembly
cell wall macromolecule catabolic process
cellular response to amino acid stimulus
positive regulation of protein serine/threonine kinase activity
cell division
methylation
methylglyoxal metabolic process
pigment biosynthetic process
farnesyl diphosphate biosynthetic process, mevalonate pathway
mitotic spindle disassembly
cell population proliferation
cellular process
circadian rhythm
glycerol catabolic process
carbohydrate phosphorylation
SREBP signaling pathway
RNA splicing
positive regulation of cell growth
actin filament severing
NADH oxidation
recognition of pollen
response to calcium ion
mitochondrion morphogenesis
nitrogen compound metabolic process
cytokinin biosynthetic process
apoptotic process
response to stimulus
sporulation

Supplemental Figure 5. Differential gene expression between wet and dry ecotypes**.** Heatmap of differentially expressed genes (adjusted $p < 0.05$) between the wet and dry ecotypes when grown at the driest site of Colby KS, illustrating transcriptional responses under water-limited conditions.

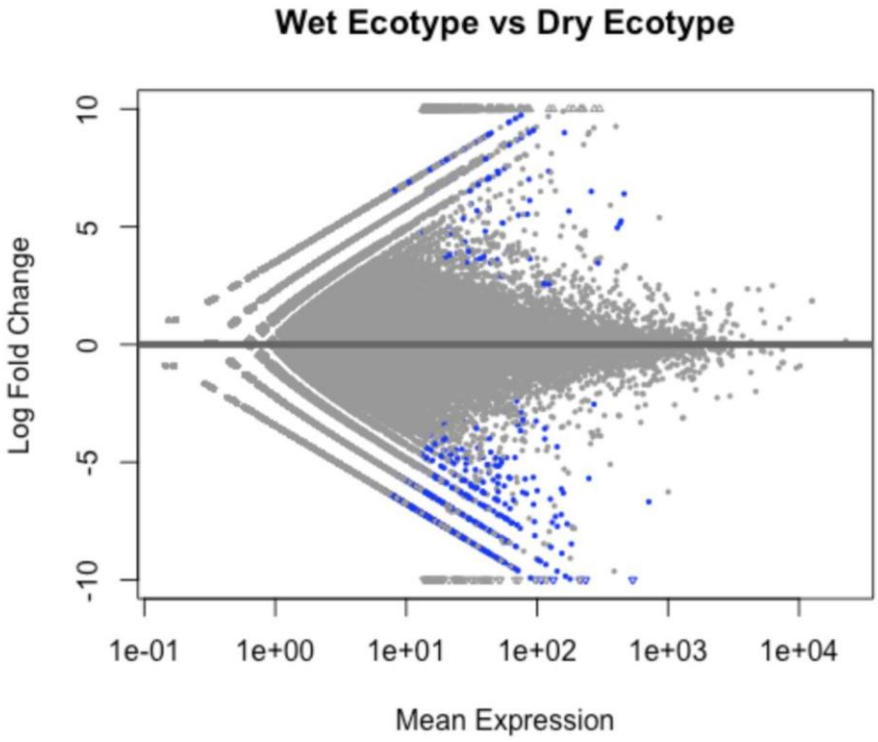

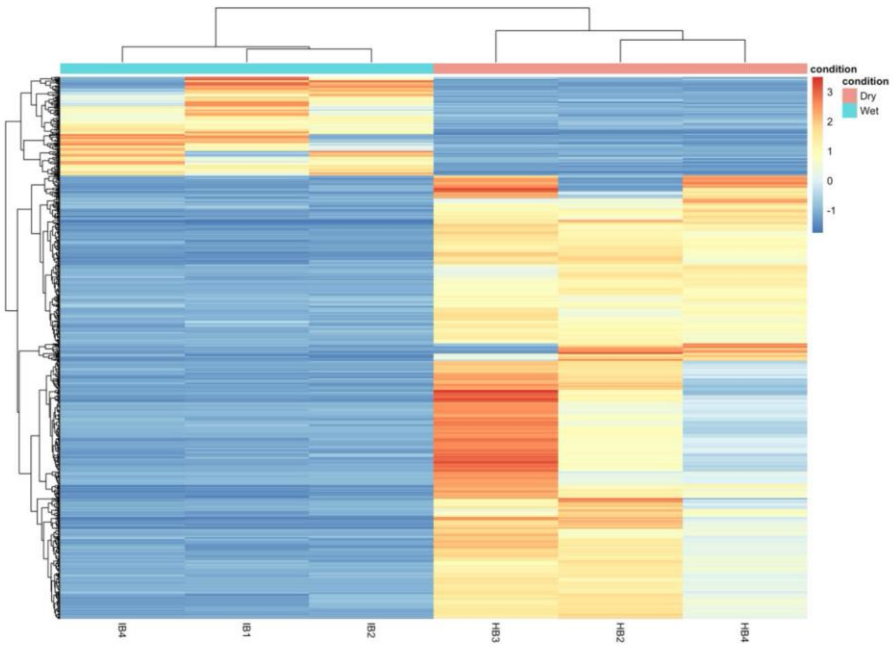

Supplemental Figure 6. A. Soil moisture throughout the growing season of 2022 in ambient and rainout treatments across sites (Western Kansas (Colby, Kansas), Central Kansas (Hays, Kansas), Eastern Kansas (Manhattan, Kansas), and Southern Illinois (Carbondale, Illinois). B. Ground light availability in peak season 2022 in ambient and rainout conditions across sites (Western Kansas (Colby, Kansas), Central Kansas (Hays, Kansas), Eastern Kansas (Manhattan, Kansas), and Southern Illinois (Carbondale, Illinois).

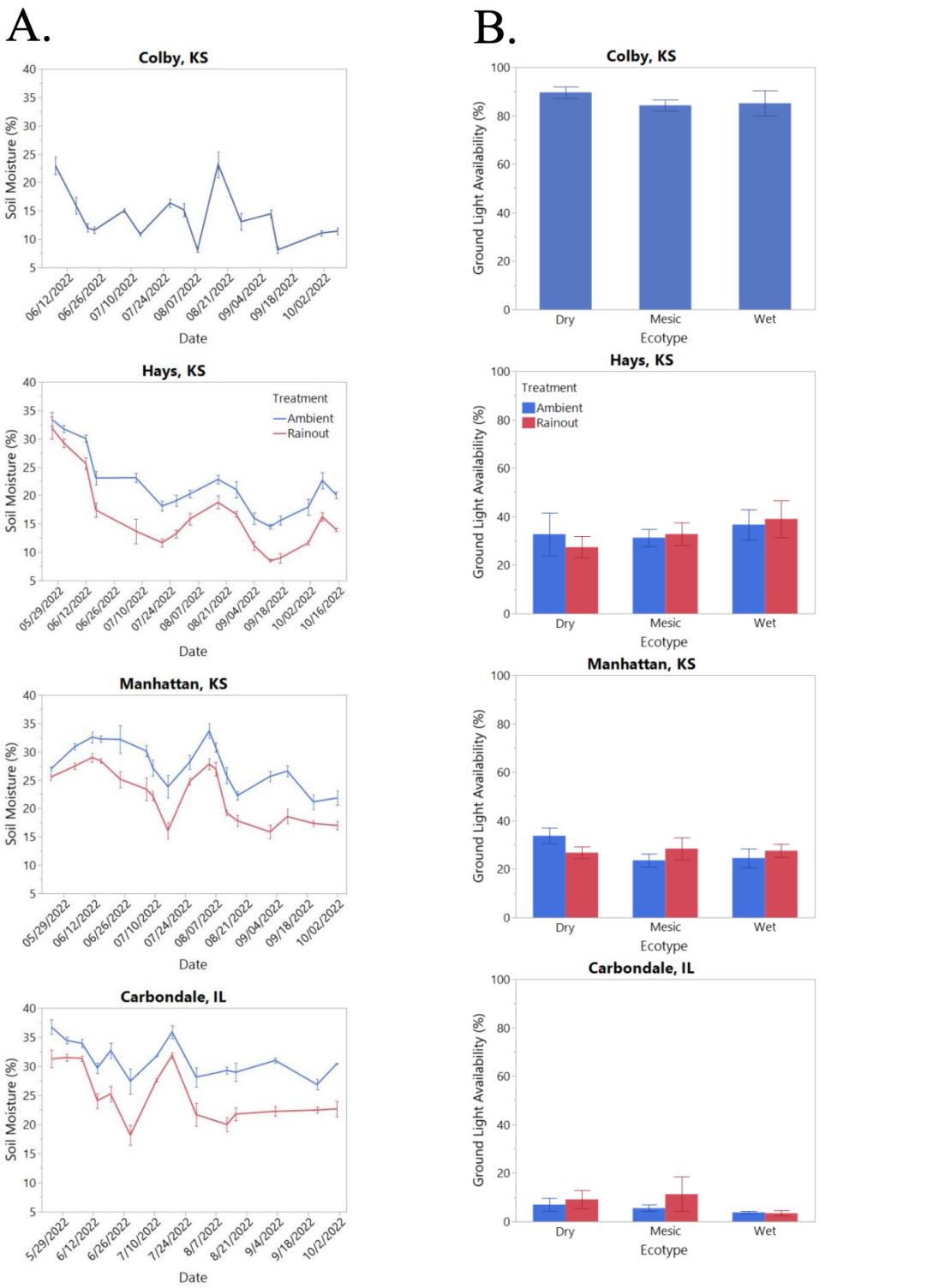

Supplemental Figure 7. Mean annual precipitation over the study period (2010-2022) in western Kansas (Colby, Kansas), central Kansas (Hays, Kansas), eastern Kansas (Manhattan, Kansas), and southern Illinois (Carbondale, Illinois).

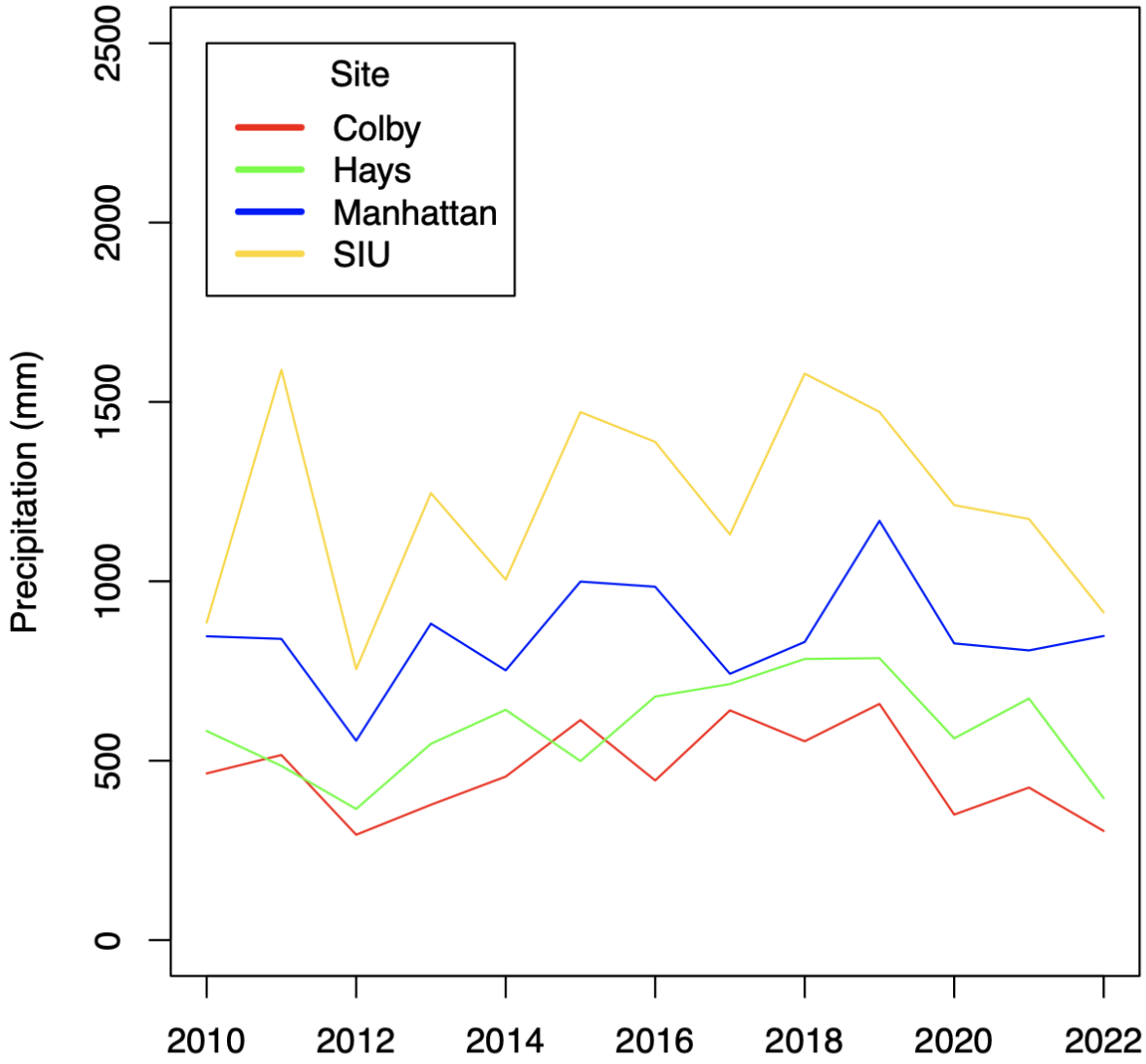

Table 2.1. Seed sources with location, soil type, size, and elevation per plant ecotype. Four populations of each ecotype were collected from each region (dry, mesic, and wet regions).

Ecotype	Prairie	Size (ha)	County, State (USA)	Elevation (m)	Soil Type	Latitude	Longitude
Dry	Webster Reservoir	356	Rooks, KS	606	Wakeeney-Hamey Silt Loam	39.41	99.50
Dry	Saline Experimental Range	880	Ellis, KS	641	Bogue-Armo Clay Loam	38.76	99.14
Dry	Cedar Bluffs Reservoir	850	Trego, KS	688	Armo Clay Loam	38.76	99.83
Dry	Relict Prairie	14	Ellis, KS	640	Armo Gravelly Loam	38.85	99.37
Mesic	Konza Prairie	1557	Riley, KS	366	Benfield Silty Clay Loam	39.08	96.56
Mesic	Tallgrass National Preserve	4409	Chase, KS	392	Irwin Silty Clay Loam	38.25	96.60
Mesic	Carnahan Cove	99	Pottawatomie, KS	389	Benfield Silty Clay Loam	39.34	96.62
Mesic	Top of the World Park	61	Riley, KS	379	Orthents Silty Loam	39.22	96.62
Wet	Desoto Prairie	0.4	Jackson, IL	119	Orthents Silty Loam	37.85	89.14
Wet	Twelve Mile Prairie	28	Effingham, IL	160	Cisne Silty Loam	38.78	88.83
Wet	Walters Prairie	5	Jasper, IL	150	Atlas Silty Clay Loam	38.92	88.19
Wet	Fults Prairie	214	Monroe, IL	215	Menfro Wetty Clay Loam	38.17	90.19

Table 2.2. Historical weather data (30-year normal) for planting site locations with garden site locations relevant information. Annual rainfall and temperature at each garden, average throughout the study period, and historical average.

Reciprocal Garden Site	Elevation (m)	Latitude	Longitude	Mean Annual Temp (C)	Soil Type	Mean Annual Precip (mm)
Colby, KS, USA **Driest Site** KSU Ag Experimental Station (Thomas Co)	972	39.39	101.06	10.9	Ulysses Silt Loam	495
Hays, KS, USA **Dry Site** KSU Ag Experimental Station (Ellis Co)	603	38.85	99.34	12.3	McCook Silt Loam	550
Manhattan, KS, USA **Mesic Site** USDA Plant Material Center (Riley Co)	315	39.19	96.58	12.8	Belvue Silt Loam	871
Carbondale, IL, USA **Wet Site** SIU Ag Research Station (Jackson Co)	127	37.73	89.17	13.5	Story Silt Loam	1267

Table 2.3. List of all planted species in each reciprocal garden site with family, functional group, and seeding rate per species, seeds sown by hand in 2009.

Planted Species	**Family**	**Functional Group**	**Seeding Rate (live seed m^{-2})**
Andropogon gerardi Vitman	Poaceae	C_4 Grass	270
Sorghastrum nutans (L.) Nash	Poaceae	C_4 Grass	70
Elymus canadensis (L.)	Poaceae	C_3 Grass	30
Asclepias tuberosa (L.)	Asclepiadaceae	Forb	30
Chamaecrista fasciculata (Michx.) Greene	Fabaceae	Forb	30
Dalea purpurea Vent.	Fabaceae	Forb	30
Monarda fistulosa (L.)	Lamiaceae	Forb	30
Oligoneuron rigidum (L.) Nutt. es Sims	Asteraceae	Forb	30
Penstemon digitalis Nutt. ex Sims	Scrophulriaceae	Forb	30
Ruellia humilis Nutt.	Acanthaceae	Forb	30
Total Seeds (m^{-2})			**580**

Table 2.4. Candidate genes differentially expressed between wet and dry ecotypes at the driest, dry, and wet sites. Candidate genes are selected based on significant differential expression (padj<0.05), at least 70% sequence similarity to known gene annotations, logFoldChange > 2.0, and functional relevance to plant metabolism, development, or stress response.

Site	Ecotype	Annotation	FoldChange
Homesite	**Wet**	SANT/MYB protein	-4.5593581
Homesite	**Wet**	fasciclin-like arabinogalactan protein 3	-8.38942
Homesite	**Wet**	FTSHI 3, chloroplastic	-7.866185
Homesite	**Wet**	DUF3511 domain protein	-5.0129582
Homesite	**Wet**	Sterol 14-demethylase	-8.91182998
Homesite	**Wet**	pectinesterase inhibitor 45	-6.967393
Homesite	**Wet**	S-type anion channel SLAH2-like	-7.2385787
Homesite	**Wet**	transcription factor bHLH041	-6.7595963
Homesite	**Wet**	protein SAR DEFICIENT 1-like isoform X2	-3.7687974
Homesite	**Wet**	Cinnamoyl-CoA reductase 1	-2.8128343
Homesite	**Wet**	RICESLEEPER 2	-5.8183863
Homesite	**Wet**	Aldo-keto reductase/ oxidoreductase	-6.3425512
Homesite	**Wet**	MutS homolog2	-6.8253362
Homesite	**Wet**	disease resistance protein RPP13-like isoform X3	-7.0901084
Homesite	**Dry**	actin 2	8.85668688
Homesite	**Dry**	PHLOEM PROTEIN 2-LIKE A1	8.70057059
Homesite	**Dry**	ZIPPER1	8.50656289
Homesite	**Dry**	protein RGA1	8.18660133
Homesite	**Dry**	CASP-like protein 1D1	3.601507
Homesite	**Dry**	bundle sheath cell specific protein 1	7.55461811
Homesite	**Dry**	Protein TIFY 10a	3.7863904
Homesite	**Dry**	Solanesyl-diphosphate synthase 2, chloroplastic	5.52201116
Homesite	**Dry**	chloroplast accumulation response 1	6.69501861
Homesite	**Dry**	ABC transporter G family member 34	6.67136964
Homesite	**Dry**	sphingolipid transporter spinster	6.44389195
Homesite	**Dry**	Arabinosyltransferase XEG113	4.01115304
Homesite	**Dry**	gelation factor	6.9751171
Homesite	**Dry**	probable glucose repressible protein Grg1	7.33426661
Homesite	**Dry**	Cytochrome P450 71A26	4.18107892
Dry Site	**Wet**	HARBI1	-8.802745
Dry Site	**Wet**	protein DJ-1 homolog A	-9.346891
Dry Site	**Wet**	plant-specific domain TIGR01589	-5.7961223
Dry Site	**Wet**	GSTU6	-4.0775171
Dry Site	**Wet**	16.9 kDa class I heat shock protein 1	-5.2119373
Dry Site	**Wet**	S-acyltransferase 4	-3.971462

Wet Site	**Dry**	ketol-acid reductoisomerase, chloroplastic	5.2426357
Wet Site	**Dry**	chloroplast accumulation response 1	5.79237287
Wet Site	**Dry**	Remorin family protein	6.4036166
Wet Site	**Dry**	polygalacturonase	6.72045716
Wet Site	**Dry**	Aldo/keto reductase	7.72500371
Wet Site	**Dry**	thioredoxin H-type 5	9.48833385
Wet Site	**Dry**	Pib variant protein	6.93483109
Wet Site	**Dry**	MYB DNA-binding domain superfamily protein	10.1551959
Wet Site	**Dry**	RPP13	7.55575889
Driest Site	**Wet**	transcription factor bHLH139-like	-6.475918
Driest Site	**Wet**	mitogen-activated protein kinase	-8.2794821
Driest Site	**Wet**	EMBRYO SAC DEVELOPMENT ARREST 3	-7.9209306
Driest Site	**Wet**	Histone H2A.4	-4.8276516
Driest Site	**Wet**	polyphenol oxidase	-7.5582844
Driest Site	**Wet**	cyclophilin 1 long isoform	-7.9591091
Driest Site	**Wet**	elongation factor-1a	-7.6224908
Driest Site	**Wet**	glucosamine-phosphate N-acetyltransferase	-9.1080052
Driest Site	**Wet**	heat shock protein 90	-9.2771298
Driest Site	**Wet**	protein FAR1-RELATED SEQUENCE 6	-6.7590848
Driest Site	**Wet**	HSP30 heat shock protein Yro1p	-6.6748077
Driest Site	**Wet**	EMBRYONIC FLOWER 2	-6.7297479
Driest Site	**Wet**	cytochrome c peroxidase	-7.4043611
Driest Site	**Wet**	catalase-peroxidase	-6.9098461
Driest Site	**Wet**	GMC oxidoreductase	-7.0977046
Driest Site	**Wet**	DETOXIFICATION 44	-6.769949
Driest Site	**Wet**	Rp1-like protein	-7.154188
Driest Site	**Wet**	translation initiation factor eIF-5A	-6.7282403
Driest Site	**Wet**	fatty acid hydroxylase superfamily protein	-7.2372462
Driest Site	**Wet**	fad dependent oxidoreductase	-7.7878634
Driest Site	**Wet**	glucose-repressible protein Grg1	-10.35467
Driest Site	**Wet**	general substrate transporter	-9.1378997
Driest Site	**Wet**	putative fggy-family carbohydrate kinase	-8.7443103
Driest Site	**Dry**	pectinesterase	8.46765816
Driest Site	**Dry**	tic20-like protein	7.16094026
Driest Site	**Dry**	Bowman-Birk type trypsin inhibitor	9.088026
Driest Site	**Dry**	Photosystem I subunit O	9.73907089
Driest Site	**Dry**	23.2 kDa heat shock protein-like	5.49344593
Driest Site	**Dry**	putative r40c1 protein	2.59004126
Driest Site	**Dry**	L-ascorbate oxidase homolog	3.79540458
Driest Site	**Dry**	Nuclear transcription factor Y subunit A-8	7.08162346

Driest Site	**Dry**	seed maturation protein PM41	5.69381291
Driest Site	**Dry**	1-hydroxy-2-methyl-2-(butenyl 4 reductase	7.26661229
Driest Site	**Dry**	ABC transporter G family member 34	5.33576163
Driest Site	**Dry**	18-cineole synthase 1 chloroplastic	5.61490211
Driest Site	**Dry**	late embryogenesis abundant protein 3	7.01557646
Driest Site	**Dry**	germinated spore protein 1	6.88667454
Driest Site	**Dry**	lipid binding protein	4.68542821
Driest Site	**Dry**	threonine-protein kinase NAK	6.87928856
Driest Site	**Dry**	polygalacturonase	6.1201309

Methods S1: Statistical Analysis

We used generalized additive models (Wood, 2017) to assess each of our hypotheses. Briefly, generalized additive models are like other well-known regression-type modeling techniques such as linear models (i.e., regression and ANOVA), mixed models, and generalized linear models. The difference is that with GAMs, the effect of time, space, or other continuous variables of interest can be modeled with a so-called "smooth" effect which, in general, estimates a "curve" under limited assumptions (Wood, 2017; Hefley et al., 2017). The feature of GAMs is important for our study because the relationship between response variables like canopy cover and predictor variables like time (year) are generally unknown. For example, prior to our long-term study, it was generally unknown how canopy cover would change for a given ecotype over the thirteen years of our study. The use of GAMs enables us to use a well-developed statistical framework to learn these types of relationships through the estimation of a "curve" or "function" while imposing minimal assumptions on the functional form of such relationships. In addition, GAMs can include simple linear and categorical predictors, random effects, and non-normal response variables. We used GAMs to analyze cover and biomass data, rainout effects, and effects of ecotypes on surrounding community functional groups.

That said, this flexibility GAMs provide does come at a cost. Two limitations that are important to our study include: 1) summarizing the output of GAMs in an interpretable manner; 2) limitations on predictions. Related to the first limitation, statistical models like standard regression impose more restrictive assumptions than GAMS. For example, a standard linear regression model would impose the assumption that canopy cover monotonically increases or decreases at a constant rate over the thirteen-year period of our study. This assumption is convenient because it enables us to have simple interpretable statistics to summarize the

relationship—the slope parameter. GAMs on the other hand are flexible curves and may require bespoke statistical summaries to aid in interpretation. In our study, this includes summaries like the average value of the curve over specific time periods or time points. Related to the second limitation, GAMs, like any statistical model, warrant caution when making predictions. For example, during the period 2016-2020 we did not measure canopy cover. Therefore, we used the GAMs to predict what the % canopy cover from 2016 to 2020. In general, GAMs will appropriately inflate uncertainty measures (e.g., wider confidence intervals) for such prediction. In contrast, point estimates (e.g., the estimated "curve") should be interpreted with caution and only in conjunction with the inflated uncertainty measures.

Chapter 3 - Taking Genomics Outdoors: Linking local adaptation, trait variation, and gene expression in grass ecotypes across a rainfall gradient

Running Head: Linking traits and genomics over rainfall gradient

Authors: Jack Sytsma[1], Matthew Galliart[2], Kian Fogarty[1], Kori Howe[1], Bradley J. S. C. Olson[1], Sara G. Baer[3], David J. Gibson[4], Brian Maricle[5], Eli Hartung[1], and Loretta Johnson[1]

Addresses: [1]Department of Biology, Kansas State University; [2]Department of Biological Sciences, Fort Hays State University; [3]Kansas Biological Survey & Center for Ecological Research and Department of Ecology and Evolutionary Biology, University of Kansas; [4]School of Biological Sciences, Southern Illinois University Carbondale; [5]Department of Biology, Saginaw Valley State University, University Center, Michigan, USA

Key Words: Co-expression Networks, Drought, Functional Trait, Grasslands, Transcriptomics, RNAseq

Abstract

With increasing droughts, understanding local adaptation and drought tolerance in ecologically dominant species is crucial for enhancing ecosystem resilience. We leveraged a long-term reciprocal garden to assess local adaptation and drought responses in *Andropogon gerardi*, a foundation species in the US Great Plains. Our objectives were to identify adaptive traits, explore gene expression responses across a rainfall gradient and under experimental drought and integrate trait-based analyses with gene expression profiles to test for local adaptation. Reciprocal gardens, established a decade ago, are composed of different *A. gerardi* ecotypes sourced along a rainfall gradient (MAP 480–1167mm yr^{-1}) and sown as ecological communities in post-agricultural fields. Rainout shelters imposed experimental drought. We hypothesized that ecotypes should perform best in their homesite, reflecting local adaptation. The dry ecotype should perform best under rainouts and exhibit traits and expression profiles favoring drought tolerance; the wet ecotype should favor traits and gene expression enhancing growth and resource acquisition. We found ecotypes had highest biomass and cover in their homesite, confirming local adaptation. Under experimental drought, the dry ecotype demonstrated improved performance at the wet site, confirming its adaptive value under water limitation. The dry ecotype showed stress-tolerance strategies (shorter, more water-efficient, upregulated drought-response genes), while the wet ecotype emphasized growth strategies (taller, higher biomass, upregulation of growth hormone gibberellin). Using co-expression networks, gene clusters linked adaptive traits, revealing genetic mechanisms of adaptation. Results advance our understanding of adaptation by linking gene expression and trait variation to drought responses in locally-adapted ecotypes, informing ecotype climate-matching under drought.

Introduction

Increasing frequency of drought has motivated research on how changes in rainfall affect the functioning of grasslands (Cook et al., 2015; Li et al., 2018; Griffin-Nolan et al., 2021). Drought is considered one of the most severe of environmental stresses to plants (Seleiman et al., 2021), therefore understanding plant tolerance to water limitation is particularly important (Smith et al., 2024). Furthermore, grasslands are sensitive to drought (Cherwin & Knapp, 2012; Knapp et al., 2015) and the impact of drought on grassland productivity has been underestimated (Smith et al., 2024). This sensitivity highlights the importance of understanding local adaptation as a mechanism of drought tolerance in grassland species, especially dominant grasses. Dominant grass species may play a crucial role in maintaining productivity (Zhang et al., 2025a) and ecosystem resilience in the face of changing rainfall (Van der Meer & Jansen, 2019).

Despite the well-documented importance of drought in grasslands (Cherwin & Knapp, 2012; Craine et al., 2013; Knapp et al., 2015), predictions of grassland functioning under drought are not well characterized in the context of the potential for species to adapt. This is despite the fact that intraspecific variation plays a key role in climate response by providing the raw material for adaptation (Westerband et al., 2021). Understanding local adaptation—where populations exhibit peak fitness in their home environments (Savolainen et al., 2007)—is essential to predict how plants respond to environmental variation and climate stressors (Savolainen et al., 2013). Significant progress has been made by separately studying local adaptation in ecology (Leimu & Fischer, 2008; Wadgymar et al., 2022) and genomics (Savolainen et al., 2007; Kang et al., 2023) Yet, a critical gap remains in bringing genomics into ecological field experiments (Ungerer et al. 2008, Johnson et al. 2022, Sytsma et al., accepted). Bridging this gap is essential for understanding how genetic variation drives responses to environmental stressors under realistic,

complex field conditions. By combining trait-based analyses with modern genomic approaches, we can both characterize phenotypic variation (Fortunato & Pires, 2020) and uncover gene expression profiles associated with ecotypic drought response (Pardo et al., 2020).

Several studies have identified drought-responsive genes in plants, especially in the model plant *Arabidopsis thaliana* (Lovell et al., 2015; Kang et al., 2023). However, knowledge of gene expression in wild plants is limited, particularly in long-lived perennial C_4 grasses that endure long periods of drought (Weaver, 1968). Research on some grasses such as *Panicum* spp. (Lovell et al., 2016; Heckman et al., 2025) and *Brachypodium* spp. (Song et al., 2019; Decena et al., 2021) shows that substantial intraspecific variation in drought-responsive genes exists within species. Uncovering such intraspecific variation in stress response under field conditions is crucial for identifying traits that enhance drought resilience and inform restoration strategies to guide selection of climate-resilient seed sources (Torok et al., 2024). Many ecological genomic studies are conducted using single-species trials and most are short-term (Johnson et al. 2022, Sytsma et al., accepted). By contrast, our research platform, set in ecological communities, extends for over a decade, thus encompassing interannual rainfall variation.

We focus on local adaptation in big bluestem (*Andropogon gerardi* Vitman), a dominant C_4 perennial grass that contributes up to 70% of aboveground biomass in tallgrass prairies (Knapp et al., 1998) and can disproportionately shape community and ecosystem structure (Mendola et al., 2015; Ren et al., 2023). This species spans a steep rainfall gradient across the U.S. Great Plains (mean annual precipitation MAP 480–1167 mm yr^{-1}) putatively resulting in dry, mesic, and wet ecotypes (Gray et al., 2014; Johnson et al., 2015; Galliart et al., 2019, 2020). While *A. gerardi*'s responses to rainfall are well studied (Fay et al., 2003; Slette et al., 2023), its drought tolerance at the transcriptomic level remains poorly understood. To address this, we used

an existing reciprocal garden experiment, established in 2009 across the rainfall gradient, with ecotypes cross-transplanted planted in prairies and part of the plots subjected to ~50% rainfall reduction via rainout shelters (Johnson et al., 2015, 2022). This design enables testing for local adaptation under realistic ecological conditions. Measurements taken ten years post-establishment reflect long-term successional dynamics critical for evaluating adaptation in long-lived grassland perennials (Ren et al., 2023, 2024; Gibson et al., 2024).

The overall goal of this study was to assess local adaptation in *A. gerardi* ecotypes combining both trait-based and genomic analyses. To achieve this, the first objective was to evaluate phenotypic evidence for local adaptation using trait-based analyses to test whether phenotypic differentiation among ecotypes corresponds to environmental gradients and aligns with adaptive strategies under drought. We hypothesized that local ecotypes would perform best in their home environments, with reduced performance when transplanted to non-native sites, consistent with local adaptation. We expected the dry ecotype to exhibit a drought-tolerant strategy such as shorter stature and higher water-use efficiency (Grime, 1988; Jardine et al., 2021), while the wet ecotype would show traits related to growth and resource acquisition, including greater height and higher biomass (Grime, 1988; Moles et al., 2009; Jardine et al., 2021). Experimental drought was predicted to reduce biomass, photosynthetic rates, and delay flowering across all ecotypes, with the dry ecotype being least impacted.

Our second objective was to investigate transcriptomic signatures of local adaptation and their alignment with ecotypic strategies across the natural rainfall gradient and under experimental drought. Specifically, we aimed to test how gene expression differs and whether gene expression patterns reflect the functional adaptive strategies of each ecotype. We hypothesized that the dry ecotype would upregulate drought-response genes (e.g., DREB; Zhang

et al., 2025b), while the wet ecotype would upregulate genes related to growth (e.g., gibberellin response; Shah et al., 2023) and resource acquisition. Additionally, we expected that rainout treatments would induce stress-related genes, including heat shock proteins (Rahman et al., 2022) and ABA-regulated genes involved in stomatal control (Aimar et al., 2014).

Our final objective was to uncover genomic basis of local adaptation by integrating both phenotypic and transcriptomic data. We used co-expression network analysis (Aoki et al., 2007; Serin et al., 2016) and hypothesized that specific gene modules would correlate with physiological traits. For example, we predicted that genes involved in ABA signaling would be co-expressed with stomatal conductance. Similarly, we expected that genes associated with growth, such as the growth hormone gibberellin (Shah et al., 2023), would be co-expressed with plant height.

This study is among the first to link local adaptation, trait variation, drought response, and gene expression profiles in realistic and long-term ecological communities across a broad rainfall gradient, offering a rare window into the role of local adaptation to rainfall. By combining trait-based analyses with genomic characterization, we identify genetic and physiological adaptations that enable dry-adapted ecotypes to thrive under water limitation. Our findings will offer critical guidance for matching seed sources to future climate conditions (Doherty et al., 2017), informing restorations that prioritize climate-adapted ecotypes to improve long-term ecosystem function under increasing drought frequency and intensity (Baer et al., 2019).

Materials and Methods

Focal Species

Andropogon gerardi is distributed across most of eastern North America (USDA Plants Database, 2022) spanning broad rainfall gradients and dominates in the center of the range (~450-1250mm yr^{-1}). In addition to its dominance as part of the tallgrass prairie, it is also an important forage for cattle, accounting for $8 billion USD of the US rangeland's economy (USDA NASS, 2023). Furthermore, *A. gerardi* is widely used in grassland plantings through the USDA's Conservation Reserve Program, which has converted over 3.2 million ha of cropland to grassland (CRP, 2023).

We used the newly annotated genome of *A. gerardi* (*Andropogon gerardi* Hap2 v1.1; Joint Genomics Institute, 2023) that enables gene expression analysis. With a 2.5B bp scaffold and 88,437 protein-coding genes, it offers a valuable resource for studying genomic molecular mechanisms of drought adaptation, crucial for restoration efforts and its role as forage in future droughts. Being evolutionarily closely related to the well-studied crop plants *Zea mays* and *Sorghum bicolor* (Swaminathan et al., 2010), this relationship allows us to take advantage of knowledge of their genomes and annotations.

Reciprocal Garden Establishment Along the Natural Rainfall Gradient

We utilized a long-standing reciprocal garden platform of seeded ecological communities established over a decade ago. Full details on plot establishment can be found in Johnson et al. (2015; 2022). Briefly, in 2008, seeds of *A. gerardi* were collected from four populations (native prairies) in each of three distinct regions along a precipitation gradient (Figure 3.1a; Table 3.1), which at the time defined regional putative climate ecotypes. Reciprocal transplant gardens were established in 2009 with each ecotype sown into plots in Colby, KS, Hays, KS, Manhattan, KS, and Carbondale, IL, USA (driest to wet sites, MAP 480-1167mm yr^{-1}, Figure 3.1a). All plots were also sown with the same mix of nine native subordinate species representing multiple

functional groups to assemble a community and simulate a restoration (Table 3.1; Johnson et al., 2015). Colby KS had no local ecotype and was included to test ecotypic threshold to drier conditions as might be experienced in the future. Ecotypes were assigned to plots in each site according to a completely randomized block design where each block consisted of three 4 m x 4 m plots each sown with one of three ecotypes (Figure 3.1b). Plots were not weeded and volunteers from the regional species pool also established in the plots. The community aspects of the reciprocal garden platform are described elsewhere (Ren et al., 2023; 2024; Gibson et al., 2024).

To test for the specific role of rainfall in local adaptation, experimental rainouts on all ecotypes were established in 2011 in three of the sites (Hays, KS, USA, dry site-MAP 546 mm yr^{-1}, mesic site-Manhattan, KS, USA, MAP 891 mm yr^{-1}, and wet site-Carbondale, IL, USA, MAP 1256 mm yr^{-1}, Figure 3.1b). Rainouts were not established in Colby KS, the driest site, because precipitation is already low there. Rainouts were designed to reduce ~50% of ambient rainfall over half of each plot by using the design of Yahdjian and Sala (2002) and 2 m x 2 m roofs were installed in mid-June and taken down after the growing season each year. Rainfall runs into gutters and is then collected in rain barrels and disposed of away from the plots. At the wet site, using tubing connected to the gutter, excess water is drained away from the plots.

To assess soil moisture, we used METER volumetric soil moisture probes at 20cm depth (ECH20 Onset S-SMD-M005 Large Volume Soil Moisture Sensor; Meter Group, Pullman, WA, USA). Probes were installed in one block per site (n=4 per site) all three sites, including under rainouts. For Colby that did not have rainouts, we measured moisture in each block (total 28 probes). We took readings approximately once a week per block in ambient and rainout

conditions at each site. Rainouts reduced soil moisture by ~10-15% compared to ambient (Figure S1).

Objective 1: Testing for Local Adaptation

Response Variables: Cover and Biomass

To assess local adaptation, we measured vegetative cover and aboveground biomass in 2021 and 2022 during peak season (late July to early August), over a decade after the establishment of the plots. Canopy cover served as a proxy for abundance, predicting success in long-lived perennials (Damgaard, 2015). For cover, we used 1m² quadrats with 81 intersections per plot and recorded *A. gerardi*, other grasses, forbs, or bare ground at each intersection. We also harvested aboveground biomass by clipping from 50 cm x 20 cm quadrats at the end of each growing season. For both cover and biomass, we used four non-overlapping quadrats per plot, for each of the three ecotypes in the four blocks at all four sites, including cover under rainouts (336 quadrats annually for cover and biomass).

Response Variables: Trait Measurements on Individual Plants

Early in the 2022 growing season, five individual *A. gerardi* plants were randomly selected from each plot and rainout treatment at each site and marked with flags. The driest site (Colby, KS, USA) did not have rainouts, so five plants were selected per each plot. We measured morphological, physiological, and reproductive traits on 420 individual plants in early, peak, and late (June, July, August) growing seasons. For brevity, here we include peak season measurements with early and late season results included as supplemental data, since the patterns are qualitatively similar.

Physiological Traits: To evaluate leaf physiological traits and gas exchange, we employed several techniques. We measured leaf chlorophyll absorbance with a SPAD-502 chlorophyll meter (Konica Minolta, Japan) of an average of at least three mature leaves. We used a LI6400-XT IRGA system (Li-Cor Biosciences, Inc., Lincoln, NE, USA) to assess gas exchange on sunny days between 10:00-14:00h. We measured photosynthesis, stomatal conductance, transpiration, water use efficiency (WUE, photosynthetic rate/ transpiration rate), and internal carbon dioxide. Gas exchange was measured on a fully expanded leaf with CO_2 levels at 400ppm, humidity and temperature at ambient levels, and photosynthetically active radiation at 1500 μmol photons $m^{-2}s^{-1}$. Measurements were made when rates had stabilized with a coefficient of variation <1 for one minute.

Morphological Traits: To assess key plant traits and growth metrics, we employed several methods for measuring plant morphology and biomass. First, we determined height by extending leaves vertically from the ground to the tip of photosynthetic tissue. We measured plant diameter as an average of two orthogonal measurements of entire plant width. We assessed leaf width as an average of three mature leaves at their broadest section. We measured thickness of three mature leaves using a hand caliper (Mitutoyo Corp. Kawasaki Japan), excluding the midvein, and averaged these values per plant. In peak season (Julian days 177-192), we collected vegetative tissue from each plant at the midsection of 3-5 mature leaves to determine %C and %N. We harvested aboveground biomass in late fall by cutting individual plants at soil level, drying at 60ºC, and weighing.

Reproductive Phenology: To track the phenological development of each plant, we assessed the date of bolting, defined as a clear presence of a flowering stalk, and the date of

flowering, defined as the first presence of anthers. Plants were monitored throughout the season every 1-2 weeks until all flowered or until the date of first frost at each site.

Statistical Analysis: Cover, Biomass, and Functional Traits

To assess plot-level cover, biomass, and functional traits, we used a standard least squares regression model with a split-plot design in JMP Pro17 statistical software (SAS Institute Inc., Cary, NC, 2023). The main plot factors were site and ecotype, while the subplot factor was treatment (ambient or rainout), with all two-way and three-way interactions included in the model. For both cover/biomass and traits, site, ecotype, and rainout treatment (ambient or rainout) were fixed factors, and block number and quadrat/plant repetitions were treated as random effects. Separate models were constructed for early, peak, and late season data, as well as a repeated measures model to assess changes over time. When normality assumptions were violated, response variables were transformed using log transformations to improve the distribution of residuals. ANOVA and Tukey's HSD tests were used to assess significance ($p<0.05$).

Ordination Analysis. We used a principal components analysis (PCA) to explore correlations of traits across ecotypes, sites, and rainout treatment. For different principal components analysis (PCA) were conducted separately under ambient conditions by ecotype, site, homesite, or treatment (ambient or rainout). All trait data were log-transformed to normalize distributions before they were used in correlation analysis and used a 95% confidence interval to show statistical significance.

Objective 2: Differential Gene Expression

Sample Collection and Extraction. Due to the strong phenotypic differences between

ecotype and site extremes (dry and wet ecotypes, the driest, dry, and wet sites), we used these for gene expression analysis. We also analyzed gene expression profiles in ambient and rainout treatments. We collected 2-3 mature leaves from one plant of wet and dry ecotypes per block (n=40) at the same plants for which phenotypes were collected on the same day as traits from peak-season, allowing linkage between traits and gene expression. The leaves were flash frozen on dry ice in the field and transferred to -80ºC freezer at the laboratory**.** Detailed methods on RNA extraction, sequencing, and analysis are found in Methods S1.

Differential Gene Expression and Identification of GO Terms. To identify differentially expressed genes (DEGs), we used DESeq2v3.112 (Love et al., 2014) on all pairwise comparisons using an adjusted probability (padj)<0.05. We categorized DEGs according to pattern of expression and up- or down-regulation over three comparisons (ecotype, site, rainout treatment). We identified genes using BLASTx (Camacho et al., 2009) to the *Zea mays* ensemble 58 and *Sorghum bicolor* rNCBlv3 reference genomes on the NCBI database at an *E*-value cut-off of 1×10^{-6} and selecting the top 20 hits.

Differentially expressed genes (|logFC| > 1, FDR-adjusted p-value) were visualized in a volcano plot (-log10 p-value vs. log fold-change) using the VolcanoPlot tool in Galaxy (https://usegalaxy.org/). The plots include only genes meeting the significance threshold (padj < 0.05; |logFC| > 1), highlighting those that are significantly upregulated or downregulated under different conditions. We visualized significant DEGs using a heatmap and clustered using "pheatmap" (Kolde et al., 2019) using R v1.0.12. Genes were hierarchically clustered by expression pattern using Pearson's correlation, and red indicates upregulation while blue indicates downregulation.

We implemented Blast2GO 5.25 (Conesa & Gotz, 2008) to determine gene ontologies

(GO terms), GO term enrichment, and annotations using 5% FDR cutoff. The complete lists were further filtered to focus on the GO terms that were within the top 10% of most significantly enriched within the original 5% FDR.

Objective 3: Linking Phenotype to Gene Expression

Weighted Gene Co-expression Network Analysis (WGCNA). We used co-expression networks using the WGCNA R package (Langfelder & Horvath, 2008) to identify significantly co-regulated gene cluster modules with phenotypic traits. Following module identification steps, we explored the correlation between module expression, ecotype (wet or dry), site (driest, dry, or wet), treatment (ambient or rainout), all two-way and three-way interactions, to the phenotype of the same plant from which the tissue was taken. Heatmaps were based on module eigengene values and included both correlation coefficients and corresponding p-values to assess the robustness of each association. Additionally, we used the R package "igraph" (Csardi & Nepusz, 2006) to construct network visualizations, illustrating the interactions between key genes and functional traits. Networks were built from adjacency matrices derived from module membership values (kME), and edges were filtered based on a minimum module membership threshold $|kME| > 0.7$, and significance of gene-trait correlations ($padj < 0.05$), retaining only the strongest connections. This filtering resulted in simplified network visualizations that highlight key hub genes and their putative functional associations with phenotypic traits.

Results

Objective 1: Ecotypic Variation and Local Adaptation

Plot-Level Cover and Biomass

At the plot level in 2022, we found significant main effects of site, ecotype, and their interaction on *A. gerardi* canopy cover and biomass (all $p<0.05$), as well as a significant interaction of site × ecotype × treatment ($p<0.05$; Table 3.2). For 2021, patterns of biomass and cover mirrored the 2022 trends (Table 3.2b, Figures 3.2, S2).

Ecotype Variation by Site. We consider ecotype response at each site separately and focus mainly on 2022. Starting with the driest site (Colby, KS, USA), the dry ecotype had significantly higher cover (48.9% ±0.6) compared to the wet (8.8% ±1.2) and mesic (39.1% ±2.1) ecotypes (all $p<0.05$; Figure 3.2a). Moving on to the dry site (Hays, KS, USA), again the dry ecotype similarly had significantly higher cover (63.2% ±1.7) than the wet ecotype (15.4% ±1.8; $p<0.05$), and the mesic ecotype had intermediate values (Figure 3.2a). At the driest and dry sites, biomass showed similar trends in 2022 (Figure 3.2b). Progressing eastward to slightly wetter conditions, at the mesic site (Manhattan KS, USA), cover among ecotypes did not differ and were ~60% (Figure 3.2a). Moving to the wet site (Carbondale IL, USA) the wet ecotype demonstrated significantly highest (60.6% ±1.5) cover, while the dry ecotype had only 6.2% ±2.0 cover, and the mesic ecotype was intermediate (34.7% ±4.6; Figure 3.2a). The mesic ecotype showed intermediate cover (40-60%) at all sites (Figure 3.2a). Biomass showed similar trends as cover in 2022 (Figure 3.2b).

For 2021, biomass and cover patterns mirrored the 2022 differences across sites (Figure S2).These patterns support evidence for local adaptation of the wet and dry ecotypes, with the dry ecotype demonstrating significantly highest cover and biomass at its dry home site and the wet ecotype showing significantly highest cover and biomass its wet home site (Figure 3.2).

Rainout. Regarding rainout treatment, at the dry site, mesic and wet ecotypes demonstrated significantly reduced cover under rainouts compared to the ambient (mesic ecotype

ambient 40.4% ±0.7 vs rainout 26.2% ±3.2; wet ecotype ambient 15.4% ±1.8; vs rainout 4.8% ±0.9; Figure 3.2a). At the mesic site all ecotypes showed significantly reduced cover under rainouts (Figure 3.2a). At the wet site, the wet ecotype demonstrated a significant reduction in cover under rainouts compared to the ambient (60.6% ±1.5 vs 52.3% ±1.9; Figure 3.2a). Interestingly, also at the wet site, the dry ecotype had significantly higher cover under rainouts compared to ambient (18.7% ±3.1 rainout vs 6.2% ±2.0 ambient; Figure 3.2a). Results for biomass (Figure 3.2b) mirrored these trends. In 2021 under rainouts, biomass and cover generally showed similar trends as 2022 (Figure S2).

Functional Trait Measurements

In terms of individual plant functional traits, at peak season, all 14 traits showed significant effects of ecotype and site; four out of 14 traits demonstrated significant main effects of rainout treatment (Table 3.2). The interaction between site x ecotype was significant ($p<0.05$) for all traits in all seasons, consistent with expectations for local adaptation. All other interactions and seasons are presented in Table S3.2.

Ecotypic Trait Variation by Sites. Across sites, wet and dry ecotypes exhibited distinct functional strategies, but these differences varied by site, often reflecting local adaptation. Since the mesic ecotype and mesic site showed intermediate trait values (Figures 3.3, S3), offering limited insight into divergent adaptive strategies, we focus our comparisons on the dry and wet ecotypes at the driest, dry, and wet sites.

Driest Site. First, at the driest site**,** the dry ecotype compared to the wet ecotype demonstrated significantly greater photosynthetic rates (dry 11.2 μmol $CO_2m^{-2}s^{-1}$±1.1 vs wet 5.0±0.2), higher stomatal conductance (dry 0.139 mol $H_2Om^{-2}s^{-1}$±0.003 vs wet 0.09±0.01), greater water use efficiency (WUE; dry 3.64 μmol $CO_2/H_2Om^{-2}s^{-1}$±0.52 vs wet 1.05±0.04),

higher nitrogen concentration (dry 1.54%±0.06 vs wet 1.31%±0.05), thicker leaves (dry 0.21 mm±0.02 vs wet 0.17±0.01) but lower transpiration (dry 2.78 μmol $H_2Om^{-2}s^{-1}$±0.06 vs wet 4.28±0.06; all $p<0.05$; Figures 3.3a, S3). The dry ecotype bolted earlier than the wet ecotype by nine days (Julian date, JD dry 246.1±0.5 vs wet 255.3±2.9) and flowered earlier by 20 days (dry JD= 258.0±2.7 vs wet 278.3±3.0; Figures 3.3b, S3). However, the wet ecotype compared to the dry ecotype was nearly twice as tall (wet 32.4 cm ±5.6 vs 18.4±0.4), had wider leaves (0.74 cm±0.09 vs 0.60±0.01), and greater plant diameter by ~30 cm (wet 53.8 cm±9.5 vs dry 21.4±1.6; all $p<0.05$; Figures 3.3c, S3).

Dry Site. Next, moving on to the dry site, the dry ecotype showed generally similar patterns as the driest site. The dry ecotype, at its homesite, compared to the wet ecotype showed significantly greater photosynthetic rates (dry 19.4 μmol $CO_2m^{-2}s^{-1}$±0.08 vs wet 11.5±0.80), higher chlorophyll absorbance (dry 36.2 SPAD±1.4 vs wet 29.8±3.2), greater stomatal conductance (dry 0.174 mol $H_2Om^{-2}s^{-1}$±0.003 vs wet 0.08 ±0.005), higher WUE (dry 7.29 μmol $CO_2/H_2Om^{-2}s^{-1}$±0.8 vs wet 1.40±0.2), greater nitrogen concentration (dry 1.80±0.20% vs wet 1.39±0.18%) and thicker leaves (dry 0.19 mm± 0.03 vs wet 0.17±0.04; all $p<0.05$; Figures 3.3a, S3). Further, the dry ecotype compared to the wet ecotype had significantly lower transpiration rates (dry 2.12 μmol $H_2Om^{-2}s^{-1}$±0.2 vs wet 4.46±0.02), bolted earlier by 23 days (dry JD=219.9±3.6 vs wet 243.1±5.0) and flowered earlier by 16 days (dry JD=246.0±4.0 vs wet 262.3±4.2; Figures 3.3b, S3). This combination of traits indicate adaptation to dry conditions. Similar to the driest site, the wet ecotype compared to the dry ecotype was taller by ~20 cm (wet 71.1 cm±16.9 vs dry 54.9±3.7) and had greater diameter by ~40 cm (wet 91.3 cm±18.8 vs dry 50.3±4.0; all $p<0.05$; Figures 3.3c, S3).

Wet Site. Finally, at the wet site**,** the dry ecotype compared to the wet ecotype again demonstrated significantly greater photosynthetic rates (dry 15.0 μmol $CO_2m^{-2}s^{-1}$±0.47 vs wet 12.3±0.29), higher transpiration rates (dry 3.78 μmol $H_2Om^{-2}s^{-1}$±0.28 vs wet 2.36±0.25), and had thicker leaves (0.19 mm±0.02 vs 0.16±0.01; all $p<0.05$; Figures 3.3a, S3). Furthermore, the dry ecotype flowered earlier (dry JD = 219.0±3.5 vs wet 237.4±2.0) than the wet ecotype at the wet site (Figure 3.3b). The wet ecotype, at its homesite, compared to the dry ecotype was significantly taller by ~100 cm (wet 160.2 cm±9.2 vs dry 59.9±15.9), had greater leaf width (wet 1.1 cm±0.3 vs dry 0.6±0.04), larger diameter (wet 107.1 cm±7.3 vs dry 47.3±6.2), greater total biomass by 200 g (wet 231.0 g±52.1 vs dry 27.6±4.9) and greater seed biomass (wet 9.7 g±3.2 vs dry 0.22±0.16; all $p<0.05$; Figures 3.3c, S3). This combination of traits indicate adaptation to wet conditions, where light and nutrients are limiting.

Rainout. Rainout treatments revealed ecotype-specific response to drought, with the wet ecotype generally exhibiting the strongest negative response. At the dry site, under rainouts compared to ambient, the wet ecotype had a significant reduction in photosynthetic rate (7.1 μmol $CO_2m^{-2}s^{-1}$±0.9 lower), height (15.6 cm±1.3 lower), total biomass (18.2 g±2.4 lower), and diameter (12.4 cm±3.1 lower; Figures 3.3a-b, S3). In contrast, the dry ecotype showed significantly higher WUE (1.2 μmol $CO_2/H_2Om^{-2}s^{-1}$±0.9 increase) under rainouts relative to ambient and significantly lower transpiration rates (Figure S3), consistent with drought tolerance. Rainouts delayed flowering of all ecotypes by 5-15 days at the dry site (Figure 3.3c).

Finally, at the wet site, rainouts delayed flowering of all ecotypes by 6-17 days (Figure 3.3c). The wet ecotype demonstrated significantly reduced photosynthetic rates (4.2 μmol CO_2±0.4 decline), WUE (2.3 μmol $CO_2/\mu mH_2O$±0.09 decline), height (35.3 cm±0.9 decline), seed biomass (4.8 g±0.8 decline), and stomatal conductance (0.25 mol H_2O±0.07 decline;

Figures 3.3, S3; all $p<0.05$) under rainouts compared to ambient. In contrast, under rainouts the dry ecotype showed significantly higher chlorophyll absorbance (5.2 SPAD±0.4 increase), photosynthetic rates (2.7 μmol CO_2±0.7 increase), stomatal conductance (0.11 mol H_2O±0.4 increase), WUE (1.9 μmol H_2O±0.2 increase), height (29 cm±1.4 increase), leaf width (0.19 cm±0.05 increase), and nitrogen concentration (0.46%±0.11 increase; Figures 3.3, S3; all $p<0.05$).

Principal Components Analysis (PCA) of Functional Traits

Multivariate trait associations revealed clear ecotype differentiation and environmental clustering across sites and rainout treatment. In nearly all PCAs analyzed, axis 1 explained over 50% of the total variance, with axis 2 accounting for 15–20%. Consequently, our interpretation focuses on axis 1. In the PCA by ecotype**,** axis 1 was significantly correlated with mean annual precipitation across all three ecotypes ($p<0.05$; Figure S4), highlighting a rainfall-trait relationship consistent with local adaptation.

By Ecotype. Trait coordination differed among ecotypes: for the dry ecotype (Figure 3.4a), axis 1 was strongly associated with WUE and leaf thickness—traits aligned with a drought tolerance strategy. In contrast, for the wet ecotype (Figure 3.4b), most traits corresponded to a growth/ competition strategy such as height and total biomass.

By Site. The PCA analyzed by site demonstrated trait coordination among sites along axis 1. At the dry **(**Figure 3.4c) and driest sites (Figure S5), increased WUE, greater leaf thickness, and increased chlorophyll absorbance loaded strongly on axis 1 and were associated with the dry ecotype. At the wet site (Figure 3.4d), nearly all morphological traits were associated with the wet ecotype. These patterns indicate that site-level environmental conditions shape trait integration and ecotype performance.

Homesite. The PCA by homesite also revealed strong evidence for local adaptation through trait coordination. The dry homesite (Figure 3.4e) showed positive loading of total biomass, seed biomass, transpiration rate, SPAD, and bolting with axis 1, while WUE and leaf thickness were negatively associated. At the wet homesite (Figure 3.4f), canopy diameter, leaf thickness, and total biomass were positively associated with axis 1, whereas internal CO_2 concentration, carbon concentration, transpiration rate, and flowering were negatively associated. These patterns of trait coordination at homesites support local adaptation, with each ecotype exhibiting trait combinations optimized for performance at their homesite.

Rainouts. Comparing PCA under rainouts, we identified specific traits linked to each ecotype. For example, under rainouts, leaf thickness, WUE, bolting, flowering, photosynthetic rate, and nitrogen concentration were linked to the dry ecotype (Figure S6a). However, in ambient conditions, canopy diameter, height, total biomass, carbon concentration, and leaf width were associated with the wet ecotype (Figure S6b).

Objective 2: Gene Expression Analyses

Gene Expression Characteristics. Here we focus on a subset of plants for differential gene expression analysis: the dry and wet ecotypes, driest, dry, and wet sites, and treatment (ambient and rainout). In the differential gene expression analysis, we identified 77,471 genes among these samples with each sample with a FastQC score of 97.5% or higher. Of the identified genes, 66,037 genes had annotations. A list of candidate genes identified by ecotype, site, and rainout treatment is presented in Table 3.5.

Ecotype. We identified 11,278 differentially expressed genes (DEGs) with a main effect of ecotype (Figure 3.5a, Table 3.3). In the dry ecotype, GO terms were significantly enriched for root epidermal cell, root differentiation, chlorophyll metabolism, and regulation of stomatal

closure (Figure S7a; Table 3.4). In the wet ecotype, GO terms were significantly enriched in genes related to gibberellin response, trichome differentiation, and auxin-activated pathway (Figure S7a; Table 3.4). Taken together, this indicates a strategy of water conservation and belowground investment for the dry ecotype and growth promotion and aboveground development for the wet ecotype.

Site. Site comparisons identified 24,927 DEGs between dry and wet sites (Figure 3.5b, Table 3.3). At the dry site, GO terms were significantly enriched for root cap of primary root, response to stress, defense response, and lateral root tip (Table 3.4; Figure S7b). In contrast, at the wet site, GO terms were significantly enriched in growth-related processes such as biosynthetic and metabolic processes and auxin response shoot system meristem, response to auxin, chloroplast organization, and reproductive bud (Table 3.4; Figure S7b). Comparing the wet and the driest site, we found 10,015 DEGs (Table 3.4), showing enrichment for GO terms related to defense response and abscisic acid transport at the driest site (Table 3.4). Taken together, this indicates a strategy of stress tolerance and root-driven resource acquisition for the dry site and growth and reproductive development for the wet site.

Homesite. Most informative are comparisons of gene expression between ecotypes at their homesites revealing genetic signatures of local adaptation. Specifically, comparing the dry ecotype at the dry site and wet ecotype at the wet site, we identified 19,054 DEGs (Figure 3.5c). In the wet homesite, 8,713 genes were significantly enriched for GO terms related to seed maturation, gibberellin mediated signaling pathways, shoot system morphogenesis, and apical meristem (Figure S7c; Table 3.4). In the dry homesite, 10,341 genes were significantly enriched for ABA signaling, photosynthesis, root epidermis, and pollen development (Figure S7c; Table 3.7). In summary, this indicates a strategy of stress-adaptation at the dry homesite and growth-

oriented development at the wet homesite, consistent with local adaptation to contrasting environments.

Rainout. Gene expression patterns reflected distinct responses to rainout and ambient treatment (across sites and ecotypes) with 407 DEGs showing a treatment effect (Figure 3.5d, Table 3.3). Under rainouts, GO terms were significantly enriched for root apical meristem, cellular water homeostasis, heat shock protein signaling, and chloroplast modification (Figure S7d; Table 3.4). In ambient conditions, GO terms were significantly enriched for vascular growth, stem epidermis, first order inflorescence axis, and regulation of growth (Figure S7; Table 3.4). This indicates a strategy of stress mitigation under experimental drought, and developmental progression and structural investment under ambient conditions.

Objective 3: Linking Gene Expression to Phenotype with Co-expression Networks

Ecotype. To uncover the molecular basis of adaptive divergence between ecotypes, we analyzed gene co-expression networks linked to phenotypic traits. These networks reveal a striking contrast in adaptive strategies between wet and dry ecotypes that may drive local adaptation. First, in the dry ecotype (Figures 3.6a, S8a), we identified upregulated genes involved in stress responses, photosynthesis, and gene regulation (notably, *chlorophyll A-B binding, drought-induced-19, chloroplast drought-induced protein,* Cluster 26; *DREB2A,* Cluster 13) which were co-expressed with transpiration rate, internal carbon dioxide concentration, and height (red stars, Figure 3.6a). Upregulated genes related to growth (e.g., *ARF-16,* Cluster 33) were co-expressed with growth rate and transpiration rate (Figure 3.6a; Table 3.6). These patterns reveal that the dry ecotype coordinates gene expression around stress-response pathways, reflecting a strategy prioritizing resource conservation in challenging environments.

In contrast, in the wet ecotype, we identified genes linked to ten traits (Figure S8b; Table 3.6) such as flowering, stomatal conductance, height, and total biomass, co-expressed with upregulated genes related to auxin and growth (e.g., *ARF-75, PHABULOSA*, Cluster 11; Figure 3.6b; Table 3.6). Furthermore, upregulated genes involved in response to the growth hormone gibberellin (*gibberellin 2-O*, Cluster 30; *gibberellin response*; *GASR3* Cluster 29; Figure 3.6b; Table 3.6) that were co-expressed with nine traits including height and growth rate. This network suggests that the wet ecotype's adaptive strategy emphasizes growth and biomass accumulation in favorable conditions.

Site. Site-specific gene–trait associations underscore how local environment shape both traits and gene expression. At the dry site, genes involved in osmotic regulation (e.g., *DROUGHT SENSITIVE 1,* Cluster 5; Figures 3.6c, S8c; Table 3.6) were co-expressed with stomatal conductance, growth rate, and photosynthetic rate. Genes involved in floral meristem regulation (e.g., *CLAVATA1,* Cluster 6) and stress response (e.g., *drought-responsive protein*, Cluster 6; Figure 3.6c) were co-expressed with seed biomass and stomatal conductance. Heat-shock-related genes (e.g., *Heat-Shock STI,* Cluster 4) were positively linked to nitrogen concentration, carbon concentration, and bolting. Finally, genes involved in root growth (e.g., *STRUBBELING-RECEPTOR FAMILY 7*, Cluster 18), was co-expressed with chlorophyll absorbance (Figures 3.6c, S8c; Table 3.6). These networks highlight how stressors at the dry site selectively upregulate genes related to stress tolerance.

In contrast, at the wet site, genes involved in regulating flowering (e.g., *FCA*, Cluster 8) and those involved in growth regulation (e.g., *Growth Regulator*, *DIMINUTO,* Cluster 8) were co-expressed with height and diameter (Figures 3.6d, S8d; Table 3.6). Genes involved with flowering (e.g., *RNA flowering locus*, Cluster 10) were co-expressed with bolting. Finally, genes

related to growth (e.g., *DWARF1:* Cluster 2) were co-expressed with nitrogen and carbon concentration (Table 3.6; Figure 3.6d). Co-expression networks at the wet site suggest that favorable conditions promote a strategy geared toward maximizing growth and development.

Homesite. Gene–trait associations of the ecotypes reflected local environmental conditions, supporting local adaptation. At the dry homesite, several genes involved in regulation of flowering (e.g., *FRIGIDA*, Cluster 16; Figures 3.7a; S8e) were co-expressed with six traits including total biomass and leaf width. Further, we identified downregulated genes involved in root growth (e.g., *root hair defective-5,* Cluster 10) were co-expressed with nine traits including transpiration rate and WUE (Figure 3.7a; Table 3.6). Other upregulated genes were involved in auxin response and photosynthesis (notably *auxin response-8, photosystem reaction center*, Cluster 9) were each linked to multiple traits including WUE, photosynthetic rate, and growth rate (Figure 3.7a; Table 3.6). Several genes involved in root formation (e.g., *aberrant root formation-P4*, Cluster 17) were linked to seed biomass, height, and stomatal conductance at the dry homesite (Figure 3.7a; Table 3.6). Our network reflects local adaptation of the dry ecotype to water-limited conditions, with coordinated regulation of genes that optimize water-use efficiency under low moisture.

In comparison, at the wet homesite, many gene clusters were strongly associated with multiple traits (Figure S8f). For example, downregulated genes involved in nitrogen regulation (e.g., *Nitrogen Regulation Transcription Factor*, Cluster 26*)* were co-expressed with nitrogen concentration. Genes involved in vascular tissue generation (e.g., *VASCULAR-RELATED DOMAIN-6*, Cluster 23) were co-expressed with several traits including flowering, seed biomass, and photosynthetic rate (Figure 3.7b; Table 3.6). Additionally, gibberellin-related genes (e.g., *Gibberellin 20-Oxidase 1,* Cluster 5*, Gibberellin 2-beta-dioxygenase-7*, Cluster 6) and genes

involved in flowering (e.g., *Early Flowering 6*, Cluster 23) were broadly co-expressed with most traits, including height, photosynthetic rate, and seed biomass (Figure 3.7b; Table 3.6). This network highlights local adaptation of the wet ecotype, with genes promoting growth and reproduction, reflecting optimization of development under abundant soil moisture.

Rainout Treatment. Of the 407 DEGs expressed under rainouts across sites and ecotypes, 146 were significantly correlated with a measured phenotype (Figure S8g-h). For example, under rainouts we identified several upregulated genes that are involved in root development and stress response (notably *Aberrant Root Formation-4, stress-responsive-AB, DROUGHT SENSITIVE-1, drought responsive protein,* and *Panicle Inflorescence*, Cluster 3). These genes were co-expressed with nine traits including WUE and bolting (Figure 3.7c; Table 3.6). In contrast, in ambient conditions (Figure 3.7d), genes involved in flowering (e.g., *FLOWERING LOCUS C,* Cluster 1) or nutrient uptake (e.g., *Haloacid dehalogenase* (*HAD*), Cluster 1) were co-expressed with chlorophyll absorbance (Figure 3.7d). Also in ambient conditions, genes involved in vascular tissue growth (e.g., *shoot apical meristem A2, Albino Leaf* 4, Cluster 3) were co-expressed with five traits including flowering, photosynthetic rate, and stomatal conductance. Taken together, our networks demonstrate gene–trait linkages associated with stress tolerance, highlighting adaptive responses to both natural rainfall gradients and experimental drought conditions.

Discussion

This study sheds light on how form, function and growth of plant ecotypes are influenced by rainfall gradients and experimentally reduced rainfall, by linking gene expression and plant functional traits to characterize local adaptation (summarized in Figure 3.8). Here, we explore

how local adaptation is indicated by plant traits indicating coordination of trait strategies (Grime, 1988): stress tolerant traits in the dry ecotype in response to water limitation and competitive growth traits (Jardine et al., 2021) in the wet ecotype due to light and nutrient limitation. We then discuss the gene expression differences between ecotypes, which at the genetic level, support the divergent adaptive phenotypes. Further, using the experimental rainfall manipulation, we show that rainfall is the driving selective force leading to divergence of these ecotypes. Finally, by connecting gene expression to traits like photosynthetic rate, biomass, and height, we reveal the genetic basis of adaptive phenotypes as related to rainfall. This integrative approach offers a unique perspective on the genetic basis of ecological performance in natural plant communities (Johnson et al., 2022) under changing climatic conditions (Benning et al., 2023).

Evidence of plot-level local adaptation to rainfall linked to functional traits

We found the highest cover and biomass of the wet and dry ecotypes at the plot-level in their home site and lower at foreign sites, supporting local adaptation of *A. gerardi* (Galliart et al., 2019; 2020). It is well-established that climate drives intraspecific variation and local adaptation (Turesson, 1922; McMillan, 1965; Savolainen et al., 2013) where numerous studies have demonstrated that populations often exhibit higher fitness in their home environments, reflecting patterns of local adaptation (Joshi et al., 2001; Leimu & Fischer, 2008; Lortie & Hierro, 2022). However, few studies integrate local adaptation with transcriptomics and traits across environmental gradients, especially in native, non-model species in ecological communities (Johnson et al., 2022; Sytsma et al., in press). We address this gap by integrating ecological and genomic approaches to reveal mechanisms of local adaptation in *A. gerardi* across a natural rainfall gradient and in response to experimental drought (Figure 3.8) in grassland

communities. Since rainfall putatively drives ecotypic differentiation (Gray et al., 2014), our use of cross-transplantation in community settings enabled realistic detection of local adaptation.

Our findings reveal clear physiological and morphological divergence and coordinated trait strategies among ecotypes that underpin local adaptation to the rainfall gradient. The dry ecotype exhibited classic drought-adaptive traits, including higher photosynthetic rates, improved water-use efficiency, thicker leaves, and elevated leaf nitrogen despite smaller stature (Grime, 1988; Jardine et al., 2021; Ochola et al., 2024). Its earlier flowering suggests a drought escape strategy at the end of the growing season or adaptation to shorter growing seasons (Shavrukov et al., 2017), consistent with patterns seen in arid-adapted species showing early phenology, reduced size, and efficient water use (Castillioni et al., 2022). In contrast, the wet ecotype prioritized growth, producing wider leaves and more biomass, and growing taller particularly at the wet site. This reflects a broader trend in which ecotypes from wetter regions favor rapid growth and resource acquisition (Jardine et al., 2021). These differences illustrate trade-offs between growth and stress tolerance (Grime, 1988), providing mechanistic evidence of local adaptation through trait divergence (Figure 3.8).

Rainout manipulations demonstrated that rainfall is the selective pressure driving divergent ecotypes, further corroborating support for regional climate ecotypes and local adaptation. Rainfall imposes strong selective pressure in many organisms, often driving population differentiation in traits related to growth, reproduction, and survival (Siepielski et al., 2017). Consistent with this, rainouts delayed flowering in all ecotypes, especially at the dry site, linking water availability to reproductive timing in *A. gerardi* (Dietrich & Smith, 2016). In general, rainouts reduced the performance of all ecotypes but disproportionately impacted the

wet ecotype, underscoring its adaptation to high-moisture environments and reduced drought tolerance.

At the wet site, we found additional strong evidence of rainfall as a selective pressure. Interestingly, under rainouts, the dry ecotype's biomass, cover, photosynthetic rate, and height *increased* compared to ambient, suggesting that reduced rainfall in wetter environments may favor drought-adapted ecotypes (Metz & Tielborger, 2023). Additionally, under rainouts at the dry site, the wet ecotype showed reduced WUE compared to ambient, while the dry ecotype showed increased WUE, indicating greater drought tolerance (Tardieu, 2022). These results demonstrate that rainfall not only drives local adaptation but may also shapes functional trait divergence in ecological communities.

Gene expression profiles reflect divergent adaptive phenotypes

Distinct patterns of gene expression were correlated between ecotypes, sites, and rainfall treatments, suggesting local genetic adaptation (Savolainen et al., 2013; Hoffman et al., 2018; Figure 3.8). These findings suggest that key physiological pathways were selected in each ecotype to optimize their physiological responses to local environmental conditions.

First considering ecotype, the wet ecotype upregulated genes involved in carbon gain and growth, reflecting an adaptive strategy favoring resource acquisition and growth investment in high-moisture environments. Building on findings by Galliart et al. (2020), our data also show further upregulation of gibberellic acid pathways (*gibberellin 2-O*, *GASR3*)—key to germination, shoot elongation, and reproductive transitions (Shah et al., 2023)—likely contributing to the wet ecotype's greater height and biomass. In contrast, the dry ecotype upregulated genes related to root development (*Chaperonin 60*), dehydration response (*DREB2A)* and stomatal complex formation (*chloroplast drought-induced protein*), aligning with drought-adaptive strategies

aimed at enhancing water uptake and regulating gas exchange (Pardo et al., 2020; Gupta et al., 2024; Zhang et al., 2025b). These contrasting gene expression profiles reflect distinct physiological strategies and reinforce the role of local adaptation at the genetic level (Figure 3.8).

The impact of precipitation on gene expression is further evident when comparing sites, with ecotypes combined, with contrasting wet and dry rainfall patterns. First, at the wet site, genes involved in growth (*Growth Regulator*, *DIMINUTO*) and flowering (*FCA, RNA Flowering Locus*) were upregulated, reflecting an earlier onset of the growing season. In contrast, at the dry site, we found enrichment of genes involved in abscisic acid signaling (*ABI-3*), a key pathway in drought response (Aimar et al., 2014). These findings suggest that rainfall drives significant shifts in gene expression (Hamann et al., 2021), with the wet site promoting growth and reproductive pathways, while the dry site upregulates drought response mechanisms. Similarly, other studies (Lovell et al., 2016; Bhaskara et al., 2023) reported differential expression of drought-responsive genes across a precipitation gradient in *Panicum hallii*, supporting the idea that aridity selects for transcriptomic shifts associated with water conservation.

Considering gene expression of ecotypes in their homesite, our analysis revealed strong transcriptomic differentiation between wet and dry ecotypes where they have been strongly selected for by regional climate over thousands of years (Axelrod, 1985). At the wet homesite, enrichment of genes related to gibberellin signaling (*Gibberellin 20-Oxidase 1, Gibberellin 2-beta-dioxygenase 7*) suggests an environment-driven developmental shift favoring growth, resource acquisition, and competitive ability in resource-rich environments (Shah et al., 2023). Conversely, in the dry homesite, gene enrichment in processes related to early flowering (*FRIGIDA*), gas exchange (*photosystem reaction center),* and root growth (*root hair defective-5, aberrant root formation-P4)* indicates an adaptive focus on survival and resource conservation

under water-limited conditions (Cardoso et al., 2015). Similar patterns have been observed in *Panicum* spp., where wet populations exhibit enrichment of genes involved in growth, while dry populations express genes associated with stress tolerance (Meyer et al., 2014; Lovell et al., 2018; Heckman et al., 2025). Together, homesite comparisons uncover expression patterns that show local adaptation is driven by transcriptome patterns leading to divergent physiological strategies (Figure 3.8).

Finally, under experimental drought, the enrichment of genes related to stress response (*stress-responsive-AB, DROUGHT SENSITIVE-1)* and regulation of flowering (*Panicle Inflorescence*) suggests a coordinated developmental response to water limitation. These shifts in gene expression support a strategy of water balance, reduced growth, and reproduction under stress (Wu et al., 2022). Similar patterns in other species show enrichment in the same pathways during drought, highlighting convergent adaptive responses to water limitation (Lovell et al., 2016; Shrestha et al., 2023). Together, these results underscore how ecotypes cope with drought by modulating development and phenology to enhance drought resilience (Napier et al., 2023).

Co-expression networks link genes to traits and highlight the role of rainfall

Our co-expression networks connect gene expression to phenotypic traits, providing insight into the genetic architecture behind local adaptation (Figure 3.8). Specifically, co-expression networks connect transcriptomic profiles with traits and are instrumental in understanding plant biology and informing restoration efforts (Aoki et al., 2007). These findings underscore the importance of exploring how gene expression patterns influence adaptive traits, offering a deeper insight into the mechanisms that drive local adaptation (Savolainen et al., 2013; Kang et al., 2023).

Ecotype-specific patterns of gene expression and trait correlations reveal distinct adaptive strategies. In the dry ecotype, genes involved in photosynthesis and stress tolerance (e.g., *ARF-16, drought-induced-19, DREB2A;* Wu et al., 2022; Zhang et al., 2025b) were correlated with traits such as transpiration rate and height, pointing to regulatory networks that enhance water-use efficiency and growth in arid conditions. These findings are consistent with drought-adaptive strategies observed in *Brachypodium* sp. (Verelst et al., 2013; Wang et al., 2025). In contrast, the wet ecotype upregulated genes involved in gibberellin response and growth (*gibberellin response*, *GASR3, ARF-75;* Shah et al., 2023; Zheng et al., 2023) which were linked to competitive traits (Grime, 1988) including height and biomass. These ecotype-specific networks highlight distinct strategies—drought resilience in the dry ecotype versus growth in wet ecotype—offering insights into local adaptation and potential responses to changing environmental conditions.

Looking at the site differences, at the dry site, several genes were correlated with functional traits across ecotypes. Notably, genes known to be involved in drought tolerance (*drought-responsive protein, DROUGHT SENSITIVE 1,* and *Heat-Shock STI*; Soma et al., 2021; Ni et al., 2021) were linked to stomatal conductance and growth rate, suggesting that stress-response genes can influence growth under water stress. Similar patterns have been observed in *Arabidopsis*, where genes related to drought tolerance regulate growth and reproduction under water-limited conditions (Alam et al., 2022). At the wet site, genes associated with growth regulation and flowering control (*Growth Regulating Factor* and *FCA;* Wang et al., 2020), were co-expressed with traits linked with height and bolting. These site-specific gene-trait correlations highlight how environmental conditions shape ecotypic adaptations, supporting the genetic basis of local adaptation (Figure 3.8).

Considering gene expression differences at homesites (wet and dry), the clear differentiation observed between co-expression networks of the local ecotypes is particularly striking. At the wet homesite, genes related to growth (*VASCULAR-RELATED NAC DOMAIN-6*; Wang et al., 2022), were co-expressed with many adaptive traits including flowering and photosynthetic rate. Notably, genes involved in gibberellin response *(Gibberellin 20-Oxidase 1, Gibberellin 2-beta-dioxygenase 7)* were correlated with nearly all traits, emphasizing the importance of gibberellins in promoting growth in wet environments (Shah et al., 2023). In contrast, at the dry homesite, genes (*FRIGIDA*, *auxin response-8;* Hrmova & Mussain, 2021; Xu et al., 2022*)* were correlated with numerous traits including flowering, total biomass, and leaf width confirming results found in other species (Heckman et al., 2025). The contrasting co-expression networks provide strong evidence of how local conditions shape both gene expression and trait variation, supporting the role of local adaptation in plant survival.

Under rainouts, genes like *drought responsive protein* (Ying et al., 2023), *stress-responsive-AB* (Ji et al., 2016), and *DROUGHT SENSITIVE-1* (Abdel-Ghany et al., 2020) were correlated with traits including biomass and photosynthetic rate under experimental drought, demonstrating their involvement in stress response. Similar patterns have been observed in other studies (Hayford et al., 2022; Bhaskara et al., 2023), where drought-responsive genes were correlated with key traits such as biomass production and photosynthetic rate under drought. These co-expression patterns under rainouts highlight core stress-response genes as key to adaptation to rainfall (Figure 3.8), offering molecular targets for enhancing drought resilience in grasslands.

Conclusions

Our results demonstrate the value of linking gene expression to traits to uncover mechanisms of local adaptation under increasing drought. As a dominant foundation species, *Andropogon gerardi* shapes grassland community structure and function (Gibson, 2009; McCain et al., 2010; Ren et al., 2024), making its adaptation critical for predicting grassland responses to rainfall. By integrating trait and gene expression data, we identified genes associated with drought response and competitive ability—key fitness strategies—revealing molecular trade-offs between stress tolerance and growth. These insights provide targets for restoration, biofuels, and improving resilience in drought-prone systems (Zhang et al., 2015; Baer et al., 2019). One of the few ecological genomic studies conducted in long-term, realistic field settings (Johnson et al., 2022; Sytsma et al., accepted), our work highlights the need to understand genetic and phenotypic responses to rainfall to address challenges such as reduced productivity and forage in drought-prone ecosystems (Bao et al., 2019; Smith et al., 2020; Habte et al., 2022). Given that drought is a major driver of crop loss and reduced primary productivity (Dietz et al., 2021; Liu et al., 2023), our findings are timely and support more effective grassland restoration using climate-matched ecotypes.

Author Contributions

Jack Sytsma: Writing- original draft, conceptualization, data curation, formal analysis, investigation, methodology, **Matthew Galliart:** Writing- review & editing, software, validation, **Kian Fogarty:** Writing- review & editing, data curation, investigation, **Kori Howe:** Writing- review & editing, investigation, **Bradley Olson:** Writing- review & editing, validation, software, **Sara Baer:** Writing- review & editing, resources, **David Gibson:** Writing- review & editing,

resources, **Brian Maricle:** Writing- review & editing, resources, **Eli Hartung:** Writing- review & editing, investigation, **Loretta Johnson:** Writing- review & editing, conceptualization, funding acquisition, methodology, resources, project administration.

Acknowledgements

Thanks to Z. Ren, D. Barfknecht, and N. Bishop for help in the field. Thanks to the National Center for Genome Resources and New Mexico State University INBRE for assisting in analysis and access to their server. Funding was provided by USDA Grant 2020-03665 and partially funded by the Kansas Academy of Science 2023 Student Research Grant, the 2023 Kansas Native Plant Society Bancroft Grant, and the U.S Department of Education Graduate Assistance in Areas of National Need Grant P200A240009 awarded to Sytsma.

Conflicts of Interests

The authors declare that they have no competing interests.

Data Accessibility

All data supporting the findings of this study will be available in a public repository upon publication. Raw sequencing reads, and processed genetic data will be deposited in the EMBL/GenBank repository, and trait measurements in a publicly accessible dryad repository Any additional data or materials can be made available upon reasonable request to the corresponding author.

Benefit-Sharing Statement

This research was conducted within the United States on native plant species without involving genetic resources requiring prior informed consent under the Nagoya Protocol. Results will be shared through open-access publication, conference presentations, and outreach to land managers and restoration practitioners to support sustainable grassland management and conservation.

Figure 3.1. A. Aerial photograph of the mesic garden site, showing the spatial arrangement of plots within the prairies. This image highlights the ecological context of the experiment and illustrates how the reciprocal gardens are established within a grassland community. B. The location of the source populations, the garden sites along the natural rainfall gradient of the US Midwest. The location of reciprocal gardens plantings are black filled points and source populations are hollow white circles. Color gradients denote mean annual total precipitation in mm from 400-1250mm yr^{-1}. C. Transplant design for garden plots with rainouts in gray and where ecotype plots (dry, mesic, or wet ecotypes) are indicated by colors (red, green, and blue). At each planting site, there are four replicate plots and plots were randomized at each site.

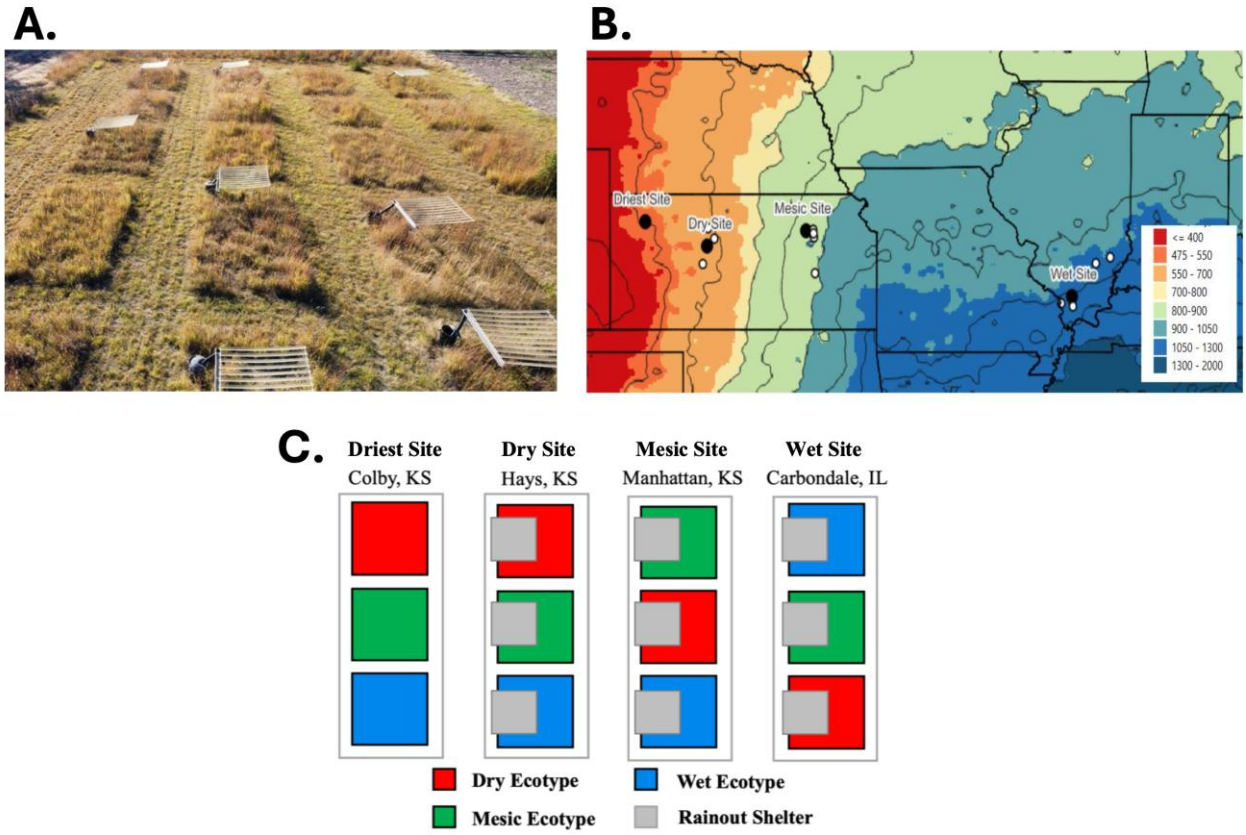

Figure 3.2. Comparisons of community-level response variables. A. canopy cover and B. aboveground biomass of *A. gerardi* in 2022. Ambient conditions are blue, and rainout is in red. The points indicate the mean, error bars represent standard errors, and the different letters denote significantly differences between ecotypes and treatments within a site and year ($\alpha = 0.05$). The first year (2021) is presented in Figure S2.

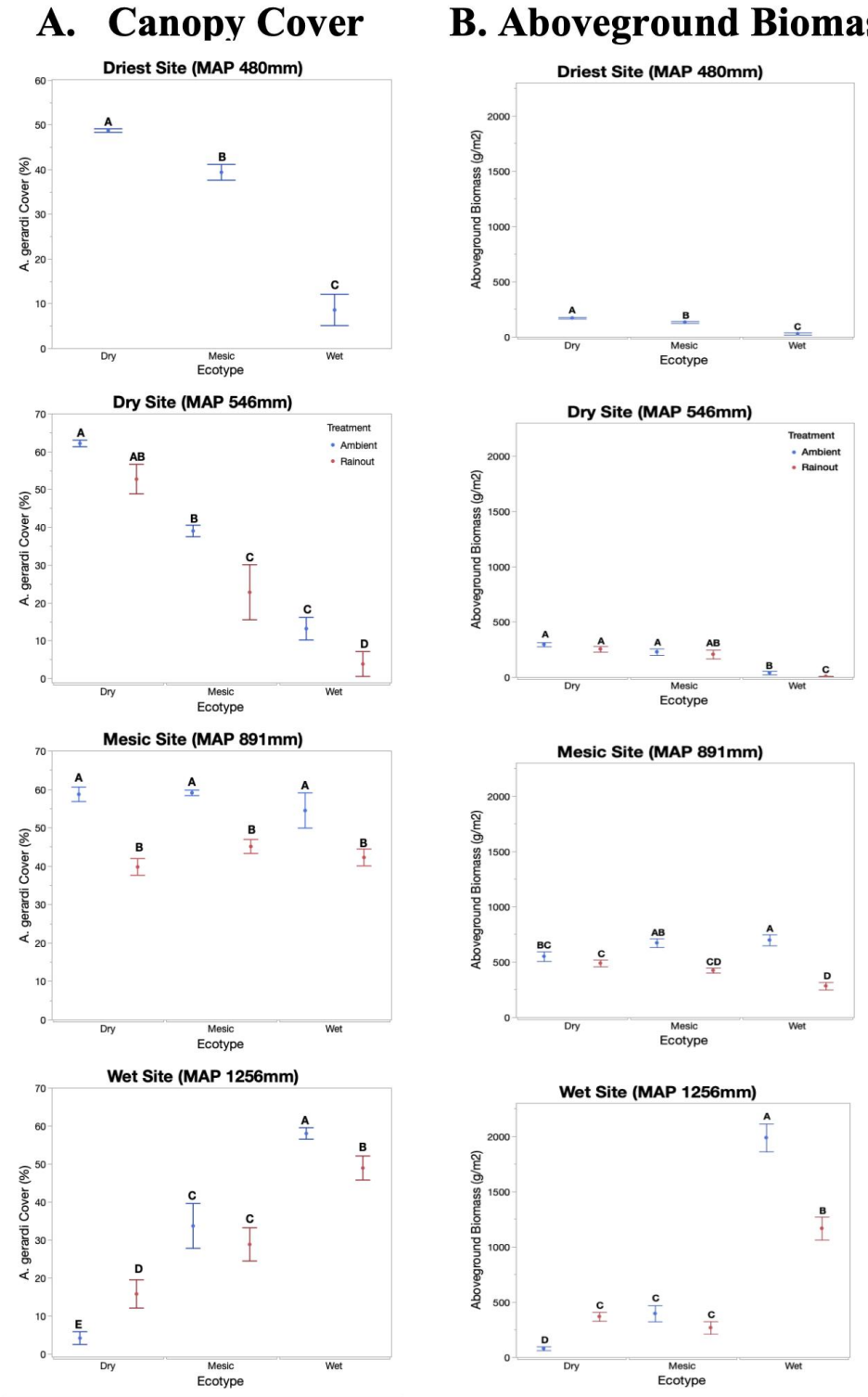

Figure 3.3. Comparisons of individual plant traits. A. photosynthetic rate, B. date of flowering, and C. vegetative height across sites (driest, dry, mesic, and wet) in peak season 2022. Ambient is blue, and rainout treatment is in red. The error bars represent standard errors, and the different letters denote significantly different groups among the comparisons within site ($\alpha = 0.05$).

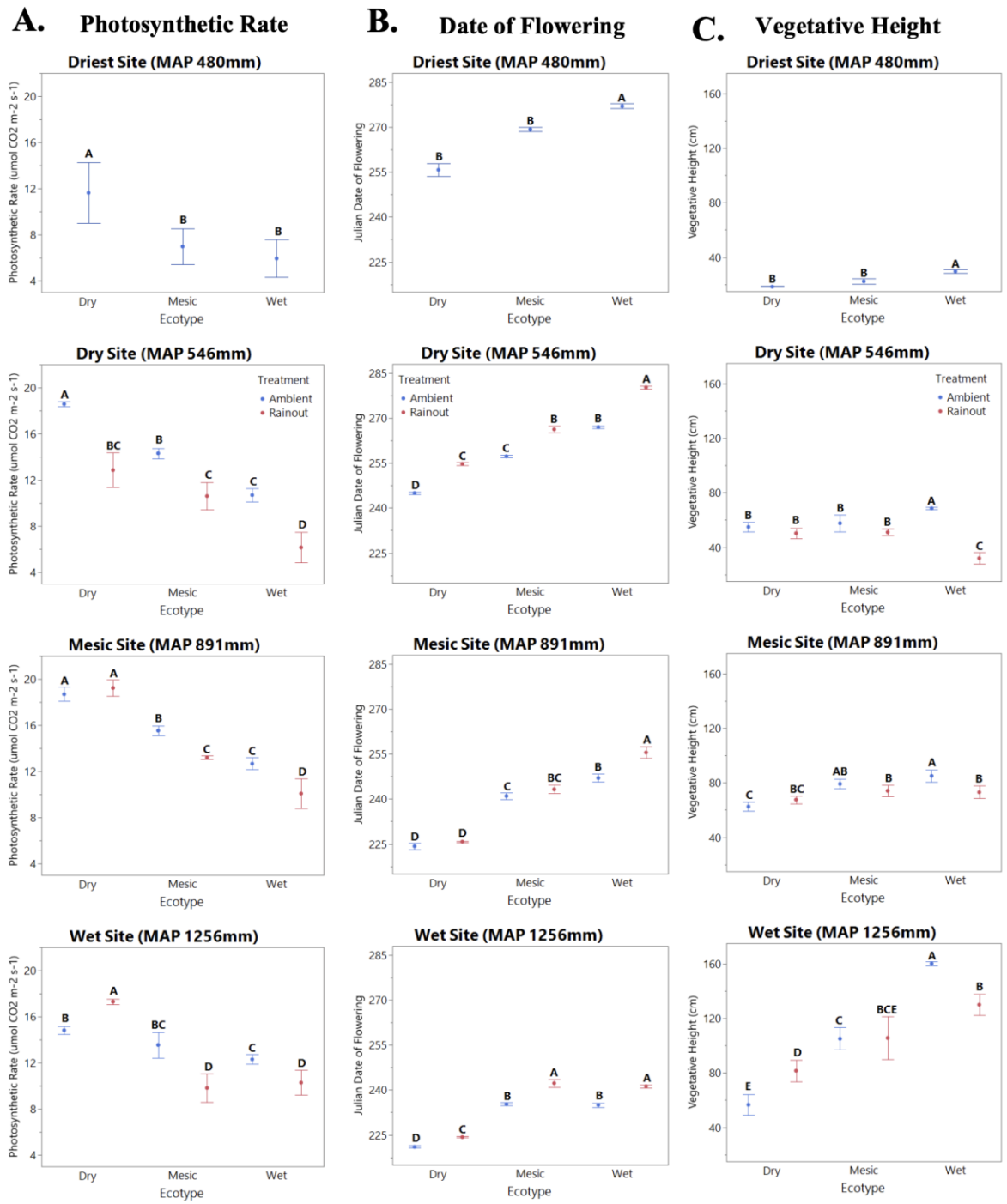

Figure 3.4. A. Principal component analysis (PCA) biplot of trait data by ecotype. A. dry ecotype and B. wet ecotype (mesic in the supplement) where colors and shapes indicate site (driest, dry, mesic, and wet). A PCA biplot of trait by site: C. dry site and D wet site in peak season (mesic and driest site in the supplement) where colors and shapes indicate ecotype (dry, mesic, or wet). A PCA biplot of trait by homesite. E. dry homesite and F. wet homesite in peak season where colors and shapes indicate ecotype (dry or wet). Lines indicate plant traits, and points are the means.

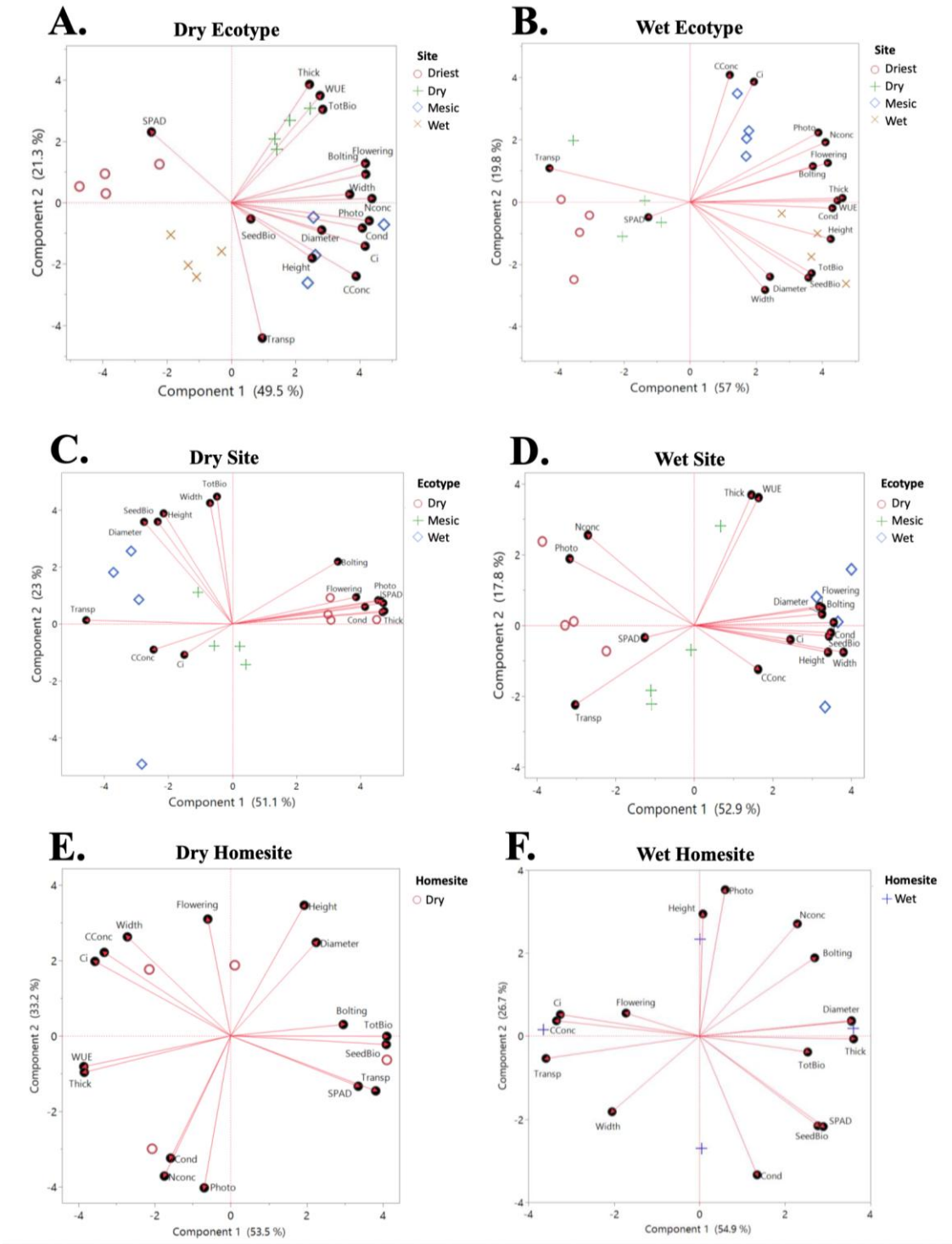

Figure 3.5. Heatmaps and volcano plots depicting the following: A. 11,278 differentially expressed genes between the wet and dry ecotypes, sites combined (ecotype main effect). B. 24,927 differentially expressed genes between the wet and dry sites, ecotypes combined (site main effect) C. 19,054 differentially expressed genes between the wet and dry ecotypes in their respective home sites (homesite effect). D. 408 differentially expressed genes between ambient and rainout conditions, ecotypes and sites combined (rainout main effect). Red points indicate upregulated genes; blue points indicate downregulated genes in volcano plots with unsignificant genes (p adj > 0.05) are indicated by gray points. The fold change in heatmaps indicated by blue (negative expression) or red (positive expression).

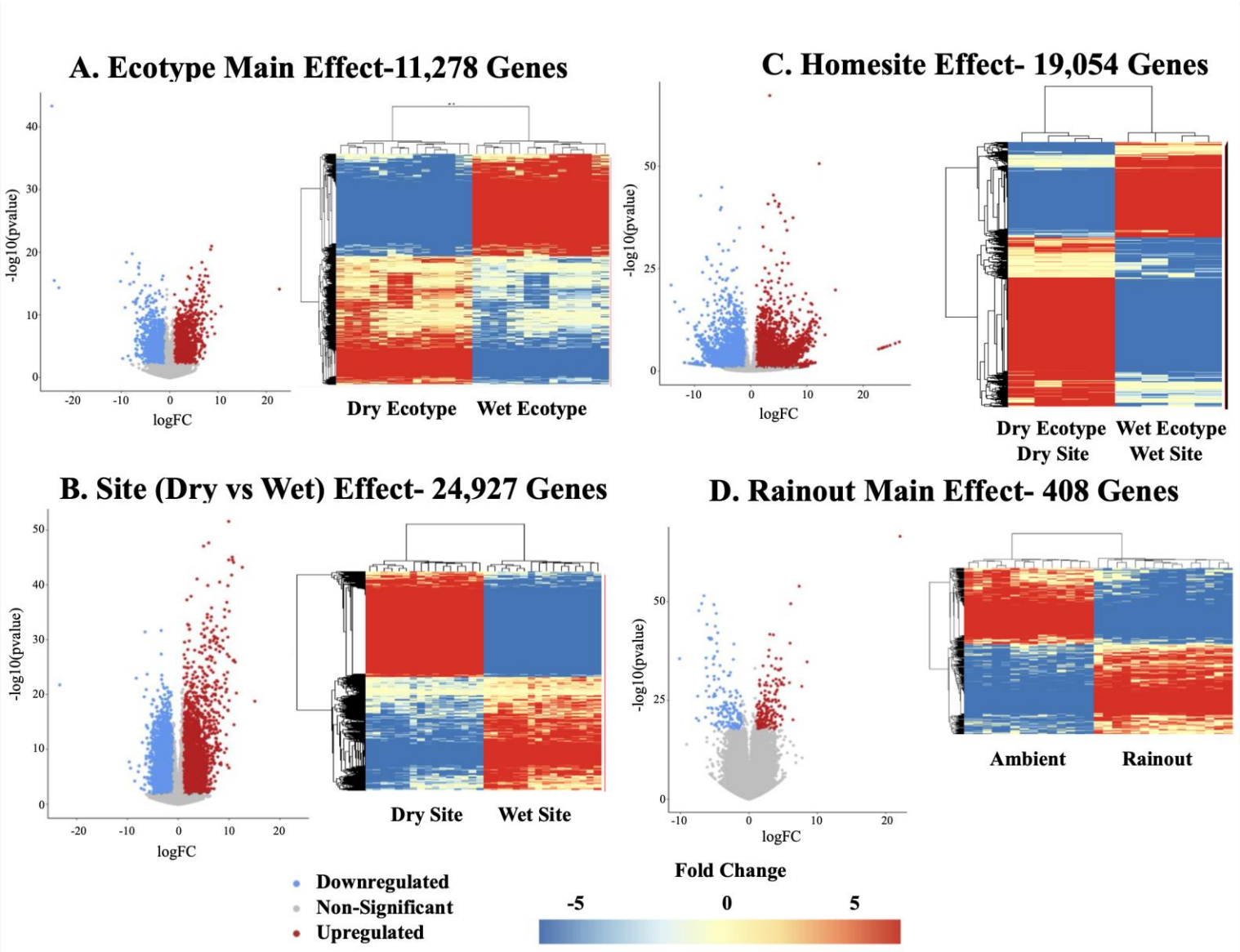

Figure 3.6. Co-expression network analysis of gene-trait associations. A. dry ecotype, B. wet ecotype, C. dry site, and D. wet site. Candidate genes were selected based on significant gene clusters from WGCNA with more than 3-fold change in expression and a known annotation. Green circles represent measured traits, while orange circles denote genes. Stars indicate genes with a well-documented function and provide insight into adaptive mechanisms. Line thickness corresponds to the strength of the association, with red lines indicating positive correlations and blue lines representing negative correlations. This network visualization highlights key relationships between gene expression and phenotypic traits, providing insights into potential functional connections underlying trait variation.

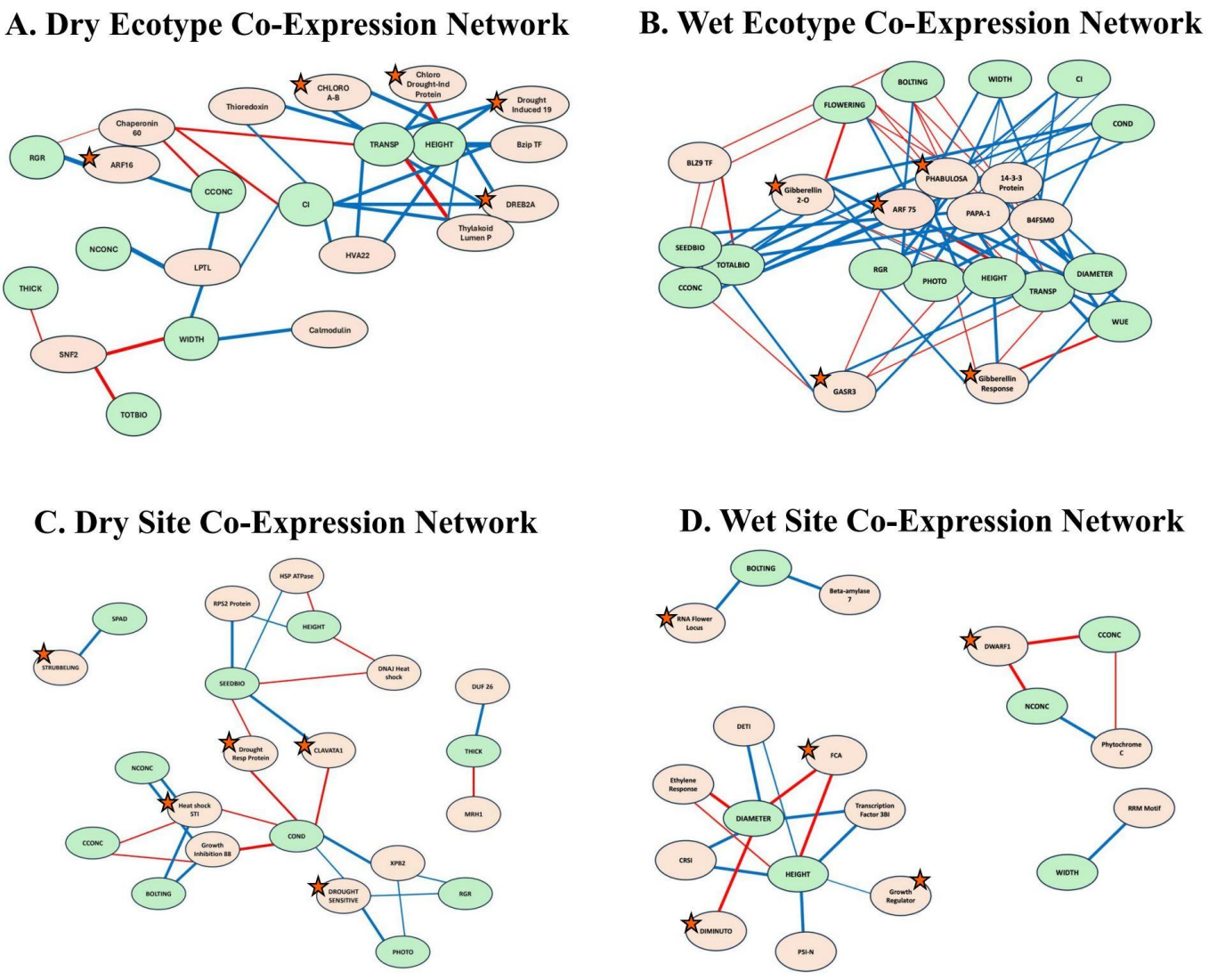

Figure 3.7. Co-expression network analysis of gene-trait associations. A. dry homesite and B. wet homesite, C. rainout, D. ambient treatments. Candidate genes were selected based on significant gene clusters from WGCNA with more than 3-fold change in expression and a known annotation. Green circles represent measured traits, while orange circles denote genes. Stars indicate genes with a well-documented function and provide insight into adaptive mechanisms. Line thickness corresponds to the strength of the association, with red lines indicating positive correlations and blue lines representing negative correlations. This network visualization highlights key relationships between gene expression and phenotypic traits, providing insights into potential functional connections underlying trait variation.

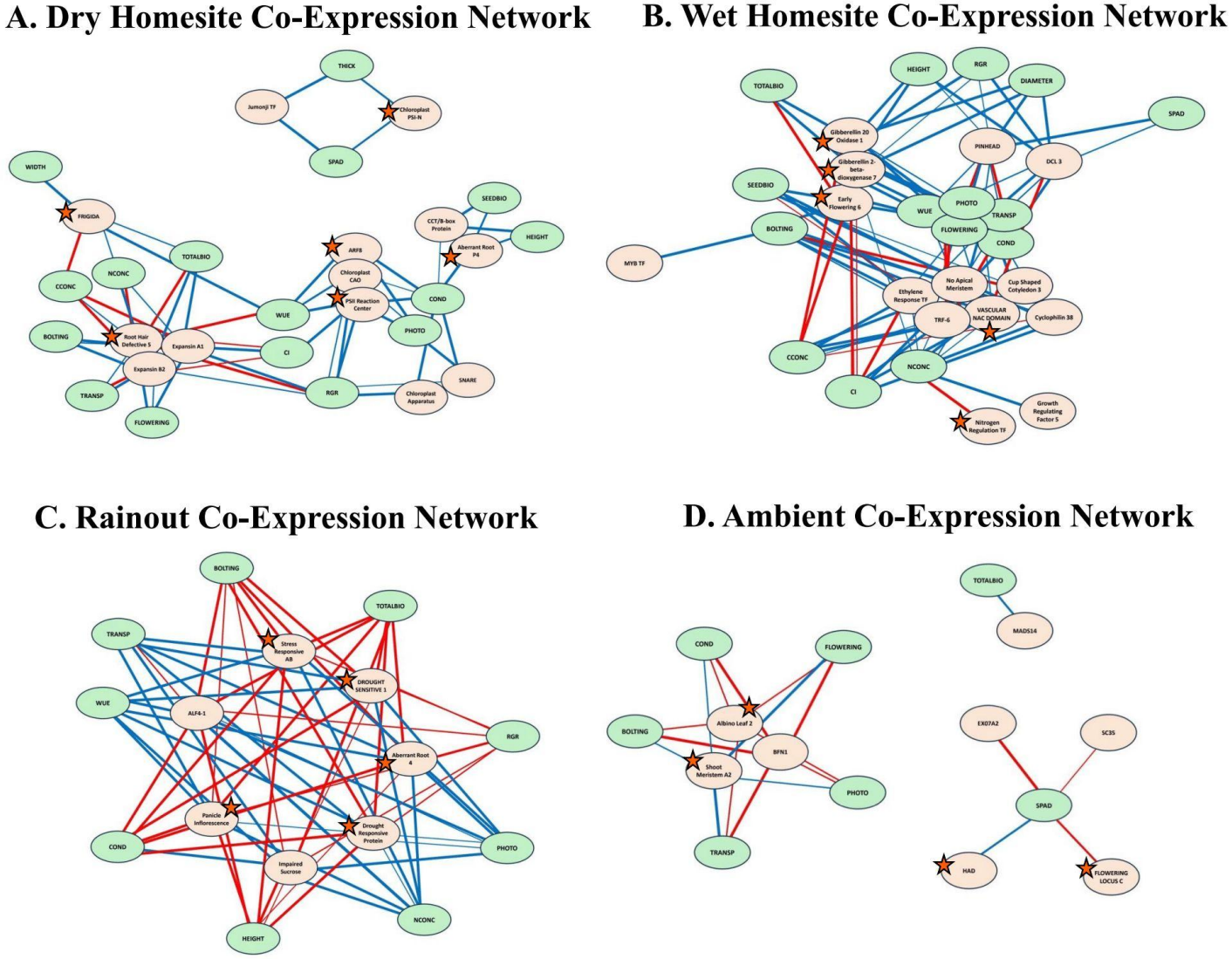

Figure 3.8**.** This model illustrates the adaptive strategies of wet and dry ecotypes in response to their respective home sites. In the wet ecotype, upregulated genes related to growth regulation, gibberellin signaling, and biomass accumulation are associated with increased resource capture and competitive success under favorable moisture conditions. In contrast, the dry ecotype shows enhanced expression of drought-tolerant genes involved in water retention, photosynthetic efficiency, and stress response mechanisms, enabling survival in arid environments. The lower panel illustrates the influence of experimental drought by rainouts on plant performance, trait variation, and gene expression. Our conceptual model highlights the role of gene-environment interactions in local adaptation and the importance of assessing both trait and transcriptomic data to understand the molecular basis of ecological success in plant communities.

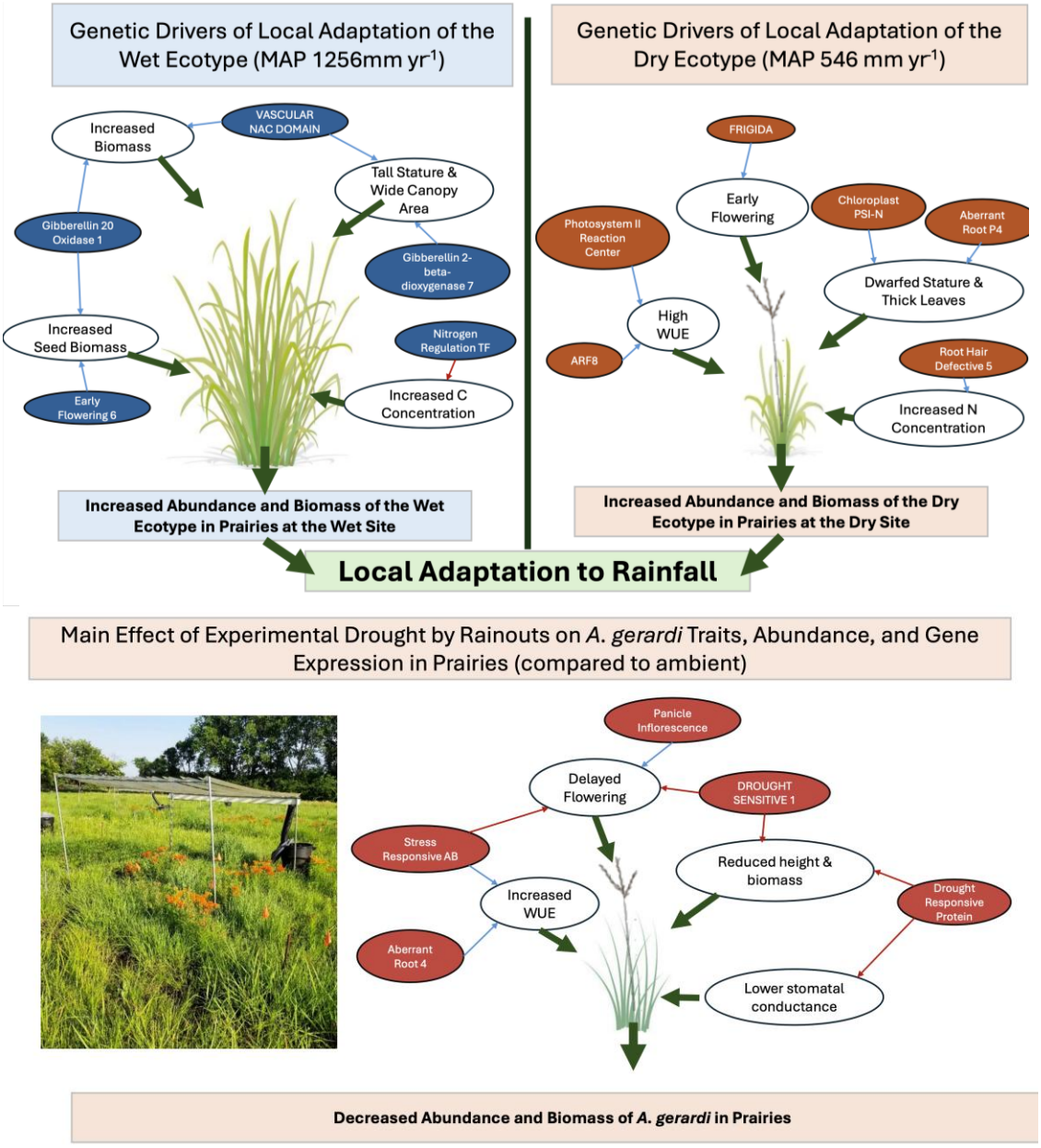

Supplemental Figure 1. Soil volumetric water content in each of the sites. A. driest, B. dry, C. mesic, and D. wet sites in 2022. Points indicate the mean of four blocks and error bars are the standard error. Ambient is indicated with blue and rainout treatment is indicated with red.

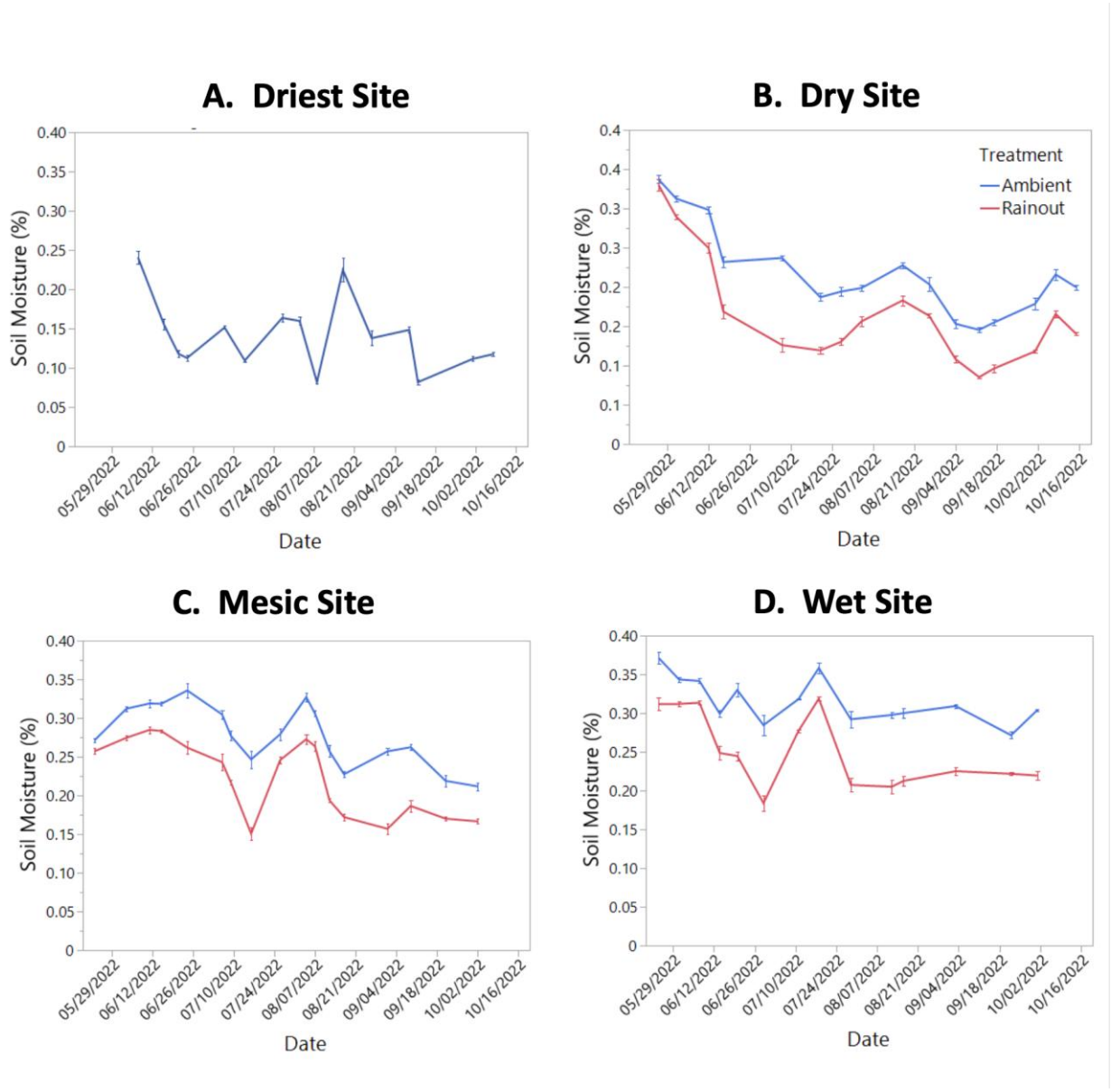

Supplemental Figure 2. Comparisons of community-level response variables. A. canopy cover and B. aboveground biomass in 2021. Ambient conditions are in blue, and rainout is in red. The points indicate the mean, error bars represent standard errors, and the different letters denote significantly differences between ecotypes and treatments within a site and year ($\alpha = 0.05$).

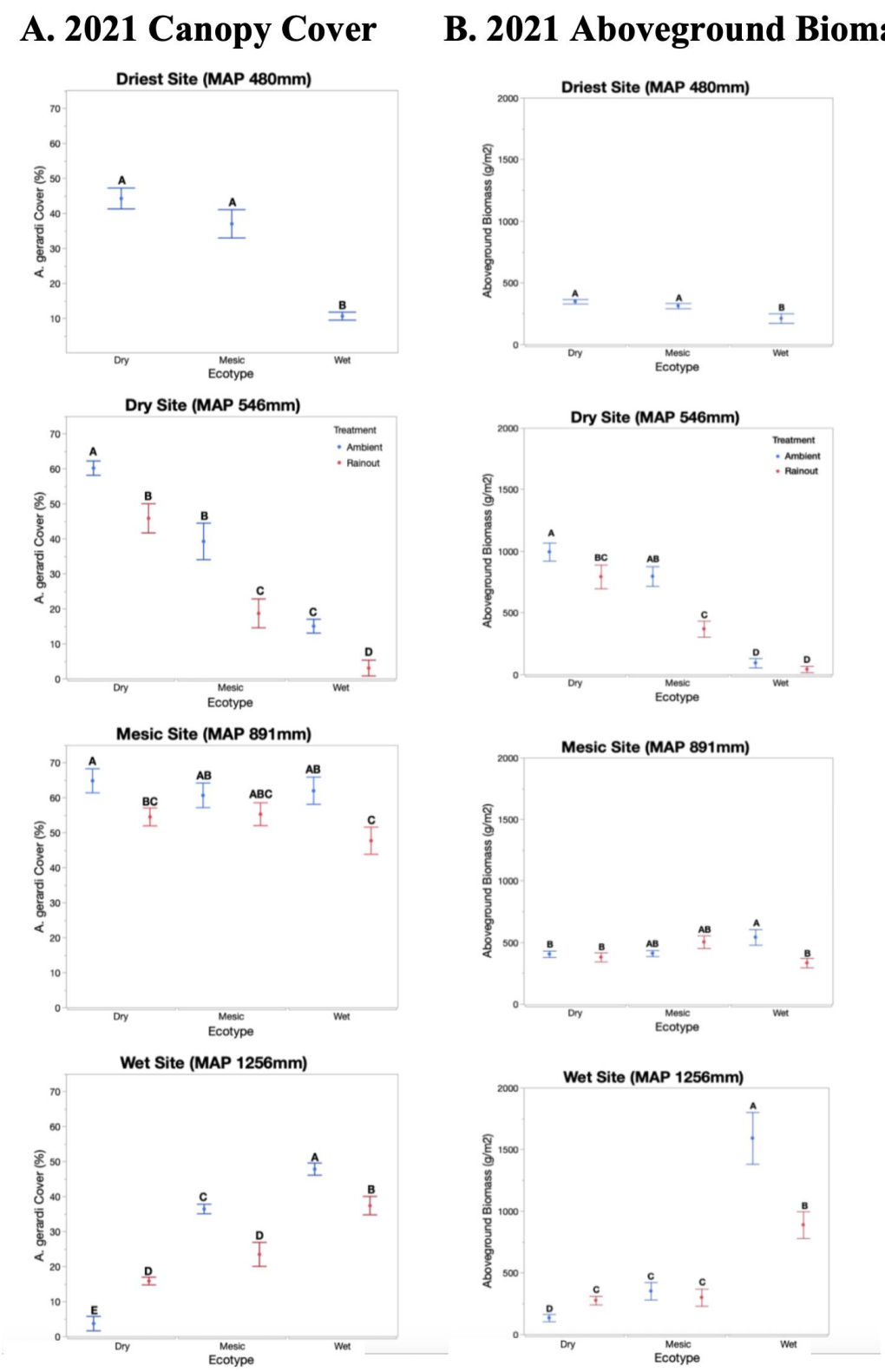

Supplemental Figure 3. Comparisons of traits. A. chlorophyll absorbance, B. stomatal conductance, C. transpiration rate, D. water use efficiency, E. blade width, F. seed biomass, G. total biomass, H. canopy diameter, I. leaf thickness, J. leaf nitrogen concentration, K. leaf carbon concentration, L. internal carbon dioxide concentration, and M. Julian date of bolting across sites (driest, dry, mesic, or wet) in peak season 2022. Ambient is blue, and rainout treatment is in red. The error bars represent standard errors, and the different letters denote significantly different groups among the comparisons within site ($\alpha = 0.05$).

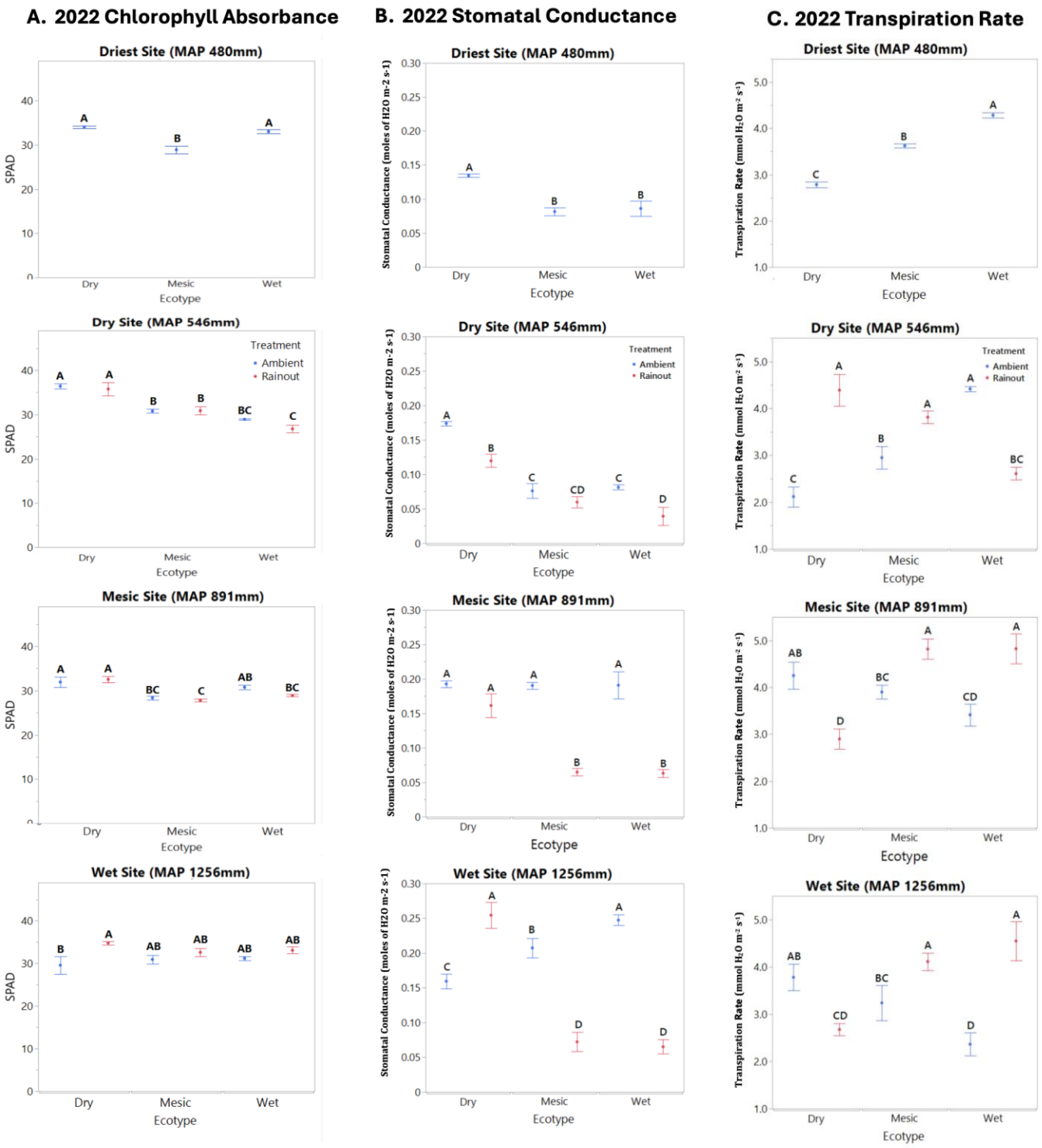

D. 2022 Water Use Efficiency

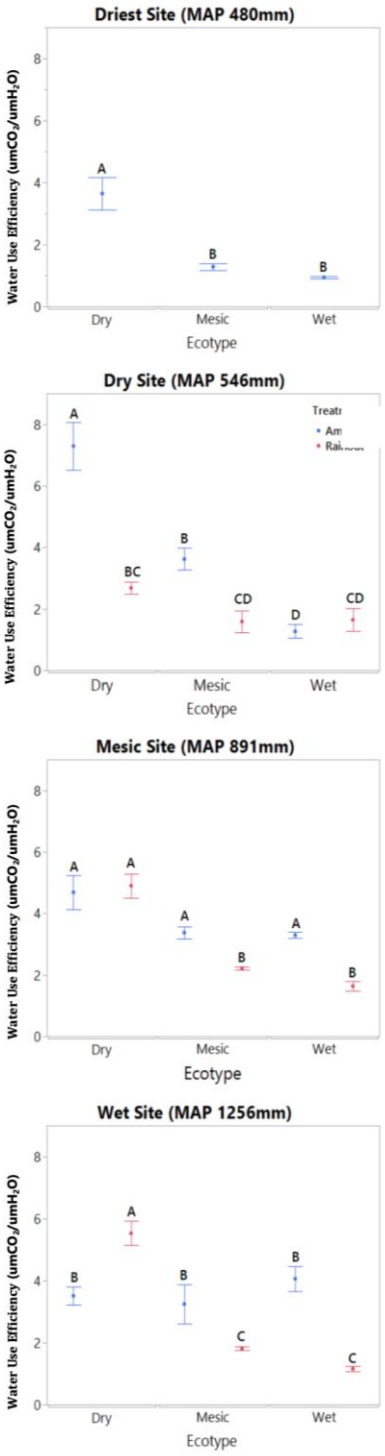

E. 2022 Blade Width

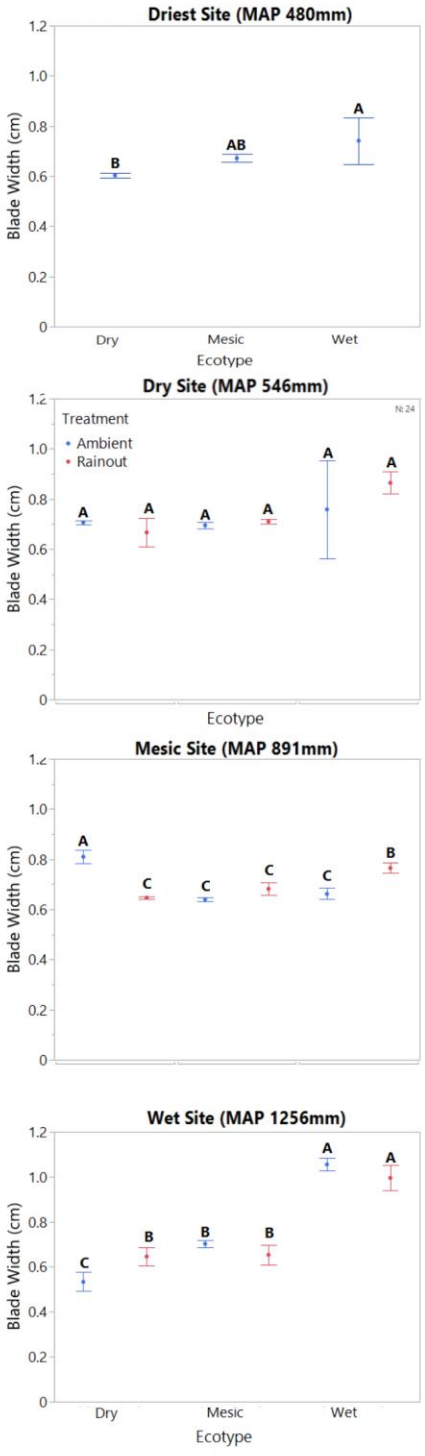

F. 2022 Seed Biomass

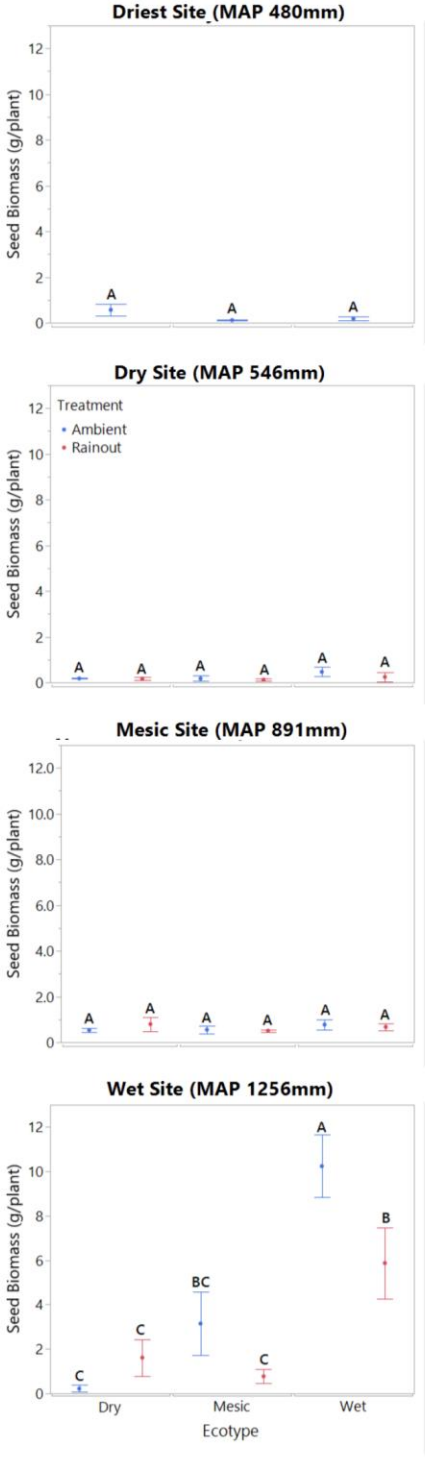

G. 2022 Total Biomass

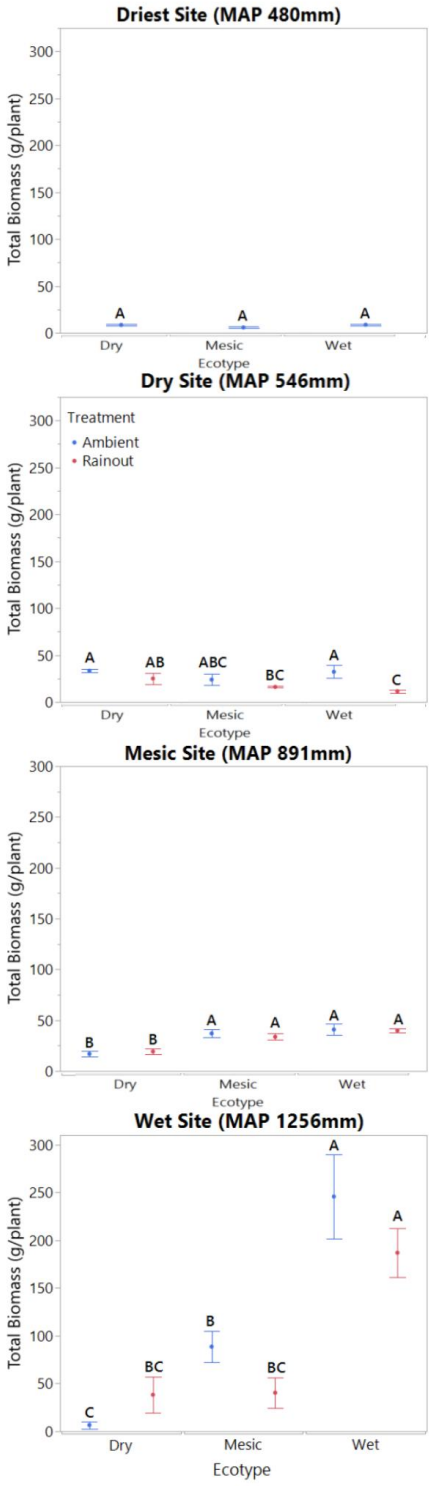

H. 2022 Canopy Diameter

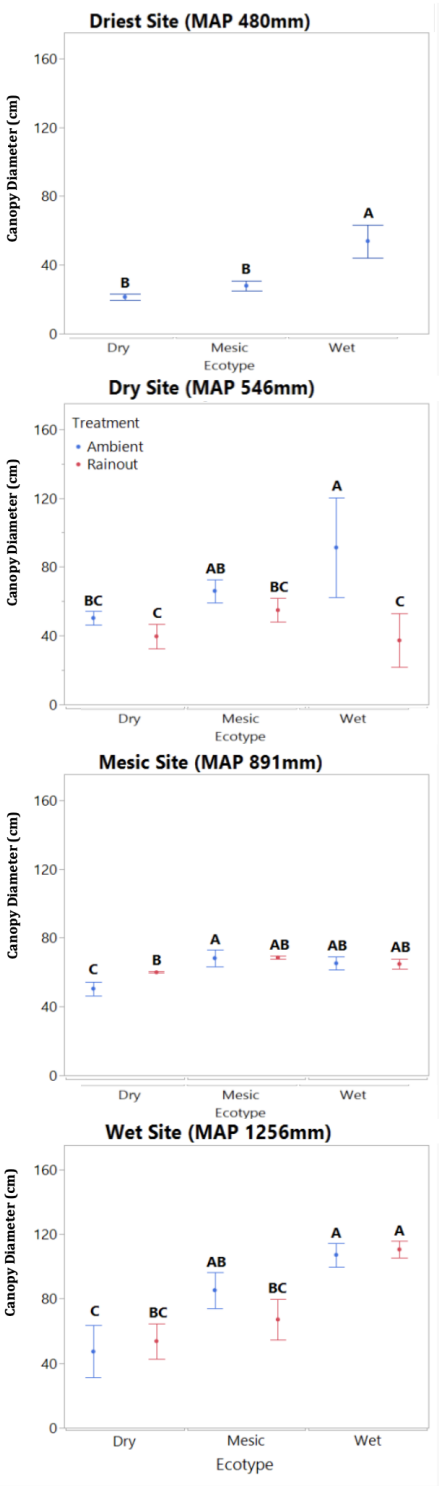

I. 2022 Leaf Thickness

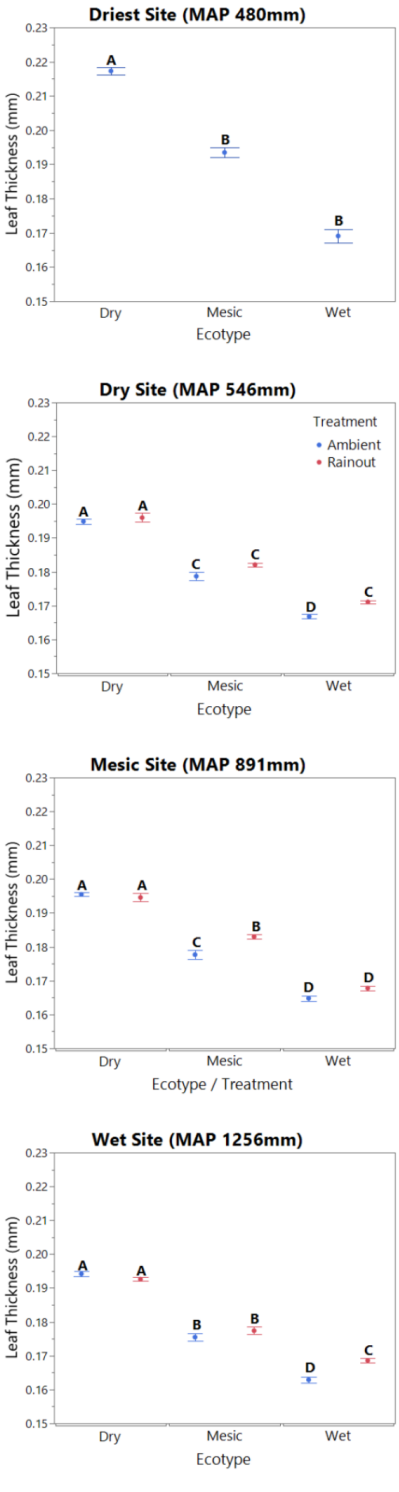

J. 2022 Nitrogen Concentration

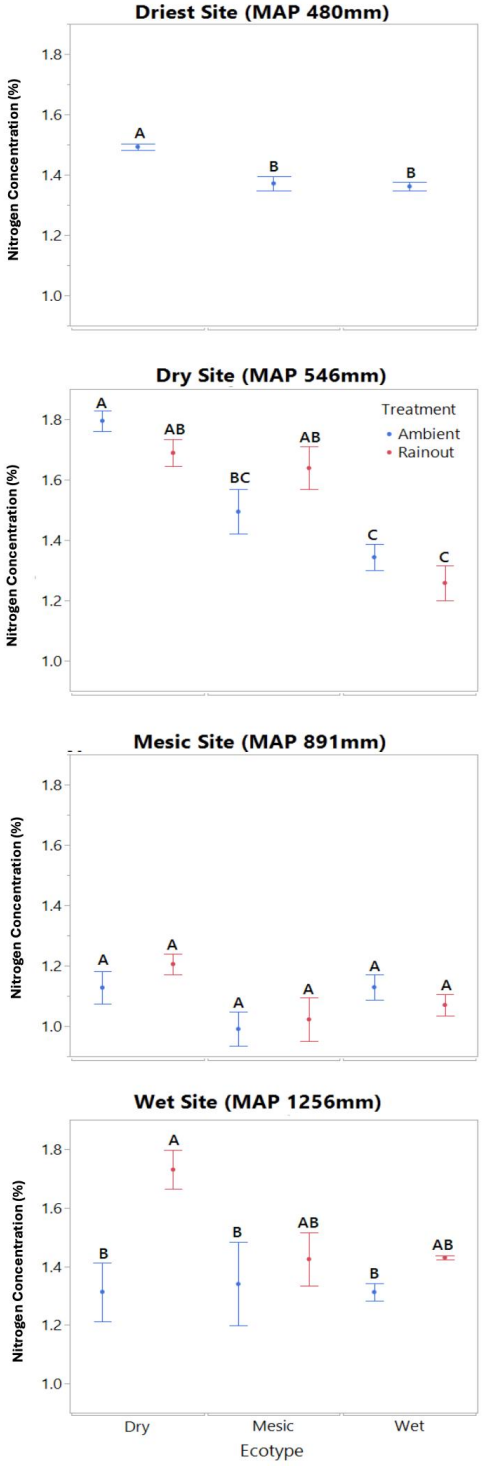

K. 2022 Carbon Concentration

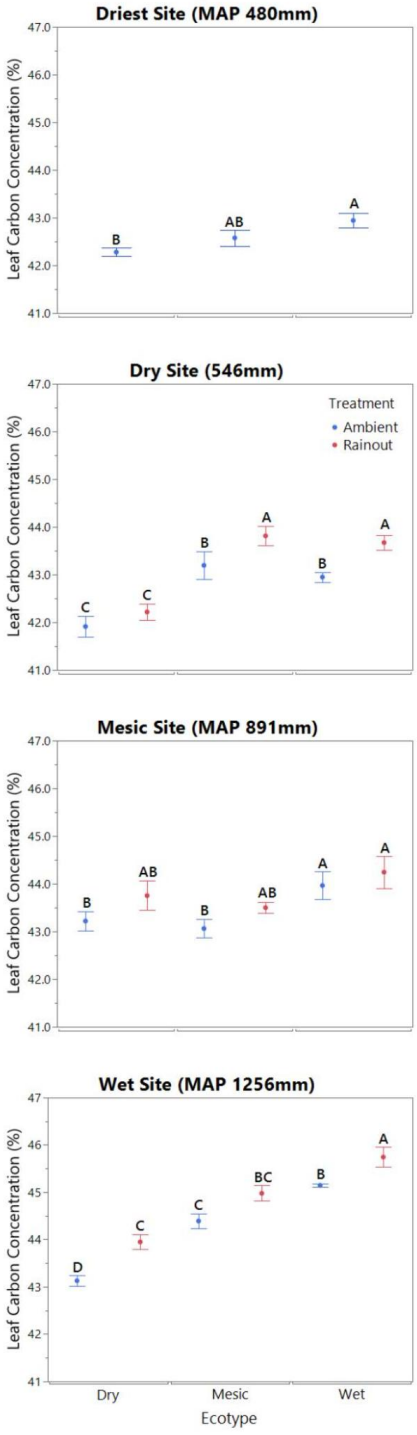

L. 2022 Internal CO_2 Concentration

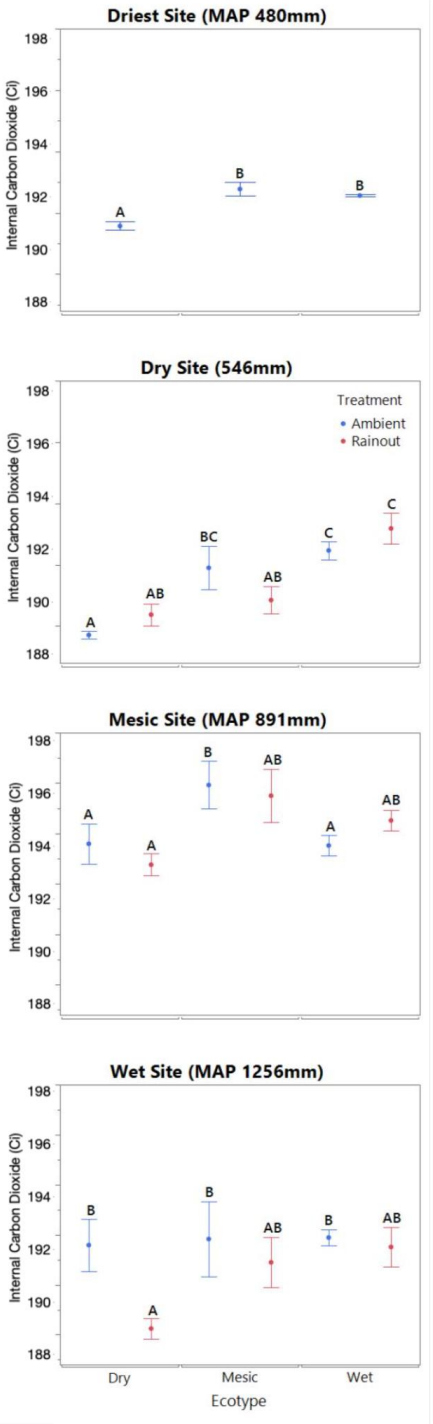

M. 2022 Date of Bolting

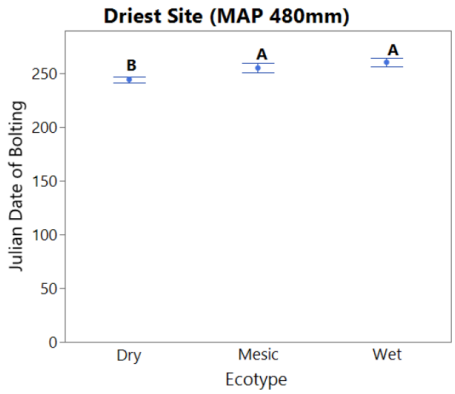

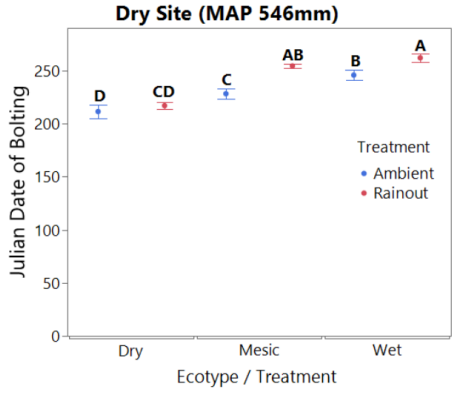

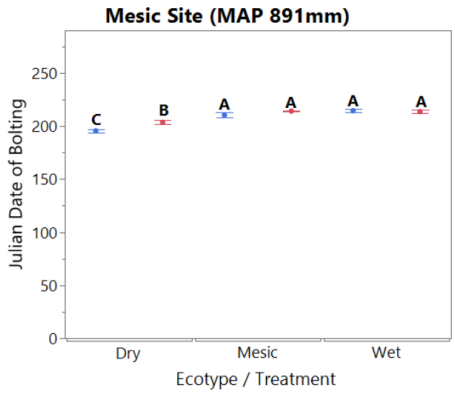

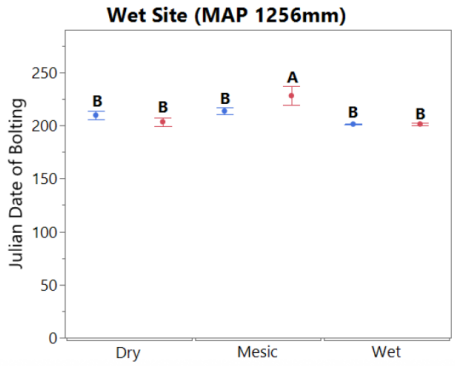

Supplemental Figure 4. Association between PCA axis 1 and annual precipitation across A. dry, B. mesic and C. wet ecotypes. This shows the relationship between the first principal component (PCA axis 1) and mean annual precipitation (MAP) across sites. Each panel presents a regression analysis to assess the correlation between PCA axis 1 and MAP within each ecotype. Data points represent the mean PCA axis 1 scores for each ecotype, and the regression lines indicate the trend in the relationship between PCA axis 1 and MAP.

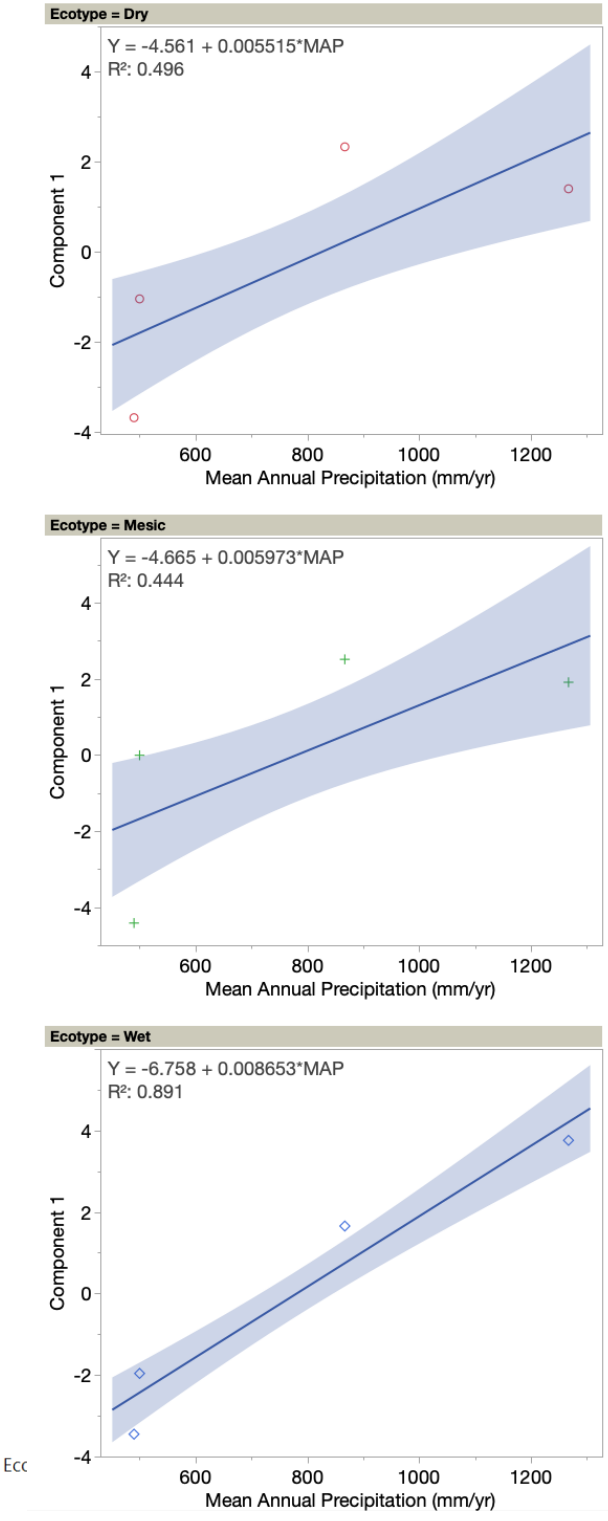

Table 3.1. A. Seed source of the dry, mesic, and wet ecotypes of *A. gerardi* sown into the reciprocal gardens.

Ecotype	Prairie	Size (ha)	County, State (USA)	Elevation (m)	Soil Type	Latitude	Longitude
Dry	Webster Reservoir	356	Rooks, KS	606	Wakeeney-Hamey Silt Loam	39.41	99.50
Dry	Saline Experimental Range	880	Ellis, KS	641	Bogue-Armo Clay Loam	38.76	99.14
Dry	Cedar Bluffs Reservoir	850	Trego, KS	688	Armo Clay Loam	38.76	99.83
Dry	Relict Prairie	14	Ellis, KS	640	Armo Gravelly Loam	38.85	99.37
Mesic	Konza Prairie	1557	Riley, KS	366	Benfield Silty Clay Loam	39.08	96.56
Mesic	Tallgrass National Preserve	4409	Chase, KS	392	Irwin Silty Clay Loam	38.25	96.60
Mesic	Carnahan Cove	99	Pottawatomie, KS	389	Benfield Silty Clay Loam	39.34	96.62
Mesic	Top of the World Park	61	Riley, KS	379	Orthents Silty Loam	39.22	96.62
Wet	Desoto Prairie	0.4	Jackson, IL	119	Orthents Silty Loam	37.85	89.14
Wet	Twelve Mile Prairie	28	Effingham, IL	160	Cisne Silty Loam	38.78	88.83
Wet	Walters Prairie	5	Jasper, IL	150	Atlas Silty Clay Loam	38.92	88.19
Wet	Fults Prairie	214	Monroe, IL	215	Menfro Wetty Clay Loam	38.17	90.19

Table 3.1**.** B. Site information of the reciprocal gardens.

Reciprocal Garden Site	Elevation (m)	Latitude	Longitude	Mean Annual Temp (C)	Soil Type	Mean Annual Precip (mm)	Annual Precip 2021 (mm)	Annual Precip 2022 (mm)
Colby, KS, KSU Ag Experimental Station (Thomas Co)	972	39.39	101.06	10.9	Ulysses Silt Loam	480	491.1	459.8
Hays, KS, KSU Ag Experimental Station (Ellis Co)	603	38.85	99.34	12.3	McCook Silt Loam	546	550.8	601.1
Manhattan, KS, USDA Plant Material Center (Riley Co)	315	39.19	96.58	12.8	Belvue Silt Loam	891	882.9	840.0
Carbondale, IL, SIU Ag Research Station (Jackson Co)	127	37.73	89.17	13.5	Story Silt Loam	1256	1279.8	1196.2

Table 3.2. A. Statistical response with main and interactive effect in early season 2022 at p<0.05.

Response variable	Site	Ecotype	Treatment	Significant Interactions
Morphological				
Plant Height	<.0001	0.006	<0.0001	Site x Eco: <0.0001 Site x Trt: 0.0009
Canopy Diameter	<0.0001	0.009	<0.0001	Eco x Site: 0.01 Site x Trt: <0.0001
Leaf Width	<0.0001	0.63	<0.0001	Eco x Site: <0.0001 Eco x Trt x Site: 0.02
Leaf Thickness	<0.0001	0.003	0.07	Eco x Site: 0.01 Eco x Site x Trt: <0.0001
Physiological				
SPAD	<0.0001	0.25	<0.0001	Eco x Site: 0.02 Trt x Site: <0.0001 Trt x Eco x Site: 0.002
Photosynthetic Rate	<0.0001	<0.0001	<0.0001	Site x Eco: 0.014 Trt x Site: <0.0001
Transpiration Rate	<0.0001	0.01	0.16	Site x Trt: <0.0001 Site x Eco x Trt: <0.0001
Stomatal Conductance	<0.0001	0.03	<0.0001	Trt x Site: <0.0001 Eco x Site x Trt: <0.0001
Water Use Efficiency	0.06	<0.0001	0.03	Eco x Site: <0.0001 Trt x Site: <0.0001 Eco x Site x Trt: <0.0001
Internal Carbon Dioxide Concentration	0.23	0.10	0.02	Trt x Site: <0.0001 Eco x Site x Trt: <0.0001
Reproductive				
Flowering	<0.0001	0.47	<0.0001	Eco x Site: <0.0001
Bolting	0.003	0.11	0.002	Eco x Site: 0.04

Table 3.2. B. Statistical response with main and interactive effect in peak season 2022 at p<0.05.

Response variable	Site	Ecotype	Treatment	Season	Significant Interactions
Morphological					
Plant Height	<.0001	<.0001	0.26	<0.0001	Site x Eco: <0.0001
Canopy Diameter	<0.0001	<0.0001	0.005	0.05	Eco x Site: 0.0005 Eco x Trt x Site :0.03
Leaf Width	0.02	<0.0001	0.39	0.26	Eco x Site: <0.0001 Eco x Trt x Site: 0.007
Nitrogen Concentration	<0.0001	<0.0001	0.06	N/A	Site x Trt: 0.008 Eco x Site: 0.002
Carbon Concentration	<0.0001	<0.0001	0.15	N/A	Eco x Site: <0.0001
Leaf Thickness	<0.0001	<0.001	0.74	0.54	Eco x Site: <0.0001 Trt x Site: 0.02 Trt x Site x Eco: 0.02
Physiological					
SPAD	0.0001	<0.0001	0.09	<0.0001	Seas x Site: <0.0001 Eco x Site: <0.0001 Trt x Site: 0.008
Photosynthetic Rate	<0.0001	<0.0001	0.0006	<0.0001	Site x Eco: 0.01 Trt x Site: 0.0008 Site x Eco x Trt: 0.01
Stomatal Conductance	0.01	<0.0001	0.09	<0.0001	Seas x Site: 0.001 Site x Eco x Trt: 0.01
Transpiration Rate	0.003	0.01	0.08	<0.0001	Eco x Site: 0.0005 Eco x Trt x Site :0.03
Water Use Efficiency	0.0001	<0.0001	0.002	<0.0001	Eco x Site: <0.0001 Eco x Trt x Site: 0.007

Internal Carbon Dioxide Concentration	0.02	<0.0001	0.06	0.04	Seas x Site: <0.0001 Site x Eco x Trt: 0.01
Reproductive					
Flowering	<0.0001	<0.0001	0.06	N/A	Eco x Site:0.0005
Bolting	0.04	0.005	0.01	N/A	Eco x Site: 0.01
2021 Cover	0.0001	0.07	<0.0001	N/A	Eco x Site: <0.0001 Site x Eco x Trt: 0.03
2022 Cover	0.02	0.12	<0.0001	N/A	Eco x Site: <0.0001 Site x Eco x Trt: 0.02
2021 Biomass	0.0008	0.37	0.04	N/A	Eco x Site: <0.0001 Site x Trt:0.02 Site x Eco x Trt: 0.01
2022 Biomass	<0.0001	0.10	0.07	N/A	Site x Eco x Trt: 0.02 Site x Eco: <0.0001

Table 3.2. C. Statistical response with main and interactive effect in late season 2022 at p<0.05.

Response variable	**Site**	**Ecotype**	**Treatment**	**Significant Interactions**
Morphological				
Plant Height	<.0001	0.02	0.29	Site x Eco: <0.0001 Site x Trt: 0.0009 Trt x Eco: 0.0009
Canopy Diameter	<0.0001	<0.0001	0.02	Eco x Site: <0.0001 Site x Trt: <0.0001 Eco x Trt x Site :0.001
Leaf Width	0.005	0.48	0.67	Eco x Site: <0.0001 Eco x Trt x Site: <0.0001
Leaf Thickness	0.25	0.008	0.007	Eco x Site: <0.0001 Eco x Trt x Site: <0.0001
Total Biomass	0.0003	0.04	0.08	Eco x Site: <0.0001 Eco x Trt x Site: <0.0001
Seed Biomass	0.001	0.24	0.08	Eco x Site: <0.0001 Site x Trt: 0.003 Eco x Trt x Site: <0.0001
Physiological				
SPAD	0.04	0.017	<0.0001	Seas x Site: <0.0001 Eco x Site: <0.0001 Trt x Site: <0.0001 Trt x Eco x Site: 0.014
Photosynthetic Rate	<0.0001	0.01	0.02	Site x Eco: <0.0001 Trt x Site: <0.0001 Site x Eco x Trt: 0.03
Transpiration Rate	<0.0001	0.01	0.02	Site x Trt: <0.0001 Site x Eco x Trt: <0.0001
Stomatal Conductance	0.0003	0.0002	<0.0001	Eco x Site: <0.0001 Trt x Site: 0.03 Eco x Site x Trt: <0.0001
Water Use Efficiency	0.006	0.04	0.15	Site x Eco: <0.0001 Trt x Site: <0.0001
Internal Carbon Dioxide Concentration	0.45	0.15	0.05	Site x Eco: 0.01 Trt x Site: 0.002 Site x Eco x Trt: <0.0001
Reproductive				
Flowering	<0.0001	0.009	0.10	Eco x Site: <0.0001 Eco x Site x Trt: 0.014
Bolting	0.03	0.16	0.41	Eco x Site: 0.01 Eco x Site x Trt: 0.04

Table 3.3. The total number of up- and down-regulated differentially expressed genes at all comparison points and at the individual comparison points for each ecotype (wet or dry), site (wet, dry, or driest), homesite (wet or dry homesite), and treatment (rainout or ambient).

Comparison	Upregulated genes (padj<0.05)	Downregulated genes (padj<0.05)	Total differentially expressed genes
Ecotype (dry vs wet)	6099 in dry ecotype	5,179	11,278
Dry Homesite	8404 in dry ecotype	8820	17,224
Wet Homesite	7,328 in dry ecotype	8,951	16,279
Site, Driest and Dry	672 in driest site	683	1,355
Site, Dry and Wet	12,956 in dry site	11,971	24,927
Site, Driest and Wet	4,631 in driest site	5,384	10,015
Treatment (ambient or rainout)	221 under rainouts	187	408

Table 3.4. Significantly enriched Gene Ontology (GO) terms among differentially expressed genes associated with the main effects of ecotype, site, and rainout treatment. Only GO terms with a false discovery rate (FDR) < 0.05 are included. GO term annotations were obtained using Blast2GO. "u" indicates GO terms enriched among upregulated genes, and "d" indicates enrichment among downregulated genes for each main effect.

Effect	Gene Function	GO Term
Wet Ecotype	flower bud (u)	GO:0060572
	auxin metabolism processes (u)	GO:0042446
	ATP generation/binding (u)	GO:0005524
	shoot system morphogenesis (u)	GO:0010016
	response to gibberellin (u)	GO:0009739
	gibberellic acid mediated signaling pathway (u)	GO:0009740
	vascular tissue generation (u)	GO:0001944
	RNA modification (u)	GO:0009451
	response to blue light (u)	GO:0009637
	trichome differentiation (u)	GO:0010026
Dry Ecotype	root differentiation (u)	GO:0015994
	plant organ senescence (u)	GO:0090693
	regulation of stomatal closure (u)	GO:0015994
	root hair cell differentiation (u)	GO:0048765
	electron transport in photosynthesis (u)	GO:0009767
	guard cell development (u)	GO:0010441
	root epidermis (u)	GO:0010054
	chlorophyll metabolic process (u)	GO:0015994
	stomatal complex development (u)	GO:0010374
	primary root growth (u)	GO:0080022
	defense response (u)	GO:0006952
	regulation of photoperiodism (u)	GO:0048573
	flowering (u)	GO:0048573
Wet Site	biosynthetic process (u)	GO:0008152
	metabolic processes (u)	GO:0008152
	regulation of biosynthetic process (u)	GO:0009889
	salicylic acid mediated signaling pathway (u)	GO:2000031
	cellular response to amino acid starvation (u)	GO:0034198
	abscisic acid catabolic process (d)	GO:0046345
	auxin response (u)	GO:0009733
	shoot system meristem (u)	GO:0010016
	reproductive bud (u)	GO:0009908
	vascular system (u)	GO:0010051
	chloroplast organization (u)	GO:0015994
Dry Site	primary root growth (u)	GO:0010102
	regulation of metabolism (d)	GO:0019222
	electron transporter (u)	GO:0009772
	defense responses (u)	GO:0006952
	DNA-binding transcription factor activity (d)	GO:0003700
	regulation of transcription (u)	GO:0006357
	stress response (u)	GO:0006952
	DNA repair (u)	GO:0006281

	root cap of primary root (u)	GO:0048829
	ATP binding (u)	GO:0005524
	hydrolase activity (u)	GO:0016787
	lateral root growth (u)	GO:0010102
Driest Site	Defense responses (u)	GO:0006952
	DNA-binding transcription factor activity (d)	GO:0003700
	cellular copper ion homeostasis (u)	GO:0006878
	abscisic acid transport (u)	GO:0080168
	programmed cell death (u)	GO:0012501
	lateral root tip (u)	GO:0048527
	chitinase activity (u)	GO:0004568
	flower bud (d)	GO:0048573
Wet Homesite	apical meristem growth (u)	GO:0040008
	seed maturation (u)	GO:0048573
	flower growth (u)	GO:0048573
	hormone metabolism processes (u)	GO:0006106
	shoot system morphogenesis (u)	GO:0010016
	response to gibberellin (u)	GO:0009739
	hormone extracellular transport (u)	GO:0006858
	gibberellic acid mediated signaling pathway (u)	GO:0009740
	response to hypoxia (u)	GO:0001666
Dry Homesite	pollen development (u)	GO:0010431
	regulation of metabolism (u)	GO:0019222
	electron transporter (u)	GO:0009772
	transferring electrons for photosynthesis activity (u)	GO:0009767
	guard cell development (u)	GO:0010377
	photosynthesis (u)	GO:0009658
	root epidermis (u)	GO:0010053
	abscisic acid-activated signaling pathway (u)	GO:0080168
	chloroplast modification (u)	GO:0009658
Rainout	root apical meristem (u)	GO:0048829
	chloroplast modification (u)	GO:0009507
	DNA damage checkpoint signaling (u)	GO:0000077
	heat shock protein signaling (u)	GO:0031072
	cellular water homeostasis (u)	GO:0009992
	negative regulation of meristematic growth (u)	GO:0010075
	root apical meristem (u)	GO:0010071
	acyl-CoA dehydrogenase activity (u)	GO:0003995
	lateral root cap (u)	GO:0048829
Ambient	vascular growth (u)	GO:0001944
	first order inflorescence axis (u)	GO:0009672
	stem epidermis (u)	GO:0090558
	hormone transport (u)	GO:0009914
	regulation of metabolism (u)	GO:0019222
	positive regulation of seed maturation (u)	GO:2000693
	intracellular monoatomic ion homeostasis (u)	GO:0006873
	regulation of growth (u)	GO:0040008

Table 3.5. List of selected candidate genes identified across ecotypes, sites, treatment, and homesite. The table includes gene annotations, associated Gene Ontology (GO) terms, and fold change values indicating the direction and magnitude of differential expression.

Effect	Gene	Annotation	GO Term	Fold Change
Ecotype	06BG063200	abscisic stress-ripening	0006950	+3.57
Dry Ecotype	05BG130400	3-ketoacyl-CoA synthase	0006633	+5.47
	04BG198300	*ARF16*	0005524	+6.29
	01CG411500	chloroplastic drought-induced stress protein	0045454	+6.34
	02CG047700	Chlorophyll A-B binding family protein	0005515	+6.11
	09CG201100	heat shock protein 17.4	0006950	+6.92
	04AG294100	chloroplasts 55-II	0016491	+5.44
	04BG127400	salt stress root protein RS1	0051716	+4.02
	07BG164800	rotamase FKBP 1	0006457	+6.47
	05AG094300	Heat shock protein 22H	0005515	+5.06
	01CG303500	SAUR-like auxin-responsive protein	0009733	+4.44
	09BG190100	indole-3-butyric acid response 1	0008667	+4.39
	10CG027000	early nodulin 93	0016757	+4.31
	10AG161400	multiprotein bridging factor 1C	0043565	+4.24
Ecotype	02AG195700	gibberellin receptor GID1L2	0016491	+4.52
Wet Ecotype	03CG144300	auxin response factor 75	0006281	+3.15
	05BG011300	WRKY64	0006355	+4.11
	03BG273300	gibberellin 2-oxidase 1	0005506	+3.90
	01CG090600	BEL1-like homeodomain 4	0006355	+3.23
	01CG314300	myb domain protein 94	0003677	+4.10
	08CG126900	Auxin-responsive Aux/IAA gene family	0005634	+4.46
	03CG275000	HVT1 Vascular Tissue Tapetum	0005524	+4.09
	10BG199700	auxin response factor 16	0005634	+3.20
	01CG072700	GASR3	0008080	+4.78
	02AG291100	gibberellin-responsive protein	0008080	+3.06
Site	03AG057500	FASCICLIN-like arabinogalactan-protein 11	0006351	-3.11
Dry Site	01AG088000	senescence-associated gene 12	0008234	+4.20
	04BG038400	STRUBBELIG-RECEPTOR FAMILY 1	0008324	+3.87
	01AG264300	transcription factor MYC7E	0004559	+3.01
	08BG013400	GRAS transcription factor	0055114	-4.15
	06BG118800	TRS120	0003676	-3.64
	07CG097100	phototropin 2	0004672	+3.05
	05CG174200	Stigma-specific Stig1	0003723	-4.09
	02CG360600	Ethylene insensitive 3	0003700	+4.60
	03BG256400	senescence-associated protein	0050662	+3.22
	04AG218300	cold-regulated 47	0009415	-4.06
	10AG102800	heat shock protein DnaJ	0008168	+3.44
	06AG010600	heat shock protein 90.1	0006457	+6.13
Site	10AG189900	alpha/beta-Hydrolases	0008236	-9.06
Wet Site	02AG172700	auxin-repressed protein	0009733	-6.14
	02AG115500	aquaporin protein 2	0005215	+3.25
	03CG094900	DNAJ Heat Shock 20	0005743	+3.12
	09AG005900	auxin-induced protein 5NG4	0016021	+5.14
	07BG171400	ascorbate peroxidase 6	0055114	-3.21
	05BG105600	BRASSINOSTEROID INSENSITIVE 1	0005515	+3.81
	10AG218700	Amidase 1	0016884	+3.31
	02BG022000	photosynthetic electron transfer A	0009055	+5.44
	01AG387800	MYB family transcription factor	0003677	+3.74
	04AG206000	aldehyde dehydrogenase 3F1	0004030	-3.11
Site	03BG150100	hypoxia-responsive family protein	0020037	-6.94
Driest Site	07CG071600	photosystem II subunit	0009523	+4.78
	04AG268100	Chloroplast ATP synthase delta chain	0046933	-3.75
	04BG108300	Flowering Locus T gene	0006468	-4.64
	10AG184500	cytochrome P450	0005506	+3.37
	06CG013300	heat shock protein 90.1	0006457	-4.72

	04AG254400	ATP-BINDING TRANSPORTER ABC	0016020	+3.45
	02AG115600	aquaporin protein	0006810	+6.73
	02AG053400	SHOOT1 protein	0005515	+6.09
	03BG135200	universal stress protein domain	0006950	+5.18
	05BG075500	gibberellin receptor G3	0055114	-4.49
Rainout Main effect	05AG211000	stachyose synthase	0003824	+5.28
	02CG154300	armadillo/beta-catenin	0005488	+5.87
	03BG099300	stress responsive protein	0006355	+6.27
	03BG099200	no apical meristem protein	0003677	+3.40
	01AG088000	senescence-associated gene 12	0008234	+3.44
	04CG017700	DROUGHT SENSITIVE 1	0005506	+3.13
	07AG141100	panicle inflorescence	0005515	+3.79
	03BG198000	stress responsive A/B Barrel	0005515	+3.75
	10BG085100	annexin 7	0005509	+4.03
Ambient Main effect	03BG392900	glutathione S-transferase TAU 8	0005515	-5.52
	03CG305900	NAC Transcription Factor	0006355	+5.61
	04CG017700	Abscisic acid-responsive (TB2/DP1, HVA22)	0005515	-4.98
	03CG188600	MADS14	0003676	-3.05
	03BG161400	EX07A2	0000145	-3.14
	03CG380400	ALOG2 Shoot Apical Meristem	0003676	+3.40
	03CG182000	FLOWERING LOCUS C	0003676	+3.45
	03BG381500	Haloacid dehalogenase (HAD)	0000287	-3.51
	03CG182300	Albino Leaf 2	0003676	-3.15
	09CG098800	Dehydrin	0009415	-3.91
Homesite Dry Ecotype x Dry Site	03AG271600	Flowering Locus T	0003676	+5.22
	08BG118900	FRIGIDA-like protein	0005509	+3.17
	06CG133000	Photosystem II reaction center PsbP protein	0005488	+3.26
	01BG420000	heat shock protein 17.4	0005515	+4.47
	10BG141200	DAWDLE	0005515	+6.52
	04CG269300	heat shock 22 kDa protein	0005515	+5.86
	04AG159700	STRUBBELIG-RECEPTOR FAMILY 7	0004713	+6.26
	02BG224700	Chaperonin	0006457	+6.10
	02BG224200	photosystem I light harvesting complex gene 6	0016020	+6.46
	05AG023100	acyl-CoA synthetase protein	0008152	+5.27
	06AG091500	auxin response factor 1	0005634	+3.15
	07BG137500	EXPANSIN-A1	0009664	+4.76
	03BG188700	Chaperone DnaJ	0005515	+4.69
	02AG130800	flowering time control protein FCA	0003676	+3.12
Homesite Wet Ecotype x Wet Site	09AG131900	gibberellin receptor GID1L2	0016787	+4.49
	02CG241200	SAUR-like auxin-responsive protein	0009733	+3.71
	05BG170800	SCARECROW	0005202	+3.43
	01AG142600	Auxin-responsive gene family	0009733	+4.11
	08BG148200	senescence-related gene 1	0055114	-3.55
	03CG003900	growth-regulating factor 5	0005524	-3.58
	03CG122300	Plant regulator RWP-RK family protein	0003677	+3.99
	03CG017400	HMG box protein with ARID/BRIGHT	0003676	+4.12
	03CG014300	histone H3	0003676	-3.45
	06AG110600	GASR4 - Gibberellin-regulated GASA	0008080	+3.07

Table 3.6. The DEGs co-expressed with plant phenotype and their candidate genes associated, annotation, WGCNA cluster number, and GO term. Phenotype abbreviations: Ph= Photosynthetic Rate, Co= Stomatal conductance, Tr=Transpiration Rate, Wu= Water Use Efficiency, Sp= SPAD, Ci= Internal Carbon Dioxide Concentration, Bw=Blade Width, Rg= Relative Growth Rate, He=Height, Th= Leaf Thickness, Di= Canopy Diameter, Sb=Seed biomass, Tb=Total Biomass, Nc= Leaf Nitrogen Concentration, Cc= Leaf Carbon Concentration, Bo=Bolting, and Fl=Flowering.

Effect	Gene	Annotation	Gene Ontology	Phenotype(s) code	Cluster (Fig S10)	Fold Change
Ecotype Dry Ecotype	04BG198300	*ARF16*	0005524	Tr, Ci, He, Rg, Cc	33	+6.29
	09CG180800	chlorophyll A-B binding protein	0009765	Tr, Ci, He	26	+4.40
	02CG351100	drought induced protein 19	0003676	Ci, Wi, Nc, Cc	26	+3.98
	01CG411500	chloroplastic drought-induced stress protein	0045454	Tr, Ci, He	26	+3.34
	03AG366700	thylakoid lumenal protein, chloroplast precursor	0008152	Tr, Ci, He, Cc	33	+3.17
	01CG308200	HVA22	0045454	Tr, Ci, He, Cc	33	+3.11
	08AG143200	SNF2	0005524	Wi, Th, Tb	12	-2.99
	08AG043900	LPTL	0008270	Ci, Wi, Nc, Cc	19	+3.36
	08AG131200	Calmodulin	0005516	Wi	1	+3.47
	04AG325000	Bzip txn factor	0043565	Tr, Ci, He	26	+3.55
	09AG159900	Thioredoxin	0045454	Tr, Ci, He, Cc	33	+3.87
	08AG074800	DREB2A	0046872	Ci, He	13	+4.15
	08AG174800	Chaperonin 60	0042026	Tr, Ci, He, Rg, Cc	33	-3.66
Ecotype Wet Ecotype	10BG190500	PAPA-1-like conserved family protein	0031011	Ph, Tr, Wu, Rg, He, Di, Sb, Tb, Cc, Bo, Fl	8	+3.61
	01AG027500	GASR3 - Gibberellin-regulated family protein	0016491	Ph, Tr, Wu, Rg, He, Di, Sb, Tb, Cc	29	+3.98
	03AG306700	cellular response to gibberellin	0016491	Ph, Tr, Wu, Rg, He, Di, Sb, Tb, Cc	29	+3.37
	03BG134600	SH2 motif	0006139	Ph, Tr, Wu, Rg, He, Di, Sb, Tb, Cc, Bo, Fl	8	+3.67
	03CG144300	ARF-75	0006281	Ph, Co Tr, Wu, Rg, Sb, Tb, Cc, Bo, Fl	11	+3.15
	10AG219900	gibberellin 2-oxidase 1	0030896	Ph, Co Tr, Wu, Rg, Sb, Tb, Cc, Bo, Fl	30	+4.11
	04AG308700	basic leucine zipper 9 Transcription Factor	0003700	Di, Cc, Nc	30	+3.45
	10BG070600	nudix hydrolase homolog 3	0016787	Co, Tr, Wu, Ci, Rg, Sb, Tb, Bo, Fl	3	+3.97
	10BG153500	14-3-3 Protein	0019904	Ph, Co Tr, Wu, Rg, Sb, Tb, Cc, Bo, Fl	9	-3.59
	10BG150800	OMP85 family protein	0019867	Ph, Co Tr, Wu, Rg, Sb, Tb, Cc, Bo, Fl	11	+5.37
	03CG144300	PHABULOSA	0032784	Ph, Co Tr, Wu, Rg, Sb, Tb, Cc, Bo, Fl	11	+3.88
	10BG155600	B4FSM0, Anther-specific protein APG	0048653	Ph, Co Tr, Wu, Rg, Sb, Tb, Cc, Bo, Fl	11	+3.06
Site Dry Site	07AG194100	DROUGHT SENSITIVE 1	0005515	Ph, Co, Rg	5	+3.83
	06CG148400	DNAJ heat shock N-terminal protein	0003677	He, Sb	11	+3.45
	03BG201200	growth inhibition & differentiation protein 88	0005506	Co, Nc, Cc, Bo	4	+4.24
	04AG059600	XPB2	0003677	Ph, Co, Rg	5	+3.97
	07AG184300	heat shock protein STI	0005515	Co, Nc, Cc, Bo	4	+3.15
	03CG129700	Drought-responsive family protein	0003676	Co, Sb	6	+3.57
	05CG083100	CLAVATA1	0004672	Co, Sb	6	+4.77
	05CG144800	MRH1	0004672	Th	8	-3.56
	05CG160700	DUF26	0004672	Th	8	+3.68
	05CG091400	RPS2 protein	0003684	He, Sb	11	+4.11
	03CG062100	heat shock protein ATPase	0001671	He, Sb	11	+3.07
	05CG022600	STRUBBELIG-RECEPTOR FAMILY 7	0004672	Sp	18	+3.95
Site Wet Site	03BG175900	phytochrome C	0000155	Nc, Cc	2	+3.12
	08AG163200	growth-regulating factor	0005524	He, Di	8	+3.07
	03BG285900	flowering time control protein FCA	0000166	He, Di	8	+3.71
	04BG018000	chloroplast splicing factor CRS1	0003723	He, Di	8	+3.50
	04CG101100	DWARF1	0003824	Nc, Cc	2	-3.45
	04BG203700	light-mediated development protein DET1	0003824	He, Di	8	+4.97
	08AG138500	PSI-N	0005516	He	5	+4.22
	04CG097900	DIMINUTO	0003824	He, Di	8	-3.69
	03BG173900	ethylene receptor	0000155	He, Di	8	+3.99
	03BG271200	translation initiation factor 3B1	0000166	He, Di	8	+3.95
	03CG181700	RNA Binding flowering time control	0003676	Bo	10	-3.88
	03BG247900	RRM/RBD/RNP motifs family protein	0000166	Wi	15	+3.22
	03BG361500	beta-amylase 7	0000272	Bo	16	-3.17
Site Driest Site	04CG002300	3-ketoacyl-CoA synthase precursor	0003824	Nc, Cc	5	+4.94
	03CG339100	OsLonP2 protease	0003684	He, Di	12	+3.66
	03CG336100	AP2/B3-like transcriptional factor protein	0003677	He, Di	12	+3.08
	04CG023900	hydrolase, alpha/beta fold family	0003824	Bo	14	+3.96
	03CG334200	GROWTH INHIBITION	0000166	Nc	22	+4.88
	03CG331900	chalcone synthase	0003824	He, Cc	24	-3.15
	04CG056200	OPC-8:0 CoA ligase1	0003824	Rg, He, Di, Bo	26	+3.88
	03BG188900	two-component response regulator	0000160	He, Di	12	+3.55
	04CG016400	methyl-CpG binding domain	0003677	He, Di	12	+3.96
Rainout Main effect	06BG244400	aberrant root formation protein 4	0005488	Ph, Co, Tr, Wu, Rg, He, Tb, Nc, Bo	3	+3.93
	07AG210300	stress responsive A/B Barrel	0005515	Ph, Co, Tr, Wu, Rg, He, Tb, Nc, Bo	3	+3.75
	07AG141100	DROUGHT SENSITIVE 1	0005506	Ph, Co, Tr, Wu, Rg, He, Tb, Nc, Bo	3	+3.13
	06CG056900	Drought-responsive family protein	0005515	Ph, Co, Tr, Wu, Rg, He, Tb, Nc, Bo	3	+3.04
	06BG244100	Impaired sucrose induction 1	0005488	Ph, Co, Tr, Wu, Rg, He, Tb, Nc, Bo	3	+4.99

	07AG210300	stress-inducible protein	0000166	Ph, Co, Tr, Wu, Rg, He, Tb, Nc, Bo	3	+3.67
	03BG198000	panicle inflorescence	0005515	Ph, Co, Tr, Wu, Rg, He, Tb, Nc, Bo	3	+3.79
	06BG244300	ALF4-1	0005488	Ph, Co, Tr, Wu, Rg, He, Tb, Nc, Bo	3	-3.97
Ambient Main effect	03CG182300	Albino Leaf 2	0003676	Ph, Tr, Ci, Bo, Fl	3	-3.15
	03CG182000	FLOWERING LOCUS C	0003676	Sp	1	+3.45
	03BG381500	Haloacid dehalogenase (HAD)	0000287	Sp	1	-3.51
	03BG258200	SC35	0000166	Sp	1	+3.94
	03CG188600	MADS14	0003676	Tb	7	-3.05
	03BG161400	EX07A2	0000145	Sp	1	-3.14
	03CG380400	ALOG2 Shoot Apical Meristem	0003676	Ph, Tr, Ci, Bo, Fl	3	+3.40
	03CG178300	BFN1	0003676	Ph, Tr, Ci, Bo, Fl	3	-3.66
Homesite Dry Ecotype x Dry Site	08BG113900	expansin B2	0005576	Tr, Wu, Ci, Rg, Tb, Nc, Cc, Bo, Fl	10	+3.08
	08BG118900	FRIGIDA-like protein	0005509	Wu, Wi, Tb, Nc, Cc, Bo	16	+3.17
	06CG133000	Photosystem II reaction center PsbP protein	0005488	Ph, Co, Wu, Ci, Rg	9	+3.26
	06BG242400	aberrant root formation P4	0005525	St, He, Sb	17	+3.02
	08BG071800	Root hair defective 5	0005525	Tr, Wu, Ci, Rg, Tb, Nc, Cc, Bo, Fl	10	-3.94
	08BG159100	auxin response factor 8	0005634	Ph, Co, Wu, Ci, Rg	9	+3.91
	08AG085500	chloroplast signal recognition (CAO)	0005515	Ph, Co, Wu, Ci, Rg	9	+4.12
	08BG154800	transcription factor jumonji	0005634	Sp, Th	20	+2.05
	08AG138400	chloroplast PSI-N	0005516	Sp, Th	20	+3.47
	08BG154700	chloroplast import apparatus 2	0005509	Ph, Co, Rg	6	+3.46
	08BG138600	CCT/B-box zinc finger protein	0005622	Co, He, Sb	17	+3.87
	08BG130200	SNARE-like superfamily protein	0005622	Ph, Co, Rg	6	+3.95
	08BG113800	EXPANSIN-A1	0005576	Tr, Wu, Ci, Rg, Tb, Nc, Cc, Bo, Fl	10	+3.66
Homesite Wet Ecotype x Wet Site	03CG374700	myb family transcription factor	0003677	Bo	2	+3.01
	04AG186600	cup-shaped cotyledon 3	0000413	Ph, Co, Tr, Wu, Ci, Nc, Cc, Bo, Sb, Fl	23	+3.42
	03CG190500	PINHEAD	0003676	Ph, Co, Tr, Wu, Sp, Rg, He, Di, Fl	25	+4.05
	06CG068600	gibberellin 2-beta-dioxygenase 7	0003677	Ph, Co, Tr, Wu, Rg, He, Di, Sb, Tb, Bo, Fl	6	+3.96
	06CG071100	gibberellin 20 oxidase 1	0003676	Ph, Co, Tr, Wu, Rg, He, Di, Sb, Tb, Nc, Cc,	5	+3.66
	03CG351600	nitrogen metabolism transcription factor	0003677	Nc	26	+5.16
	03CG003900	growth-regulating factor 5	0005524	Nc	26	-3.58
	03CG122300	Plant regulator RWP-RK family protein	0003677	Nc	26	+3.99
	03CG017400	HMG box protein with ARID/BRIGHT	0003676	Nc	26	+4.12
	03CG014300	histone H3	0003676	Nc	26	-3.45
	03CG190500	DCL3	0003676	Nc	25	-4.00
	03CG326800	TRF-like 6	0003677	Ph, Co, Tr, Wu, Sp, Rg, He, Di, Fl	23	+3.22
	04AG185300	no apical meristem protein	0000413	Ph, Co, Tr, Wu, Ci, Nc, Cc, Bo, Sb, Fl	23	-3.76
	04AG182900	VASCULAR-RELATED NAC-DOMAIN 6	0003676	Ph, Co, Tr, Wu, Ci, Nc, Cc, Bo, Sb, Fl	23	+4.21
	03CG242200	cyclophilin 38	0000413	Ph, Co, Tr, Wu, Ci, Nc, Cc, Bo, Sb, Fl	23	+3.28
	03CG402000	growth-regulating factor 3	0005524	Ph, Co, Tr, Wu, Ci, Nc, Cc, Bo, Sb, Fl	23	+3.83
	03CG127400	early flowering 6	0003676	Ph, Co, Tr, Wu, Ci, Nc, Cc, Bo, Sb, Fl	23	+3.26
	03CG388900	ethylene-responsive transcription factor	0003676	Di	17	+4.79

Methods S1: Extraction and Mapping

Total RNA was isolated and purified using the QIAGEN RNeasy kit according to the manufacturer's recommended protocol for plants. The concentration and purity of total RNA was evaluated on the Nanodrop Spectrophotometer (Thermo Scientific). The intactness of RNA samples was assessed using the Agilent Bioanalyzer 2100 (Agilent Technologies). To eliminate genomic DNA contamination of the RNA samples were treated with RNase-Free DNase I (Qiagen). cDNA libraries were constructed from messenger RNA and prepared for sequencing on the Illumina NovaSeq 600 in two lanes. The pooled libraries were then loaded onto Illumina NovaSeq 600 at a concentration of 14 pM and sequenced for 100 cycles from each end of the fragments plus 7 cycles for the index read according to the manufacturer's instructions (Illumina, San Diego, CA). Raw files were converted to fastq files with Casava 1.8.2. Average quality scores were ≥30 across sequencing cycles and reads were 150 bp in length.

Prior to mapping, raw reads were processed using Trimmomatic v.0.33 (Bolger et al., 2014) to remove adapters and the quality of resulting trimmed and cleaned reads was assessed using *FastQC v0.11.9 (*Andrews, 2010). Reads were then mapped to the assembly version of the *Andropogon gerardi* Hap2 v1.1 genome (Joint Genomics Institute, 2023) using the splice-aware mapper Hitsat2 v.2.0.0 (Wen, 2017). We used HiSat2 (Wen, 2017) to index the reference genome and each of the individual samples was mapped to the indexed reference genome. Next, gene counts were obtained using the *feature Counts (*Liao et al., 2014) procedure as implemented in HISat2 (Wen, 2017).

Chapter 4 - Testing core vs. margin paradigms: Abundance, traits, and genetic patterns of a dominant grass across a broad native range

Running Title: Range-Wide Trait and Genetic Variation of a Dominant Grass

Authors: Jack Sytsma[1], Allison Louthan[1], Helen Winters[1], Matthew Galliart[2], Adam B. Smith[3], Erica Newman[3,4,5], Sonny Lee[1], Ari Jumpponen[1], Brooke Vogt[1], Anna Kazarina[1], and Loretta Johnson[1]

Institutions: [1]Division of Biology, Kansas State University; [2]Department of Biological Sciences, Fort Hays State University; [3]The Missouri Botanical Garden; [4]Department of Integrative Biology, University of Texas at Austin; [5]James Madison University

Abstract

The Abundant Center Hypothesis (ACH) predicts species' abundances are highest in the range core and decline towards margins. By extension, fitness-related traits and genetic diversity may follow the same trends. Alternatively, abundance and traits may differ along environmental clines (Clinal Pattern Model, CPM), irrespective of range position. We tested the ACH and CPM using *Andropogon gerardi* (big bluestem; Poaceae), a widespread perennial grass of North America. Our objectives were to define the core distribution, to measure abundance and functional traits and to evaluate genetic diversity across its range. We modeled the species' climatic suitability to define the core, then measured abundance and traits using 26 field populations across the range of *A. gerardi*, spanning broad temperature (4-21°C, North Dakota-Texas, US) and rainfall (418-1467 mm yr^{-1}, Colorado-North Carolina) gradients. We hypothesized that abundance and genetic diversity would peak in the core (ACH), whereas traits would vary along environmental clines (CPM), and arid populations would possess drought-tolerant traits (higher water-use efficiency, reduced stature), whereas mesic populations would favor competitive traits (greater height, broader leaves). Following the ACH, abundance and genetic diversity were highest in the core compared to non-core sites. In contrast, functional traits followed the CPM, increasing linearly with precipitation or aridity, but not temperature alone. Arid populations showed drought-adaptive traits (increased water-use efficiency, thicker leaves), whereas mesic populations had competitive traits (greater height and biomass). We present a compelling case study that tests the long-standing ACH concept using a widespread species across ~2100 km and broad climate gradients. The ACH and CPM provide complementary insights into range dynamics: the ACH explains patterns of abundance and genetic diversity, while the CPM captures climate-linked trait variation. Our findings highlight

the importance of integrating both frameworks to conserve populations facing changing climates and increased droughts.

Key Words: Intraspecific variation, ecological gradients, clinal patterns, genetic diversity, abundant center hypothesis, *Andropogon gerardi*

Introduction

A long-standing concept in ecology and biogeography is that abundance tends to peak at the center of a species' range and decline toward margins (Brown, 1984; Eckert et al., 2008; Sheth et al., 2020; Sporbert et al., 2020). This concept, known as the "abundant center hypothesis" (ACH, Brown, 1984), provides valuable insights into differences among populations across species 'ranges. The ACH has been used to describe potential drivers of range limits (Sexton et al., 2011) and has also been used in conservation ecology to forecast extinction risks (Lesica & Allendorf, 1995; Sagarin et al., 2006). While originally focused on abundance, the ACH can be extended to other organismal facets. For example, the high dispersal and low genetic drift at the center of the range should lead to high within-population genetic diversity (Sagarin et al., 2006; Fréjaville et al., 2020). By contrast, at the range margin, the few, widely dispersed populations will have small population sizes with reduced within-population genetic diversity (Sexton et al., 2011). Despite these challenges, populations at the range margin may be pivotal in driving adaptation and range shifts under changing climates (Räikkönen et al., 2017) because these populations are usually the first to experience climate extremes. Thus, populations at range margins may be critical to conservation and restoration (Nadeau & Urban, 2019).

Empirical support for the ACH remains limited in predictions of abundance (Dallas et al., 2020) and genetic diversity (Dixon et al., 2013; Wang, 2020). An alternative hypothesis, the clinal pattern model (CPM), proposes that performance varies with environmental conditions regardless of range position. Numerous studies show species 'abundance shifts along environmental gradients such as precipitation (Soliani et al., 2020), elevation (Lynn et al., 2019), and nutrient availability (Ohdo & Takahashi, 2020). Similarly, intraspecific trait variation—linked to fitness—can also follow environmental gradients, driven by local adaptation (Savolainen et al., 2007) or phenotypic plasticity (Stotz et al., 2021; Estarangue et al., 2022). The CPM suggests that suites of traits, shaped by shared evolutionary and ecological pressures, co-vary along these gradients—forming trait assemblages (Rueda et al., 2018). Selective pressures are expected to shift across gradients, leading to distinct, inheritable trait combinations. For instance, dry-climate populations may possess stress-tolerant traits (e.g., narrow leaves, high water-use efficiency; Grime, 1988; Zhang & Tielbörger, 2019), whereas those in wetter climates may favor competitive traits (e.g., greater height and leaf area; Grime, 1988; Bennett et al., 2016). Understanding such patterns is critical for predicting population responses to environmental change, as genetic diversity underlies adaptive potential (Jump et al., 2009).

The ACH and CPM are not necessarily mutually exclusive—abundance and genetic diversity can peak in the range center, whereas traits may vary across environmental gradients. When gradients and core-marginal geography coincide (e.g., a species prefers wet conditions, and the range core is the wettest area across its range), traits, genetics, and abundance can covary. However, when gradients and core-margin are incongruent, the ACH and CPM may be less correlated. We can test congruence by examining associations between abundance, population genetics, and traits along both geographic and environmental gradients.

To better understand how empirical studies support the predictions of the ACH and CPM in plants, a systematic review of 152 publications (details in Methods S1) indicated that patterns of abundance and genetic diversity generally align with the predictions of the ACH. Just over half of the studies demonstrated peak abundance (56.5%, 35 of 62 papers) and greatest genetic diversity (62%, 31 of 50 papers; Table 4.1) in the core and declines toward the margins. In contrast, approximately a third of studies examining trait variation supported the ACH (33.8%, 23 of 68 papers), whereas most studies reported patterns consistent with the CPM (66.2% 45 of 68 papers). In these studies, traits often corresponded with linear clines along environmental gradients, rather than with the spatial position within a species' range (Table 4.1). Notably, only 3% of studies (five of 152 papers) simultaneously evaluated the abundance, genetic diversity, and trait variation, limiting our ability to assess how these dimensions of intraspecific variation may interact. As such, there remains a critical need for integrative studies that jointly assess these components to more fully understand the mechanisms shaping range-wide variation.

In this study, we tested the predictions of the ACH and CPM by quantifying intraspecific variation in abundance, functional traits, and genetic diversity. We used *Andropogon gerardi* (Vitman) as a study system as it is a dominant grass in the US Great Plains (Knapp et al., 1998), with a range spanning broad temperature and precipitation gradients. Although regional climate variation can drive local abundance patterns in this species (Galliart et al., 2019; 2020), understanding how climate variation across the species' geographic range influences both abundance and genetic diversity is critical for identifying the processes that shape adaptation and persistence under environmental change.

Our study has four primary objectives: 1) Define the *A. gerardi* range core using niche modeling; 2) Test whether abundance, and fitness-related traits are better predicted by range

position (supporting the ACH; Figure 4.1A) or by climate (supporting the CPM; Figure 4.1B); 3) Test whether genetic diversity varies systematically with range position (supporting the ACH; Figure 4.1C/D) or with climate; and, 4) Determine whether assemblages of traits occur together, to identify if climatic gradients lead to predictable intraspecific assemblages of traits.

Materials and Methods

Study species. Our focal species, *A. gerardi,* occurs in every state in the USA east of the Rocky Mountains and eastern Canada, and at especially high densities in the tallgrass prairie (Epstein et al., 1996) of the US Great Plains region. It is a long-lived, clonal (Keeler et al., 2002), warm season perennial grass (Lauenroth & Adler, 2008) that is wind pollinated, and wind dispersed (Johnson & Tausch, 2009). Its range spans mean annual temperatures of ~5–24°C (Mexico to Canada) and mean annual precipitation from ~300–1500 mm yr^{-1} (Rocky Mountains to East Cost USA; USDA Plants Database, 2022). *Andropogon gerardi* is also economically important as the preferred forage cattle in the central grasslands of the US (Gibson et al., 2017), contributing to the $86.1 billion US cattle ranching industry annually (USDA NASS, 2023). This species is also widely used in prairie restoration efforts including the US Conservation Reserve Program spanning over 3.2 million ha (CRP, 2023).

Field site sampling locations

We sampled *A. gerardi* field populations at 26 sites spanning ~2100 km north-south and ~2500 km east-west, and nearly the entire range of environmental conditions the species inhabits (418-1467mm yr^{-1} 30-year mean annual precipitation and 5.9-21.2°C mean annual temperature; Figure 4.2, Table 4.2; ClimateNAv7.3, https://climatena.ca/mapVersion; Wang et al. 2016). *Andropogon gerardi* range encompasses 80% of the North-South geographic range axis and 84%

of the East-West axis. To locate sampling sites, we subdivided the currently occupied climatic space into zones based on variation in key climatic variables (*e.g.,* temperature and precipitation gradients) and targeted at least one site in most zones (Perret & Sax 2022). For site-level analyses, we obtained climate data from the ClimateNA web-based tool (version 7.30; https://climatena.ca), which provides 1-km resolution data averaged over the 1990–2020 period. We sampled each site when *A. gerardi* biomass was highest, at 50-60% growing degree days (Table 4.2) during 2023. Growing degree data was retrieved from the USA National Phenology Network (2023) and confirmed with the agricultural degree calendar database from GreenCast (https://www.greencastonline.com/). All populations were located at unrestored, native prairies with similar management history (see site details in Table 4.2).

To characterize site edaphic conditions, we sampled 10 cm soil deep cores at the base of each plant at each site (3 per plant x 6 plants/ site = 18 cores per site). The core samples were composited and analyzed at the site level at the Kansas State University Soils Testing Lab for soil carbon and nitrogen, pH and texture (sand, silt, or clay content; Recommended Chemical Soil Test Procedures, 1998). Detailed methods are described in supplemental methods and soil conditions (Table 4.2).

Objective 1- Defining the species core distribution: Ecological niche modeling

To delineate the species niche and define core and non-core populations (Obj. 1) key to test the ACH and CPM, we constructed an environmental niche model that predicted species abundance as functions of five climate predictors (30-year averages of mean annual precipitation, growing season precipitation, mean annual temperature, aridity index (defined as [mean annual temperature + 10)/(mean annual precipitation / 1000)]; Wang et al. 2016), and maximum temperature of the warmest month). Briefly, we obtained occurrence data from Smith

et al. (2017) and supplemented them with records in BIEN (Maintner et al., 2020). For each climate predictor, we constructed a series of univariate niche models to predict abundance using R v12.1 (R Core Team, 2024) using nimble (de Valpine et al., 2017; full model description in Methods S2).

Objective 2- Abundance and functional traits

To assess abundance across the range (Obj. 2), we used *A. gerardi* aboveground percent cover (hereafter, abundance) at each site. We used a pin-hit method (Greig-Smith, 1983) and four replicate 1.0-m^2 quadrats with 81 evenly spaced sampling points at each population. The four non-overlapping quadrats were haphazardly placed at least five meters apart. At every sampling point, we recorded the presence of *A. gerardi*, other graminoids, forbs, or bare ground.

To quantify functional trait variation across the range (Obj. 2), we measured 15 traits of six haphazardly selected *A. gerardi* individuals at each population (hereafter, focal plants). The individuals were at least 10 meters apart. In total, we measured traits of 156 individual plants (six focal plants/population x 26 populations=156 plants).

Our physiological traits included gas exchange, chlorophyll absorbance, midday water potential, and carbon isotopic discrimination. We recorded gas exchange on focal plants with a LICOR-6400XT IRGA system (Li-Cor Biosciences, Inc., Lincoln, Nebraska, USA; Tamayo & Weiss, 2001) and measured photosynthesis (μmol CO_2 $m^{-2}s^{-1}$), stomatal conductance (μmol H_2O $m^{-2}s^{-1}$), transpiration (μmol H_2O $m^{-2}s^{-1}$), water use efficiency (photosynthetic/transpiration rate), and internal CO_2 concentration. We measured gas exchange on a fully expanded leaf with CO_2 levels at 400 ppm, humidity and temperature at ambient levels, and photosynthetically active radiation at 1500 μmol photons $m^{-2}s^{-1}$. We measured on sunny days between 10:00-13:00h to

minimize plants 'adjustment time to leaf chamber conditions and when photosynthetic rates had stabilized (coefficient of variation remained <1 for more than one minute).

To further assess physiological differences among populations, we measured leaf chlorophyll absorbance on focal plants using a portable chlorophyll meter (SPAD, Soil Plant Analysis Development**,** SPAD-502, Minolta, Japan), using the average of three readings of fully expanded mature leaves. We also measured the midday leaf water potential with a pressure chamber (PMS Instrument Co., Albany, OR, USA) on one leaf of each focal plant in the field. We measured carbon isotope discrimination to assess water use efficiency differences among populations (Farquhar et al., 1989; Ellsworth & Cousins, 2016) by collecting three 5-7 cm leaf samples from the midsection of four focal plants. Samples from each plant were homogenized, dried at 60°C for at least 48 hours, finely ground, redried, and analyzed for ^{13}C isotope ratios (Farquhar et al., 1982) in the Stable Isotope Mass Spectrometry Laboratory at Kansas State University (see Methods S2).

Our morphological traits included plant height and diameter, leaf width and thickness, as well as vegetative and total biomass. We determined vegetative height by extending the longest leaf vertically, measuring from the ground to the highest point of extension. Reproductive stalks were excluded. For plant diameter, we averaged two perpendicular measurements. For leaf width, we averaged maximum widths of three mature leaves. For leaf thickness, we measured thicknesses of three mature leaves at the widest point of the blade using a hand caliper (Mitutoyo Corp. Kawasaki Japan), excluding the midvein, and averaged these values. We harvested aboveground biomass of at least five individual plants (*i.e.*, separated by 20m; distinct from the six focal plants for which we measured other traits) by collecting all aboveground tissue and

drying it at 60ºC. We subsequently divided dried biomass into vegetative (leaves) or reproductive (stalks, flowers, and seeds) allocations and weighed each.

To quantify leaf nitrogen (N) concentration, as an indicator of nutrient status, we collected three 5-7 cm leaf samples from the midsection of each focal plant and dried them at 60°C for at least 48hrs. We finely ground the samples, redried, and analyzed a ~0.15 g sample for %N on a LECO TruSpec Nitrogen combustion analyzer (LECO Direct, St. Joseph MO, USA) at the Soils Testing Laboratory at Kansas State University (Manhattan, KS, USA).

Statistical Analyses. We used a model selection approach to test whether variation in abundance and traits was better explained by range position (supporting ACH) or by climate (supporting CPM). For abundance and for each of the 15 traits, we fit mixed models that included either effects of longitude or latitude (to test ACH) or any climate predictor (see Table 4.2; to test CPM) as well as any edaphic predictors (Table 4.2). We compared models that included a linear effect of longitude or latitude, linear and quadratic effects of longitude or latitude, linear effects of mean annual precipitation, linear and quadratic effect of mean annual precipitation, and similar models for the other climate (e.g., mean annual temperature, aridity index, maximum temperature of the warmest month; Table 4.2) and edaphic (e.g., soil nitrogen, soil pH, soil silt content; Table 4.2) predictors. All models included population as a random effect. We compared the model fits using AICc and assumed that if the best-fit model contained a negative quadratic effect of longitude (concave), the ACH was supported. Support for any of the climate predictor models suggested support for the CPM.

To gain insights into whether within-population trait variation is highest in core or non-core populations, we also analyzed the coefficient of variation in trait values (CV, 100 × standard deviation/mean of a population) using the same model selection as trait means.

Objective 3- Genetic diversity

To quantify genetic diversity at each of the 26 populations across the range (Obj. 3), we sampled five leaf midsections of our six focal plants for "Genotyping by Sequencing" (GBS, Poland and Rife, 2012). We flash froze the 156 samples (6 plants x 26 populations) on dry ice in the field, freeze dried them for at least 72hrs, finely ground them using a GENO/GRINDER 2010 (Cole-Palmer Metuchen, NJ, USA), and stored them at −80°C until DNA extraction. DNA was extracted using a modified CTAB protocol (Doyle and Doyle, 1987; Methods S3). Full details regarding DNA extraction and GBS sequencing are available in Methods S3.

To assess population genetic diversity, we used *PopGenome* v2.7.5 (Pfeifer et al., 2014). We utilized the R package *hierfstat* v0.5-11 (Goudet et al., 2015) to calculate pairwise F_{ST} among populations, as well as populations 'allelic richness and observed heterozygosity (full details on analysis of genetic diversity is in Methods S3).

To evaluate support for the predictions of the ACH and the CPM, we used a similar model selection approach as outlined in Obj. 2 to test whether range position or climate variables best predicted genetic diversity. We used nucleotide diversity, allelic richness, and observed heterozygosity as response variables and fit 10 models as described for the previous objective, comparing among models using AICc. We used linear models rather than mixed models, because each population had one measurement of genetic diversity. We again assumed that support for a quadratic longitudinal term would indicate support for the ACH, whereas support for climate predictors would suggest support for CPM.

Objective 4- Climate-trait associations

To examine how climate correlated with trait assemblages (Obj. 4), we first conducted a Principal Component Analysis (PCA) on our four climate predictors at the sites. We conducted a second PCA on all 15 traits. We extracted the first principal component (PCA Axis 1) from both the climate and trait PCAs, as this axis captured the majority of variance in each dataset (60.2% and 56.7%, respectively). To assess the relationship between climate and trait variation, we conducted a linear regression analysis, treating PCA axis 1 scores from the climate PCA as the predictor variable and PCA axis 1 scores from the trait PCA as the response variable.

We also performed redundancy analyses (RDA; R package 'vegan'; Oksanen et al., 2010) alongside our PCA analysis to identify the primary climate and range drivers of trait variation across the range. For the RDA, we first standardized all trait data using the Bray-Curtis transformation. We then used multivariate linear regressions to relate traits to climate and range predictors, generating matrices of fitted values. To quantify the variance in traits explained by different sets of predictors, we performed four variance partitioning analyses using the following explanatory variable sets: (1) a combined model including mean annual precipitation, mean annual temperature, aridity index, latitude, and longitude; (2) climate variables only (precipitation, temperature, and aridity index); (3) geographic variables only (latitude and longitude); and (4) precipitation and aridity alone. We calculated the variances explained by each of the four models with a one-way analysis of variance ANOVA, with $\alpha<0.05$.

Results

Niche modeling identifies the range core of *A. gerardi*

Our niche model indicated that 8 of the 26 populations (IA, IN, KS-1, KS-2, MO, OK, NE-1, and WI) were within the core of *A. gerardi* distribution (top 5% of expected abundance

values; Figure 4.3A). Predicted abundance based on the niche model showed highest abundance at intermediate longitudes and latitudes (Figure 4.3A). These spatial predictions align with the ACH with abundance peaking in the center of the range. By identifying core and peripheral populations quantitatively, the niche model provides a foundation for testing whether abundance, genetic diversity, and trait variation follow similar spatial patterns.

Abundance provides evidence for the ACH, but traits generally support the CPM

For the 26 field populations, site-level abundance was highest in the core (Figure 4.3A) and lowest at low and high longitudes (Figures 4.3B, C, R^2=0.30; Tables S3-4). The best-fit model for abundance included linear and quadratic effects of longitude (Figure 4.3C; Table 4.5).

Unlike the unimodal relationship of abundance with longitude, most traits varied linearly across environmental clines. Climate predictors, rather than longitude or latitude, best explained trait variation (Tables S3-5), supporting the CPM. For morphological traits, mean annual precipitation was included in the best-fit model for all traits except leaf thickness, which correlated best with the aridity index (Tables S3-5). Plant height increased linearly with precipitation (R^2=0.50; ~35 cm in dry to ~100 cm in wet populations; Figure 4.4A), as did vegetative biomass (R^2=0.53; ~5-100 g), canopy diameter (R^2=0.62; ~40-120 cm), leaf width (R^2=0.54; ~0.6-1.1 cm), and total aboveground biomass (R^2=0.43; ~10-140 g; Figures 4.4 B-D, S1). Leaf N concentration decreased with precipitation (R^2=0.49; 1.5% to 1.0% N; Figure S1C), whereas leaf thickness increased with aridity (R^2=0.60; ~0.15 mm to ~0.25 mm; Figure 4.4C).

Physiological traits mainly showed linear (5 of 8 traits) or quadratic (3 of 8) responses to climate. Six of the eight best-fit models included aridity; fewer including precipitation (1 of 8) or temperature (1 of 8; Tables S3-5). For example, photosynthetic rate had a quadratic relationship with aridity (R^2=0.37), peaking near 20 μmol CO_2 m^{-2} s^{-1} before declining at the most arid sites

(Figure 4.4C). Unlike morphological traits tied to precipitation, most physiological traits increased with aridity: chlorophyll absorbance (R^2=0.52; ~28-39 SPAD), water use efficiency (WUE; R^2=0.59; ~3.0-9.0 μmol CO_2/μmol H_2O), and internal CO_2 concentration (R^2=0.19; ~175-255 μmol CO_2) all rose linearly (Figures 4.4D-E, S1). Expectedly, midday water potential decreased with aridity (R^2=0.41), from -0.8 MPa in least arid to -1.5 MPa in most arid populations (Figure 4.4F). Leaf ^{13}C discrimination also increased with aridity (R^2=0.42), indicating greater WUE due to more closed stomata in the most arid sites (Figure S1F).

Two physiological traits showed unimodal climate responses: transpiration rate had a concave relationship with mean annual precipitation (R^2=0.44), lowest (~1.5 μmol H_2O m^{-2} s^{-1}) in driest sites, peaking (~3.0 μmol H_2O m^{-2} s^{-1}) at intermediate rainfall (Figure S1G). Stomatal conductance showed a concave relationship with warmest month temperature (R^2=0.30), lowest (~0.075 μmol H_2O m^{-2} s^{-1}) at warmest populations, peaking (~0.22 μmol H_2O m^{-2} s^{-1}) at intermediate temperatures (Figure S1H). All traits are mapped across the contiguous US for visualization (Figure S2).

Nearly half of trait CVs (7 of 15) showed a significant response ($p<0.05$) to predictor variables (climate or range). In contrast, no model for CV in abundance was significant (all $p>0.05$). The within-population CV (Figure S3) showed the strongest relationship with mean annual precipitation for five traits, and the CV of WUE was best explained by aridity. Only the CV of stomatal conductance was best explained by temperature. Additionally, five trait CVs had a quadratic relationship with mean annual precipitation, with lowest at intermediate rainfall and highest at extremes. Specifically, height (R^2=0.25), canopy diameter (R^2=0.21), leaf N concentration (R^2=0.47), total biomass (R^2=0.33), and transpiration rate (R^2=0.61; Figure S3A-E) all had the lowest within population CV in the intermediate core populations and the highest

CV in the non-core populations (Figure S3 A-E). Similarly, the CV of WUE and stomatal conductance had a convex relationship with climate predictors (aridity, R^2=0.29, and temperature R^2=0.25, respectively; Figure S3F-G).

Genetic diversity peaks in core populations, confirming the ACH

We aimed to characterize how geographic vs. environmental factors influence genetic variation (Obj. 3). Our data best align with ACH: the best-fit model for nucleotide diversity, allelic richness, and observed heterozygosity exhibited unimodal relationships with longitude, similar to our results for abundance. Core populations had greater nucleotide diversity than non-core populations (R^2=0.39) with the highest nucleotide diversity (π=0.205-0.24) in the core (Figure 4.5A). Similarly, allelic richness (R^2=0.37) and observed heterozygosity (R^2=0.32) varied unimodally with longitude and were highest in the core (Figures 4.5B, S34; Table 4.6).

We also used metrics of genetic similarity among populations to assess whether non-core populations diverged substantially from one another, as predicted by the ACH. The F_{ST} estimates ranged from 0.0141-0.092 between the core populations indicating high similarity among them (Figure 4.5C). In general, geographically disparate populations showed large differences in F_{ST} expected from reduced gene flow. For example, the F_{ST} estimate between MS and KS1 was 0.269 and between NM and MO F_{ST} was 0.184 (Figure 4.5C). These results support the ACH as the core populations had higher genetic diversity and were more similar (lowest F_{ST}), whereas the geographically more distant populations showed greater genetic differentiation.

Trait assemblages are shaped by precipitation and aridity, not temperature

To test whether trait groups differed with climatic predictors (Obj. 4), we first quantified trait assemblages using principal component analysis (PCA; Figure 4.6A). The first PCA axis in

this analysis explained 56.7% of the variation. In similar analyses with climate variables (Figure 4.6B), the first PCA axis explained 60.2% of the trait variation. The climate PC1 scores increased linearly with precipitation (R^2=0.68, Figure 4.6C) suggesting that trait assemblies across populations shifted linearly with precipitation, not temperature. Similarly, PC1 of the traits was strongly positively related to mean annual precipitation (R^2=0.81; Figure 4.6D) indicating that traits are associated with a gradient in precipitation.

To evaluate the relative effect of range position vs. climate predictors on trait assemblages, we used RDA to partition variance and assess the relative contributions of geography and climate. The first two eigenvectors explained 76.8% of the overall variation in traits among populations. Variance partitioning showed that geographic range (latitude and longitude) and climatic variables jointly explained 70.1% of this explained variation (Table 4.7). Climate was the main contributor to variance in traits, accounting for 62.0% of the explained variance, followed by longitude and latitude (4.0%; Table 4.7). Partial redundancy analysis of climate, conditioned by geography and temperature alone (i.e., the precipitation and aridity only model) showed 63.2% of the overall variation was explained by RDA1 and RDA2 and 77.9% explained by the first four RDAs. These axes demonstrate that precipitation and aridity are the primary drivers of trait variation across the range, rather than range position. Together, these findings indicate that trait assemblages correspond strongly with climatic predictors, suggesting that environmental filtering shapes suites of co-varying traits across populations.

Discussion

This study addresses the long-standing ecological question of how environmental gradients, geographic range position, trait variation and genetic diversity influence plant adaptation and

distribution. We test the ACH and CPM using a widespread perennial grass to better understand intraspecific variation in abundance, traits, and genetic diversity, by combining niche modeling using herbarium records and field sampling across >2000 km and 3-fold differences in climate. Patterns of abundance supported the ACH and variation in traits aligned with the CPM, highlighting the need to explore how these frameworks might be used to better understand species' range dynamics. We also found evidence for the predictions of the ACH for genetic diversity *(i.e.*, lesser genetic diversity in non-core populations). However, despite the lesser genetic diversity, non-core population traits were highly variable and had climate-matched adaptive traits. Trait assemblages were more tightly associated with the climate than geographic variables, highlighting how trait coordination changes together across climate gradients. Precipitation—not temperature—was the dominant driver of trait-climate relationships across the range. In sum, the ACH and CMP provide alternative—but not mutually exclusive—hypotheses explaining intraspecific variation in abundance, genetic diversity, morphology, and physiology, and how these relate to geographic and environmental gradients. Most studies to date have explored just one of these two hypotheses (Table 4.1). Our results highlight the need for approaches that capture multiple facets to better understand how organisms relate to their environments.

Niche modeling and abundance patterns empirically confirm the ACH

Both the niche model and field sampling of abundance provided strong evidence for the ACH in *A. gerardi* populations across its extensive range (~2100 km North-South, ~2500 km East-West). Peak abundance occurred in core sites at intermediate longitudes, both in the niche model and *in-situ* in the field*,* with declining abundance towards peripheries. These results align with occurrence-based niche modeling of this species presented here (Figure 4.3A) and in earlier

studies (Smith et al., 2017) and support the relevance of the ACH in explaining species' abundances (Brown, 1984). While empirical support for the ACH remains mixed (Dallas et al., 2020), our study highlights its utility in understanding the ecological and evolutionary dynamics of a dominant grassland species.

Several mechanisms may explain the observed ACH pattern of abundance, such as differences in fitness or fragmentation across its range. Survival and reproductive output can differ along environmental gradients (e.g., Riesch et al., 2018; Keep al., 2021; Buckley et al., 2021). Thus, lower survival and reproductive rates that commonly lead to low abundance (e.g., Howard & Goldberg, 2001; Germain & Lutz, 2020; Nomoto & Alexander, 2021), could explain results in the non-core populations. In addition, non-core populations with less suitable habitat are typically more fragmented than those in the core (Oppido et al., 2023). Thus, even if local survival and reproduction is high at non-core populations, fragmentation at non-core populations might lead to lower abundance due to the loss of genetic diversity and limited dispersal. In addition, smaller patches in a fragmented matrix can support fewer individuals, increasing the risk of local extinction (Makishima et al., 2021) in the non-core populations.

Despite their low abundance and low genetic diversity, non-core populations may hold critical adaptive value. For example, their exposure to extreme climate conditions, such as droughts or excessive rainfall, may drive local adaptation (Savolainen et al., 2007) that enables survival in less favorable environments (Anderson & Song, 2020). Supporting this claim, we observed that non-core populations in dry locations tend to possess traits that are commonly associated with drought tolerance (Jardine et al., 2021), such as greater WUE and thicker leaves (Figure 4.4). Take together this suggests that non-core populations could be vital in the species ' persistence under climate change (Nadeau & Urban, 2019). As global temperatures and

precipitation shift (Robinson et al., 2021; IPCC, 2023), these non-core populations might serve as reservoirs of adaptive traits, allowing for range shifts into more drought-borne areas (Anderson & Song, 2020). Conserving non-core populations will thus be crucial for maintaining this species' long-term viability in the face of ongoing environmental changes.

Clinal trait variation reflects climate-driven trait shifts across the range

Trait variation supported the CPM rather than the ACH, highlighting the contrasting drivers behind trait variation and local abundance. While we hypothesized that traits related to increased fitness (e.g., biomass) are likely to vary like the abundance (since higher fitness should lead to higher abundance), we observed contrasting patterns in these two responses. One reason for this discrepancy may be that, while abundance might be highly plastic, trait variation might be primarily a product of selection (Geber & Griffen, 2003). In this scenario, abundance may peak under optimal climatic conditions, but if traits evolve more gradually, variation in abundance and traits might differ—particular given recent changes in climate (IPCC, 2023). Similar patterns of adaptation to climate are common in plant species (Etterson, 2004; Woods et al., 2012) and documented in other studies of *A. gerardi* (Johnson et al., 2015, 2022 ; Galliart et al., 2019, 2020).

While abundance and trait means followed linear or concave patterns, within-population trait variation (CV) often peaked in the non-core populations with a modest convex trend (Figures 4.1D, S3). This variation in non-core populations may reflect microclimatic heterogeneity or plastic responses (Pierce et al., 2019), and could contribute to adaptive potential under changing conditions (Nicotra et al., 2010; Bonamour et al., 2019). Together, our results suggest that trait variation is more strongly shaped by climate, rather than by range position,

highlighting that traits and abundance may respond to different ecological and evolutionary pressures.

High nucleotide diversity in the core further reinforces the ACH

Highest genetic diversity (nucleotide diversity, allelic richness, and observed heterozygosity) occurred in the core populations, consistent with the ACH (Figures 4.1C & 4.5). The ACH predicts that genetic diversity should decline from the range core as populations on the periphery are often fragmented and genetically depauperate (Eckert et al., 2008), leading to less gene flow and greater genetic drift (Sexton et al., 2011). As a result, non-core populations should experience lesser gene flow due to geographic isolation, reducing the genetic diversity overall. Consistent with this expectation, pairwise F_{ST} estimates revealed greater genetic differentiation between the core and the non-core sites, indicating a more limited connectivity between these populations.

Genetic diversity is fundamental for adaptation as it determines the potential to adapt to environmental change (DeWoody et al., 2021). Yet, for many species it is unclear to what extent core and non-core populations differ in genetic diversity (Eckert et al., 2008). Our study unequivocally demonstrates that genetic diversity peaks within the core populations, providing strong support for the ACH. Information on how genetic diversity varies across species ranges is needed to advance conservation practice and to better understand geographic range limits (Sexton et al., 2016), especially in a foundational species like *A. gerardi*. Thus, investigating the genetic diversity across a species range is crucial for predicting its response to future climate shifts and for guiding effective conservation efforts (Shaw et al., 2025).

Previous studies have demonstrated that population size affects genetic diversity (Jump & Peñuelas, 2005; Mijangos & Koo, 2021), potentially explaining the low genetic diversity in

populations with low abundance. Small populations at non-core sites may experience greater genetic drift effects (Bohm et al., 2025), resulting in lower genetic diversity compared to the core. Taken together, these factors reduce the genetic variability of non-core populations, potentially compromising their long-term viability, potentially resulting in low abundance. Conservation of these non-core *A. gerardi* populations with low genetic diversity and low abundance is essential to prevent further genetic loss and to maintain the species 'overall adaptive potential in the face of environmental change (Nadeau & Urban, 2019).

Climate gradients shape divergent trait assemblages across the range

Correlations between climate variables and trait assemblages suggest that trade-offs between precipitation and light acquisition shape the evolution of trait assemblages (Raffard et al., 2017). Our analysis of trait assemblages suggests that populations share a set of traits that correspond to their position along environmental gradients. For example, our ordination analyses demonstrated correlations between photosynthetic rate and leaf thickness in arid populations, whereas other traits like height and vegetative biomass were strongly associated with increased precipitation. Trade-offs among traits might generate these patterns: at wet sites, plants had a greater canopy diameter, height, and leaf width, perhaps to optimize light and resource acquisition (Moles et al., 2009; Baird et al., 2021), because strong competition means that light availability, rather than water, may be the key limiting factor for plant growth. In contrast, plants in arid sites possessed trait assemblages reflective of a conservative resource-use strategy (e.g., higher chlorophyll absorbance and photosynthetic rate, thicker leaves, and greater water use efficiency; Grime, 1988), that allows plants to maintain physiological function and productivity under water-limited conditions (Wright et al., 2001; Matos et al., 2021). Similar trait syndromes have been observed in other grassland species, where mesic conditions favor competitive,

growth-enhancing traits and arid conditions promote drought-resilient traits (Jardine et al., 2021; Yan et al., 2025).

These findings have important implications for restoration efforts. Predicted climate change in North America—including rising temperatures and more frequent droughts (IPCC, 2023)—poses significant risks to grasslands (Smith et al., 2024), underscoring the importance of understanding intraspecific phenotypic and genetic variation (Anderson & Song, 2020). In *A. gerardi*, non-core populations, though less abundant and genetically depauperate, exhibited traits potentially valuable for climate adaptation and restoration. Arid populations showed high water-use efficiency and low water potentials, making them candidates for drought resilience, while wetter non-core populations expressed traits like greater height and biomass, suited for maximizing yield. These findings highlight the conservation importance of rear-edge populations, which often harbor unique stress-tolerant traits (Hampe & Petit, 2005; Thomas, 2022) but face heightened extinction risk due to low abundance and limited genetic diversity (Gilbert et al., 2020). Protecting these marginal populations may be critical for preserving the species 'adaptive potential under ongoing climate change.

Conclusions

Our study confirms that the ACH and CPM provide complementary insights into range dynamics of *Andropogon gerardi*. The ACH effectively explains patterns of abundance and genetic diversity, with core populations showing higher abundance and genetic variation. In contrast, the CPM better captures trait variation and adaptive trait assemblages linked to climate gradients, revealing how plants adjust their functional traits to local environmental conditions. Together, these frameworks highlight different facets of species adaptation: the ACH reflects

demographic and genetic constraints shaping population size and connectivity, while the CPM captures how trait variation across climatic gradients likely results from adaptation to local climate conditions. Recognizing their distinct utility allows for a more nuanced understanding of species 'distribution across the range. Overall, our findings underscore the importance of integrating both frameworks to fully understand and conserve species in the face of changing climates.

Data Archiving Statement. All data supporting the findings of this study are in a private for peer review Dryad repository (DOI: 10.5061/dryad.905qfttzm). The data will be released to the public upon publication.

Figure 4.1. Conceptual models of A. increased plant performance (ex. height, photosynthetic rate, abundance) in core sites at intermediate longitudes (ACH). B. An alternative model of clinal variation (CPM) in plant traits across a mean annual precipitation gradient. C. increased nucleotide diversity in core sites at intermediate longitudes (ACH) or D. increased genetic diversity in non-core sites (PTV). The core distribution of *A. gerardi,* indicated by a red circle, is between either intermediate longitudes or precipitation, which is indicated by red dashed lines.

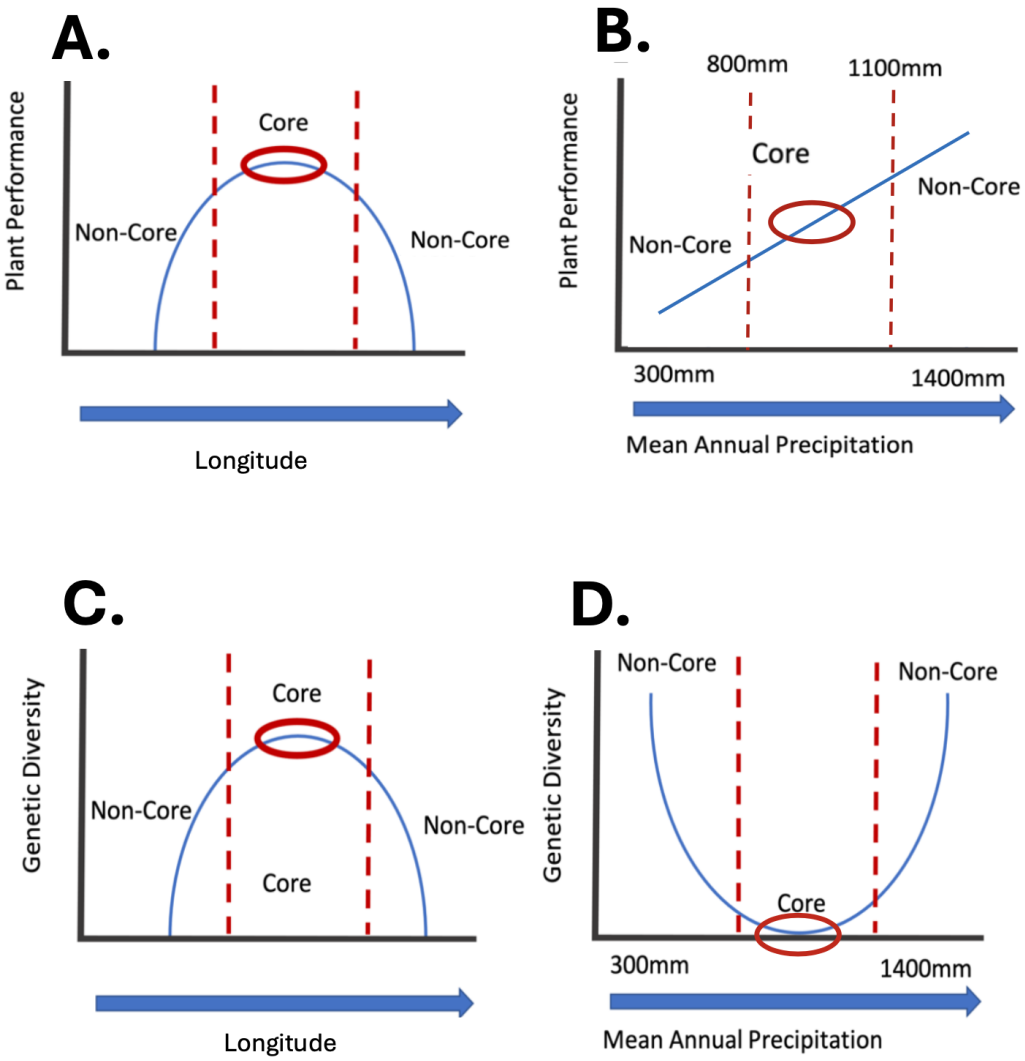

Figure 4.2. Sampling sites across the US where each site is indicated by a black point. A. Mean annual precipitation (mm/yr) is overlayed from low precipitation in warm colors to high precipitation in cool colors. B. Mean annual temperature (ºC) is overlayed from low temperatures in cool colors and high temperatures in warm colors. Sites were sampled mid-season, growing degree days 50-60%, 2023.

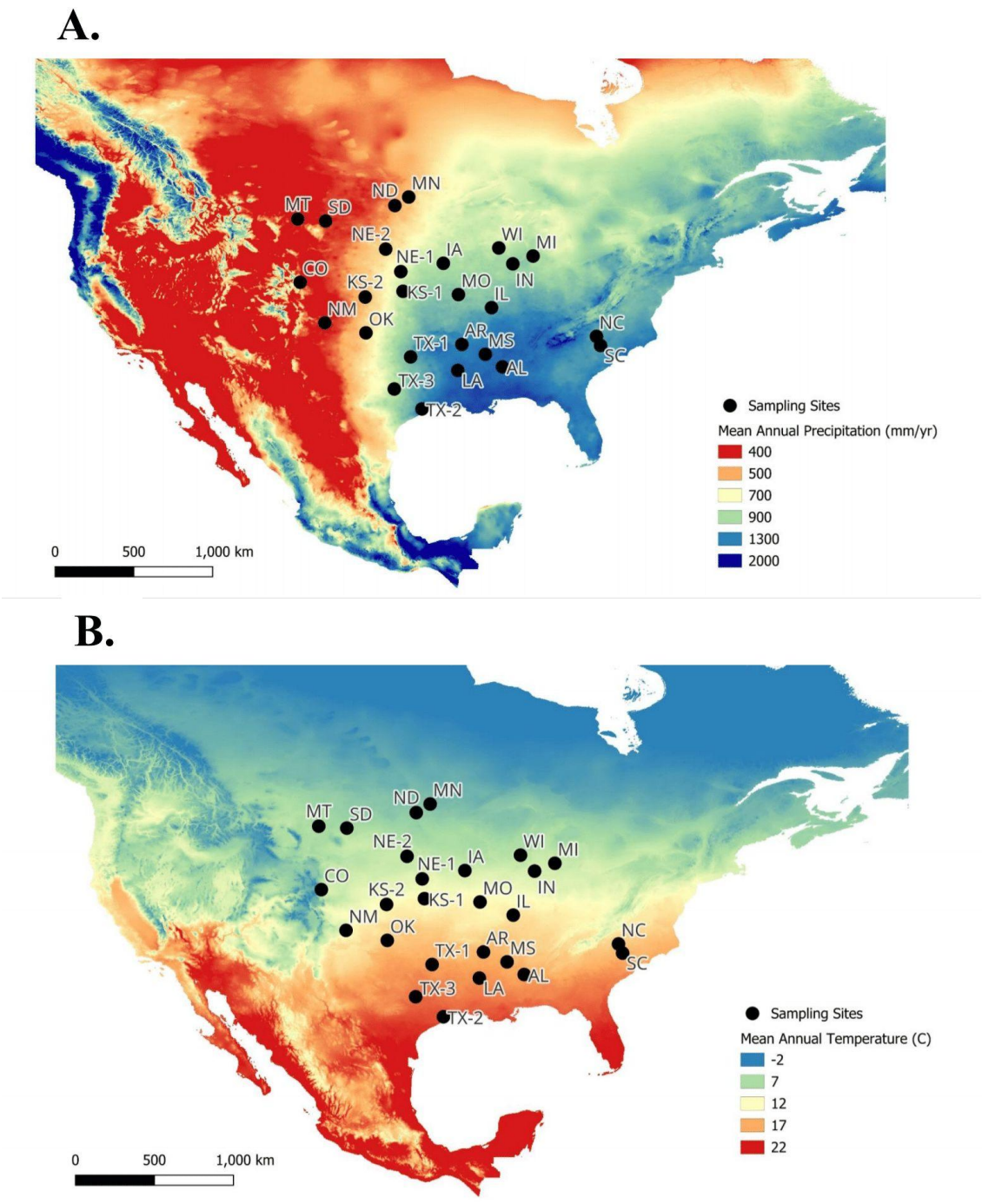

Figure 4.3. A. Map of climatic suitability from a multivariate, Bayesian species distribution model. Values represent the mean estimated relative abundance, λ, across all MCMC chains in the Bayesian model. Points represent locations of sampling sites. The current suitability is overlayed on the map and represented by contour lines. We define the range "core" to be the portion in the top 5th percentile of the distribution of λ. B. Abundance (canopy cover) of *A. gerardi* overlayed on a map of North America. Points indicate the site mean and the color indicates the high (red) or low (blue) cover. C. A quadratic regression of the relationship between *A. gerardi* abundance (canopy cover) and longitude. Points indicate the site mean, error bars indicate standard error, and the shaded is the 95% confidence interval. Green squares indicate core sites (within the current suitability), and black circles indicate non-core sites.

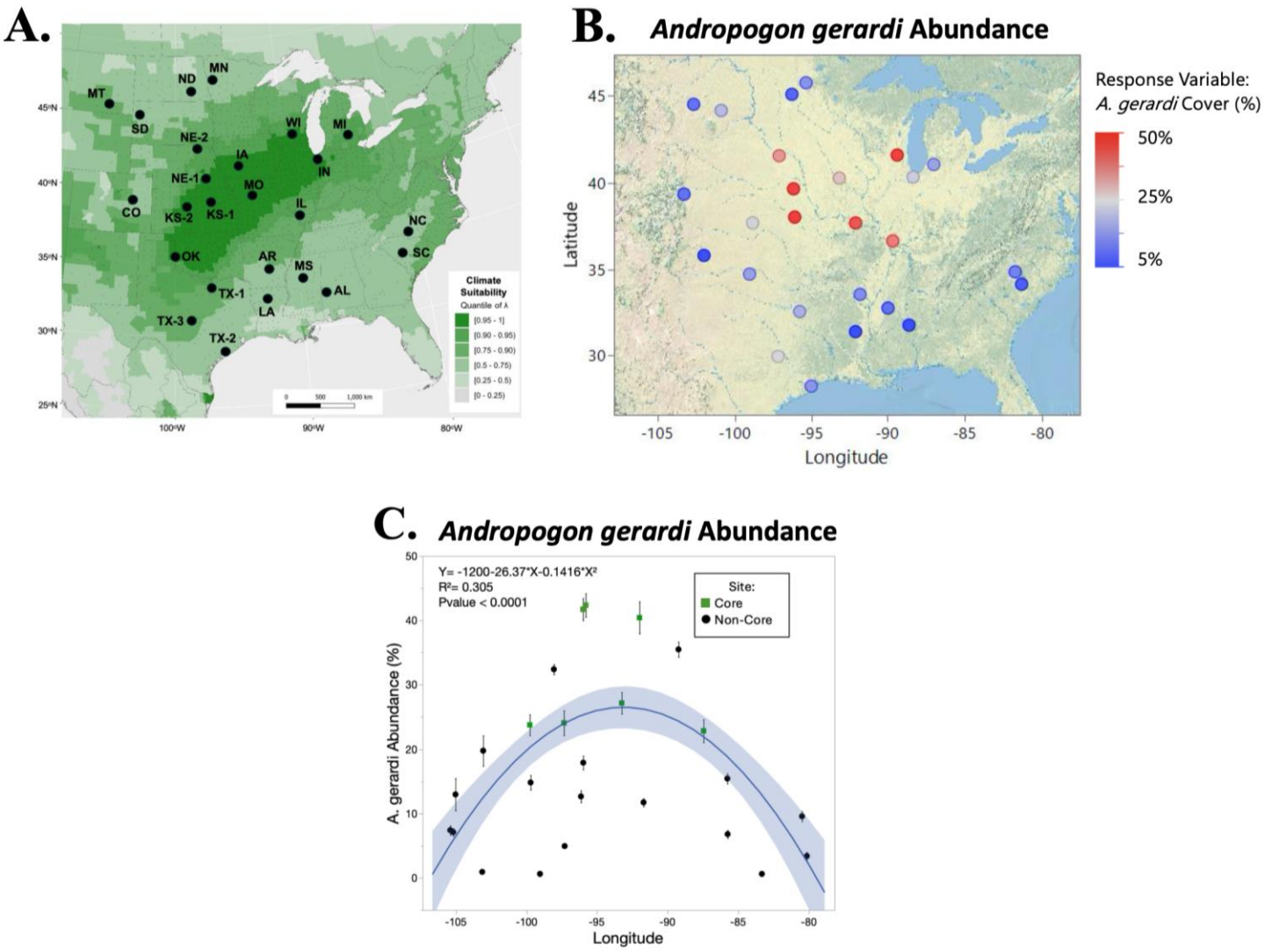

Figure 4.4. Regressions of A. plant height, B. vegetative biomass, C. leaf thickness, D. photosynthetic rate, E. water use efficiency, and F. water potential. Each trait is regressed based on the predictor with the lowest AICc in regression analysis. The solid line is the regression, shaded area indicates the confidence interval, points indicate site mean, and error bars indicate site standard error. Green squares indicate core sites (within the current suitability), and black circles indicate non-core sites.

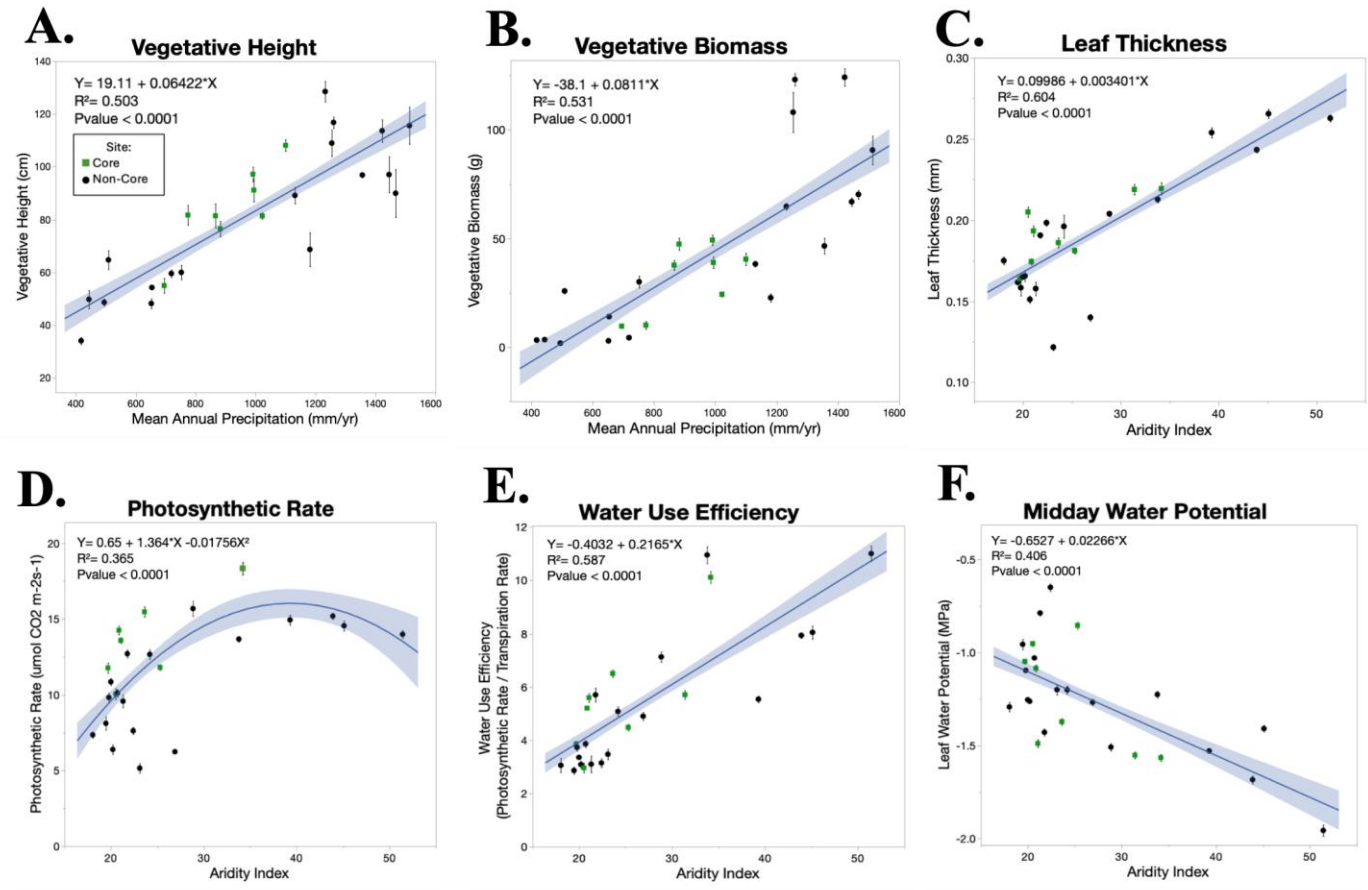

Figure 4.5. A. Regression of nucleotide diversity (π) and B. allelic richness across longitude. The solid line is the regression, shaded area indicates the confidence interval, points indicate site mean. Green squares indicate core sites (within the current suitability), and black circles indicate non-core sites. C. Heatmap of pairwise F_{st} comparisons between sites. High F_{st} is indicated by red and low by blue values.

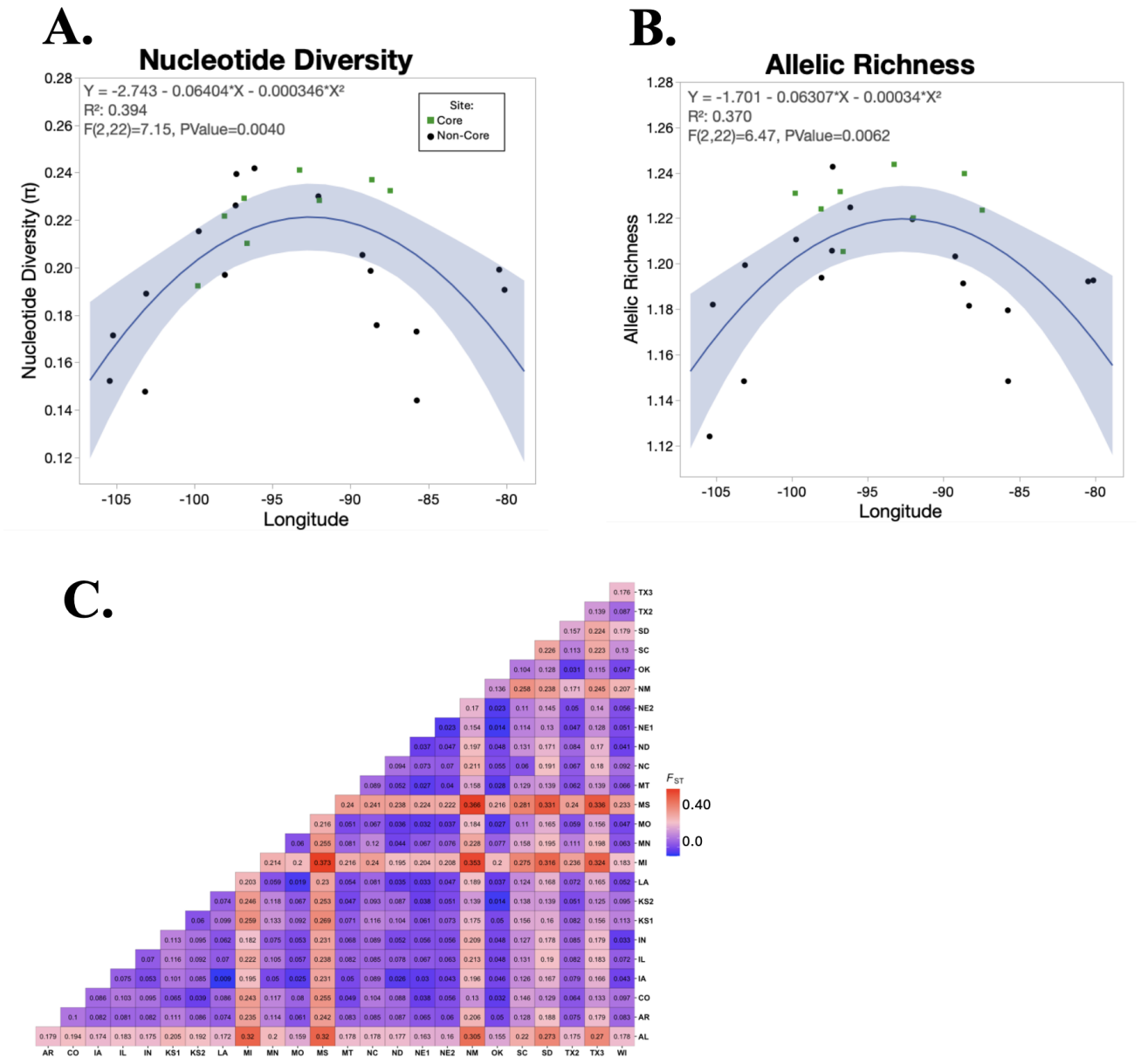

Figure 4.6. A. A principal components analysis (PCA) plot of climate variables across all populations. Points indicate site mean and green squares indicate core sites (within the current suitability), and black circles indicate non-core sites. B. A PCA loading plot where traits are displayed as vectors. The length of the vector indicates its magnitude of influence. C. Linear regression of the trait PC1 across climate PC1 where points indicate site means. D. Linear regression of the climate PC1 across a mean annual precipitation gradient. E. Correlation network analysis of plant traits and climatic conditions across all sites. Network hubs (ie hub traits) have the most connections (highest edge density). Hollow points indicate a variable, the correlation direction is indicated by color (blue = positive, red = negative), and the length of the edge indicates closeness among nodes and shorter lines indicate increased correlation. Variables with no significant (Pearson's -0.7<x<0.7) do not have an edge drawn and are not shown. LEGEND: Photo= photosynthetic rate, Transp= transpiration rate, Ci= internal carbon dioxide concentration, WUE= water use efficiency, SPAD= chlorophyll absorbance, WaterPot= midday water potential, d13C= carbon isotope discrimination, NConc = leaf nitrogen concentration, Thickness= leaf thickness, Diameter= canopy diameter, Height= vegetative height, Width= blade width, VegBio= vegetative biomass, TotalBio= total aboveground biomass, MAP = mean annual precipitation, MAT= mean annual temperature, and WMT = temperature of the warmest month.

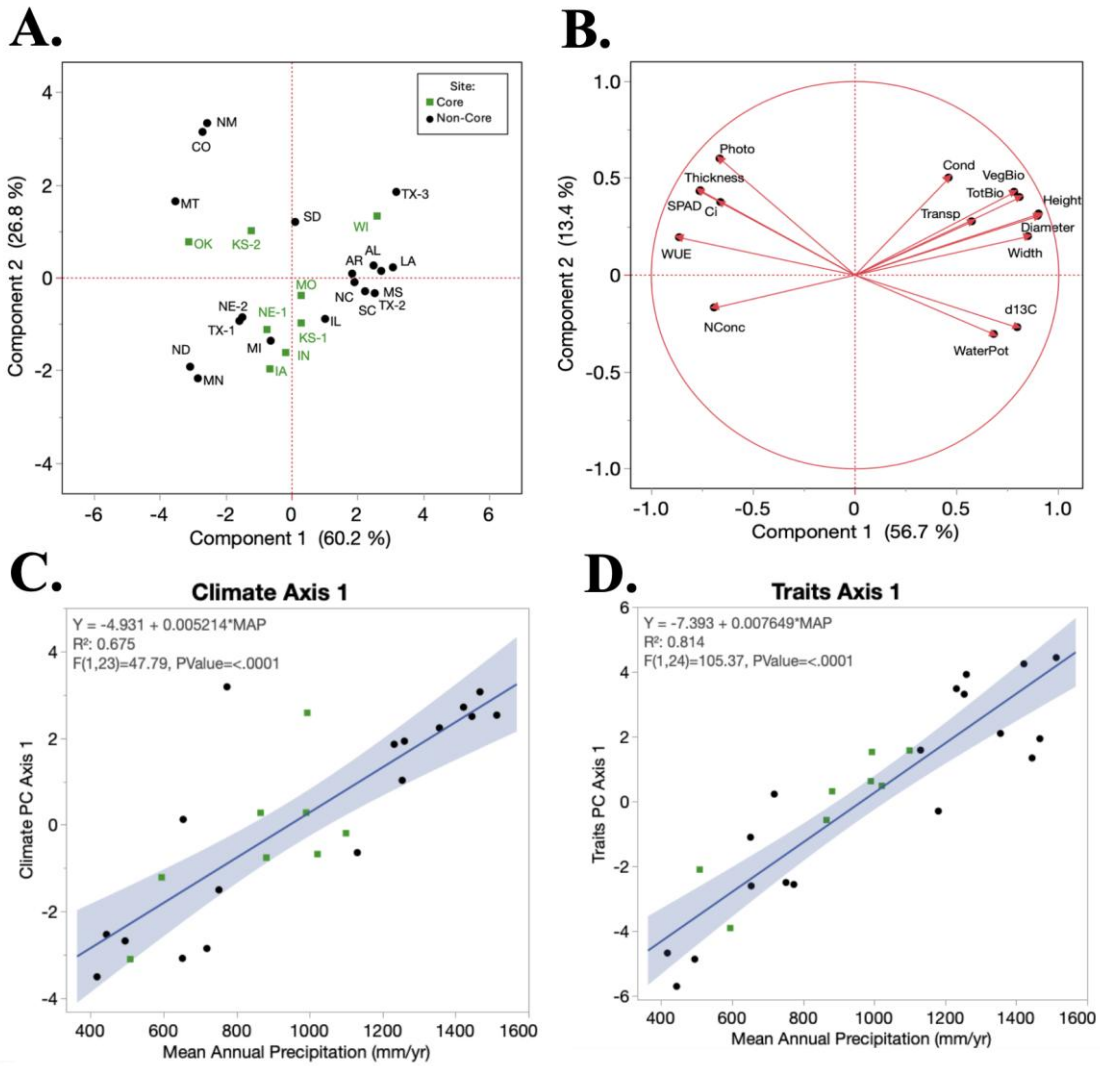

Supplemental Figure 1. Regressions of A. canopy diameter B. leaf width, C. leaf nitrogen concentration, D. total aboveground biomass, E. chlorophyll absorbance, F. carbon isotope discrimination, G. transpiration rate, H. stomatal conductance, and I. internal carbon dioxide concentration based on the variable contributing most to the variation explained by bivariate model analysis. The solid line is the regression, shaded area indicates the confidence interval, points indicate site mean, and error bars indicate site standard error. Green squares indicate core sites (within the current suitability), and black circles indicate non-core sites.

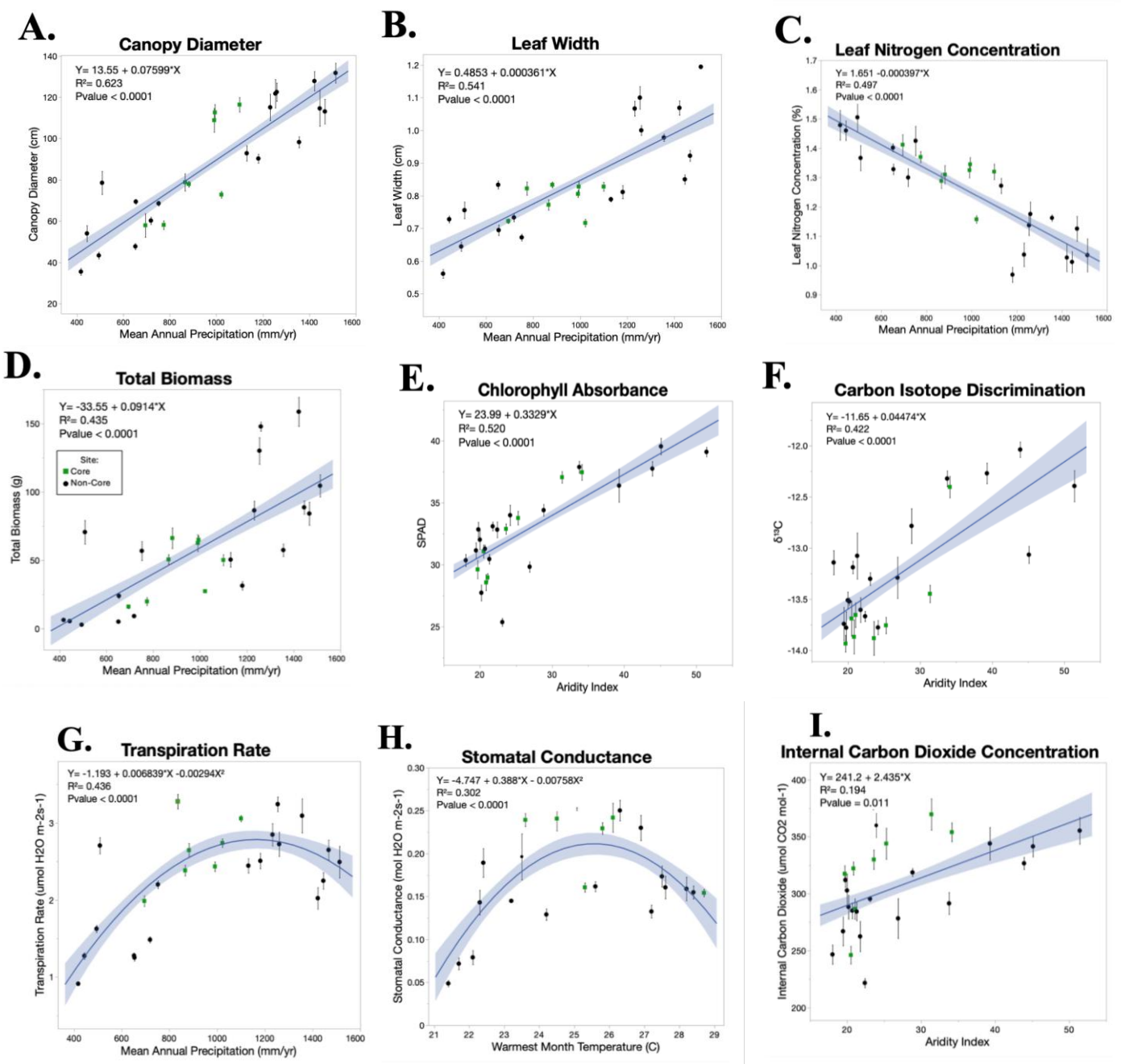

Supplemental Figure 2. A. Height, B. biomass, C. diameter, D. thickness, E. blade width, F. leaf nitrogen concentration, G. photosynthetic rate, H. chlorophyl absorbance (SPAD), I transpiration rate, J. water use efficiency, K. water potential, L. internal carbon dioxide, M. species richness and N. carbon isotope discrimination overlayed on a map of North America. Points indicate the site mean and the color indicates the high (red) or low (blue) values.

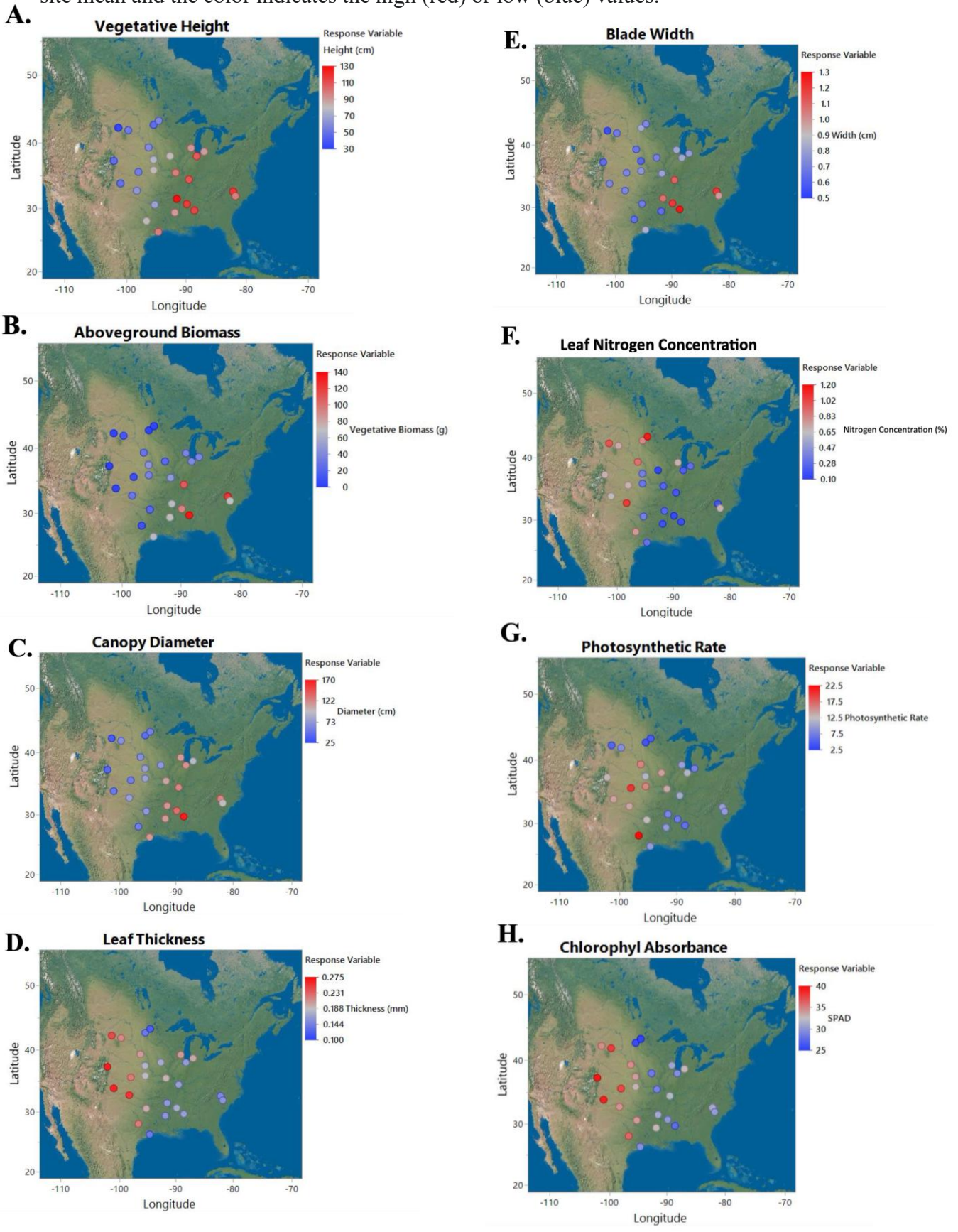

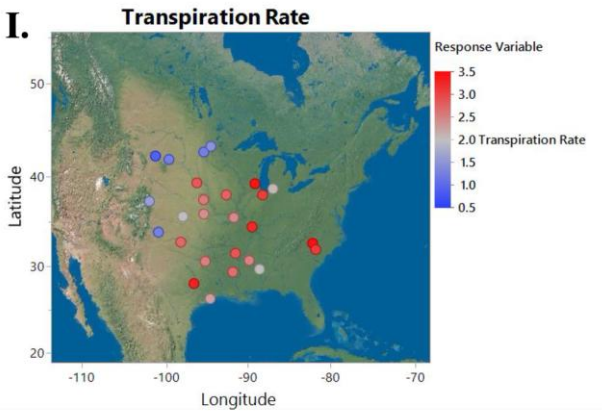
I.
Transpiration Rate
Response Variable
3.5
3.0
2.5
2.0 Transpiration Rate
1.5
1.0
0.5
Latitude
50
40
30
20
-110
-100
-90
-80
-70
Longitude

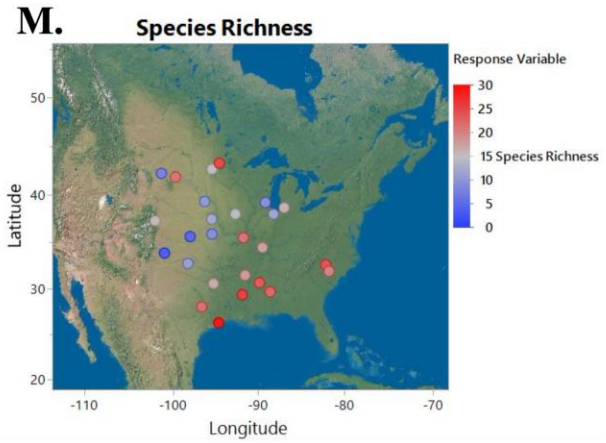
M.
Species Richness
Response Variable
30
25
20
15 Species Richness
10
5
0
Latitude
50
40
30
20
-110
-100
-90
-80
-70
Longitude

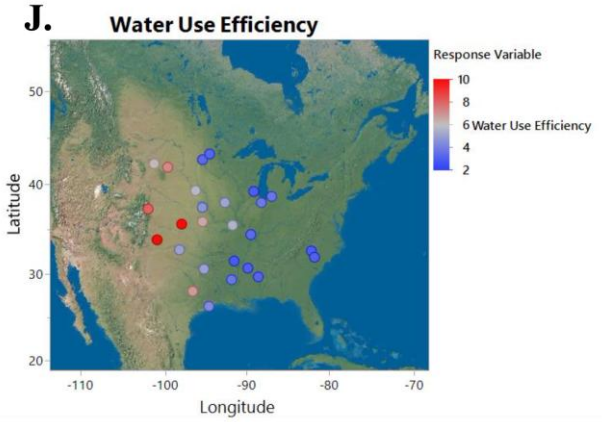
J.
Water Use Efficiency
Response Variable
10
8
6 Water Use Efficiency
4
2
Latitude
50
40
30
20
-110
-100
-90
-80
-70
Longitude

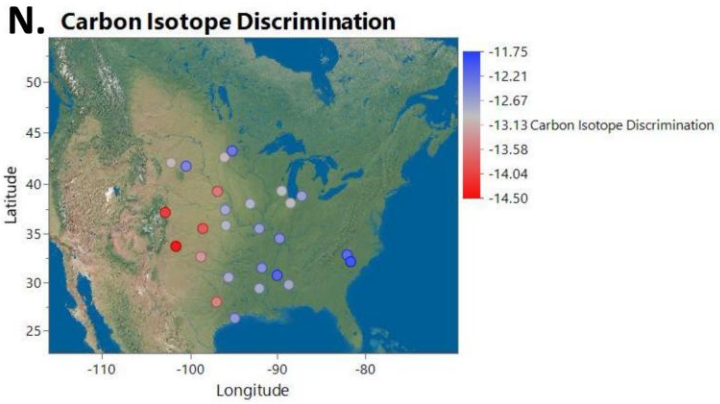
N.
Carbon Isotope Discrimination
-11.75
-12.21
-12.67
-13.13 Carbon Isotope Discrimination
-13.58
-14.04
-14.50
Latitude
50
45
40
35
30
25
-110
-100
-90
-80
Longitude

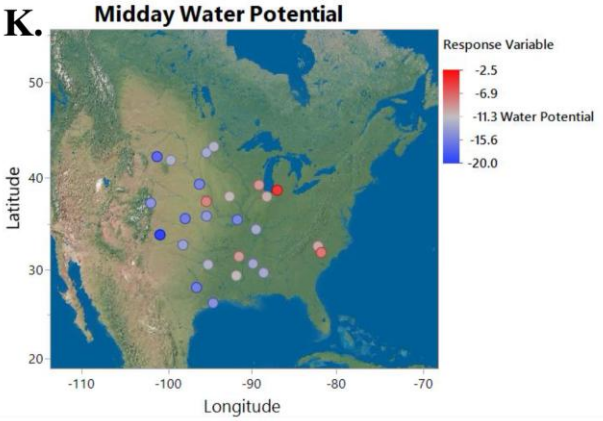
K.
Midday Water Potential
Response Variable
-2.5
-6.9
-11.3 Water Potential
-15.6
-20.0
Latitude
50
40
30
20
-110
-100
-90
-80
-70
Longitude

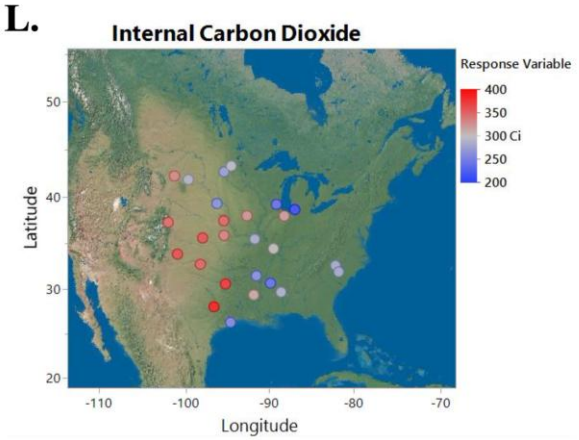
L.
Internal Carbon Dioxide
Response Variable
400
350
300 Ci
250
200
Latitude
50
40
30
20
-110
-100
-90
-80
-70
Longitude

Supplemental Figure 3. Quadratic regressions of the coefficient of variation (CV) for A. vegetative height, B. canopy diameter, C. leaf nitrogen concentration, D. total biomass, E. transpiration rate, F. water use efficiency, and G. stomatal conductance. The CV of each trait is regressed based on the variable contributing most to the variation explained by bivariate model analysis. Points indicate the site mean and the shaded is the 95% confidence interval. Green squares indicate core sites (within the current suitability), and black circles indicate non-core sites.

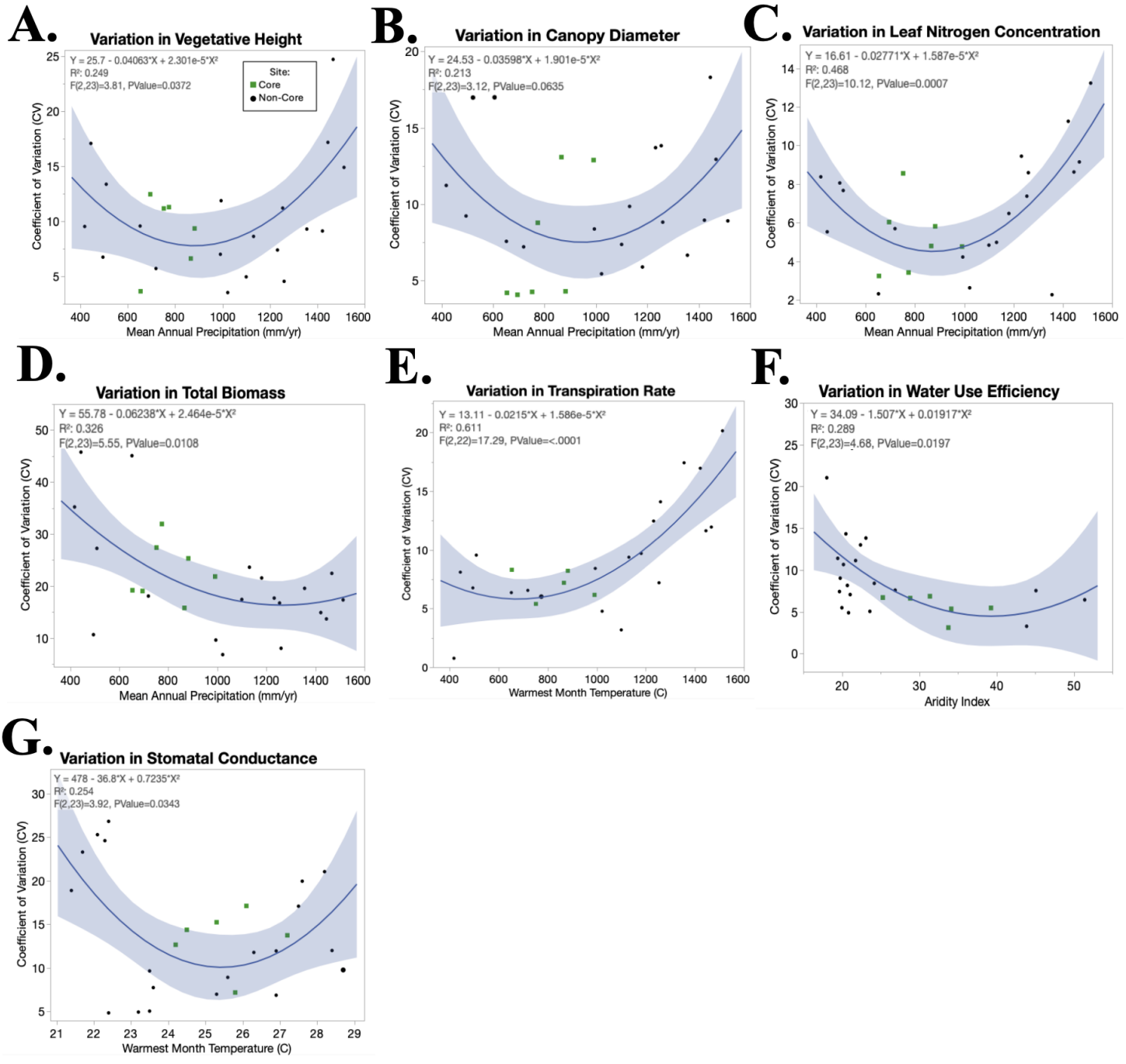

Supplemental Figure 4. Regression of observed heterozygosity based on the variable contributing most to the variation explained by bivariate model analysis. The solid line is the regression, shaded area indicates the confidence interval, points indicate site mean. Squares indicate core sites (within the current suitability), and black circles indicate non-core sites.

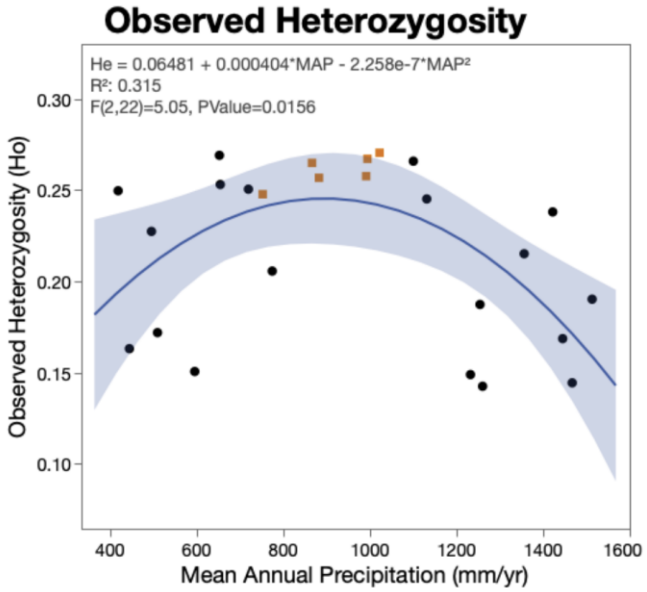

Supplemental Figure 5**.** Regressions for canopy cover of A. forb cover, B. other grass species, and C. bare ground based on the variable contributing most to the variation explained by bivariate model analysis D. A quadratic regression of species richness based on the variable contributing most to the variation explained by bivariate model analysis. Points indicate the site mean, error bars indicate standard error, and the shaded is the 95% confidence interval. Green squares indicate core sites (within the current suitability), and black circles indicate non-core sites.

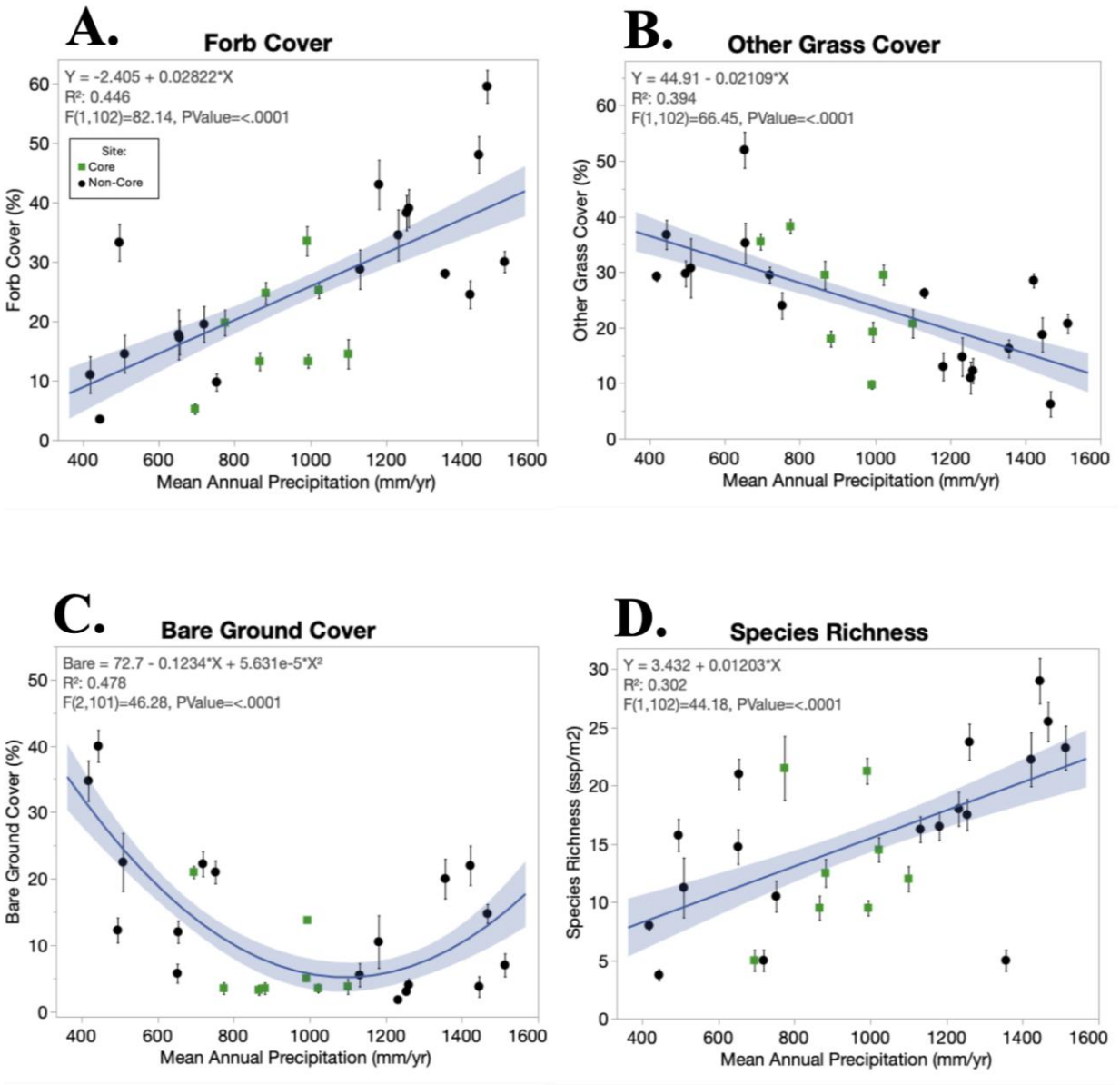

Supplemental Figure 6. Regressions of A. soil moisture (volumetric water content) and B. soil temperature (ºC) based on the variable contributing most to the variation explained by bivariate model analysis. The solid line is the regression, shaded area indicates the confidence interval, points indicate site mean, and error bars indicate site standard error.

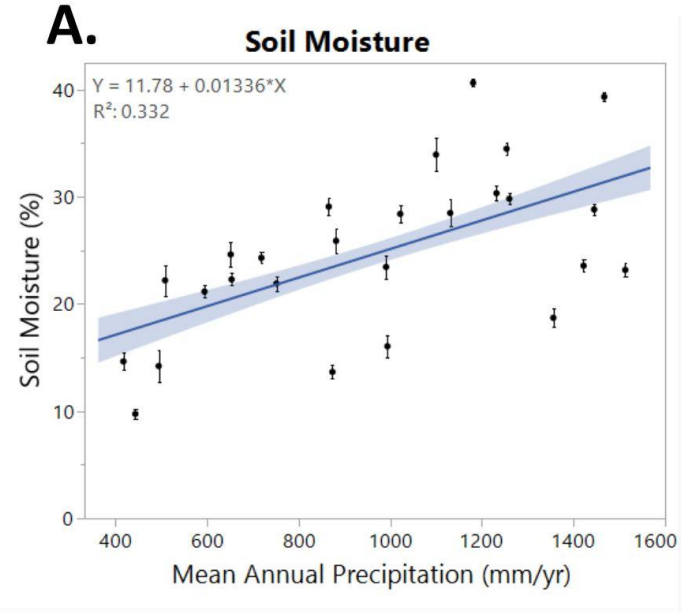

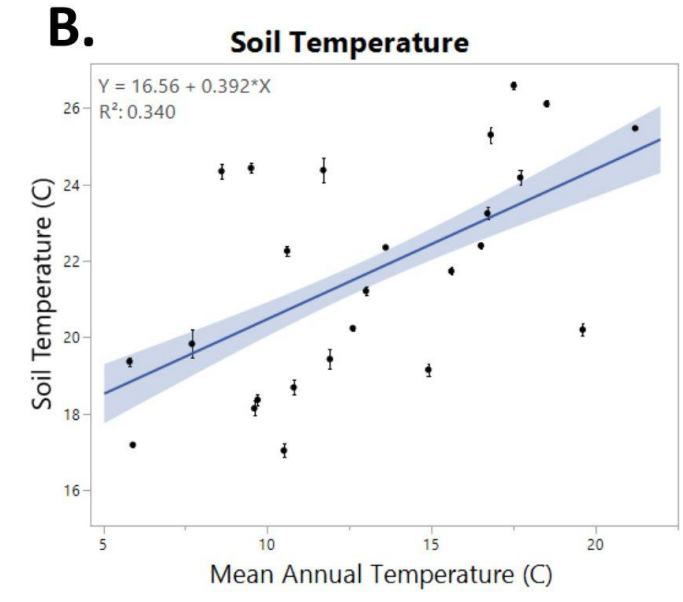

Table 4.1. Literature view of Web of Science of 152 papers demonstrating: Data type used in the study where A=abundance, T=traits, and G=genetic. The response curve of either the ACH or CPM where L= linear, NL= nonlinear, and cat = categorical.

Study	Data types	ACH Support	ACH Response	CPM Support	CPM Response
Panteret al. 2023	A	Mixed	L	Yes	L
Martinet al. 2020	A	No	NL	No	NL
Murphyet al. 2006	A	No	NL	No	NL
Samiset al. 2007	A	No	Cat	No	Cat
Tzortzaki et al. 2017	A	Mixed	Cat	Mixed	NL + Cat
Roux et al. 2012	A	Yes	NL	No	NL
Sugiyamaet al. 2002	A	No	L	Mixed	L
Bañares de Dioset al. 2020	A	No	L	Yes	L
de Oliveiraet al. 2014	A	Yes	NL	No	NL
Freitaset al. 2022	A	Yes	NL	No	NL
Pirononet al. 2022	A	Yes	Cat	No	Cat
Picardet al. 2022	A	Yes	Cat	No	Cat
Pagugaet al. 2018	A	Yes	Cat	No	Cat
Boekenet al. 1998	A	No	Cat	No	Cat
Wilsonet al. 1998	A	Yes	NL	No	NL
Antunezet al. 2025	A	Yes	NL	No	NL
Murrayet al. 1999	A	Yes	NL	No	NL
Xuet al. 2021	A + G	Yes	NL	No	NL
Dixonet al. 2013	A + G	Mixed	NL + L	Mixed	NL + L
Wróblewskaet al. 2008	A + G	No	L	Mixed	L + Cat
Kapralovet al. 2004	A + G	Yes	Cat	No	Cat
de Mattoset al. 2023	A + G	Yes	NL	No	NL
Karbsteinet al. 2023	A + G + T	Yes	NL	Mixed	NL
Pfeiferet al. 2010	A + G + T	Mixed	NL + Cat	Mixed	NL + L + Cat
Herlihyet al. 2005	A + G + T	Yes	NL	Yes	L
Buschet al. 2005	A + G + T	Yes	NL	Mixed	NL
Ducciet al. 2021	A + G +T	Mixed	NL + L	Mixed	NL + L
Kietyket al. 2018	A + T	Yes	NL	Mixed	NL
Moutouamaet al. 2022	A + T	No	L	Yes	L
Pirononet al. 2014	A + T	Mixed	NL	No	Cat
Radulaet al. 2025	A + T	No	Cat	No	Cat
Jumpet al. 2003	A + T	Mixed	NL + L	Mixed	NL + L
Vaupel et al. 2012	A + T	Yes	NL	No	NL
Iyengaret al. 2017	A + T	No	Cat	No	Cat
Vergeeret al. 2013	A + T	Yes	NL	No	NL
Wanget al. 2019	A + T	Yes	NL	No	Cat
Wedelet al. 2021	A + T	No	NL	No	NL
Kulmatiskiet al. 2020	A + T	No	NL	No	NL
Levineet al. 2002	A + T	Mixed	NL	No	NL
Dostalet al. 2016	A + T	Yes	NL	Mixed	NL

Paulo et al. 2019	A + T	Yes	NL	Mixed	NL + L
Chenet al. 2024	A + T	Yes	NL	No	NL
Bakkeret al. 2004	A + T	Yes	NL	No	NL
Salazar Villegaset al. 2023	A + T	Yes	Cat	Mixed	NL + Cat
Munozet al. 2011	A + T	No	L	Yes	L + Cat
Silket al. 2013	A + T	No	L	Yes	L
Pareueloet al. 1996	A + T	No	L	Yes	L
Vaupelet al. 2012	A + T	Yes	NL	Yes	L
Yakimowskiet al. 2007	A + T	Yes	L	No	L
Asplundet al. 2022	A + T	No	L	Yes	L
Fontaineet al. 2022	A + T	Yes	Cat	Yes	Cat
Serrano et al. 2015	A + T	No	L	Yes	L
Prioret al. 2021	A + T	No	L	Yes	L
Quero Perezet al. 2008	A + T	No	L	Yes	L + Cat
Bertilleret al. 2000	A + T	Yes	NL	Yes	L
Marchandet al. 2020	A + T	Mixed	NL	Mixed	NL + L
Wrightet al. 2003	A + T	No	L + Cat	Mixed	NL + L + Cat
Bastidaet al. 2015	A + T	Yes	NL	Yes	L
Andersonet al. 2012	A + T	Mixed	Cat	Mixed	L + Cat
Samiset al. 2007	A + T	Mixed	NL + L	Mixed	NL + L
Russellet al. 2025	A + T	No	L	Yes	L + Cat
Moelleret al. 2012	A + T	No	L	Mixed	L
Hirschet al. 2015	G	Yes	Cat	No	L
Pérez?Collazoset al. 2009	G	No	NL	No	NL
Renet al. 2022	G	No	Cat	Mixed	Cat
Casazzaet al. 2021	G	No	Cat	Yes	Cat
Bontrageret al. 2018	G	No	NL	No	NL
Dauphinet al. 2020	G	Yes	NL	Mixed	L
Goughertyet al. 2020	G	Yes	NL	No	NL
Kitamuraet al. 2020	G	Yes	NL	Yes	L
Lazaro-Nogal et al. 2017	G	No	Cat	Mixed	Cat
Liuet al. 2025	G	Yes	Cat	Yes	L
Liu et al. 2020	G	Mixed	NL + L	Mixed	NL + L
Lopez-Delgadoet al. 2020	G	Yes	Cat	Yes	L
Ochoa-Zavalaet al. 2022	G	Yes	NL	No	NL
Ramirez-Orozcoet al. 2022	G	Mixed	L	No	L
Therarozet al. 2024	G	Yes	NL	No	NL
Wang et al. 2025	G	Mixed	NL	Mixed	L
Xuet al. 2021	G	Mixed	L	Yes	L
Yakimowskiet al. 2008	G	No	Cat	Mixed	Cat
Vanrellet al. 2024	G	Mixed	NL	No	NL + L + Cat
Fantet al. 2014	G	No	L	Yes	L
Kerfahiet al. 2019	G	Yes	NL	Mixed	NL + L
Premarathneet al. 2021	G	Mixed	NL + L	Mixed	NL + L
Gaete-Loyolaet al. 2017	G	No	Cat	Yes	L + Cat

Therarozet al. 2024	G	Yes	NL	No	NL
Tanet al. 2012	G	Yes	NL	No	NL
Latronet al. 2020	G	Yes	L	No	L
Rameriz-Orozcoet al. 2022	G	Yes	NL	No	NL
Wagneret al. 2011	G	Yes	L	No	L
Rotaet al. 2024	G	Mixed	Cat	Mixed	L + Cat
Kottleret al. 2021	G	Mixed	Cat	Mixed	Cat
Kennedyet al. 2020	G + T	Yes	L + Cat	Mixed	L
Pfeilstickeret al. 2021	G + T	Yes	NL	Yes	L
Volis et al. 2022	G + T	Mixed	NL	No	Cat
Byrne et al. 2016	G + T	No	Cat	Yes	L + Cat
Thompsonet al. 2010	G + T	No	NL + Cat	Yes	NL + Cat
Zaretskaya et al. 2022	G + T	No	L	Yes	L
Pfeiferet al. 2009	G + T	Yes	NL	No	NL
Pfeilstickeret al. 2021	G + T	Yes	NL	Yes	L
Doudaet al. 2020	G + T	Mixed	Cat	Mixed	Cat
Lammiet al. 1999	G + T	No	L	Yes	L + Cat
Boratynka et al. 2005	T	No	L	Yes	L + Cat
Campset al. 2021	T	Yes	NL	Mixed	Cat
Dacoet al. 2024	T	No	L	Yes	L
Macriet al. 2020	T	Mixed	NL + Cat	Mixed	NL + Cat
Thomet al. 2021	T	No	Cat	Mixed	Cat
Estaragueet al. 2021	T	Mixed	NL	No	NL
Wangneret al. 2011	T	No	Cat	Yes	Cat
Zhaoet al. 2019	T	No	L	Mixed	L
Imbertet al. 2001	T	Yes	NL	No	NL
Montiet al. 2016	T	No	Cat	No	L + Cat
Gallenmülleret al. 2015	T	No	Cat	Mixed	L + Cat
Schmiegeet al. 2021	T	No	L	Yes	L
Brumet al. 2023	T	No	L	Yes	L + Cat
Bolinet al. 2018	T	No	Cat	Yes	Cat
Benning et al. 2019	T	Mixed	NL + Cat	Mixed	NL + Cat
Benning et al. 2021	T	No	L	Yes	L + Cat
Volis et al. 1998	T	No	L	Mixed	NL + L
Santamariaet al. 2003	T	No	NL	Mixed	NL + L

Table 4.2. A. Site information for sampling of *A. gerardi* showing site (state) name, county, vegetation type based on Kuchler vegetation category (Kuchler, 1947), geographic coordinates. Historic temperature & precipitation values, aridity (annual heat moisture index, temperature/ precipitation), climatic ranges, and 2023

precipitation and temperature are included. Data downloaded from ClimateNA based on site coordinates. Edaphic conditions and additional climatic variables are presented in Supplemental Table 1. B. Site environmental variables showing elevation, additional climatic variables, 2023 growing degree days, and relevant management history. Site soil nitrogen concentration, pH, sand, silt, and clay are included.

State/ Site	County	Vegetation Category (Kuchler)	Longitude	Latitude	Mean Annual Precip (mm)	Aridity Index	Growing Season Precip (mm)	Mean Annual Temp (C)	Warmest Month Temp (C)	Growing Season Temp (C)	Coldest Month Temp (C)	2023 Annual Precip (mm)	2023 Annual Temp (C)	2023 Aridity Index
AL	Dallas	Hardwood Forest	-87.12	32.31	1422	20.2	508	17.7	27.6	27.3	7.0	1528	17.6	19.6
AR	Lonoke	Hardwood Forest	-91.70	34.77	1232	19.5	463	16.5	27.5	21.5	4.3	1494	14.8	19.2
CO	Boulder	Short Grass	-105.28	39.99	495	45.1	139	10.8	23.2	22.6	0.5	416	10.8	25.4
IA	Jasper	Tallgrass	-93.01	41.56	1022	20.9	418	9.7	23.6	24.7	-6.2	1101	14.9	22.6
IL	Williamson	Savanna	-88.83	38.78	1254	19.9	483	13.6	25.6	21.9	0.4	1190	11.5	19.7
IN	Lake	Savanna	-87.45	41.52	1100	19.7	400	10.5	23.5	25.2	-3.8	1193	13.4	19.6
KS-1	Riley	Tallgrass	-96.61	39.22	866	23.6	325	12.6	26.1	24.6	-1.7	783	12.8	22.1
KS-2	Logan	Mixed Grass	-100.81	38.77	595	34.2	228	11.9	25.8	27.6	-1.2	597	18.8	34.2
LA	Ouachita Parish	Hardwood Forest	-92.04	32.60	1467	19.8	574	18.5	28.2	28.8	7.9	1331	19.6	22.2
MI	Kalamazoo	Hardwood Forest	-85.76	42.17	1131	22.4	382	9.6	22.4	20.9	-4.2	1150	10.7	20.8
MN	Clay	Tallgrass	-96.14	47.10	719	19.1	364	5.9	21.4	21.2	-8.2	772	6.6	19.0
MO	Calloway	Tallgrass	-91.99	38.94	991	21.1	389	13	25.3	24.6	-0.2	947	14.3	20.8
MS	Yalobusha	Hardwood Forest	-89.75	33.94	1513	18.0	598	16.7	26.9	26.8	5.5	1499	17.8	19.8
MT	Rosebud	Short Grass	-105.41	45.260	418	43.9	194	7.7	22.1	20.5	-4.9	482	8.4	40.3
NC	Cabarrus	Hardwood Forest	-80.51	35.44	1260	20.7	497	15.6	26.3	24.8	4.9	1442	16.2	19.2
ND	Ransom	Mixed Grass	-97.30	46.39	652	26.9	297	5.8	21.7	21.2	2.4	641	6.2	25.3
NE-1	Lancaster	Tallgrass	-96.80	40.86	882	25.3	361	10.6	24.5	23.5	-4.7	844	11.4	25.4
NE-2	Knox	Tallgrass	-98.06	42.75	652	28.8	270	9.5	24.2	23.3	-5.1	788	9.9	29.3
NM	Union	Short Grass	-104.22	36.23	444	51.4	170	11.7	23.5	22.2	1.0	438	11.9	50.7
OK	Beckham	Mixed Grass	-99.68	35.61	509	39.3	240	7.7	22.4	20.8	1.2	518	8.4	40.3
SC	Chesterfield	Hardwood Forest	-80.13	34.37	1256	21.3	352	16.8	26.9	25.6	5.2	1305	17.3	20.6
SD	Lawrence	Short Grass	-103.07	45.10	654	33.8	184	14.9	27.2	26.2	-2.6	650	15.8	33.9
TX-1	Fannin	Tallgrass	-95.03	29.37	1181	21.8	419	17.5	28.4	28.5	6.1	1207	18.5	23.6
TX-2	Galveston	Mixed Grass	-97.34	31.06	1445	31.4	569	21.2	28.7	29.5	7.3	1432	22.1	32.4
TX-3	Bell	Tallgrass	-95.97	33.72	874	24.2	384	8.6	22.3	21.2	6.6	911	9.8	24.7
WI	Walworth	Savanna	-88.62	42.84	994	20.5	398	19.6	29.3	31.0	-2.1	1056	21	20.1

Site	Elevation (m)	GDD on Sample Date	2023 GDD	GDD %	Mean Diurnal Range	Temp Annual Range	Precip Season	2023 Warmest Month Temp (C)	2023 Growing Season Precip (mm)	Soil N (%)	Soil pH	Sand (%)	Silt (%)	Clay (%)
AL	50	3164	5707	55.4	13.4	33	21.5	23.2	408	0.18	5.8	54	29	17
AR	68	3065	5906	51.9	11.8	34.4	19.9	28.1	495	0.24	5.6	36	54	10
CO	1676	1561	3046	51.2	16.3	39.4	44.4	22.9	453	0.13	6.2	59	26	15
IA	272	1873	3470	53.9	11.5	37.1	17.9	26	476	0.25	6.3	44	41	15
IL	183	2367	4188	56.5	11.5	37.1	18.0	22.9	492	0.37	5.6	15	67	18
IN	190	1814	3092	58.6	10.9	39.3	27.6	26.2	645	0.25	6.5	59	29	10
KS-1	308	2676	4626	57.8	12.8	41	52.6	25.7	403	0.21	7.8	17	61	22
KS-2	703	2600	4451	58.4	15.3	43.3	59.0	28.9	570	0.2	7.7	43	40	17
LA	22	3072	5881	52.2	12.4	32.4	18.6	30.3	486	0.14	8	14	73	13
MI	260	1563	2904	53.8	11.2	37.7	22.4	22.3	494	0.15	6	67	19	14
MN	363	1474	2688	54.8	12.3	47.8	60.2	21.8	515	0.22	5.8	31	52	17
MO	363	2134	4259	50.0	11.9	39.3	28.4	25.7	432	0.39	6.5	22	59	19
MS	128	2870	5117	56.0	12.9	33.5	21.0	27.7	463	0.35	5.8	48	46	6
MT	1085	1459	2735	53.3	15.5	43.5	61.4	21.8	354	0.58	7.5	32	50	18
NC	215	2669	4938	54.0	13.1	33.6	11.3	26.5	577	0.26	5.6	22	28	50
ND	327	1479	2682	55.1	12.8	47.8	62.9	22.1	557	0.26	7.5	64	27	12
NE-1	393	2023	3897	51.9	13.0	42.6	52.1	23.8	496	0.3	7.7	22	59	19
NE-2	380	1828	3557	51.4	13.1	43.5	60.5	23.9	543	0.33	6.9	20	32	48
NM	1563	1860	3598	51.7	16.1	38.5	68.6	23.8	485	0.34	7.1	88	6	6
OK	891	2552	4933	51.7	14.7	40.2	53.1	21.7	426	0.16	5.9	16	64	20
SC	134	2827	5264	53.7	13.0	32.8	16.4	29.8	783	0.32	6.5	26	59	15
SD	697	2827	5264	53.7	14.7	45.2	62.8	28	475	0.26	7.9	50	35	15
TX-1	251	1599	2973	53.7	12.6	35.3	29.1	22.2	419	0.13	6	60	36	4
TX-2	153	3153	6211	50.7	8.8	25.4	25.4	30.6	433	0.34	5.9	11	37	51
TX-3	202	3545	6943	51.4	12.6	33.3	29.2	30.5	569	0.36	7.5	22	38	40
WI	175	3537	6621	53.4	11.4	41	37.0	32.6	339	0.26	5.8	17	52	31

Table 4.3. Results from regression analysis using climate variables or biogeographic range position as predictors. P-values shown ($\alpha<0.05$) with significant variables in bold and highest contributing variable (lowest p-value) bold and underlined.

Response Variable (Linear)	Mean Annual Precip (mm)	Growing Season Precip (mm)	Aridity Index	Mean Annual Temp (°C)	Warmest Month Temp (°C)	Coldest Month Temp (°C)	Lat.	Long.	Elev. (m)	Temp Ann. Range (°C)	Precip Seasonal.	Mean Diurnal Range (°C)	Growing Season Temp.(°C)	2023 Annual Precip (mm)	2023 Annual Temp (°C)	2023 Warmest Month Temp (°C)	2023 Grow. Season Precip (mm)	2023 Aridity Index
LINEAR RESPONSE																		
Morphological																		
Vegetative Height (cm)	**<u>0.001</u>**	**0.001**	<0.001	**0.03**	**0.04**	**0.001**	**0.04**	**0.01**	**0.01**	**0.01**	**0.01**	0.40	0.33	0.06	0.06	**0.001**	**0.01**	**0.02**
Blade Width (cm)	**<u>0.001</u>**	**0.01**	<0.001	0.08	0.14	0.10	0.77	**0.01**	**0.04**	0.17	0.12	0.32	0.24	<0.001	0.06	**0.003**	**0.03**	**0.02**
Diameter (cm)	**<u>0.001</u>**	**0.002**	<0.001	**0.01**	0.09	0.10	0.07	**0.02**	<0.001	**0.04**	**0.001**	0.55	0.48	0.12	0.26	**0.001**	<0.001	**0.05**
Leaf Thickness (mm)	<0.001	<0.001	**<u>0.001</u>**	0.32	0.11	0.63	0.09	**0.001**	**0.01**	0.09	**0.02**	0.25	0.31	<0.001	0.79	0.23	<0.001	**0.001**
Vegetative Biomass (g)	**<u>0.001</u>**	**0.03**	<0.001	0.10	**0.01**	0.10	0.90	0.08	**0.001**	0.05	0.06	0.74	0.85	**0.04**	0.07	**0.04**	**0.04**	0.08
Total Biomass (g)	**<u>0.001</u>**	0.12	<0.001	0.42	0.23	0.38	0.06	**0.03**	0.05	0.09	**0.03**	0.74	0.85	**0.001**	0.08	**0.08**	**0.04**	**0.03**
Leaf Nitrogen Concentration (%)	**<u>0.001</u>**	**0.03**	<0.001	**0.01**	**0.01**	0.12	0.07	**0.04**	**0.01**		**0.01**	0.62	0.61	**0.02**	0.10	0.09	**0.04**	**0.01**
Physiological																		
Chlorophyl Absorbance (SPAD)	<0.001	**0.001**	**<u>0.001</u>**	0.21	0.65	0.34	**0.02**	**0.01**	**0.001**	0.22	0.07	0.31	0.40	**0.02**	0.86	0.37	0.10	**0.02**
Photosynthetic Rate (μmol CO_2 m^{-2} s^{-1})	<0.001	**0.003**	**<u>0.001</u>**	0.99	0.51	0.66	0.49	**0.001**	**0.001**	0.30	0.05	0.52	0.60	**0.03**	0.06	**0.04**	0.27	0.05
Transpiration Rate (mol H_2O m^{-2} s^{-1})	<0.001	<0.001	<0.001	0.08	**0.01**	**0.01**	0.07	**0.01**	0.06	0.34	0.15	0.05	**0.04**	<0.001	0.14	**0.001**	**0.004**	**0.03**
Stomatal Conductance (mol H_2O m^{-2} s^{-1})	<0.001	**0.001**	<0.001	0.10	0.07	0.11	0.52	0.20	0.09	0.10	**0.02**	0.72	0.67	<0.001	0.14	0.37	**0.02**	0.07
Water Use Efficiency (Transpiration/ photosynthetic rate)	<0.001	<0.001	**<u>0.001</u>**	0.06	**0.04**	0.07	0.16	**0.01**	0.13	0.76	0.05	0.14	0.18	<0.001	0.38	0.34	0.13	**0.004**
Water Potential (MPa)	<0.001	<0.001	**<u>0.001</u>**	0.08	0.09	0.67	0.07	<0.001	0.05	0.08	<0.001	0.07	0.09	<0.001	0.07	0.06	**0.001**	**0.003**
Internal CO_2 (μmol CO_2 mol^{-1})	<0.001	0.06	<0.001	0.20	**0.02**	0.10	0.12	0.06	0.05	0.09	**0.01**	0.76	0.78	<0.001	0.14	0.09	**0.03**	<0.001
13C Carbon Isotope ($\Delta^{13}C$)	<0.001	<0.001	**<u>0.001</u>**	0.19	0.05	0.28	0.52	0.09	0.30	0.06	0.11	0.11	0.10	**0.005**	0.25	**0.04**	**0.002**	**0.02**
Ecological																		
A. gerardi cover (%)	<0.001	**0.001**	**0.02**	0.91	0.25	0.29	0.06	<0.001	**0.04**	0.30	<0.001	**0.02**	0.30	**0.001**	0.26	0.12	**0.001**	**0.001**
Grass cover (%)	<0.001	**0.01**	<0.001	0.10	0.12	0.20	0.09	0.12	0.11	0.11	**0.001**	**0.01**	**0.01**	**0.004**	0.12	**0.03**	**0.005**	**0.06**
Forb cover (%)	<0.001	**0.003**	<0.001	0.07	**0.01**	**0.02**	0.20	0.19	**0.001**	**0.01**	**0.001**	0.19	0.10	<0.001	0.07	**0.02**	**0.002**	<0.001
Bare cover (%)	<0.001	<0.001	<0.001	0.10	**0.03**	0.27	0.10	<0.001	0.05	0.09	<0.001	**0.01**	**0.03**	<0.001	0.09	**0.02**	**0.04**	<0.001
Genetic																		
Nucleotide Diversity (π)	**0.04**	**0.04**	**0.02**	0.25	0.42	0.57	0.36	**0.01**	0.50	0.97	0.10	0.18	0.05	**0.02**	0.83	0.26	0.08	**0.04**
Allelic Richness	**0.02**	0.07	**0.02**	0.05	0.16	**0.04**	0.57	**0.02**	0.77	0.85	**0.04**	0.42	0.06	**0.04**	0.10	0.97	**0.03**	0.06
Observed Heterozygosity	**0.03**	**0.04**	**0.04**	0.09	0.11	0.05	0.09	**0.02**	0.22	0.07	0.09	0.99	**0.04**	**0.04**	0.09	0.10	0.05	0.07

Response Variable (Linear)	Mean Annual Precip (mm)	Growing Season Precip (mm)	Aridity Index	Mean Annual Temp (°C)	Warmest Month Temp (°C)	Coldest Month Temp (°C)	Lat.	Long.	Elev. (m)	Temp Ann. Range (°C)	Precip Seasonal.	Mean Diurnal Range (°C)	Growing Season Temp.(°C)	2023 Annual Precip (mm)	2023 Annual Temp (°C)	2023 Warmest Month Temp (°C)	2023 Grow. Season Precip (mm)	2023 Aridity Index
QUADRATIC RESPONSE																		
Morphological																		
Vegetative Height (cm)	**<0.001**	**0.001**	**<0.001**	**0.03**	**0.04**	**0.001**	**0.04**	**0.01**	**0.01**	**0.01**	**0.01**	0.40	0.33	0.06	0.06	**0.001**	**0.01**	**0.02**
Blade Width (cm)	**<0.001**	**0.001**	**<0.001**	0.08	0.14	0.10	0.77	**0.01**	**0.04**	0.17	0.12	0.32	0.24	**<0.001**	0.06	**0.003**	**0.03**	**0.02**
Diameter (cm)	**<0.001**	**0.002**	**<0.001**	**0.01**	0.09	0.10	0.07	**0.02**	**<0.001**	**0.04**	**0.001**	0.55	0.48	0.12	0.26	**0.001**	**<0.001**	0.05
Leaf Thickness (mm)	**<0.001**	**<0.001**	**<0.001**	0.32	0.11	0.63	0.09	**0.001**	**0.01**	0.09	**0.02**	0.25	0.31	**<0.001**	0.79	0.23	**<0.001**	**0.001**
Vegetative Biomass (g)	**<0.001**	**0.03**	**<0.001**	0.10	**0.01**	0.10	0.90	0.08	**0.001**	0.05	0.06	0.74	0.85	**0.04**	0.07	**0.04**	**0.04**	0.08
Total Biomass (g)	**<0.001**	0.12	**<0.001**	0.42	0.23	0.38	0.06	**0.03**	0.05	0.09	**0.03**	0.74	0.85	**0.001**	0.08	**0.08**	**0.04**	**0.03**
Leaf Nitrogen Concentration (%)	**<0.001**	**0.03**	**<0.001**	**0.01**	**0.01**	0.12	0.07	**0.04**	**0.01**		**0.01**	0.62	0.61	**0.02**	0.10	0.09	**0.04**	**0.01**
Physiological																		
Chlorophyl Absorbance (SPAD)	**<0.001**	**0.001**	**<0.001**	0.21	0.65	0.34	**0.02**	**0.01**	**0.001**	0.22	0.07	0.31	0.40	**0.02**	0.86	0.37	0.10	**0.02**
Photosynthetic Rate (μmol CO_2 m^{-2} s^{-1})	**<0.001**	**0.003**	**<0.001**	0.99	0.51	0.66	0.49	**0.001**	**0.001**	0.30	0.05	0.52	0.60	**0.03**	0.06	**0.04**	0.27	0.05
Transpiration Rate (mol H_2O m^{-2} s^{-1})	**<u>0.001</u>**	**<0.001**	**<0.001**	0.08	**0.01**	**0.01**	0.07	**0.01**	0.06	0.34	0.15	0.05	**0.04**	**<0.001**	0.14	**0.001**	**0.004**	**0.03**
Stomatal Conductance (mol H_2O m^{-2} s^{-1})	**<0.001**	**0.001**	**<0.001**	0.10	0.07	0.11	0.52	0.20	0.09	0.10	**0.02**	0.72	0.67	**<0.001**	0.14	0.37	**0.02**	0.07
Water Use Efficiency (Transpiration/ photosynthetic rate)	**<0.001**	**<0.001**	**<0.001**	0.06	**0.04**	0.07	0.16	**0.01**	0.13	0.76	0.05	0.14	0.18	**<0.001**	0.38	0.34	0.13	**0.004**
Water Potential (MPa)	**<0.001**	**<0.001**	**<0.001**	0.08	0.09	0.67	0.07	**<0.001**	0.05	0.08	**<0.001**	0.07	0.09	**<0.001**	0.07	0.06	**0.001**	**0.003**
Internal CO_2 (μmol CO_2 mol^{-1})	**<0.001**	0.06	**<0.001**	0.20	**0.02**	0.10	0.12	0.06	0.05	0.09	**0.01**	0.76	0.78	**<0.001**	0.14	0.09	**0.03**	**<0.001**
13C Carbon Isotope ($\Delta^{13}C$)	**<0.001**	**<0.001**	**<0.001**	0.19	0.05	0.28	0.52	0.09	0.30	0.06	0.11	0.11	0.10	**0.005**	0.25	**0.04**	**0.002**	**0.02**
Ecological																		
A. gerardi cover (%)	**<0.001**	**0.001**	**0.02**	0.91	0.25	0.29	0.06	**<u>0.0001</u>**	**0.04**	0.30	**<0.001**	**0.02**	0.30	**0.001**	0.26	0.12	**0.001**	**0.001**
Grass cover (%)	**<u>0.001</u>**	**0.01**	**<0.001**	0.10	0.12	0.20	0.09	0.12	0.11	0.11	**0.001**	**0.01**	**0.01**	**0.004**	0.12	**0.03**	**0.005**	**0.06**
Forb cover (%)	**<u>0.001</u>**	**0.003**	**<0.001**	0.07	**0.01**	**0.02**	0.20	0.19	**0.001**	**0.01**	**0.001**	0.19	0.10	**<0.001**	0.07	**0.02**	**0.002**	**<0.001**
Bare cover (%)	**<u>0.001</u>**	**<0.001**	**<0.001**	0.10	**0.03**	0.27	0.10	**<0.001**	0.05	0.09	**<0.001**	**0.01**	**0.03**	**<0.001**	0.09	**0.02**	**0.04**	**<0.001**
Genetic																		
Nucleotide Diversity (π)	**0.04**	**0.04**	**0.02**	0.25	0.42	0.57	0.36	**<u>0.005</u>**	0.50	0.97	0.10	0.18	0.05	**0.02**	0.83	0.26	0.08	**0.04**
Allelic Richness	**0.02**	0.07	**0.02**	0.05	0.16	**0.04**	0.57	**<u>0.002</u>**	0.77	0.85	**0.04**	0.42	0.06	**0.04**	0.10	0.97	**0.03**	0.06
Observed Heterozygosity	**0.03**	**0.04**	**0.04**	0.09	0.11	0.05	0.09	**<u>0.001</u>**	0.22	0.07	0.09	0.99	**0.04**	**0.04**	0.09	0.10	0.05	0.07

Table 4.4. Results from regression model analysis using edaphic (soil N, pH, sand, silt, or clay content) variables as predictors. P-values shown (**α<0.05)** with significant variables in bold and highest contributing variable (highest F statistic and lowest p-value) bold and underlined.

Response Variable (Linear)	Soil N (%)	Soil pH	Soil Sand (%)	Soil Silt (%)	Soil Clay (%)
LINEAR RESPONSE					
Morphological					
Vegetative Height (cm)	0.40	**0.04**	**0.006**	**0.007**	**0.04**
Blade Width (cm)	0.08	**0.04**	0.09	**0.04**	0.36
Diameter (cm)	**0.01**	**0.008**	**0.01**	**0.002**	0.33
Leaf Thickness (mm)	0.08	**0.03**	**0.01**	**0.01**	0.94
Vegetative Biomass (g)	**0.02**	**0.03**	**0.01**	**0.01**	**0.01**
Total Biomass (g)	**0.01**	**0.01**	**0.05**	**0.001**	**0.001**
Leaf Nitrogen Concentration (%)	**0.01**	**0.02**	**0.01**	0.07	0.39
Physiological					
Chlorophyl Absorbance (SPAD)	**0.04**	**0.02**	0.08	**0.01**	0.53
Photosynthetic Rate (µmol CO_2 m^{-2} s^{-1})	0.08	**0.05**	0.05	**0.01**	**0.01**
Transpiration Rate (mol H_2O m^{-2} s^{-1})	0.11	0.16	**0.01**	**0.01**	**0.01**
Stomatal Conductance (mol H_2O m^{-2} s^{-1})	0.18	**0.05**	0.76	**0.01**	**0.02**
Water Use Efficiency (Transpiration/ photosynthetic rate)	0.06	0.08	**0.02**	0.11	**0.01**
Water Potential (MPa)	**0.01**	**0.05**	0.26	**0.02**	0.21
Internal CO_2 (µmol CO_2 mol^{-1})	0.80	0.09	0.65	0.95	0.49
13C Carbon Isotope ($\Delta^{13}C$)	0.25	**0.003**	**0.05**	**0.03**	0.96
Ecological					
A. gerardi cover (%)	0.22	0.13	**0.05**	0.11	**0.03**
Grass cover (%)	0.17	0.33	0.14	0.24	**0.01**
Forb cover (%)	**0.03**	0.11	**0.01**	**0.004**	**0.01**
Bare cover (%)	0.07	0.19	**0.02**	0.09	**0.01**
Genetic					
Nucleotide Diversity (π)	0.95	0.55	0.06	0.10	**0.04**
Allelic Richness	0.77	0.48	0.08	0.07	**0.02**
Observed Heterozygosity	0.97	0.21	0.12	0.18	0.09

Table 4.5. AICc results from regression analysis of either A. linear or B. quadratic terms. The top two models are bold, and the best model (lowest AICc) is bold and underlined.

Response Variable	Mean Annual Precip (mm)	Growing Season Precip (mm)	Aridity Index	Mean Annual Temp (°C)	Warmest Month Temp (°C)	Coldest Month Temp (°C)	Lat.	Long.	Elev. (m)	Temp Ann. Range (°C)	Precip Seasonal.	Mean Diurnal Range (°C)	Growing Season Temp.(°C)	2023 Annual Precip (mm)	2023 Annual Temp (°C)	2023 Warmest Month Temp (°C)	2023 Grow. Season Precip (mm)	2023 Aridity Index
Morphological																		
Vegetative Height (cm)	**1279.4**	1414.9	1351.9	1412.1	1418.3	1432.6	1427.7	**1332.0**	1381.7	1469.9	1339.3	1467.9	1472.1	1441.1	1439.3	1451.5	1470.1	1467.6
Blade Width (cm)	**123.6**	142.5	215.8	187.1	185.4	158.0	188.0	**132.2**	205.0	132.2	249.6	150.1	136.1	163.9	152.1	144.2	139.2	140.0
Diameter (cm)	**1315.8**	1478.6	1392.2	1458.5	1467.2	1480.5	1469.1	**1344.7**	1432.0	1505.0	1354.8	1493.4	1510.4	1493.3	1486.2	1492.2	1510.9	1507.9
Leaf Thickness (mm)	651.5	647.6	**554.7**	579.9	583.1	579.0	579.1	**562.0**	712.3	577.7	752.6	598.5	580.0	597.9	579.0	580.4	596.7	591.7
Vegetative Biomass (g)	**1134.8**	1343.2	1303.3	1325.3	1322.0	1352.4	1325.4	**1183.5**	1321.6	1360.0	1278.2	1355.1	1368.6	1360.0	1358.4	1363.8	1368.9	1368.1
Total Biomass (g)	**1320.2**	1403.4	1368.2	1382.7	1380.4	1409.0	1379.5	1351.8	1379.4	1411.5	1356.4	1407.3	1422.3	1416.9	1414.0	1418.1	1422.4	1422.0
Leaf Nitrogen Concentration (%)	**91.1**	131.3	178.5	118.9	125.4	111.4	151.2	143.8	166.6	118.6	188.0	106.8	107.5	110.9	106.7	103.0	**97.2**	100.9
Physiological																		
Chlorophyl Absorbance (SPAD)	818.0	829.4	721.8	871.8	871.8	871.0	871.0	792.5	786.8	873.4	755.3	860.0	871.1	866.1	871.3	871.8	869.1	866.5
Photosynthetic Rate (µmol CO_2 m^{-2} s^{-1})	824.8	864.2	816.1	867.1	866.2	861.0	865.9	816.2	841.2	854.3	790.4	838.7	866.8	865.8	859.4	863.5	866.8	863.6
Transpiration Rate (mol H_2O m^{-2} s^{-1})	261.0	269.5	282.4	303.9	320.9	295.7	312.7	266.5	275.6	338.8	284.2	346.5	340.3	297.5	298.1	310.1	336.2	339.6
Stomatal Conductance (mol H_2O m^{-2} s^{-1})	442.8	449.3	436.8	417.2	419.3	433.2	435.6	450.4	423.4	**404.5**	437.0	413.0	406.1	425.6	431.5	418.5	411.9	409.4
Water Use Efficiency (Transpiration/photosynthetic rate)	627.5	675.8	577.6	722.2	728.0	728.3	723.0	590.9	612.6	731.7	568.1	726.7	727.9	707.2	729.0	728.8	727.5	717.1
Water Potential (MPa)	41.4	38.0	32.0	64.4	66.6	63.7	66.4	34.6	65.3	66.7	36.5	38.4	64.5	39.6	64.1	63.4	56.2	58.7
Internal CO_2 (µmol CO_2 mol^{-1})	1598.7	1632.6	1591.6	1625.9	1630.0	1630.1	1632.5	1589.3	1610.4	1634.7	1586.3	1623.9	1633.6	1628.5	1630.8	1628.7	1633.4	1631.1
13C Carbon Isotope ($\Delta^{13}C$)	130.6	136.0	**100.0**	178.6	178.5	181.0	182.7	127.3	**103.3**	190.8	110.5	191.2	177.8	164.7	183.8	186.2	187.7	168.8
Ecological																		
A. gerardi cover (%)	847.5	837.9	842.5	848.5	848.6	848.5	841.2	848.6	844.0	820.4	831.4	849.9	847.5	848.0	847.2	846.1	845.1	848.2
Grass cover (%)	725.3	796.9	773.1	792.6	794.7	793.5	789.1	773.0	788.5	803.3	761.9	804.5	793.6	791.6	795.7	799.5	804.2	796.6
Forb cover (%)	790.9	843.3	825.5	840.6	838.7	844.4	821.9	836.7	835.5	844.9	823.3	851.1	842.4	835.0	846.4	849.0	852.1	834.3
Bare cover (%)	770.9	747.0	742.1	789.4	785.9	788.8	792.6	777.6	755.1	794.3	737.7	794.3	785.8	772.1	785.9	786.9	792.5	769.4
Genetic																		
Nucleotide Diversity (π)	694.3	715.1	702.8	716.3	717.1	714.7	717.0	673.2	709.7	706.9	688.7	718.7	718.6	692.2	716.5	719.3	700.1	705.3
Allelic Richness	46.3	85.7	75.3	100.1	97.3	99.5	100.7	58.1	94.8	109.8	49.9	117.2	118.9	108.8	101.5	109.6	118.9	117.4
Observed Heterozygosity	278.0	305.8	298.0	288.2	280.7	300.9	687.2	309.8	467.1	501.8	500.1	316.4	389.3	308.4	303.1	305.0	313.4	313.8

Response Variable	Mean Annual Precip (mm)	Growing Season Precip (mm)	Aridity Index	Mean Annual Temp (°C)	Warmest Month Temp (°C)	Coldest Month Temp (°C)	Lat.	Long.	Elev. (m)	Temp Ann. Range (°C)	Precip Seasonal.	Mean Diurnal Range (°C)	Growing Season Temp.(°C)	2023 Annual Precip (mm)	2023 Annual Temp (°C)	2023 Warmest Month Temp (°C)	2023 Grow. Season Precip (mm)	2023 Aridity Index
Morphological																		
Vegetative Height (cm)	1301.2	1395.0	1309.3	1403.5	1414.8	1426.6	1423.8	1310.7	1429.4	1463.6	1467.9	1469.9	1416.2	1424.5	1423.3	1443.9	1472.1	1467.6
Blade Width (cm)	280.0	194.1	249.6	187.0	183.8	156.0	187.1	242.3	169.7	136.3	150.1	142.2	182.7	174.4	152.9	145.3	137.7	140.0
Diameter (cm)	1317.0	1427.2	1344.8	1445.8	1461.0	1467.7	1466.9	1361.9	1471.2	1502.3	1493.4	1505.0	1459.4	1483.9	1467.9	1489.2	1512.6	1507.9
Leaf Thickness (mm)	676.9	731.8	752.6	581.7	584.8	590.0	587.7	690.8	584.2	598.4	598.5	577.7	582.2	604.7	577.8	579.2	599.8	591.7
Vegetative Biomass (g)	1233.5	1324.8	1278.2	1311.4	1315.4	1341.6	1323.2	1282.8	1331.7	1357.0	1355.1	1360.0	1328.3	1357.0	1340.6	1361.4	1371.0	1368.1
Total Biomass (g)	1320.4	1385.0	1356.4	1373.7	1374.4	1399.5	1377.2	1349.7	1388.8	1403.6	1407.3	1411.5	1384.3	1415.8	1401.6	1417.6	1424.2	1422.0
Leaf Nitrogen Concentration (%)	249.8	159.7	188.0	118.8	126.6	113.4	152.5	162.8	107.7	100.8	106.8	118.6	119.7	116.7	111.8	103.0	95.3	100.9
Physiological																		
Chlorophyl Absorbance (SPAD)	797.3	770.2	**725.3**	870.1	873.6	869.0	869.9	**750.3**	866.4	858.3	860.0	873.4	872.5	866.0	873.2	873.9	871.2	866.5
Photosynthetic Rate (µmol CO_2 m^{-2} s^{-1})	825.5	806.5	**790.4**	863.1	859.5	859.0	857.8	815.5	865.2	863.6	838.7	854.3	868.9	867.6	859.9	861.7	868.8	863.6
Transpiration Rate (mol H_2O m^{-2} s^{-1})	**251.1**	271.2	284.2	306.0	313.0	297.8	295.1	**247.1**	316.0	312.1	346.5	338.8	305.6	282.3	299.2	312.2	338.0	339.6
Stomatal Conductance (mol H_2O m^{-2} s^{-1})	454.3	447.5	437.0	461.6	**400.3**	467.0	463.9	449.0	419.3	409.6	413.0	404.5	415.7	436.7	490.3	439.1	411.7	409.4
Water Use Efficiency (Transpiration/photosynthetic rate)	617.1	652.5	**548.1**	712.6	727.1	725.2	724.5	**551.3**	726.0	710.6	726.7	731.7	724.1	700.2	728.1	727.2	728.9	717.1
Water Potential (MPa)	34.3	42.2	**30.5**	66.3	67.9	65.8	67.1	**33.0**	66.3	47.6	33.4	66.7	62.8	36.4	63.6	34.3	34.8	58.7
Internal CO_2 (µmol CO_2 mol^{-1})	1600.8	1592.1	**1586.3**	1628.0	1632.0	1632.1	1630.2	**1591.0**	1631.9	1633.8	1623.9	1634.7	1626.1	1626.4	1632.8	1600.8	1786.4	1631.1
13C Carbon Isotope ($\Delta^{13}C$)	127.5	133.3	110.5	175.5	174.4	179.6	177.7	124.0	176.5	158.6	191.2	190.8	179.0	166.6	184.7	127.5	147.2	168.8
Ecological																		
A. gerardi cover (%)	**753.7**	786.2	761.9	779.8	788.7	780.7	782.7	**744.2**	783.9	785.3	804.5	803.3	788.8	789.8	780.1	799.7	804.9	848.2
Grass cover (%)	789.8	837.7	823.3	842.2	834.3	845.9	821.1	836.4	844.9	847.4	851.1	844.9	844.6	827.3	846.6	851.1	849.6	796.6
Forb cover (%)	**729.2**	745.3	**737.6**	790.6	787.7	790.9	794.6	758.9	795.5	783.4	794.3	794.3	783.8	743.8	785.9	783.0	789.2	834.3
Bare cover (%)	696.4	714.1	**688.7**	712.5	717.6	712.9	714.7	**670.4**	715.3	711.3	718.7	706.9	714.1	686.5	707.8	698.2	698.2	769.4
Genetic																		
Nucleotide Diversity (π)	**677.4**	705.4	700.1	690.3	683.6	702.9	705.9	**658.9**	694.5	713.6	716.4	701.8	691.4	708.2	704.3	706.3	702.9	705.3
Allelic Richness	**44.0**	80.0	49.9	69.5	87.4	76.9	92.5	**40.5**	102.5	120.9	117.2	109.8	101.6	101.6	59.7	97.9	120.9	117.4
Observed Heterozygosity	**180.0**	194.1	249.6	187.0	183.8	256.0	187.1	**169.7**	242.3	196.3	250.1	192.2	182.7	184.4	182.9	195.3	197.7	313.8

Table 4.6. Estimates of nucleotide diversity, allelic richness, and observed heterozygosity among *A. gerardi* populations.

Site	Allelic Richness	Nucleotide Diversity (π)	Observed Heterozygosity
AL	1.18	0.179	0.24
AR	1.19	0.189	0.15
CO	1.20	0.222	0.27
IA	1.24	0.240	0.27
IL	1.20	0.199	0.18
IN	1.23	0.232	0.27
KS1	1.21	0.202	0.25
KS2	1.19	0.184	0.15
LA	1.22	0.216	0.144
MI	1.18	0.177	0.25
MN	1.25	0.244	0.31
MO	1.22	0.217	0.16
MS	1.15	0.145	0.19
MT	1.22	0.220	0.25
NC	1.19	0.189	0.14
ND	1.24	0.239	0.27
NE1	1.23	0.228	0.26
NE2	1.22	0.221	0.25
NM	1.15	0.145	0.16
OK	1.21	0.207	0.17
SC	1.19	0.189	0.22
SD	1.20	0.196	0.30
TX2	1.19	0.190	0.17
TX3	1.17	0.163	0.21
WI	1.24	0.236	0.27

Table 4.7. Variance partitioning analysis of plant traits by a full model of biogeographic range position and climatic variables with the total variation explained and unexplained. Model 1 is geographic variables alone, and model 2 is climatic variables alone with the total variation explained and unexplained in each model. Model 3 is precipitation and aridity alone (conditioned by geography and temperature alone).

Response variables	**Full Model Joint latitude, longitude, and climate**	**Model 1 (latitude and longitude, conditioned by climate)**	**Model 2 (climate, conditioned by latitude and longitude)**	**Model 3 (climate, conditioned by latitude, longitude, and temperature alone)**
Constrained (total explained)	4216.2	220.7 (4.0%)	1755.9 (32.0%)	3028.8 (55.7%)
Total joint explained	76.8%			
Total unexplained	1272.9 (23.2%)			
Significance Tests	F= 5.89, p=0.0001	F = 1.37, p=0.22	F = 4.51, p=0.01	F = 5.18, p=0.001

Supplemental Methods 1: Literature Review

To evaluate how empirical data across plant species' geographic ranges support theoretical expectations about range dynamics, we conducted a systematic literature review focused on two key frameworks: the Abundant Center Hypothesis (ACH) and a clinal pattern model (CPM). These models make distinct predictions about the distribution of abundance, traits, and genetic diversity across a species' range, yet it remains unclear how often and under what conditions each is supported. Our goal was to synthesize existing evidence to assess the relative support for each model across plant systems.

We conducted the review using the Web of Science database and included studies published between January 1, 1900, and July 7, 2025. To identify relevant studies, we used the following search string: *("Abundant Center" OR "Center Periphery" OR "Center Margin" OR "Center Edge" OR "Central Marginal Hypothesis") AND plant* AND (trait OR genetic*) NOT animal*. This search was designed to capture studies that explicitly addressed center–periphery dynamics in plants, while excluding research focused on animals or reviews of existing data. This search yielded a total of 152 peer reviewed papers.

We then applied the following inclusion criteria: studies had to (1) focus on plant species, (2) measure empirical trait or genetic data across a geographic range, and (3) include information relevant to evaluating the ACH or CPM. We excluded studies that were reviews, meta-analyses, or that involved experimental manipulation of plants (e.g., genetic manipulation of plant traits), as our goal was to synthesize empirical evidence across natural gradients.

Each study that met the inclusion criteria was then assessed and categorized according to the following parameters: Data Type(s): A = Abundance, T = Trait, G = Genetic; ACH Support: Whether the study supported the Abundant Center Hypothesis (yes/no/mixed); ACH

Response Type: L = Linear, NL = Nonlinear, Cat = Categorical; CPM Support: Whether the study supported the clinal pattern model (yes/no/mixed); CPM Response Type: L = Linear, NL = Nonlinear, Cat = Categorical (i.e., studies that did not model a continuous response across the range, but instead grouped sites into discrete categories such as “core” vs. “margin”);

This structured approach allowed for consistent categorization of studies and facilitated comparison across the different types of data and patterns reported.

Methods S2: Ecological Niche Model

We used an N-mixture model (Royale 2004) and assumed the density of *A. gerardi* followed an inhomogeneous Poisson point process with a mean value varying as a log-linear function of the climate predictor variables (Kéry & Royale 2020). This analysis corrects for spatial autocorrelation. We conducted two analyses to handle problems with collinearity. First, we estimated the effect of linear, quadratic, and two-way interaction terms among all non-collinear climate predictors (mean annual precipitation, growing season precipitation, maximum temperature of the warmest month, mean annual temperature, and aridity index) on abundances (we call this the multivariate model). Second, we fit a series of univariate models, one for each climate predictor, that fit abundances are functions of a linear and quadratic effects of that climate predictor. For each climate variable, we used both the multivariate and univariate models to predict expected (latent) abundance, λ, as a function of each climate predictor (holding other climate predictors constant).

Owing to the limited number of quadrature (background) sites (counties; cf. Warton & Shepherd 2010), we interpret the predicted abundance of *A. gerardi* as relative abundance. Thus, our interest is in the form of the trends of λ with each climate variable, not their absolute magnitudes. To provide context for the analysis of morphological, physiological, and community traits, we constructed multivariate and univariate niche models of the species' response to each of the climate variables. Occurrence data was obtained from Smith et al. (2017), who compiled 5784 records of *A. gerardi* across its native range collected from 1950 to 2013. These records were obtained from publicly-available databases (e.g., the Global Biodiversity Information Facility; https://gbif.org), plus by personally contacting herbaria within the species' range, with special emphasis on cases near the species' climatic limits. These records were supplemented

with specimen and plot-type data from 2014 to 2020 from BIEN version 4 (Maintner et al. 2018). We georeferenced records to the level of a county or equivalent, expect for some provincial-level records in Canada. While the coarse spatial resolution introduces some uncertainty in the output, we believe the tradeoff is justified because applying stringent quality filters resulted in loss of many records, especially near the edge of the range where climatic conditions are likely limiting. Thus, we used the number of records in each county as the observed response in the models.

We constructed Bayesian N-mixture models (Royale 2004) for each climatic variable, wherein the latent (unobserved) number of *A. gerardi* individuals follows an inhomogenous Poisson point process (Kéry & Royale 2020), with a mean (expected) value at site i of λ:

Eq. S1 $$\log(\lambda_i) = \boldsymbol{X}\beta$$

where $\boldsymbol{X}$ is a model design matrix including an intercept, and β a column vector of coefficients to be fit by the model. For the univariate models, we used a linear and quadratic term; i.e., if written in long form:

Eq. S2 $$\log(\lambda_i) = \beta_0 + \beta_0 x_i + \beta_0 x_i^2$$

where the β's are coefficients to be fit, and x is the value of the climate variable of interest. For the multivariate model we used a similar structure with linear and quadratic terms, except that we also included two-way interaction terms between each pair of variables.

The realized number of *A. gerardi* individuals, N, is assumed to follow a Poisson distribution:

Eq. S3 $$N_i \sim \text{Poisson}(\lambda_i)$$

from which the samples (observed number of *A. gerardi*), y, are drawn:

Eq. S4 $$y_i \sim \text{Binomial}(p_i, N_i).$$

The parameter p is a function of sampling intensity, which we assumed was a function of the area of a county and the number of Poaceae records in the county collected between 1950 and 2000 (obtained from GBIF and BIEN), after logit-transforming p:

Eq S5 $$\text{logit}(p_i) = \alpha_0 + \alpha_1 \log(\text{county area}) + \alpha_2 \log(\text{Poaceae}).$$

All predictors were centered to 0 and scaled by their standard deviation before modeling.

We wrote the model in nimble version 1.2.1 (de Valpine et al. 2017) for R version 4.4.1 (R Core Team 2024). All coefficients were fit using a vague prior with a mean of 0 and precision of 0.1. For multivariate and univariate models, we generated 4 chains of 200,000 iterations thinned every 200 samples (for 1000 samples per chain), plus 40,000 iterations for burn-in (except for the univariate aridity model, which due to convergence issues required 1,000,000 iterations per chain, with a thinning rate of 1000, not counting 100,000 burn-in iterations). We assessed convergence using the Gelman-Rubin statistic (Gelman & Rubin 1992) and mixing and chain stability by visual inspection of trace and density plots.

To generate a map of the multivariate predictions for identifying the location of the range core, we calculated the mean λ across all MCMC iterations for each county and color-coded the respective county by a shade indicative of the value, divided into quantiles. We define the location of the range "core" to be those counties with λ in the top 5^{th} quantile.

To construct a graph of univariate responses, we created a matrix of values of the predictor spanning the minimum to the maximum observed across counties with at least one *A. gerardi* record, extended by 10% on either side of this range (but truncated to values ≥0 if values <0 were physically impossible for the given variable). We then calculated the expected value of λ for the given value of the climate variable. For each value of the climate variables, we plotted the mean value of λ across the Monte Carlo Markov chains, plus its 95% credibility intervals.

Across all models and coefficients, the upper 95% CI of the Gelman-Rubin statistic for all βs and αs was 1.06, which is below the threshold value of 1.1, indicating the models converged.

Methods S3: Plant and Environmental Analyses

Carbon Isotope Analysis. The dried samples were ground, combusted with a CE1110 elemental analyzer (Carlo Erba Instruments, Milan, Italy) and coupled to a Delta Plus mass spectrometer (Thermo Electron Corporation, Bremen, Germany) for isotope analysis using a ConFlo II Universal Interface (Thermo Electron Corporation, Bremen, Germany). The isotopic ratio of samples was calculated using delta notation as: $\delta = \left[\left(\frac{R_{sample}}{R_{s\tan dard}} - 1 \right) * 1000 \right]$ (Farquahar et al., 1982) where *R* is the ratio of the heavy to light isotope for the sample and standard, respectively.

Soil Classification. At the Kansas State University Soils Testing Lab (Manhattan KS, USA) we tested the homogenized soil for soil carbon and nitrogen content using a LECO TruSpec CN combustion analyzer and pH using a Cadmium reduction in a flow analyzer. We also assessed soil texture (sand, silt, or clay content) using the hydrometer method using sodium hexametaphosphate as the dispersing agent (Recommended Chemical Soil Test Procedures, 1998).

***DNA Extraction and Isolation*.** We used 550 µl per sample of extraction buffer added to ground samples containing 100 mM Tris-HCl, pH 8.0, 100 mM EDTA, pH 8.0, 1.4 M NaCl, 2% CTAB, 12 mM TCEP (a non-toxic substitute for beta-mercaptanethanol), 16 mM Sodium Diethyldithiocarbamate Trihydrate, 4% PVPP. This was followed by 50 µl per sample of reducing buffer containing 100 mM Tris-HCl, pH 8.0, with 120 mM TCEP and 160 mM DIECA added separately. Quality was quantified for DNA concentration with PicoGreen (ThermoFisher.com) and normalized for library preparation. All samples were prepared for genotyping-by-sequencing (Poland and Rife, 2012) using a two restriction enzyme pair of PstI and MspI. For each plate, we used 200 base paired-end sequencing in one Illumina NovaSeq+ 25b lane.

Abundance of other species. Forb cover increased linearly with longitude with the highest cover of forbs in the furthest east (high longitude) populations (Supplemental Figure 6A). Other graminoid species cover or bare ground were highest (<30% each) at the western sites (lowest longitude) and declined to <10% in wet sites (Supplemental Figure 6B, C)

Site Environmental Measurements. We made several measurements to characterize the environment of the sampled plants. Volumetric soil water content was measured using METER soil moisture probes (ECH20 10HS Onset S-SMD-M005 Soil Moisture Sensor) to assess soil moisture (volume/volume, %). The probes were established at 15cm depth and one reading was measured at the base of each focal plant (6 readings per site). Soil temperature was measured using a Zoro Digital 20cm Soil Thermometer (Zoro Tools, Buffalo Grove IL, USA) at the base of each plant (6 readings per site). *S*oil moisture and soil temperature varied but in general, soil moisture increased with annual precipitation, soil temperature increased with annual temperature, and ground light availability increased with aridity (Supplemental Figure 2A-C).

Chapter 5 - Drivers of Intraspecific Trait Variation and Drought Response of a Dominant North American Great Plains Grass: Disentangling the Role of Climate and Genetic Background

Running Title: Climate and Genetics Shape Trait Variation

Authors: Jack Sytsma[1], Helen Winters[1], Matthew Galliart[2], Ryann Patterson[1], Brian Maricle[3], and Loretta Johnson[1]

Institutions and Addresses: [1]Division of Biology, Kansas State University, Manhattan, Kansas, USA, [2]Department of Biological Sciences, Fort Hays State University, Hays, Kansas, USA, [3]Department of Biology, Saginaw Valley State University, University Center, Michigan, USA

Key Words: *Andropogon gerardi,* C_4 Grass, Environmental Gradients, Functional Trait, Greenhouse, Grasslands, Phenotypic Plasticity

Abstract

Intraspecific trait variation (ITV) is critical for plant adaptation, particularly under increasing drought. ITV arises from phenotypic plasticity and genetic differentiation, so identifying its sources improves understanding of population responses to drought. This study investigates how climate and genetics shape ITV and drought responses in *Andropogon gerardi*, a foundational Great Plains grass. To quantify climatic determinants of ITV, we conducted a common-garden greenhouse experiment with 25 *A. gerardi* populations spanning wide temperature (4–21°C; Minnesota–Texas) and precipitation (350–1400 mm yr^{-1}; Colorado–North Carolina) gradients, measuring 17 functional traits. To test drought as a selective pressure, eight populations across a precipitation gradient (470–1350 mm yr^{-1}) were exposed to experimental drought (15% moisture vs. 30% control). Populations were also genotyped to assess the genetic basis of ITV, and greenhouse–field trait comparisons were used to separate genetic and environmental effects. We hypothesized that climate of origin, particularly precipitation, predict ITV: dry populations would express drought-adaptive traits (higher water-use efficiency, shorter stature), whereas wet populations would exhibit competitive traits (greater height, biomass). We further predicted that drought would reduce growth and delay flowering, with stronger effects in wet populations, and that trait variation would correspond with genetic differentiation. Precipitation and aridity were the strongest predictors of ITV. Principal component analyses revealed that wet populations displayed competitive traits (taller stature, larger leaves), while arid populations showed drought-adaptive traits (higher water-use efficiency, reduced stature). Under drought, wet populations exhibited greater declines in biomass and photosynthesis, indicating drought as a key selective force. Congruent genetic and trait PCAs confirmed a strong genetic basis for ITV, and consistent greenhouse–field patterns reinforced genetic control. Overall, ITV in *A. gerardi* is primarily shaped by precipitation through coordinated, genetically based trait responses, offering a predictive framework for grassland adaptation under future climate change.

Introduction

Trait variation is a cornerstone of ecological and evolutionary processes, influencing how organisms acquire resources, tolerate stress, and interact with their environment (McGill et al., 2006; Violle et al., 2007; Laughlin et al., 2020a). While often examined across species, intraspecific trait variation (ITV)—variation within species—is increasingly recognized as equally important (Bolnick et al., 2011; Des Roches et al., 2018; Westerband et al., 2021a) as interspecific variation. For example, ITV helps explain how populations adapt to environmental change (Malyshev et al., 2016), accounting for up to 25% of trait variation within communities (Siefert et al., 2015). Plant ITV is a powerful driver of ecosystem dynamics—at times surpassing interspecific differences in shaping communities and ecosystem functions (Des Roches et al., 2018). Yet, ITV varies widely within species (Westerband et al., 2021b), fueling a growing recognition of the role of ITV in shaping species' responses to climate (Valladares et al. 2014).

Common gardens, where all experimental plants share the same conditions, are foundational tools for disentangling sources of ITV (Turesson, 1922; VanWallendael et al., 2022; Schwinning et al., 2022; Johnson et al., 2022). This approach is particularly powerful in the context of climate gradients: it allows researchers to test whether populations from contrasting environments consistently exhibit differences in functional traits and whether those differences align with their climate-of-origin (Schwinning et al., 2022)

When paired with targeted environmental manipulations (e.g., water availability), common gardens can reveal not only whether climate-of-origin predicts trait values, but also how populations respond to stress under standardized conditions (Schwinning et al., 2022; Johnson et al., 2022). Such experiments allow researchers to evaluate whether trait–climate associations—especially those linked to rainfall (Johnson et al., 2015; 2022)—reflect responses to historical

selective pressures such as climate. Identifying whether populations differ in their tolerance to drought, and whether this variation corresponds to climate-of-origin, is critical for anticipating species' responses to increasing water limitation under predicted droughts (Gazol et al., 2023).

A key portion of ITV is genetically based, arising from genetic differentiation (Westerband et al., 2021a) making it essential to consider genetic structure and adaptive variation when interpreting trait–climate relationships (Pennington et al., 2021). When common garden studies are paired with genomic data, researchers can directly test of whether trait differences among populations reflect underlying genetic divergence rather than site-level physiological adjustment to environment (Schwinning et al., 2022, Johnson et al. 2022). Experiments that integrate trait, genetic, and environmental data provide a clearer understanding of how genetic variation contributes to functional diversity within species—and how that diversity may shape future responses to drought (Sork, 2018; Pennington et al., 2021).

In contrast to controlled common garden studies in the greenhouse, field studies capture trait variation under ecologically realistic conditions, integrating the effects of local climate, soil, and species interactions (Jacobs et al., 2012; Breitschwerdt et al., 2019). These approaches are complementary: common gardens offer mechanistic insight and experimental control, while field observations provide ecological realism and context (Sork, 2018). Combining both approaches is especially powerful, as it clarifies not only how traits vary, but which sources of variation—genetic, environmental, or their interaction (Groot et al., 2018)—are driving observed patterns across a species range.

In this study, we use a common garden approach in a greenhouse to assess ITV and drought responses of *Andropogon gerardi* (Vitman, big bluestem), a dominant C_4 perennial grass and foundation species of the U.S. Great Plains (Rogler, 1944; Knapp et al., 1998). We examined

25 populations spanning over 2,000 km across the species' range, encompassing wide climatic gradients in temperature (4–21°C; Minnesota to Texas, US) and precipitation (350–1400 mm yr^{-1}; Colorado to North Carolina). In another study, these same populations were also measured in the field (Sytsma et al., in review), where striking ITV patterns—including regional trait shifts and potential drought-induced short-stature phenotypes—were observed. To test whether these patterns reflect genetic differentiation or environmental acclimation, we collected seed from the same field-measured populations and grew them under controlled greenhouse conditions, enabling direct comparisons of field and greenhouse trait variation. If these populations from dry regions remain short-statured even under well-watered conditions, this would suggest a genetic basis of the trait (Ramirez-Valiente et al., 2022); however, if short-statured plants increase growth when water limitation is removed, this would indicate strong environmental control and plasticity (Martinez-Sancho et al., 2025). While *A. gerardi* productivity is known to decrease along the east–west rainfall gradient of the U.S. Great Plains (Weaver, 1950; Sala et al., 1988; Epstein et al., 1998), the underlying cause remains unresolved. Specifically, it is unclear whether productivity declines because plants in drier environments exhibit plastic responses approaching physiological limits (Kempes et al., 2019; Pugnaire et al., 1999; Liu et al., 2021) or because they are genetically constrained (Lynch et al., 2022) to conservative, drought-adapted phenotypes.

To address how ITV in *A. gerardi* reflects climate adaptation and/ or genetic differentiation, we pursued four integrated objectives. First, we quantified ITV in 25 populations grown in a greenhouse common garden to test whether trait variation aligns with climatic gradients across the species' range. We hypothesized that populations from hotter, drier environments would express drought-tolerant trait syndromes (reduced height, narrower and thicker leaves; Grime, 1988; Jardine et al., 2021), while populations from cooler, wetter climates

would exhibit more acquisitive traits (greater height and biomass, broader leaves) to support competitive growth, resource acquisition, and carbon assimilation (Jardine et al., 2021). Second, to evaluate rainfall as a primary selective pressure (Siepeleski et al., 2017), we conducted a controlled drought experiment on a subset of populations spanning a sharp precipitation gradient (472–1356 mm yr^{-1}), hypothesizing that although all populations would perform worse under drought, populations from wetter regions would show larger declines compared to populations from drier regions since dry populations may be pre-adapted to low rainfall (De Kort et al., 2020).

Third, we assessed whether observed ITV reflects underlying genetic differentiation. We characterized genetic differentiation using genotyping by sequencing (GSB, Poland & Rife, 2012) across all populations. We predicted that populations would show strong genetic differentiation (Loveless et al., 1984; Sork, 2018; Salgotra & Chauhan, 2023) and the differentiation would correlate with morphological and physiological traits, indicating a genetic basis for observed ITV. Finally, we directly compared ITV in the greenhouse with trait data from the same populations measured in the field (Sytsma et al., in review). By integrating field and greenhouse data, we aim to clarify the extent to which climate-associated trait variation reflects evolutionary differentiation versus short-term acclimation to environment through phenotypic plasticity.

Importantly, studies with this breadth of populations, traits, and experimental approaches are rare in common garden research (Johnson et al., 2022), underscoring the novelty and significance of our design. This design allowed us to evaluate whether ITV patterns observed in natural environments are retained under common conditions—providing insight into whether trait variation is genetically based or shaped primarily by phenotypic plasticity or short-term

adjustment to local environmental conditions. By integrating field and greenhouse data with genetic data, we aim to clarify the extent to which climate-associated trait variation reflects evolutionary differentiation versus phenotypic plasticity.

Methods

Seed Collection and Germination

Seed of 25 *A. gerardi* populations were collected by hand Sept-Dec 2023 from sites located across the range of this species (Figure 5.1). These seed were collected at the same locations as the field populations studied in Sytsma et al. (in review) but not from the same exact plants, however, one population failed to germinate, leaving 25 populations represented in this study. Seed was scarified and seeded into germination trays with Berger BM2 germination blend potting soil February 22-23, 2024 in a greenhouse at Kansas State University (Manhattan, KS, USA). Trays were watered to maintain surface moisture until seedling reached a sufficient size for transplanting. Then seedlings were transplanted into pots (20 x 10 x 10 cm) containing Berger BM6 general purpose soil mix.

Experimental Design: Greenhouse Common Garden Study

We conducted two experiments to assess ITV in *A. gerardi* across 25 populations (Obj 1) and drought response from eight populations across the rainfall gradient (Obj. 2). Our main experiment (Obj. 1) included all populations sourced from gradients of temperature (4–21°C) and precipitation (350–1400 mm yr^{-1}; Figure 5.1A). Each population had six replicate plants (six replicate plants x 25 populations = 150 plants total) that were watered daily to maintain field capacity (~30% soil moisture, mean= 31.4%).

To assess response to experimental drought (Obj 2), we conducted a separate, second experiment with a subset of eight populations sourced across a precipitation gradient (472-1356 mm yr^{-1} MAP; Figure 5.1B). The drought experiment had eight replicates (eight populations × two treatments × eight replicate plants = 128 plants total). Initially, plants were watered daily to allow for establishment and early growth. Starting on the 63rd day of the experiment, watering was reduced to once every two days to maintain ~15% soil moisture for the droughted plants. For control plants, watering continued every day to maintain ~30% soil moisture.

For both experiments, plants were randomized in a block design across greenhouse benches. We maintained the greenhouse at ~25°C (range: 24–28°C) with no supplemental lighting. Light levels in the greenhouse remained between 900–1200 μmol m^{-2} s^{-1} between 10:00-14:00 throughout the course of both greenhouse experiments.

Functional Traits. To quantify ITV in relation to climate-of-origin (Obj. 1), and in response to experimental drought (Obj 2), we conducted measurements of 17 morphological, physiological, and phenological traits. For measurements that were conducted several times during the experiment, we focus our analysis on the data taken after plants had sufficient time to reach maturity (35 days after the start of the experiment) and are presented in the main narrative. Measurements taken before and after this time are included in the supplement.

Morphological Traits. To assess differences in plant morphology, we measured vegetative height, leaf width, leaf thickness, leaf area, number of leaves, and reproductive stalk diameter. For height, we extended the longest leaf vertically and recording to the nearest cm, excluding reproductive stalks. We measured leaf width by averaging three mature leaves at their broadest point. We assessed leaf thickness with a Mitutoyo hand caliper of an average of three leaves per plant, excluding the midvein. We assessed leaf surface area from images captured

using a NIKON D5500 DSLR mounted on a two-meter tripod, with plants placed on white paper to prevent background interference. A 15 cm reference ruler was included in each photo for analysis in FIJI-Image. Leaf area was measured three times in ~3-week intervals during both experiments. At the end of each experiment, we counted the number of leaves per plant and measured the reproductive stalk diameter using a Mitutoyo hand caliper 15 cm above the soil surface.

To evaluate the growth dynamics of each population throughout both experiments, we assessed relative growth rate (RGR) for height and leaf area. We used the following equation: RGR = [(height or leaf area at time t) - (height or leaf area at time 0)] / (time t - time 0); Hoffmann & Poorter, 2002).

Physiological Traits. To assess plant physiology, we assessed gas exchange, chlorophyll absorbance, and water potential. We measured gas exchange three times during both experiments using a LICOR-6400 XT IRGA system (LICOR Bioscience, Lincoln NE, USA). We measured photosynthetic rate, stomatal conductance, water-use efficiency (WUE; photosynthetic rate/ transpiration rate), transpiration rate, and internal CO_2 concentration. We took measurements 10:00-14:00 on a young, fully expanded leaf at 400 ppm CO_2, ambient humidity and temperature, and 1500 µmol photons $m^{-2}s^{-1}$ photosynthetically active radiation. Gas exchange was recorded once photosynthetic rates stabilized and the coefficient of variation remained <1 for more than one minute. Each week during both experiments, we assessed leaf chlorophyll absorbance with a SPAD-502 chlorophyll meter, obtaining the mean of at least three readings per plant on fully expanded leaves. We measured midday leaf water potential three times in both experiments using a pressure chamber (PMS Instrument Co.)

Phenological Traits: To track phenological changes in both experiments, we monitored plants daily for date of bolting (defined by the presence of a flowering stalk) and flowering (defined by the presence of anthers) until all plants that did not remain vegetative had flowered.

Above and Belowground Biomass Harvest from Drought Experiment: We harvested the plants from only the drought experiment (not the main experiment). To assess biomass allocations in the drought experiment, we harvested aboveground biomass at soil level, stored it in paper bags, and later drying it at 60ºC for at least 72hrs. Aboveground biomass was subsequently divided into vegetative (leaves), reproductive stalk, or seed allocations and weighed. We also harvested belowground biomass (rhizome and root tissue), washed thoroughly with water to remove soil, stored paper bags, and dried at 60º C for at least 72hrs. The rhizome and root tissue were weighed separately.

Pot Soil Moisture. Volumetric soil water content was measured daily using METER soil moisture probes (ECH20 10HS Onset S-SMD-M005 Large Volume Soil Moisture Sensor, 15 cm depth) were used to monitor soil moisture as volume/ volume (%). For the main experiment, one reading was measured per block (six readings per day) as well as all plants in the experiment (n=150) weekly. In the drought experiment, we randomly assigned five permanent probes to five control and five droughted plants and recorded moisture daily. We also took readings of soil moisture from all plants in the experiment (n=128) weekly. For both experiments, we also measured ambient light levels with a LI-191R Quantum Sensor above each block and recorded soil temperature using a ECOWITT Zoro temperature probe bi-weekly. Results of soil moisture, temperature, and light availability from both experiments are reported in Figures S1-S2.

Home Site Climate Data. We downloaded mean (30-year normal) climatic variable from the ClimateNA version 7.3 database based on GPS coordinates where *A. gerardi* seed was

collected. The main experiment source populations ranged from 418-1413mm yr^{-1} historic (30 year averages, 1990-2020) mean annual precipitation (MAP; Figure 5.1A), 5.8-21.2°C historic mean annual temperature (MAT), and aridity index (calculated =(MAT + 10) / (MAP / 1000); Table 5.1). The source populations from the drought experiment ranged 472-1356 mm yr^{-1} MAP (Figure 5.1B). The full climatic dataset is found in Table 5.1.

Statistical Analyses of Functional Traits

Objective 1. Trait-Climate Relationships. To investigate functional trait variation among populations (Obj. 1) in relation to climate, we used a model selection approach to test how climate influences ITV. Trait measurements after plants had sufficient time to reach maturity (35th day of the experiment) are presented and analyzed in the main narrative, while analyses of measurements taken before and after peak are included in the supplement. For each trait, we fit 20 mixed models that included linear terms for each climate predictor (from Climate NA as before; Table 5.1), linear and quadratic terms, and an intercept only model. Initially, we assessed maternal effects by including seed mass from each population as a covariate in our models. However, since seed mass was never found to be a significant predictor, it was removed from subsequent analyses. In all models, we used population as a random effect. We also tested for potential block effects, but none were significant, and blocks were excluded from final models. We compared models using AIC in JMP pro 17 (SAS Institute Inc., Cary, NC, 1989–2023).

Principal Components Analyses of Trait and Climate Variation. To assess patterns of trait and climate variation across all populations in the main experiment, we conducted separate principal components analyses (PCA) on trait data and climate variables. All variables were log-transformed for standardization prior to analysis. Both PCAs were conducted in JMP Pro

17 (SAS Institute Inc.) using correlation matrices to account for differences in measurement scales. To test whether trait variation was associated with climate, we performed a linear regression between all climatic predictors (Table 5.1) and population scores on PCA axis 1, and compared models using AIC.

Plant Trait Network Analysis. To examine trait structure and interrelationships, we constructed plant trait networks (PTNs; He et al., 2020) in R (v.4.3.2) using the igraph package (Csardi & Nepusz, 2006). Networks were built from pairwise Pearson correlations among all traits, with values log-transformed, standardized (mean = 0, variance = 1), and filtered to retain only significant correlations after false discovery rate correction (Benjamini & Hochberg, 1995). We focused on two network metrics: degree (k), the number of significant connections a trait has with others (hub traits have the highest k), and betweenness (B), which captures how strongly a trait connects multiple functional clusters. In visualizations, hub traits are shown as gold circles and all others as gray; traits with high betweenness are emphasized by multiple edges (trait correlations). Edge colors indicate correlation direction (blue = positive, red = negative), and edge lengths reflect correlation strength, with shorter edges indicating stronger associations.

Objective 2: Experimental Drought Effects on Traits. To analyze the effects of drought treatment, population origin, and their interaction on all traits (Obj. 2), generalized linear models (GLMs) were performed using JMP pro 17 with treatment and population origin as fixed factors. Trait measurements after plant had been subjected to drought conditions for ~one month are presented and analyzed in the main narrative, while analyses of all other measurements taken during the experiment are included in the supplement. Trait measurements were conducted the same day for control plants. Variance components were derived by dividing the mean square of

each factor into its corresponding variance contribution. We calculated an analysis of covariance (ANCOVA) to test for the effects of population and treatment (drought or control) as well as the population x treatment interaction.

Principal Components Analysis of Trait Responses to Drought. To evaluate how functional trait variation among populations responds to drought across a precipitation gradient, we conducted separate PCAs for control and drought treatments. Prior to analysis, all traits were standardized with log transformation. Biplots were generated to visualize trait loadings and population-level variation along the first two principal components. Separate analyses for each treatment (drought or control) allowed us to assess how drought alters multivariate trait coordination and how these changes align with precipitation gradients among population origins.

Plant Trait Network Analysis of Drought Responses. To evaluate how drought treatment altered trait coordination, we also constructed separate plant trait networks for control and drought treatments using the same procedures described for Objective 1. Networks were based on morphological, physiological, and phenological traits measured 38 days after the start of drought, with log transformation, standardization, and retention of only significant (FDR-corrected) correlations. We focused on the same network characteristics described in Obj. 1 for the drought experiment analysis: edge density (ED), degree (k), and betweenness (B). Like before, in our visualizations, hub traits are shown as gold circles, betweenness is shown having the most edges, and edge color reflects the direction of the correlation (blue=positive, red=negative).

Objective 3: Genetic Differentiation of Populations

To test whether genetic differentiation underlies observed ITV (Obj. 3), we sequenced the home populations from the field study using genotyping by sequencing (GBS; Poland & Rife,

2012) from *in-situ* individuals sampled across populations. Specifically, in 2023, we collected five leaf samples from the midsection of leaves of six plants from the home populations of the main experiment. We flash froze the 150 samples (six plants x 25 populations) on dry ice in the field, freeze dried them for at least 72hrs, finely ground the tissue, and stored it at −80°C until DNA isolation. We isolated DNA using a modified CTAB protocol (Doyle & Doyle, 1987). Full description of the extraction and SNP identification are found in the supplement.

Genetic PCA. To explore individual-level genetic relationships and background, we conducted a genetic PCA using **SNPRelate** (Zheng et al., 2012) on SNP data derived from the GBS dataset. We applied the PCA to the genotype data to summarize genetic variation among individuals and extracted the first two principal components for visualization and subsequent statistical analyses.

Genetic Differentiation-Trait Association. To assess the extent to which genetic differentiation explains trait divergence (Obj. 3) in the greenhouse experiment, we explored the relationship between Trait PC1 of the main greenhouse experiment (from our trait-based greenhouse PCA from Obj.1) and the first axis from our genetic PCA using linear mixed-effects models, including population as a random effect. Statistical significance was assessed using p-values, with a threshold of 0.05 to determine significance of the genetic PCA axis in explaining trait variation. This approach enabled us to relate genetics to trait variation.

Objective 4: Traits in Greenhouse Compared to Field Setting.

To compare trait variation between controlled greenhouse and natural, field environments (Obj. 4), we used trait data from the same populations of *A. gerardi* that were measured both in the field (Sytsma et al., in review, data in dryad doi:10.5061/dryad.905qfttzm) and here in our greenhouse main experiment. The same set of phenotypic traits was compared in both

environments settings to ensure comparability. To summarize multivariate trait variation across populations, we conducted separate PCAs on greenhouse datasets and extracted PC1 scores for the field from Sytsma et al. (in review, data in dryad doi:10.5061/dryad.905qfttzm). The comparison of these PCAs were used to assess the consistency of population-level trait differences in these two settings. We log transformed any data that did not fit a normal distribution.

Because PC axis 1 explained substantial variation (68.3% and 56.7% variation, in field and greenhouse respectively), this allowed us compare trait PCA scores between the two settings. To do this, we performed a linear regression between the first principal component axis (PC1) from the greenhouse data and PC1 from the field data. This allowed us to evaluate the extent to which trait variation observed in the greenhouse predicts trait patterns expressed under natural field conditions.

Results

Trait Variation Across Climate Gradients Explained Mainly by Precipitation and Aridity

Trait variation in the main experiment comprised of 25 populations was strongly associated with climate-of-origin (Table 5.2). Specifically, 7 of 17 traits were significantly associated with home site mean annual precipitation (MAP), 6 of 17 traits with home site aridity index, and 4 of 17 traits with growing season temperature (Table 5.2).

Morphological Traits. In terms of morphological traits, vegetative height increased linearly with home MAP, nearly doubling, ($R^2 = 0.85$; $p<0.001$; Figure 5.2A), ranging from ~40 cm in dry to ~75 cm in wet populations. Also doubling or tripling with home MAP included leaf area (~110–225 cm^2; $R^2 = 0.79$; $p<0.001$), leaf width (range 0.65–1.1 cm; $R^2 = 0.49$; $p<0.001$), leaf number (range 9-25 leaves; $R^2 = 0.71$; $p<0.001$), and stalk diameter (range 2.2-6.9 mm; $R^2 =$

0.62; $p<0.001$; Figures 5.2B, S3A-C). Unlike the other morphological traits, leaf thickness showed the strongest relationship with home aridity (Table 5.2). Thickness nearly doubled in populations from more arid sites (ranging from ~0.11 mm in less arid to ~0.19 mm in more arid sites ($R^2 = 0.62$; $p<0.001$; Figure 5.2C). Vegetative height growth rates were highest in populations from warmer sites, doubling from cool to warm (0.24-0.44 cm/day; $R^2 = 0.44$; $p<0.001$). Leaf area growth rate was ~5 x greater in populations from cool to warm climates: 0.4-2.8 cm^2/day ($R^2 = 0.53$; $p<0.001$; Figure S3).

Physiological Traits. Six of seven physiological traits were most strongly predicted by home aridity index (Table 5.2). The following significantly increased positively and linearly with home aridity (Figures 5.2D–E, S3): Photosynthetic rate (range 11.2-18.1 μmol CO_2 m^{-2} s^{-1}; $R^2 = 0.48$; $p<0.001$), chlorophyll absorbance (range 31.8-39.7 SPAD units; $R^2 = 0.56$; $p<0.001$), water-use efficiency (range 3.4–5.3 μmol CO_2, $R^2 = 0.52$; $p<0.001$), water potential (range -0.40 to -0.75 MPa; $R^2 = 0.66$; $p<0.001$), and stomatal conductance (range 0.139-0.205 μmol H_2O; $R^2 = 0.49$; $p<0.001$). Transpiration rate was the only physiological trait significantly associated with MAP (Table 5.2) and decreased linearly with precipitation (range 3.5-2.2 μmol H_2O; $R^2 = 0.51$; $p<0.001$; Figure S3E).

Phenological Traits. In contrast to other traits described above, phenological traits were primarily driven by home site growing season temperature (Table 5.2). Populations sourced from cooler origins bolted earlier by up to 32 days ($R^2 = 0.68$; $p<0.001$) and flowered earlier by up to 72 days ($R^2 = 0.70$; $p<0.001$; Figures 5.2F, S3).

Ordination Analysis. Principal components analysis (PCA) of functional traits from the main experiment revealed clear separation based on climate among the 25 populations (Figure 5.3A). The first two principal components (PC1 and PC2) explained 64.9% and 19.0% of the

total variance, respectively (Figure 5.3A). Negative values on PC1 were primarily associated with leaf thickness, transpiration rate, water use efficiency, and photosynthetic rate, while positive loadings reflected differences in height, blade width, growth rate, and reproductive phenology (bolting and flowering). Regression analysis revealed a significant positive relationship between MAP and trait PCA axis 1 scores ($R^2 = 0.96$, $p < 0.001$), indicating that trait variation aligns with precipitation gradients across populations in their home site (Figure 5.3C). These results suggest that climate-of-origin, especially MAP, plays a key role in shaping functional trait divergence among populations.

Network Analysis. In our trait correlation network (Figure 5.3D), we first correlated response variables to climate variables. Starting with precipitation, the following were all positively associated with MAP: height, leaf width, stalk diameter, number of leaves, height-based growth rate, leaf area-based growth rate, flowering, bolting, water potential and leaf area (blue arrows; Figure 5.3D; all $p<0.001$). On the other hand, leaf thickness and stomatal conductance were also significantly correlated with MAP but negatively (red arrows; Figure 5.3D; both $p<0.0001$). Moving on to aridity, chlorophyll absorbance, photosynthetic rate, water use efficiency, and stomatal conductance were significantly positively correlated with aridity (blue arrows; Figure 5.3D; all $p<0.0001$). In contrast, height, leaf width, and water potential were significantly negatively correlated with aridity (red arrows; Figure 5.3D; all $p<0.0001$). Flowering, bolting, and growth rate (based both on height and leaf area) were all significantly positively correlated with home MAT (blue arrows; Figure 5.3D; both $p<0.0001$).

Consistent with these patterns, the degree (k) and betweenness (B) metrics highlighted several hub traits and climatic variables critical to network structure. In terms of climate variables, MAP had the highest degree (number of significant correlations; $k = 9$; yellow circles

in Figure 5.3D). This means that MAP was directly connected to more variables than any other climate factor and indicates that it broadly influences trait–climate relationships. Among traits, height had the highest degree (number of significant correlations with other traits; k = 8; yellow circles in Figure 5.3D), indicating it interacted with multiple other traits and potentially served as a key integrator (hub trait) within the network. Traits with high betweenness (B) reflect how often a trait lies along the shortest paths linking other traits or variables and have a stronger bridging role to other traits in the network. In our network, flowering had the highest betweenness (B = 12.5), coordinating connections among distinct traits in the network.

Population-Level Response to Experimental Drought: Wet Populations Are More Affected by Drought

In the drought experiment (Obj. 2), all traits except leaf width and leaf thickness exhibited significant responses to the main effect of experimental drought (Table 5.3). Our ANCOVA analysis revealed significant treatment × population interactions for all response variables except leaf width, leaf thickness, rhizome biomass, and aboveground:belowground biomass ratio (Table 5.3).

Morphological Traits. Under experimental drought (Figure 5.4), we observed significant reductions in ten morphological traits across populations, with the slope of the drought response differing significantly from the control (Table 5.3). Specifically, height ($R^2 = 0.74$; $p<0.001$), leaf area ($R^2 = 0.33$; $p<0.001$), total aboveground biomass ($R^2 = 0.94$; $p=0.0002$), and total belowground biomass ($R^2 = 0.87$; $p<0.001$) all declined significantly more sharply under drought conditions compared to control (Figures 5.4A–C, S4; Table 5.3). Similarly, declines were observed in number of leaves ($R^2 = 0.75$; $p<0.001$), stalk diameter ($R^2 = 0.75$; $p<0.001$),

vegetative biomass ($R^2 = 0.27$; $p=0.001$), reproductive biomass ($R^2 = 0.82$; $p<0.001$), seed biomass ($R^2 = 0.26$; $p<0.001$), and root biomass ($R^2 = 0.86$; $p<0.001$; Figure S4; Table 5.3).

Importantly, populations originating from wetter climates exhibited the steepest declines across all morphological traits, in contrast to populations sourced from drier climates were relatively unaffected by drought. Populations from wetter areas under experimental drought compared to control showed greatest reductions in height (28.1% lower), leaf area (47.7% lower), aboveground biomass (27.0% lower), and belowground biomass (46.5% lower), number of leaves (41.7% lower), stalk diameter (46.2% lower), vegetative biomass (36.5% lower), reproductive biomass (38.7% lower), seed biomass (72.3% lower), and root biomass (35.8% lower; Figures 5.4; S4). In contrast, dry populations showed minimal change under drought treatment compared to control with less than 5% change in all responses (Figures 5.4; S4). Vegetative growth rates, based on changes in height and leaf area also declined more steeply under drought compared to control (Table 5.3; Figure S4). Once again, populations from wetter climates showed the greatest reduction (height growth rate 60.6% lower; leaf area growth rate 61.2% lower), with steeper declines than those from drier origins (no significant difference in populations from dry climates; Figure S4).

Physiological Traits. Physiological traits also responded strongly to experimental drought, with significantly steeper declines observed under drought compared to control treatments for all traits but only for populations sourced from the wet areas (Table 5.3). As with morphological traits, the steepest declines in physiological performance occurred in populations from wetter environments. For example, wet populations exhibited significant reductions under drought treatment in photosynthetic rate (79.7% lower; $R^2 = 0.91$; $p<0.001$), stomatal conductance (67.7% lower; $R^2 = 0.86$; $p<0.001$), water-use efficiency (64.6% lower; $R^2 = 0.55$;

$p<0.001$), and chlorophyll absorbance (48.3% lower; $R^2 = 0.86$; $p<0.001$) were consistent across populations (Figures 5.4E, S4). Similar to morphological traits, the dry populations showed minimal changes in physiology under drought with less than 10% change compared to control (Figures 5.4; S4).

Phenological Traits. In terms of reproductive timing, across populations experimental drought significantly delayed bolting (by at least five days; $R^2 = 0.58$; $p<0.001$) and flowering (by at least nine days; $R^2 = 0.83$; $p<0.001$Figures 5.4F, S4; Table 5.3).

Ordination Analysis. Our PCA revealed distinct patterns of trait variation across the precipitation gradient under both control and drought treatments (Figure 5.5). In the control treatment (Figure 5.5A), populations exhibited a spread along PCA axis 1, where positive loadings on PC1 were primarily associated with morphological traits such as increased height, biomass, and leaf area. In contrast, negative loadings were associated with dry populations and with traits such as WUE, leaf thickness, chlorophyll absorbance, and photosynthetic rate, suggesting differences in growth and allocation strategies among populations (Figure 5.5A).

Under drought conditions (Figure 5.5B), populations shifted in PCA space, where positive loadings on PC1 were associated with dry populations, including grouping traits such as number of leaves, seed biomass, growth rate, and stomatal conductance. Negative loadings on PC1 were associated with wet populations, including traits such as flowering, bolting, leaf width, and height (Figure 5.5B).

Trait Network Analysis. Under control conditions, photosynthetic rate and height were the network hub traits (highest degree, $k = 9, 8$, respectively; yellow circles; Figure 5.5C), showing these traits were directly connected to the greatest number of other traits in the network and may influence many aspects of plant performance. Flowering, photosynthetic rate, and

transpiration rate showed the highest betweenness (shortest edges to other traits; B= 2.73, 2.68, 2.62, respectively) among traits, meaning they lay on the shortest paths between many other traits and may act as key "bridges" that link different parts of the trait network (higher values = stronger bridging role).

However, the drought treatment (Figure 5.5D) fundamentally altered networks. For example, WUE and belowground biomass were network hub traits (degree; both k=7). Under drought treatment, traits with the highest betweenness were belowground biomass (B=4.67), stomatal conductance (B=4.44), and chlorophyll absorbance (B=4.58). These results indicate that, under drought treatment, traits related to water acquisition and resource efficiency were highly connected, influencing multiple physiological processes and potentially coordinate the plant's overall drought response.

Genetic Differentiation Explains Variation in Functional Traits

Genetic PCA: We performed principal coordinates analysis (PCA) to examine genetic structure across 25 populations in the main experiment (Figure 5.6A). The first two PCs accounted for 14.3% of the total genetic variance, with PC1 explaining 9.2% and PC2 2.8%. In general, populations clustered by MAP (Figure 5.6A) suggesting a gradient of genetic variation linked to precipitation, supporting precipitation as a key factor shaping genetic structure.

We also examined the relationship between genetic PC1 scores and trait PC1 scores across populations (Figure 5.6B). A significant association was found between genetic and trait PC1 scores (R^2=0.35, p=0.002; Figure 5.6B), indicating genetic differentiation aligns with trait variation across populations. These results suggest that genetic differentiation correlates with ITV across populations, highlighting how genetic differentiation is linked to trait divergence.

Traits Consistent Across Greenhouse and Field Settings

Multivariate trait patterns similar in field and greenhouse settings. Our PCA revealed distinct patterns of multivariate trait variation among *A. gerardi* populations in both the greenhouse and field settings. Using only the same traits observed in both studies, our greenhouse trait PCA showed PC1 and PC2 accounted for 68.3% and 24.7% of the variance, respectively (Figure 5.7A). In the field dataset, PC1 and PC2 accounted for 56.7% and 17.2% of the variance, respectively (Figure 5.7B; extracted from Sytsma et al. in review, dryad doi:10.5061/dryad.905qfttzm).

In both field and greenhouse settings, positive loadings on PC1 were primarily associated with variation in WUE, leaf thickness, internal CO_2 concentration, and photosynthetic rate (Figure 5.7A-B). In comparison, variation in water potential, leaf width, and height were related to negative loadings on PC1 in both settings (Figure 5.7A-B). Together, these results suggest that underlying genetic contributions to trait variation as populations showed consistent separation along PC1 in both field and greenhouse.

Comparison of PCA axes between greenhouse and field settings. To assess whether trait differences among populations were consistent between field and greenhouse and because PC1 explained so much variation in both settings, we regressed PC1 scores from the greenhouse and field data sets. We found a significant positive relationship between greenhouse and field population PC1 scores across populations ($R^2 = 0.86$**,** $p < 0.001$; Figure 5.7C), indicating that differences among populations were highly consistent across field and greenhouse and likely reflect underlying genetic differentiation expressed in both settings. Similarly, there was a significant positive relationship between trait PC1 scores across populations in both the field and greenhouse ($R^2 = 0.80$**,** $p < 0.001$; Figure 5.7C), indicating that trait variation in the greenhouse to

reflected similar patterns in the field. This result suggests that multivariate trait variation is, in large part, genetically based and consistent across field and greenhouse settings.

Discussion

Our study demonstrates that the selection pressure of climatic variation across the natural range of *A. gerardi* is a fundamental driver of phenotypic divergence, spanning broad mean annual temperature (4–21°C) and precipitation (350–1400 mm yr^{-1}) gradients. Overall, results highlight the importance of adaptation to historical climate-of-origin in shaping functional trait variation (Wadgymar et al., 2022). Here, we explore four key aspects in detail: first, we consider how precipitation and aridity shape ITV across populations of this widespread foundation plant species, emphasizing the critical role of climate in driving adaptation and trait divergence. Second, we discuss how populations differ in their physiological, morphological and phenological responses to experimental drought, uncovering distinct strategies for survival in water-limited environments and identifying that precipitation is the likely selection pressure on trait variation. Third, we reveal how climate-driven genetic divergence underpins these population-specific adaptive trait patterns and how this genetic differentiation aligns with ITV. Fourth, we discuss how remarkably similar patterns of ITV from the same populations across greenhouse and field settings reveal consistent population-level differentiation, providing evidence that ITV is largely genetically determined. Finally, we explore the implication of this work for conservation and restoration.

Trait Variation Among Populations is Driven by Precipitation

Our results show that precipitation is a major driver of ITV in *A. gerardi*, reinforcing evidence that water availability exerts strong selective pressure even within widespread species

(Siepeleski et al., 2017). PCA and network analyses (Figures 5.3, 5.5) revealed consistent differences between populations from wetter and drier environments, indicating long-term rainfall shapes functional strategies. For example, populations from wet sites exhibited acquisitive traits such as taller stature, broader and more numerous leaves, and greater leaf area (Jardine et al., 2021), while populations from dry sites expressed conservative traits—shorter stature, reduced leaf area, and thicker leaves—adapted for water conservation (Wang et al., 2022). Height was the network hub trait (He et al., 2020) demonstrating its key role in trait networks across populations. The central role of height in the trait network echoes broader findings that key 'hub' traits can coordinate multiple functional traits, influencing species' ecological strategies and responses to environmental gradients (Wright et al., 2004; Messier et al., 2017). Similar findings have been documented in other C_4 grasses, confirming the repeated emergence of drought-adaptive syndromes such as reduced leaf area, conservative growth, and efficient water use under dry conditions (Taylor et al., 2014; Lowry et al., 2014; Aspinwall et al., 2017; Griffin-Nolan et al., 2025; Heckman et al., 2025).

Physiological traits also were related to aridity where arid populations showed higher water-use efficiency and increased chlorophyll absorbance. These patterns are consistent with broader evidence that physiological traits, such as water-use efficiency and chlorophyll content, are closely linked to aridity gradients, enabling populations to optimize water capture and photosynthetic performance under drought stress (Galmés et al., 2007; Niinemets, 2010; Fernández-de-Uña et al., 2023). Such trait adjustments highlight the role of physiological plasticity in facilitating persistence across heterogeneous environments (Brooker et al., 2022).

Phenological traits such as bolting and flowering time were influenced primarily by home-site temperature (Figure 5.2F and 5.4F). Populations of *A. gerardi* from cooler climates

flowered earlier by over two months than those sourced from warmer climates. This early flowering is likely an adaptation to shorter growing seasons going from wet to dry (Johansson et al., 2013; Bhattacharya et al., 2022). Earlier phenological transitions in cooler-origin populations mirror adaptations to short growing seasons documented in other C_4 grasses (McMillian, 1959, 1964; Lovell et al., 2021; Heckman et al., 2025) but not to the extent we document here with a 72-day difference in flowering time between the coolest and warmest populations. This pronounced difference in flowering time of *A. gerardi* populations suggests emerging reproductive isolation (Christie et al., 2022). Overall, our results highlight how *A. gerardi* populations exhibit coordinated morphological, physiological, and phenological trait variation in response to local climate, illustrating the multifaceted ways environmental gradients drive ITV.

Precipitation is the Main Selective Pressure in Population-Specific Drought Response

In our drought experiment, populations differed markedly in response: those from wetter climates showed strong trait shifts under water stress, while populations from drier regions were minimally affected (Figures 5.4–5.5). These contrasting responses suggest not only fixed trait differences but also variation in phenotypic plasticity (Schlichting, 1986; Stotz et al., 2021). Specifically, wet populations expressed greater plasticity under drought, but this came at a cost of reduced performance, likely reflecting genetic constraints on tolerance (Carrera et al., 2018; Juenger, 2013; Burnette & Eckert, 2021). In contrast, dry populations exhibited limited plasticity likely since they are already pre-adapted to low rainfall, maintaining function under stress with little adjustment. Thus, drought responses are not uniform but depend on climate-of-origin, with dry populations showing fixed adaptive traits and wet populations relying more on plasticity (De Kroon et al., 2005; Matesanz & Ramírez-Valiente, 2019; Faralli et al., 2022).

Under experimental drought, most traits declined in magnitude across all populations, with populations from wet climates showing larger reductions than those from dry climates (Figure 5.4). Our ordination analyses reveal that drought treatment not only affects trait means but also alters coordinated trait syndromes. For example, in our trait network under control treatment, growth-related traits like photosynthetic rate and height are central hubs (He et al., 2020). However, under experimental drought, hub traits shifted to water-use efficiency and belowground biomass, reflecting a focus on water conservation (Wang et al., 2023). Similar drought-driven shifts in trait networks have been documented in other plant species, indicating a common strategy of reorganizing trait relationships to enhance drought tolerance (Anderegg et al., 2018; Díaz et al., 2016; Xu et al., 2020).

Under drought treatment, dry populations maintain growth-related traits like stomatal conductance and leaf number, whereas wet populations shift toward delayed flowering and reduced size, a pattern suggesting that populations from dry sites, putatively shaped by climate selection for drought tolerance (Dickman et al., 2019), are better adapted to reduced rainfall (Brunet et al., 2025). Experimental drought also delayed bolting and flowering in all populations, as has been observed in field observations of natural and experimental prolonged drought in grasslands (Schuchardt et al., 2021). However, delays were more pronounced in wet populations, suggesting that plants adapted to wetter conditions are more strongly affected by drought stress (Campbell et al., 2019). Taken together, these results confirm that precipitation is a key selective agent underlying ITV in *A. gerardi* and that adaptation to rainfall determines populations' capacity to maintain functional traits and reorganize trait networks under drought stress.

Genetic Differentiation Explains Trait Divergence Among Populations

In our study, genetic PCA revealed strong and geographically structured genetic differentiation among populations (Figure 5.6). This genetic structure aligned closely with patterns of trait variation, as shown by a significant correlation in a regression between genetic and trait PC scores, indicating congruence between genetic and phenotypic differentiation. This suggests that genetic differentiation among populations may also reflect adaptive responses to spatially varying selective pressures (Chung et al., 2023) especially precipitation. Similar associations between genetic and phenotypic divergence have been documented in a range of species (Jarvis et al., 2005; Zhao et al., 2022; Buenaño et al., 2025), including *A. gerardi* (Gray et al., 2014; Johnson et al., 2015; Galliart et al., 2019; 2020), supporting climate in shaping genetic differentiation.

The alignment of genetic axes with trait variation suggests that populations in different climate regimes may have undergone selection for distinct trait syndromes optimized for local conditions (Le Corre & Kremer, 2012; Savolainen et al., 2013; Sork, 2018). Similar genotype–phenotype associations have been observed in other species where climatic variables like precipitation and temperature strongly predict both genetic structure and trait differentiation (Aitken et al. 2008; Galliart et al., 2019; 2020; Blanco-Sanchez et al., 2024). These patterns highlight the role of climate-driven selection in maintaining adaptive diversity across wide geographic ranges (Lait et al., 2025). Such a pattern reinforces the idea that climate-related selective pressures can leave detectable signatures in both the genome and phenotype (Savolainen et al., 2013 Lovell et al., 2014; 2021). Taken together, these results demonstrate that both climatic gradients and genetic differentiation contribute to shaping phenotypic diversity within *A. gerardi*. Together, these insights emphasize that preserving genetic and phenotypic

diversity across climate gradients is essential for sustaining the adaptive potential of species (Bomblies & Peichel, 2022) under predicted droughts.

Traits Consistent in Greenhouse and Field, Confirming Genetic Basis for Trait Variation

By comparing ITV in the greenhouse common garden and in the field setting of the same populations of *A. gerardi,* we demonstrated strong and consistent population-level differentiation underlying trait variation. Specifically, our multivariate analyses revealed that key physiological and morphological traits covary similarly in both settings, and population-level differences in trait variation were highly correlated across settings based on the congruence of the greenhouse and field-based trait PCAs (Figure 5.7). This suggests that genetic variation is a major driver of ITV (Anderson et al., 2011; Chung et al., 2023) in *A. gerardi*, with populations maintaining their distinct phenotypes even under controlled conditions in the greenhouse.

The consistent covariation of traits such as water-use efficiency, leaf thickness, and photosynthetic rate (Figure 5.7) reflects coordinated physiological strategies adapted to contrasting climates (Grime, 1998; Jardine et al., 2021). Because this pattern occurs in both greenhouse and field settings, it likely reflects genetic differentiation subject to climatic selection (Ingvarsson & Street, 2011; Westerband et al., 2021; Cooper et al., 2022), consistent with evidence for strong genetic control of ITV across environmental gradients (Sork, 2018; Schwinning et al., 2022; Iozia et al., 2023; Janikova et al., 2024). Despite the more complex biotic interactions in the field (Lambers et al., 2019; Collins et al., 2022; Fagundes et al., 2022), trait alignment between greenhouse and field plants remains strong (Figure 5.7C–D), reinforcing the role of genetic rather than environmental control. This consistency also demonstrates that common garden experiments can capture genetically based trait variation relevant to natural

conditions, highlighting the value of integrating controlled and field studies for understanding plant adaptation (Schwinning et al., 2022).

Importantly, growth and trait differences observed among populations remained the same even under well-watered greenhouse conditions. Populations originating from arid environments remain shorter and with reduced leaf area than populations from wetter regions (Figure 5.2)—indicating that these differences reflect genetically based constraints. This genetic differentiation offers a mechanistic explanation for the well-described patterns of grassland productivity decline along the precipitation gradient as documented across the Great Plains by early ecologists (Weaver, 1950; Sala et al., 1988; Epstein et al., 1998). Thus, declining productivity of *A. gerardi* in more arid regions is not simply due to short-term water limitation, but instead reflects long-term evolutionary adaptation to drought, which constrains growth potential even when water is not limiting when growing in our well-watered common garden.

Implications for Conservation and Restoration Under Predicted Droughts

The results from this study have implications for future climate scenarios**,** where more frequent and intense drought events (IPCC, 2023; King et al., 2024) could alter the distribution of species (Aldea et al., 2024) and populations (Krishnadas et al., 2021), particularly those from wetter regions (Craine et al., 2013). We found that climate-of-origin not only shapes trait variation but ultimately also determines underlying genetic structure and adaptive functional strategies. Understanding these trait-genetic relationships is vital for predicting plant responses to future drought stress. Populations with greater drought tolerance may have a better chance of surviving in more water-limited environments, potentially driving shifts in plant communities across climatic gradients (Craine et al., 2013).

Importantly, the observed patterns of ITV were also correlated with population-level genetic differentiation. This highlights the need to incorporate ITV and genetic background into conservation and restoration planning. For long-lived species like *A. gerardi*, strategies such as adaptive introgression—introducing genotypes from populations adapted to projected future climates (Suarez-Gonzalez et al., 2018)—could enhance resilience and ensure restored populations are better equipped to cope with changing precipitation and temperature regimes (Hord et al., 2025). Doing so will improve the selection of resilient plant populations, helping to sustain grassland ecosystems under future droughts. Since *A. gerardi* is a foundation grass species in tallgrass prairies (Knapp et al., 1998), its response to experimental drought provides key insights into how the prairie as a whole may respond to drought (Gitlin et al., 2006). Therefore, understanding the mechanisms of drought adaptation in *A. gerardi* can inform broader predictions of how grasslands may respond to drought.

Conclusions

This study reveals the profound influence of climate-of-origin on functional trait variation of *A. gerardi* across broad temperature (4–21°C) and precipitation (350-1400 mm yr^{-1}) gradients. Our results demonstrate that the climate-of-origin—especially precipitation and aridity—is a dominant force shaping ITV and response to experimental drought. Importantly, these trait patterns are underpinned by the population's genetic background, indicating long-term selective processes have reinforced adaptation and functional divergence. Notably, our findings offer a mechanistic explanation for the well-documented east-to-west decline in grass productivity across the Great Plains (Weaver, 1968; Sala et al., 1988; Epstein et al., 1996) for which *A. gerardi* comprises 80% of the aboveground biomass of tallgrass prairie (Knapp et al.,

1998). We show that this pattern is driven not by phenotypic plasticity and short-term physiological acclimation to declining precipitation, but by genetically based differentiation. Populations from arid regions remain smaller and less productive even under well-watered greenhouse conditions, underscoring the evolutionary constraint of drought adaptation on growth potential. These insights are especially critical in the face of predicted increased droughts (Cook et al., 2015; IPCC, 2023; King et al., 2024), where accurate predictions of plant performance under drought hinge on understanding a population's adaptive capacity (Anderson & Song, 2020). Ultimately, this research offers essential guidance for conservation strategies (Des Roches et al., 2021) and the selection of climate-resilient populations (Vitt et al., 2022) under predicted droughts.

Acknowledgements. We thank all landowners, property managers, and entities for permitting use of their sites for this study. In particular, we thank the following individuals for collecting seed used in this study: T. Smetzer, G. Hanks, S. Pennings, T. Beckert, D. Crowley, K. Shannon, C. Osborne, M. Bell, D. Testerman, J. Gruchy, J. Hill, K. R. Heidorn, M. Kroll, L. Rowley, L. Reidel, K. Viste-Sparkman, W. Williams, P. Duekrop, K. Menard, S. Wessel, A. Jarding, T. Richardson, S. Digiacomo, N. Ellingson, A. Eigirdas, and M. Ahlering.

Conflicts of Interest Statement. The authors declare no conflicts of interest related to the research, authorship, or publication of this manuscript.

Data Accessibility Statement. All data supporting the findings of this study are available in a publicly accessible Dryad repository (doi:10.5061/dryad.1vhhmgr71).

CRediT Author Contributions. Jack Sytsma: Writing – original draft, supervision, conceptualization, investigation, data curation, formal analysis, methodology. **Helen Winters:** Investigation, writing- review and editing. **Ryann Patterson:** Investigation, writing- review and editing. **Brian Maricle:** Writing- review and editing, validation. **Allison Ricker:** Investigation, writing – review and editing. **Matthew Galliart:** Investigation, Writing- review and editing, validation. **Loretta Johnson:** Conceptualization, methodology, project administration, resources, funding acquisition, writing – review and editing.

Statement on Inclusion. Our U.S.-based research team brings expertise in plant ecology, evolution, and climate adaptation. While this greenhouse-based study did not involve local fieldwork or community engagement, we consulted regional scientists and land managers for the selection of populations and seed collection. Although we were not able to collaborate with Indigenous communities, we see this as a limitation and a call for future inclusion. We are committed to equitable, inclusive science that values diverse knowledge systems and reflects the complexity of the grasslands we study.

Funding Information. Funding for this study was provided by USDA grant #2020-03665. This study is partially funded by the 2024 Grassland Heritage Foundation Research Grant and the 2024 Kansas State University Ecumenical Ministry Grant awarded to Sytsma.

Figure 5.1**.** Map of sites of *A. gerardi* A. from 25 source populations across an aridity gradient (main experiment). Aridity is defined as (mean annual temperature in °C + 10)/ (mean annual precipitation in mm/ 1000) (Wang et al. 2016). B. Source populations for the drought experiment of eight populations across a mean annual precipitation gradient.

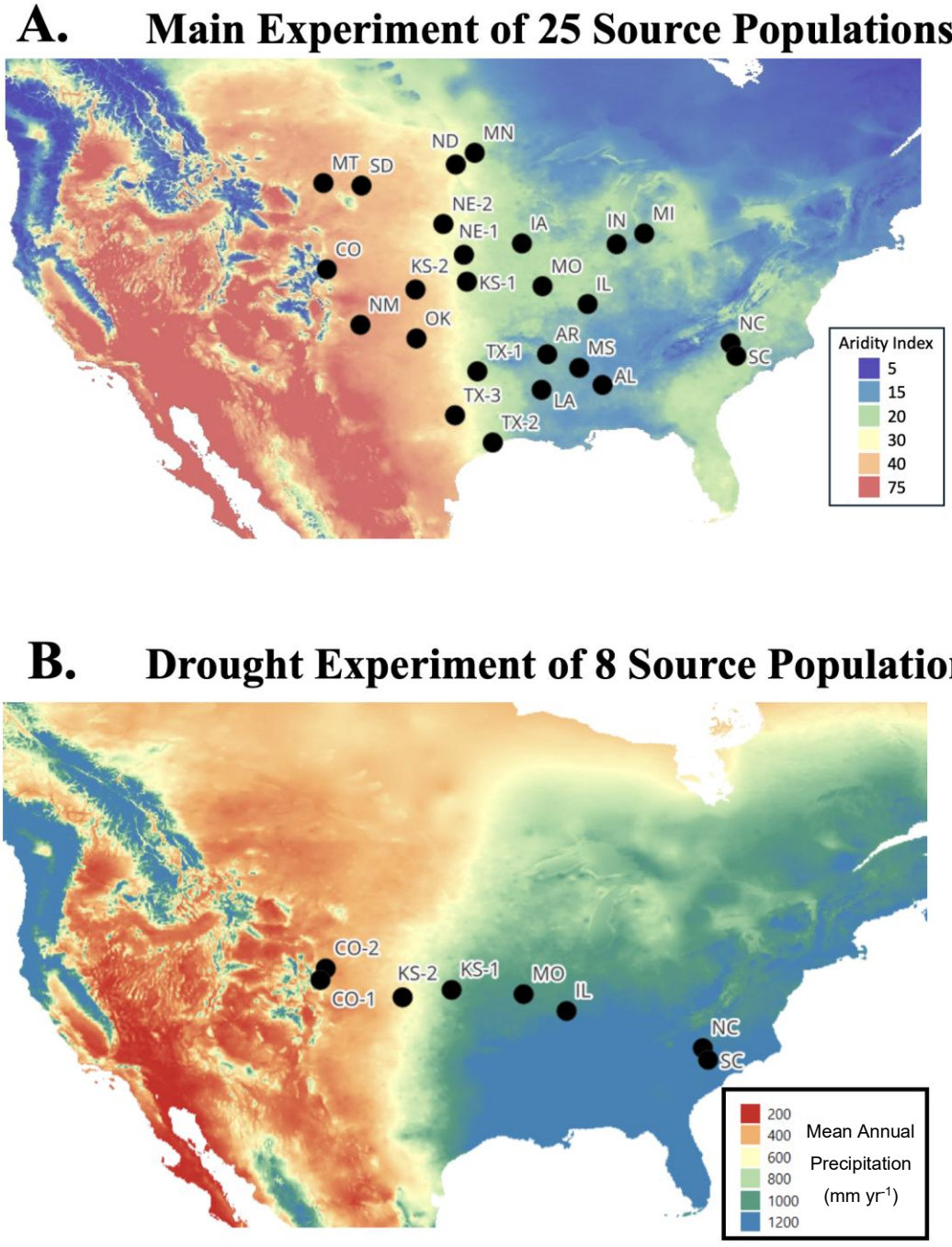

Figure 5.2. Regressions from the main experiment at mid-experiment, 95 days after transplanting. A. Vegetative height B. leaf area, C. leaf thickness D. photosynthetic rate, and E. chlorophyll absorbance, and F. date of flowering. Each trait is regressed over the best predictor by model selection. The solid line is the regression, shaded area indicates the confidence interval, points indicate site mean, and error bars indicate site standard error. The equation of the line of best fit and variance explained by R^2 is included.

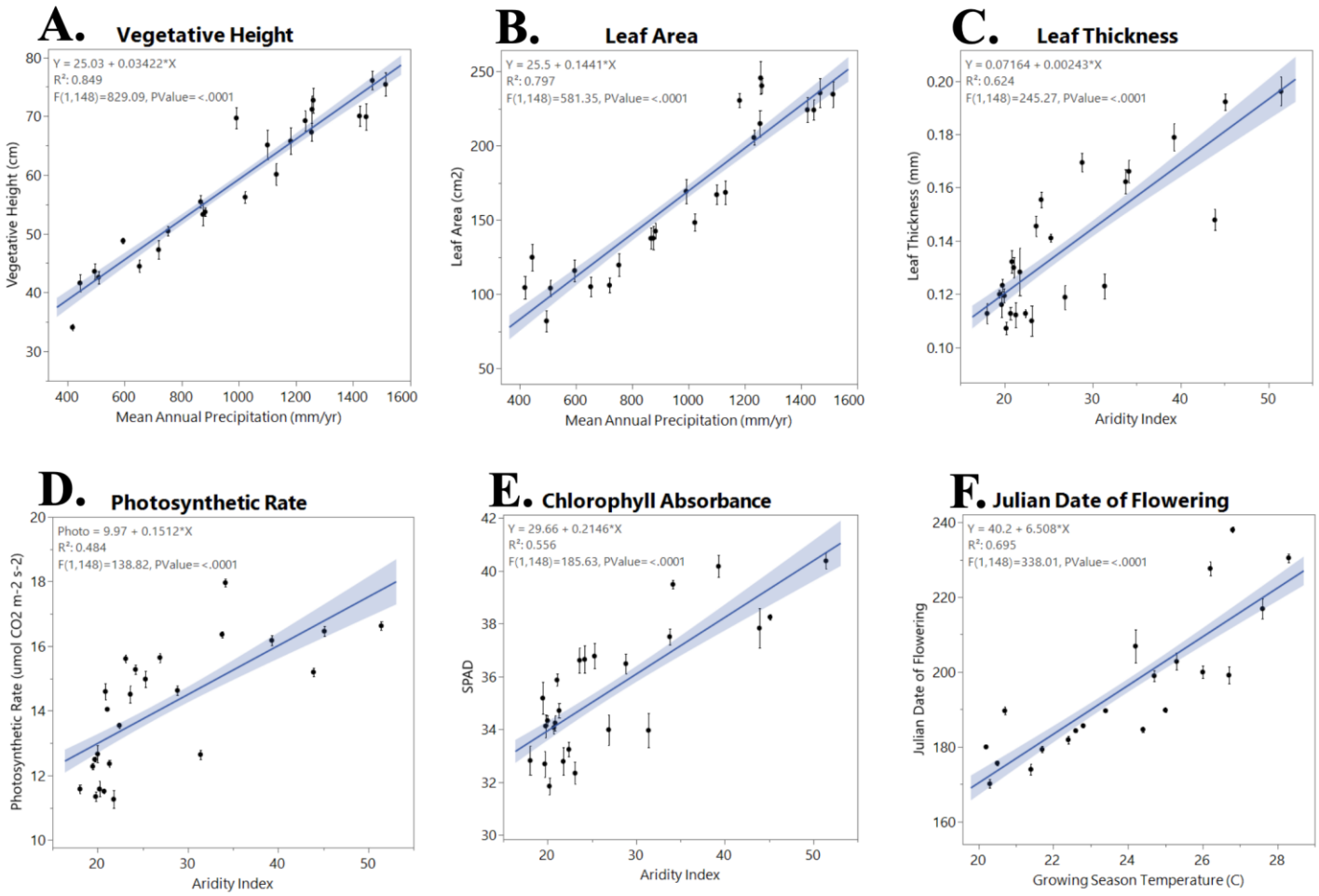

Figure 5.3. Principal Components Analyses (PCA) of trait and climate variation across 25 populations. A. PCA based on climate variables at source locations, illustrating climatic variation across populations. B. PCA based on morphological, physiological, and phenological trait data from the main greenhouse experiment, showing differentiation among populations along major trait axes. C. Linear regression showing the relationship between MAP and population scores along trait PCA axis 1. D. Plant trait network showing relationships among traits and climate variables. Nodes represent traits or climate factors, while edges indicate correlations between them. Edge color reflects the direction of the correlation: blue for positive and red for negative. The length of each edge corresponds to the strength of the correlation, with shorter edges indicating stronger connections. Hub traits—those with the highest degree (k)—are indicated in gold.

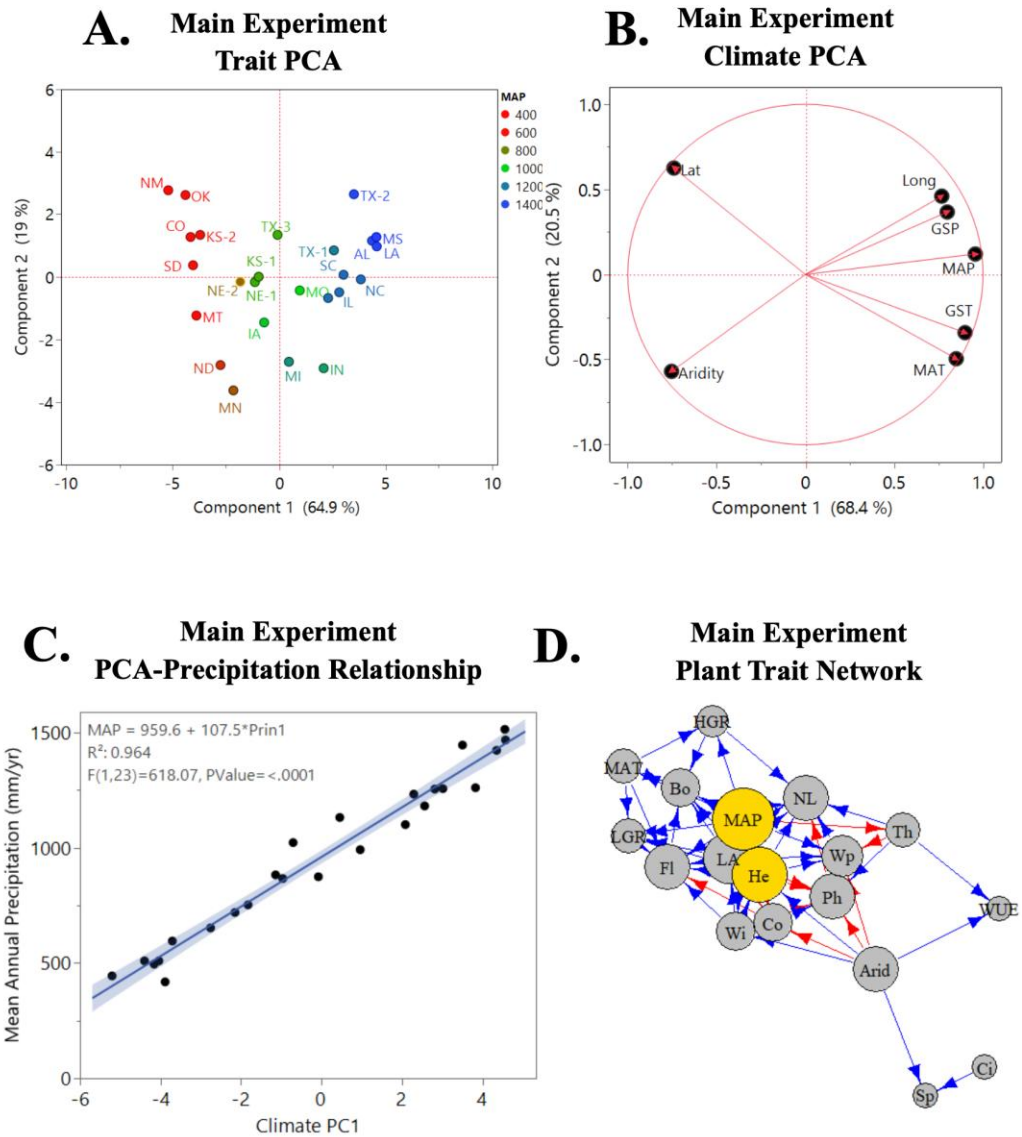

Figure 5.4. Regressions from the drought experiment, 38 days after the onset of drought. A. Plant height, B. total aboveground biomass, C. total belowground biomass, D. photosynthetic rate, E. midday water potential, and F. date of flowering across a mean annual precipitation gradient. Blue indicates control and red indicates drought. The solid line is the regression, shaded area indicates the confidence interval, points indicate site mean, and error bars indicate site standard error. The equation of the line of best fit for each treatment (control or drought) and variance explained by R^2 included.

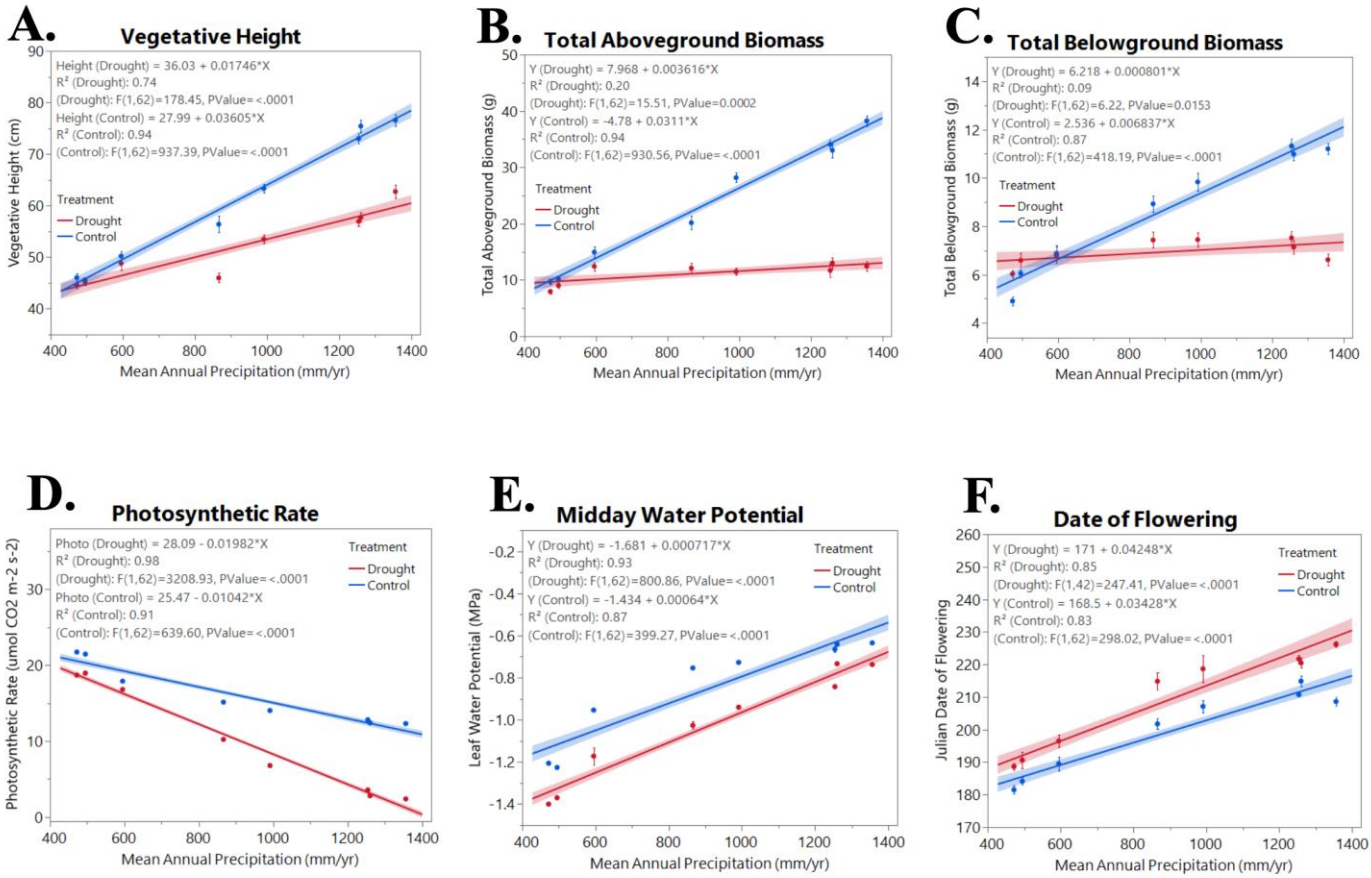

Figure 5.5**.** Principal Components Analysis (PCA) of trait variation across a precipitation gradient under control and drought treatments. A. PCA biplot of trait data from the control treatment, showing population-level variation in functional traits across the precipitation gradient. B. PCA biplot of trait data from the drought treatment, illustrating shifts in trait expression under water limitation. Arrows indicate loadings of key traits contributing to variation along PCA axes. Plant trait networks showing relationships among traits under C. control or D. drought treatment. Nodes represent traits or climate factors, while edges indicate correlations between them. Edge color reflects the direction of the correlation: blue for positive and red for negative. The length of each edge corresponds to the strength of the correlation, with shorter edges indicating stronger connections. Hub traits—those with the highest degree (k)—are indicated in gold. LEGEND: NL= number of leaves, Wi= leaf width, He= height, Th= thickness, ABio= aboveground biomass, Sp= SPAD, LA= leaf area, Wp= water potential, LGR= leaf area based growth rate, BBio= belowground biomass, Fl= flowering, Ph= photosynthetic rate, Co= stomatal conductance, Tr= transpiration rate, HGR= height based growth rate.

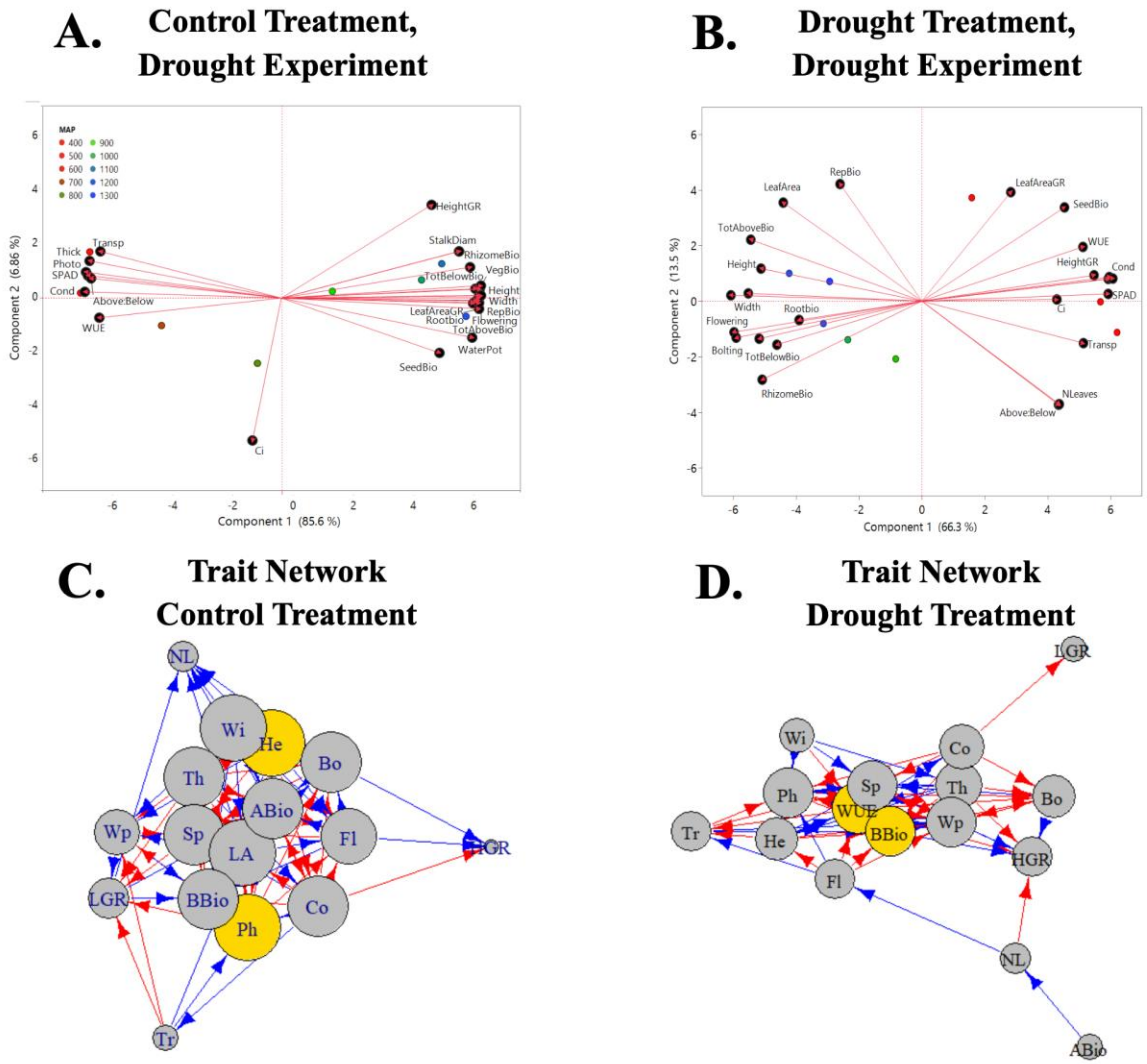

Figure 5.6. Genetic variation across *A. gerardi* populations. A. Genetic Principal Component Analysis (PCA) of populations across North America, based on SNP profiles. The first two principal components (PC1 and PC2) capture most genetic variation, and points indicate averages of populations. B. Regression analysis of trait PC1 scores across genetic PC1 scores, showing the relationship between genetic differentiation and functional trait variation across populations.

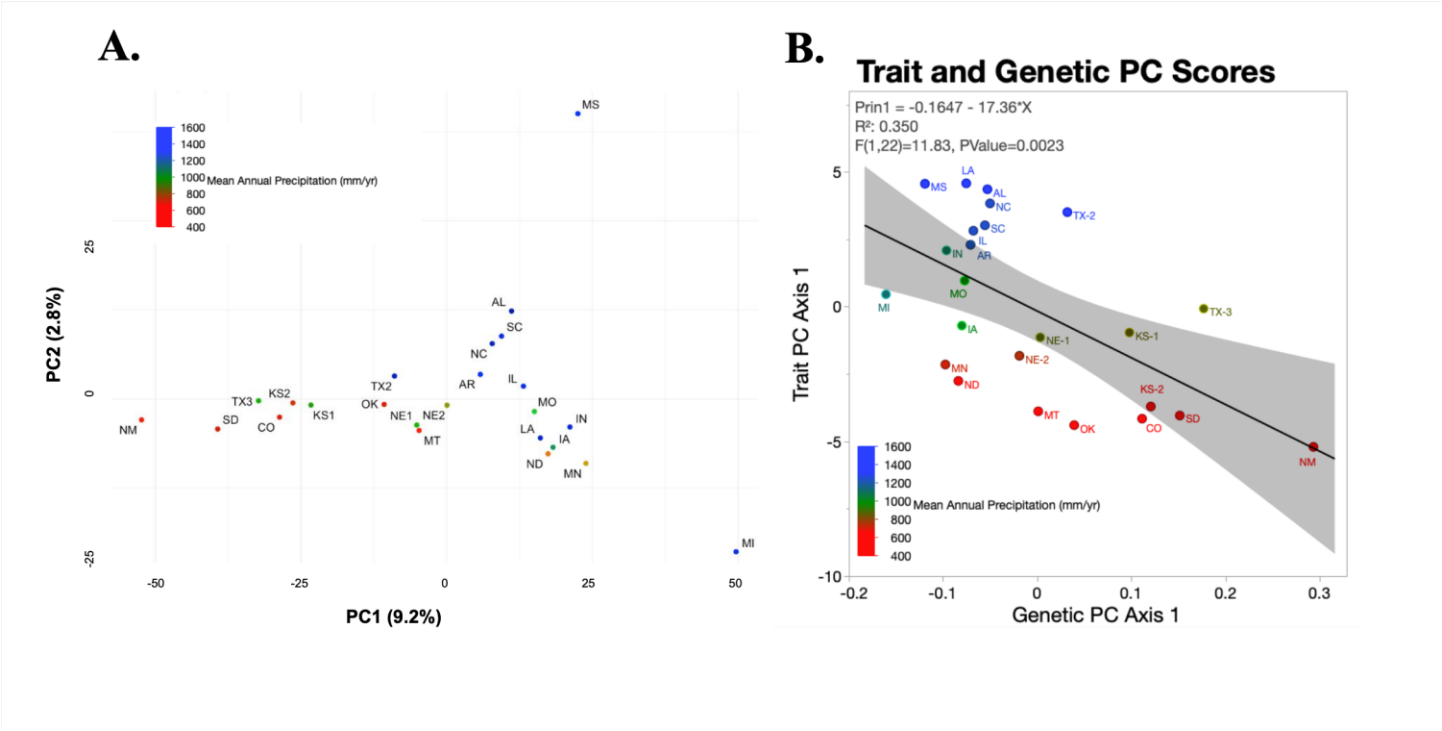

Figure 5.7. A principal component analysis (PCA) to visualize multivariate trait variation, with the same traits related to morphology and physiology across populations. ~~in~~ A. the main experiment in the greenhouse. B. the same populations in the field. C. Linear regression of PCA axis 1 scores from the greenhouse against PCA axis 1 scores from the field, assessing the consistency of population trait patterns across environments.

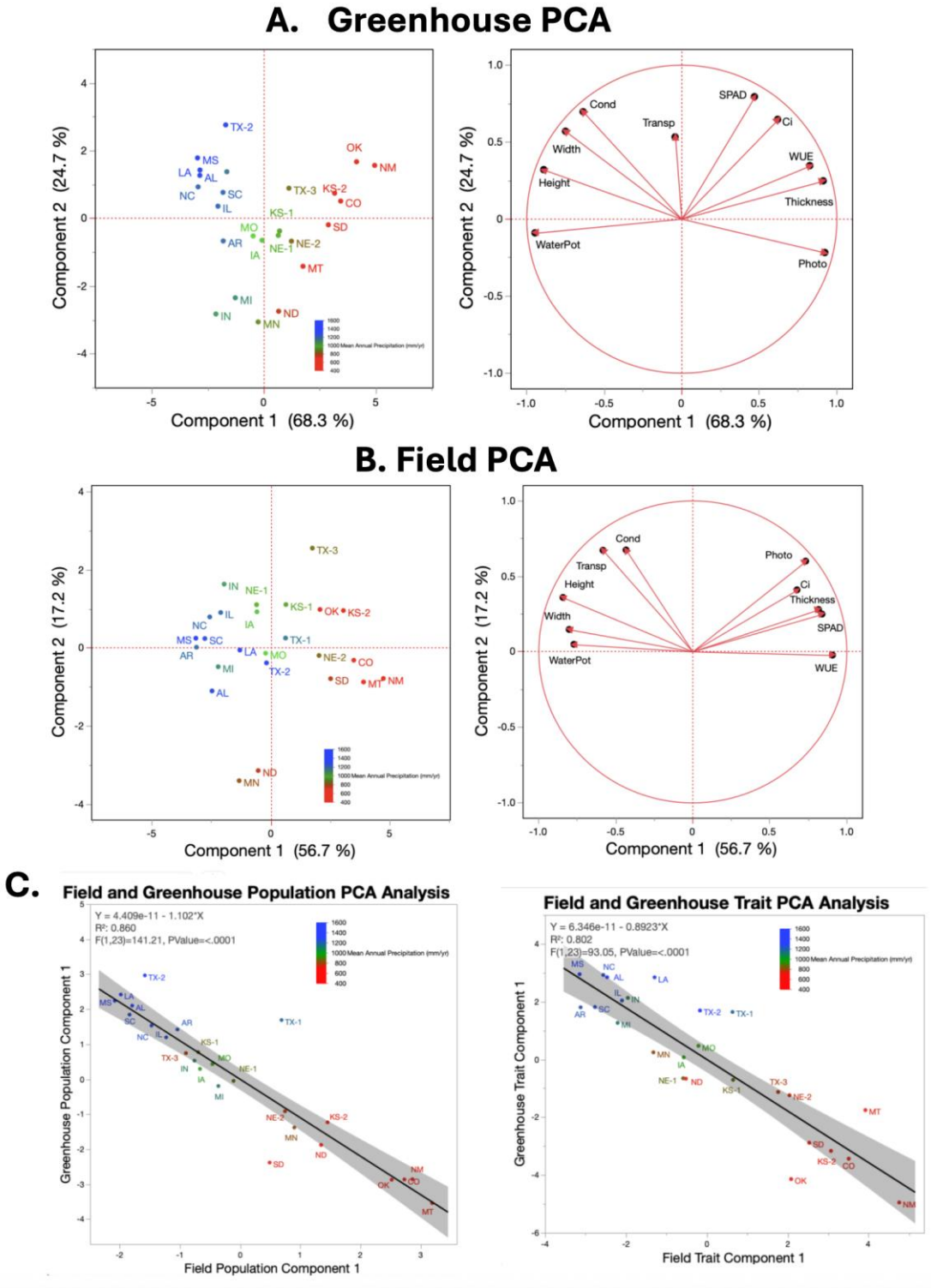

Supplemental Figure 1. Soil moisture over time in the main experiment. Data are presented as daily averages, and the line indicates the trend line. The plot illustrates the variation in soil moisture over the course of the experiment and remaining mostly near 30% soil moisture throughout the main experiment.

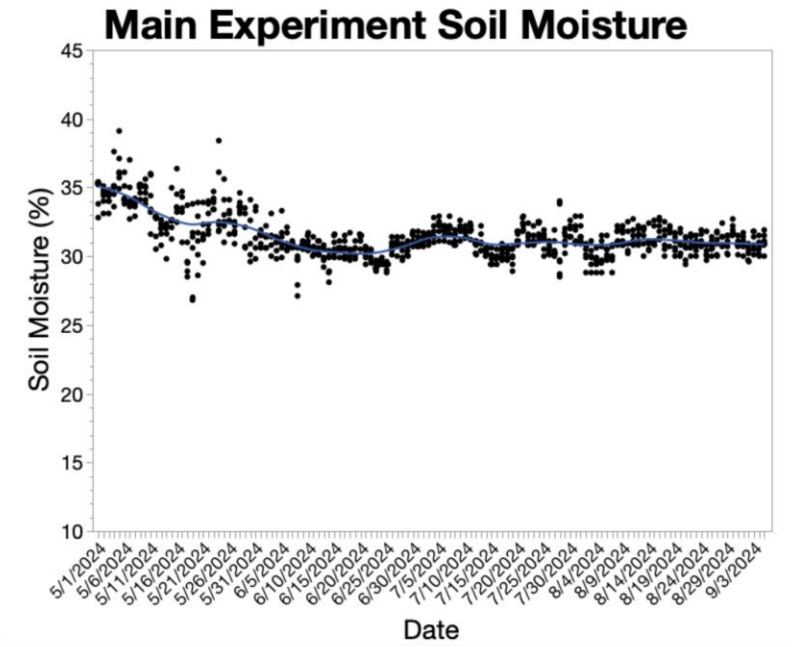

Supplemental Figure 2**.** A. Soil moisture over time in the drought experiment. Data are presented as daily averages, and the line indicates the trend line highlighting the differences in moisture availability between control (mean= 30.5%) and drought (mean = 15.2%) treatments after start of drought until the end of the experiment.

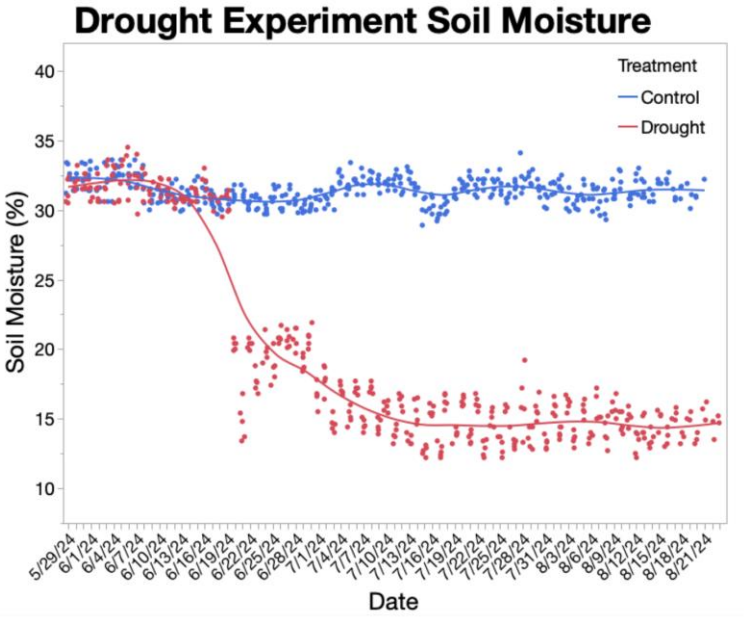

Supplemental Figure 3. Regressions from the main experiment mid-experiment, 95 days after transplanting. A. Leaf width, B. number of leaves, C. stem diameter, D. stomatal conductance, E. transpiration rate, F. water use efficiency, G. internal carbon dioxide concentration, H. water potential., I. date of bolting, J. relative height growth rate and K. relative leaf area growth rate. The solid line is the regression, shaded area indicates the confidence interval, points indicate site mean, and error bars indicate site standard error. The equation of the line of best fit and variance explained by R^2 is included.

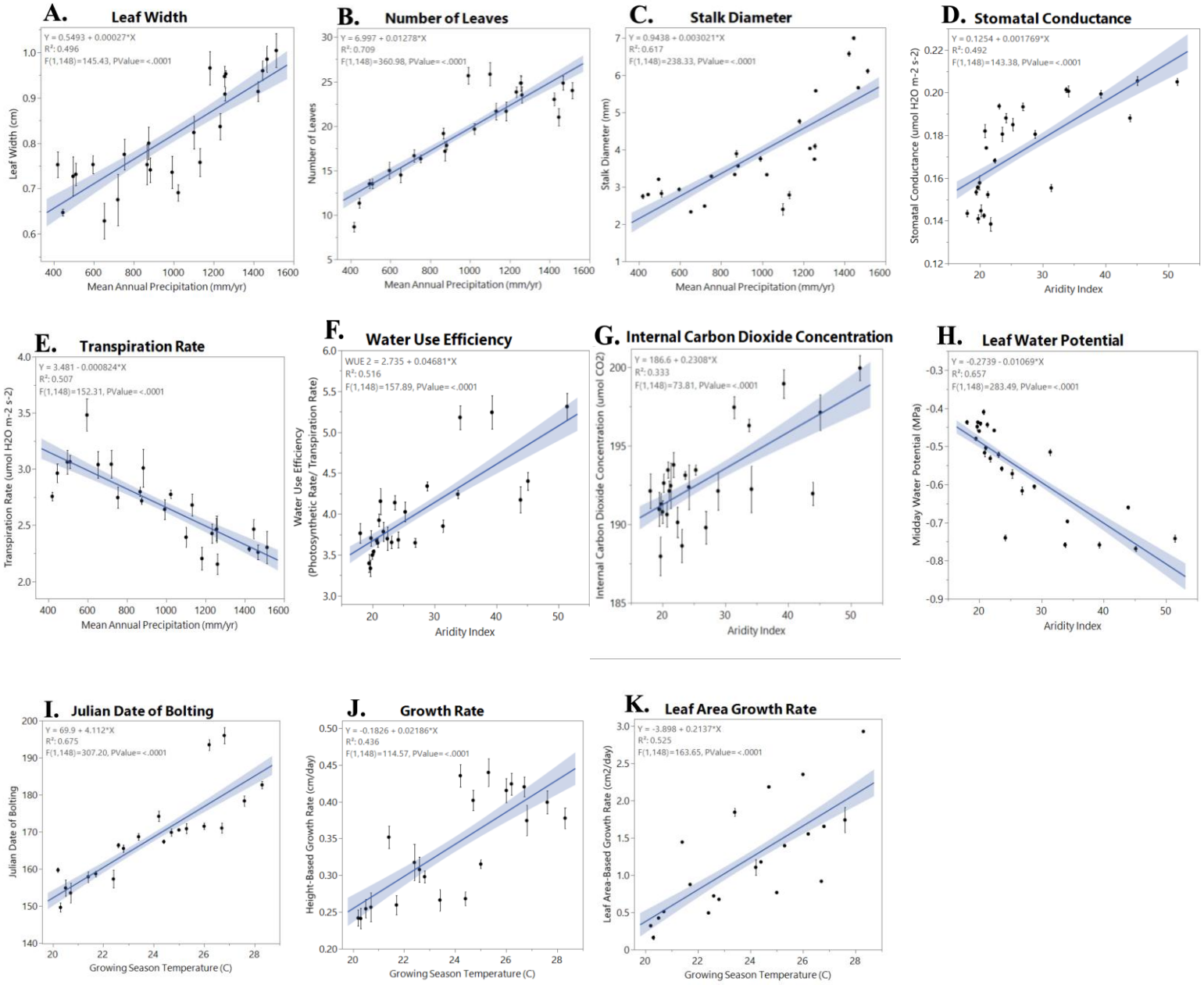

Supplemental Figure 4. Regressions from the drought experiment, 38 days after the onset of drought. A. Leaf area, B. number of leaves, C. stem diameter, D. leaf thickness, E. leaf width, F. vegetative biomass, G. reproductive biomass, H. seed biomass, I. rhizome biomass, J. root biomass, K. root to shoot ratio, L. stomatal conductance, M. transpiration rate, N. water-use efficiency, O. carbon dioxide concentration, P. chlorophyll absorbance, Q. date of bolting, R. height-based growth rate, and S. leaf area-based growth rate across a precipitation gradient. Blue indicates control and red indicates drought. The solid line is the regression, shaded area indicates the confidence interval, points indicate site mean, and error bars indicate site standard error. The equation of the line of best fit for each treatment (control or drought) and variance explained by R^2 included.

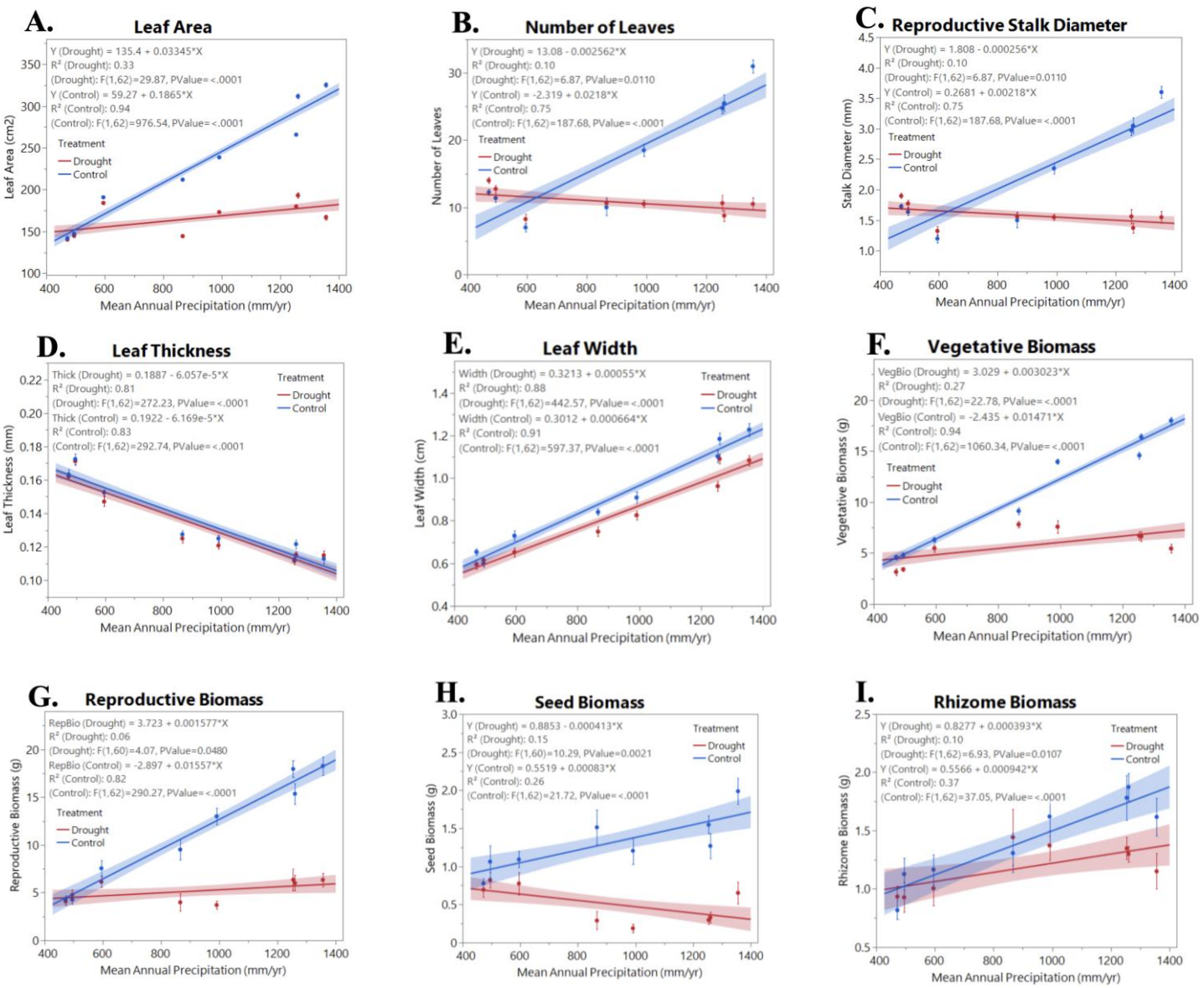

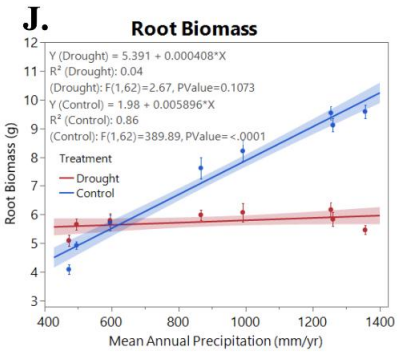
J.
Root Biomass
Y (Drought) = 5.391 + 0.000408*X
R² (Drought): 0.04
(Drought): F(1,62)=2.67, PValue=0.1073
Y (Control) = 1.98 + 0.005896*X
R² (Control): 0.86
(Control): F(1,62)=389.89, PValue=<.0001
Treatment
Drought
Control
Root Biomass (g)
Mean Annual Precipitation (mm/yr)

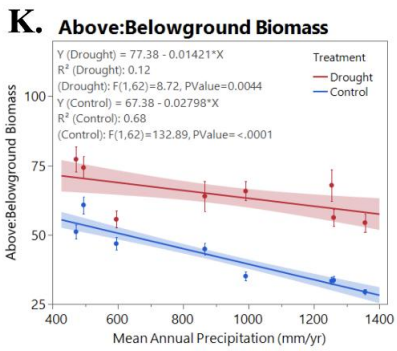
K.
Above:Belowground Biomass
Y (Drought) = 77.38 - 0.01421*X
R² (Drought): 0.12
(Drought): F(1,62)=8.72, PValue=0.0044
Y (Control) = 67.38 - 0.02798*X
R² (Control): 0.68
(Control): F(1,62)=132.89, PValue=<.0001
Treatment
Drought
Control
Above:Belowground Biomass
Mean Annual Precipitation (mm/yr)

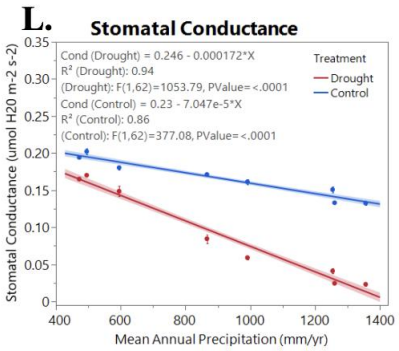
L.
Stomatal Conductance
Cond (Drought) = 0.246 - 0.000172*X
R² (Drought): 0.94
(Drought): F(1,62)=1053.79, PValue=<.0001
Cond (Control) = 0.23 - 7.047e-5*X
R² (Control): 0.86
(Control): F(1,62)=377.08, PValue=<.0001
Treatment
Drought
Control
Stomatal Conductance (umol H20 m-2 s-2)
Mean Annual Precipitation (mm/yr)

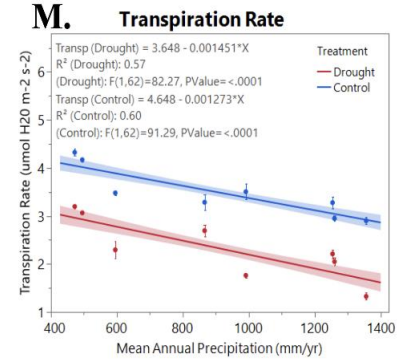
M.
Transpiration Rate
Transp (Drought) = 3.648 - 0.001451*X
R² (Drought): 0.57
(Drought): F(1,62)=82.27, PValue=<.0001
Transp (Control) = 4.648 - 0.001273*X
R² (Control): 0.60
(Control): F(1,62)=91.29, PValue=<.0001
Treatment
Drought
Control
Transpiration Rate (umol H20 m-2 s-2)
Mean Annual Precipitation (mm/yr)

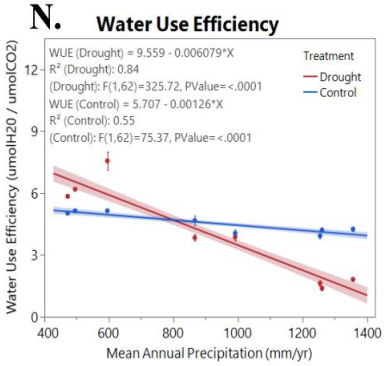
N.
Water Use Efficiency
WUE (Drought) = 9.559 - 0.006079*X
R² (Drought): 0.84
(Drought): F(1,62)=325.72, PValue=<.0001
WUE (Control) = 5.707 - 0.00126*X
R² (Control): 0.55
(Control): F(1,62)=75.37, PValue=<.0001
Treatment
Drought
Control
Water Use Efficiency (umolH20 / umolCO2)
Mean Annual Precipitation (mm/yr)

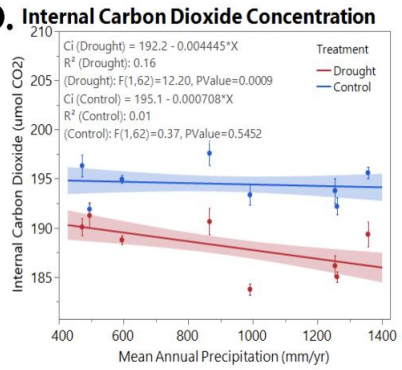
O.
Internal Carbon Dioxide Concentration
Ci (Drought) = 192.2 - 0.004445*X
R² (Drought): 0.16
(Drought): F(1,62)=12.20, PValue=0.0009
Ci (Control) = 195.1 - 0.000708*X
R² (Control): 0.01
(Control): F(1,62)=0.37, PValue=0.5452
Treatment
Drought
Control
Internal Carbon Dioxide (umol CO2)
Mean Annual Precipitation (mm/yr)

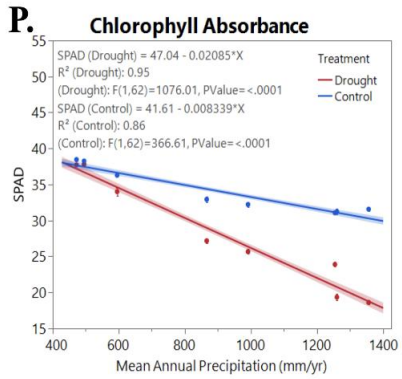
P.
Chlorophyll Absorbance
SPAD (Drought) = 47.04 - 0.02085*X
R² (Drought): 0.95
(Drought): F(1,62)=1076.01, PValue=<.0001
SPAD (Control) = 41.61 - 0.008339*X
R² (Control): 0.86
(Control): F(1,62)=366.61, PValue=<.0001
Treatment
Drought
Control
SPAD
Mean Annual Precipitation (mm/yr)

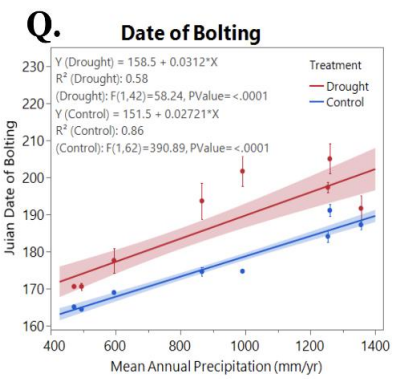
Q.
Date of Bolting
Y (Drought) = 158.5 + 0.0312*X
R² (Drought): 0.58
(Drought): F(1,42)=58.24, PValue=<.0001
Y (Control) = 151.5 + 0.02721*X
R² (Control): 0.86
(Control): F(1,62)=390.89, PValue=<.0001
Treatment
Drought
Control
Julian Date of Bolting
Mean Annual Precipitation (mm/yr)

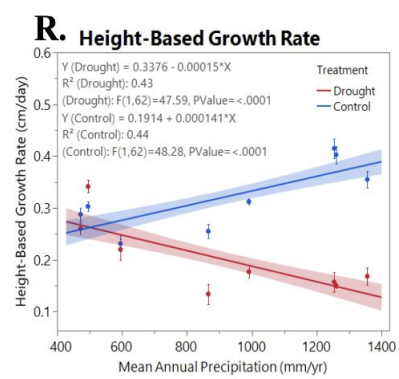
R.
Height-Based Growth Rate
Y (Drought) = 0.3376 - 0.00015*X
R² (Drought): 0.43
(Drought): F(1,62)=47.59, PValue=<.0001
Y (Control) = 0.1914 + 0.000141*X
R² (Control): 0.44
(Control): F(1,62)=48.28, PValue=<.0001
Treatment
Drought
Control
Height-Based Growth Rate (cm/day)
Mean Annual Precipitation (mm/yr)

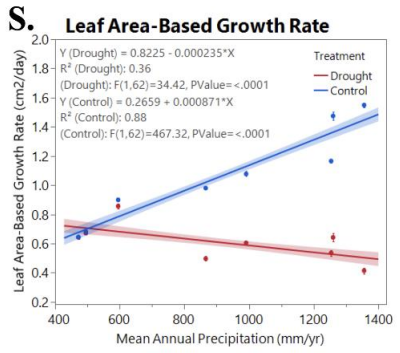
S.
Leaf Area-Based Growth Rate
Y (Drought) = 0.8225 - 0.000235*X
R² (Drought): 0.36
(Drought): F(1,62)=34.42, PValue=<.0001
Y (Control) = 0.2659 + 0.000871*X
R² (Control): 0.88
(Control): F(1,62)=467.32, PValue=<.0001
Treatment
Drought
Control
Leaf Area-Based Growth Rate (cm2/day)
Mean Annual Precipitation (mm/yr)

Table 5.1. Site information, location (longitude and latitude), and home climate variables showing historic annual temperature and precipitation, aridity (temperature/precipitation) and other relevant site details.

Site/ State	County	Longitude	Latitude	Mean Annual Precipitation (mm)	Aridity Index	Growing Season Precipitation (mm)	Mean Annual Temperature (C)	Warmest Month Temperature (C)	Growing Season Temperature (C)	Coldest Month Temperature (C)
AL	Dallas	-87.12	32.31	1422	20.2	508	17.7	27.6	27.3	7.0
AR	Lonoke	-91.70	34.77	1232	19.5	463	16.5	27.5	21.5	4.3
CO-1	Boulder	-105.28	39.99	495	45.1	139	10.8	23.2	22.6	0.5
CO-2	Boulder	-105.11	39.58	467	45.0	143	10.7	23.0	22.5	0.4
IA	Jasper	-93.01	41.56	1022	20.9	418	9.7	23.6	24.7	-6.2
IL	Williamson	-88.83	38.78	1254	19.9	483	13.6	25.6	21.9	0.4
IN	Lake	-87.45	41.52	1100	19.7	400	10.5	23.5	25.2	-3.8
KS-1	Riley	-96.61	39.22	866	23.6	325	12.6	26.1	24.6	-1.7
KS-2	Logan	-100.81	38.77	595	34.2	228	11.9	25.8	27.6	-1.2
LA	Ouachita Parish	-92.04	32.60	1467	19.8	574	18.5	28.2	28.8	7.9
MI	Kalamazoo	-85.76	42.17	1131	22.4	382	9.6	22.4	20.9	-4.2
MN	Clay	-96.14	47.10	719	19.1	364	5.9	21.4	21.2	-8.2
MO	Calloway	-91.99	38.94	991	21.1	389	13	25.3	24.6	-0.2
MS	Yalobusha	-89.75	33.94	1513	18.0	598	16.7	26.9	26.8	5.5
MT	Rosebud	-105.41	45.260	418	43.9	194	7.7	22.1	20.5	-4.9
NC	Cabarrus	-80.51	35.44	1260	20.7	497	15.6	26.3	24.8	4.9
ND	Ransom	-97.30	46.39	652	26.9	297	5.8	21.7	21.2	2.4
NE-1	Lancaster	-96.80	40.86	882	25.3	361	10.6	24.5	23.5	-4.7
NE-2	Knox	-98.06	42.75	652	28.8	270	9.5	24.2	23.3	-5.1
NM	Union	-104.22	36.23	444	51.4	170	11.7	23.5	22.2	1.0
OK	Beckham	-99.68	35.61	509	39.3	240	7.7	22.4	20.8	1.2
SC	Chesterfield	-80.13	34.37	1256	21.3	352	16.8	26.9	25.6	5.2
SD	Lawrence	-103.07	45.10	654	33.8	184	14.9	27.2	26.2	-2.6
TX-1	Fannin	-95.03	29.37	1181	21.8	419	17.5	28.4	28.5	6.1
TX-2	Galveston	-97.34	31.06	1445	31.4	569	21.2	28.7	29.5	7.3
TX-3	Bell	-95.97	33.72	874	24.2	384	8.6	22.3	21.2	6.6

Table 5.2. Statistical response for each trait in the main experiment compared to home climate. This table shows the p-values for each trait measured in the main experiment, comparing the response of traits to home climate. Values are presented for each trait, with the model with the lowest AIC value is underlined and bolded. AIC values are used to assess the relative goodness-of-fit for the models describing the relationships between traits and climate variables.

Response Variable	Population Main Effect	Mean Annual Precip (mm)	Growing Season Precip (mm)	Aridity Index	Mean Annual Temp (°C)	Warmest Month Temp (°C)	Coldest Month Temp (°C)	Lat.	Long.	Elev. (m)	Temp Ann. Range (°C)	Precip Seasonal.	Mean Diurnal Range (°C)	Growing Season Temp (°C)
Morphological														
Vegetative Height (cm)	**<0.001**	**<0.001**	**0.001**	**<0.001**	**0.03**	**0.04**	**0.001**	**0.04**	**0.01**	**0.01**	**0.01**	**0.01**	0.40	0.33
Blade Width (cm)	**<0.001**	**<0.001**	**0.01**	**<0.001**	0.08	0.14	0.10	0.77	**0.01**	**0.04**	0.17	0.12	0.32	0.24
Leaf Area (cm^2)	**<0.001**	**<0.001**	**0.002**	**<0.001**	**0.01**	0.09	0.10	0.07	**0.02**	**<0.001**	**0.04**	**0.001**	0.55	0.48
Leaf Thickness (mm)	**<0.001**	**<0.001**	**<0.001**	**<0.001**	0.32	0.11	0.63	0.09	**0.001**	**0.01**	0.09	**0.02**	0.25	0.31
Number of Leaves (count)	**<0.001**	**<0.001**	**0.03**	**<0.001**	0.10	**0.01**	0.10	0.90	0.08	**0.001**	0.05	0.06	0.74	0.85
Stalk Thickness (mm)	**<0.001**	**<0.001**	0.12	**<0.001**	0.42	0.23	0.38	0.06	**0.03**	0.05	0.09	**0.03**	0.74	0.85
Physiological														
Chlorophyl Absorbance (SPAD)	**<0.001**	**<0.001**	**0.001**	**<0.001**	0.21	0.65	0.34	**0.02**	**0.01**	**0.001**	0.22	0.07	0.31	0.40
Photosynthetic Rate (μmol CO_2 m^{-2} s^{-1})	**<0.001**	**<0.001**	**0.003**	**<0.001**	0.99	0.31	0.46	0.49	**0.04**	**0.001**	0.30	0.05	0.52	0.60
Transpiration Rate (mol H_2O m^{-2} s^{-1})	**<0.001**	**<0.001**	**<0.001**	**<0.001**	0.08	**0.01**	**0.01**	0.07	**0.01**	0.06	0.34	0.15	0.05	**0.04**
Stomatal Conductance (mol H_2O m^{-2} s^{-1})	**<0.001**	**<0.001**	**0.001**	**<0.001**	0.10	0.07	0.11	0.52	0.20	0.09	0.10	**0.02**	0.72	0.67
Water Use Efficiency (Transpiration/ photosynthetic rate)	**<0.001**	**<0.001**	**<0.001**	**<0.001**	0.06	**0.04**	0.07	0.16	**0.01**	0.13	0.76	0.05	0.14	0.18
Water Potential (MPa)	**<0.001**	**<0.001**	**<0.001**	**<0.001**	0.08	0.09	0.67	0.07	**<0.001**	0.05	0.08	**<0.001**	0.07	0.09
Internal CO_2 (μmol CO_2 mol^{-1})	**<0.001**	**<0.001**	0.06	**<0.001**	0.20	**0.02**	0.10	0.12	0.06	0.05	0.09	**0.01**	0.76	0.78
Phenological														
Bolting	**<0.001**	**0.001**	**0.001**	**0.02**	**0.001**	0.25	0.29	**0.01**	**0.04**	**0.04**	0.30	**0.01**	**0.02**	**<0.0001**
Flowering	**<0.001**	**0.01**	**0.01**	**0.003**	**0.002**	0.12	0.20	**0.001**	**0.02**	0.11	0.11	0.10	**0.01**	**<0.0001**
Relative Growth Rate (height-based)	**<0.001**	**0.01**	**0.003**	**0.01**	**0.01**	**0.01**	**0.02**	**0.02**	**0.02**	**0.001**	**0.01**	0.09	0.19	**<0.0001**

Table 5.3. The results of general linear models (GLMs) analyzed the effects of drought treatment, population origin, and their interaction on trait variation. First included is the main effect of population and home mean annual precipitation. Then, drought treatment and population origin were included as fixed factors in the models, and variance explained by each factor was calculated by the mean square of each factor into its variance component. Analysis of covariance (ANCOVA) was used to assess the effects of population of origin, drought treatment, and the population × treatment interaction over time. Significant population x treatment interaction in various time points predrought or after start of drought are bold for each response variable.

Response Variable	Population Main	Climate Main	Before Drought	Drought Time 1	Drought Time 2	Drought Time 3	Drought Time 4	Drought Time 5	Drought Time 6	Drought Time 7	Drought Time 8
Morphological											
Vegetative Height (cm)	**<0.001**	**<0.001**	0.59	**0.006**	**<0.001**	**<0.001**	**<0.001**	**<0.001**	**<0.001**	**<0.001**	**<0.001**
Blade Width (cm)	**<0.001**	**<0.001**	0.99	**0.04**	0.083						
Leaf Area (cm^2)	**<0.001**	**<0.001**	0.817	**<0.001**	**<0.001**						
Leaf Thickness (mm)	**<0.001**	**<0.001**	0.58	0.73	0.98						
Number of Leaves (count)	**<0.001**	**<0.001**	0.66	**0.02**							
Stalk Thickness (mm)	**<0.001**	**<0.001**		**0.01**							
Physiological											
Chlorophyl Absorbance (SPAD)	**<0.001**	**<0.001**	0.607	**<0.001**	**<0.001**	**<0.001**	**<0.001**	**<0.001**	**<0.001**	**<0.001**	**<0.001**
Photosynthetic Rate (µmol CO_2 m^{-2} s^{-1})	**<0.001**	**<0.001**	0.47	**<0.001**	**<0.001**	**<0.001**	**<0.001**				
Transpiration Rate (mol H_2O m^{-2} s^{-1})	**<0.001**	**<0.001**	0.73	**0.003**	**0.002**	**0.04**	**<0.001**				
Stomatal Conductance (mol H_2O m^{-2} s^{-1})	**<0.001**	**<0.001**	0.33	**<0.001**	**0.01**	**<0.001**	**<0.001**				
Water Use Efficiency (Transpiration/ photosynthetic rate)	**<0.001**	**<0.001**	0.88	**<0.001**	**<0.001**	**<0.001**	**<0.001**				
Water Potential (MPa)	**<0.001**	**<0.001**	0.59	**0.03**	**<0.001**	**0.03**					
Internal CO_2 (µmol CO_2)	**<0.001**	**<0.001**	0.20	**<0.001**	**0.04**	**0.03**	0.07				
Phenological											
Bolting	**<0.001**	**<0.001**			**0.02**						
Flowering	**<0.001**	**<0.001**			**<0.001**						
Relative Growth Rate (height-based)	**<0.001**	**<0.001**			**<0.001**						
Relative Growth Rate (leaf area-based)	**<0.001**	**<0.001**			**<0.001**						

Methods S1: DNA Extraction and Sequencing

To obtain high-quality genomic DNA, we extracted nucleic acids from ground tissue using 550 µl of extraction buffer per sample. The buffer composition (100 mM Tris-HCl, pH 8.0; 100 mM EDTA, pH 8.0; 1.4 M NaCl; 2% CTAB; 12 mM TCEP; 16 mM sodium diethyldithiocarbamate trihydrate; and 4% PVPP) was designed to lyse cells, bind polysaccharides, and neutralize phenolic compounds, which are common contaminants in plant tissues that can inhibit downstream enzymatic reactions. TCEP was used as a reducing agent in place of β-mercaptoethanol to minimize toxicity while maintaining protein denaturation efficiency. Following this, 50 µl of reducing buffer (100 mM Tris-HCl, pH 8.0, with 120 mM TCEP and 160 mM DIECA added freshly) was applied to enhance removal of metabolites.

DNA concentration and purity were quantified with PicoGreen (ThermoFisher.com), allowing normalization of samples to ensure even representation during sequencing. Libraries were prepared for genotyping-by-sequencing (GBS) following the method of Poland and Rife (2012), which leverages restriction enzymes to reduce genome complexity while retaining informative polymorphisms. We employed a two-enzyme digestion using *PstI* and *MspI* to generate reproducible, high-density markers across the genome. Sequencing was conducted using 200 bp paired-end reads on an Illumina NovaSeq+ 25b lane, providing the depth and coverage necessary for reliable SNP discovery and downstream population genetic analyses.

Chapter 6 - Chapter 6- Conclusions, Limitations, Implications, and Takeaways

Overview of Findings

Across four complementary studies, this dissertation demonstrates that climate, genetic variation, and trait differentiation jointly shape adaptation and drought tolerance in *Andropogon gerardi*, a dominant species of the North American tallgrass prairie (Knapp et al., 1998). Long-term reciprocal garden experiments (Chp. 2) provided robust evidence of local adaptation to rainfall, with local ecotypes consistently outperforming non-local ecotypes. This strong ecotypic local adaptation resulted in competitive dominance over the surrounding community, which in turn altered plant community structure. We then documented how functional traits and gene expression document possible mechanisms to strong local adaptation of wet and dry ecotypes (Chp. 3). Together, these findings highlight how environmental selection pressures shape local adaptation across climate gradients (Savolainen et al., 2007; 2013).

At a broader spatial scale, this dissertation demonstrated that different theoretical frameworks are needed to explain distinct aspects of plant population dynamics. The Abundant Center Hypothesis (ACH; Brown, 1984; Chp. 4) successfully predicted patterns of abundance and genetic diversity across the range of *A. gerardi*, where abundance and genetic diversity peaked at the range core. By contrast, the Clinal Pattern Model (CPM) more effectively explained patterns of trait variation, showing that functional traits correspond to clines following environmental gradients rather than range position. Since we provided empirical support for both frameworks, our findings deepen our understanding of how range-wide processes interact, illustrating the complexity of predicting ecological dynamics under environmental change.

Finally, greenhouse and field experiments revealed that intraspecific trait variation (ITV) is both environmentally driven and genetically constrained (Chp. 5). Populations originating from drier climates expressed drought-adaptive traits (increased water use efficiency, shorter stature), whereas populations from wetter sites exhibited traits favoring competition and growth under favorable conditions (increased canopy area, height, biomass; Grime, 1988; Jardine et al., 2021). Importantly, ITV was not purely plastic, but shaped by underlying genetic differentiation, suggesting that adaptation to precipitation regimes has left a lasting evolutionary imprint. This was corroborated by our drought experiment, confirming climate—particularly precipitation-- as a dominant selective force (Siepelski et al., 2017) and emphasize the role of ITV in buffering populations against environmental variability (Anderson et al., 2021).

Taken together, by integrating reciprocal transplants, ecological genomics, and trait-based approaches, this dissertation provides a multi-scalar perspective on adaptation, offering critical insights into both the evolutionary mechanisms and practical applications of resilience in grassland ecosystems. This work offers a multi-scale synthesis of adaptation in *A. gerardi*, advancing both ecological theory and applied restoration science. The decadal scope of the reciprocal garden experiments provides rare temporal depth compared to most reciprocal garden studies (Johnson et al., 2022; literature review in Chp. 1), which often spans only a few years (Bischoff & Müller-Schärer, 2010; Sytsma et al., in press), demonstrating that signals of local adaptation may not emerge until measured over decadal scales. At the continental scale, this research integrates two seemingly conflicting frameworks in population demography (ACH vs CPM; literature review in Chp. 1). Yet, the support for both the ACH and CPM in different contexts enriches ongoing debates about species' range dynamics (Sagarin & Gaines, 2002; Sexton et al., 2009; 2024) and parallels findings in other widespread grasses such as switchgrass

(*Panicum virgatum*), where geographic genetic structure contrasts with climate-driven trait variation (Lowry et al., 2019).

At the mechanistic scale, incorporating ecological genomics (Ungerer et al., 2008) connected functional trait divergence to underlying gene expression networks (Langfelder & Horvath, 2008), clarifying how phenotypic differentiation emerges under contrasting climatic conditions. Dry ecotypes upregulated drought-response genes (e.g., *ABA synthesis, DROUGHT SENSITIVE I*; Gupta et al. 2020) while wet ecotypes upregulated genes involved in growth and resource acquisition (e.g., gibberellins, growth regulators, Castro-Camba et al., 2022). This is consistent with studies linking local climate to gene regulatory divergence in grasses (Lowry et al., 2012; Heckman et al., 2025) and the model plant *Arabidopsis* (Des Marais et al., 2013; Savolainen et al., 2013). This integration of gene expression, trait data, and reciprocal transplants goes beyond correlative evidence to identify causal links between genotype and phenotype—a critical gap in much of the local adaptation literature (literature review in Chp. 1; Sytsma et al. in press).

Practical Implications

These findings carry significant implications for the restoration and conservation of grasslands, particularly in light of climate change and increasing droughts (Smith et al., 2024). Evidence for strong local adaptation (Chps. 2, 3) highlights the risks of using non-local seed sources (Vitt et al., 2022), which may fail to establish or destabilize community dynamics (Whitham et al., 2002; 2003; 2020). The implications extend beyond *A. gerardi*: widespread grasses and other dominant species across climate gradients may harbor similarly specialized ecotypes (e.g., ecotypes of *P. virgatum;* Lowry et al., 2014; Lovell et al., 2018; Heckman et al., 2025) that can only be detected over long timescales and in natural communities (Johnson et al.,

2022). For restoration practitioners, this means that sourcing climate-matched ecotypes is not simply beneficial but essential for ensuring long-term ecosystem stability (Vitt et al., 2022). Thus, restoration policy should prioritize regionally adapted seed sourcing to support resilient grasslands.

The integration of ecological genomics into restoration frameworks expands the toolkit available to managers and conservationists. By linking drought tolerant or growth-related trait strategies to gene expression profiles (Chp. 3), this dissertation demonstrates how genomic markers can serve as early indicators of drought tolerance (Anderson & Song, 2020). This opens the door for practical applications such as genomic screening of seed sources (Vitt et al., 2022) or the identification of functional alleles associated with drought tolerance (Gupta et al., 2020). For applied conservation, moving beyond trait-based selection toward genomics-informed restoration can accelerate the identification of populations best suited to withstand climate stress (Shaw et al., 2024). In turn, this reduces the risk of restoration failure and provides a pathway to integrate cutting-edge molecular biology into large-scale ecosystem management (Des Marais et al., 2013; Savolainen et al., 2013; Anderson et al., 2016; Shaw et al., 2024).

At broader spatial scales (Chp. 4), patterns of genetic diversity and abundance support the ACH, highlighting the importance of protecting core populations (Shaw et al., 2025). At the same time, the CPM demonstrates the need to conserve marginal populations (Nadeau & Urban, 2019; Sexton et al., 2025), which may harbor unique trait assemblages critical for adaptation to extreme environments (e.g., those conferring drought tolerance: high water use efficiency, shorter stature, more negative water potentials; Grime, 1988; Jardine et al., 2021). For practitioners, this implies that both genetic and functional diversity must be prioritized in conservation planning: losing either dimension could undermine ecosystem resilience (Moran et

al., 2016). Similarly, findings on ITV reinforce that maintaining genetic diversity is inseparable from preserving functional diversity (Chp. 5) and these heritable trait differences may mediate population responses to drought (Albert et al., 2010; Siefert et al., 2015; Volaire, 2018). Together, these insights call for -conservation strategies that balance core–margin representation (Nadeau & Urban, 2019) with functional trait diversity across climate gradients.

Taken together, this dissertation contributes to broader debates in ecology and global change biology by showing the value of integrating across scales and disciplines—field ecology, community experiments, genomics, and biogeography—to understand and manage grassland resilience under predicted droughts. The findings reinforce resilience theory's emphasis on diversity—both genetic and functional—as a cornerstone of ecosystem persistence (Folke et al., 2004; Bita-Nocalae & Dhyani, 2025). By focusing on a dominant foundation grass, this work demonstrates that conserving and restoring resilient populations of key species has disproportionate consequences for ecosystem function (Zhang et al., 2025).

Limitations

Despite the breadth and multi-scale integration of this dissertation, several limitations warrant careful consideration. First, the geographic and temporal scope, while extensive (13 years; Chp. 2), does not encompass the full environmental heterogeneity experienced by *A. gerardi* populations across North America. Certain marginal populations, particularly those at extreme ends of temperature, precipitation, or soil fertility gradients, were not sampled at these decadal scales. These unrepresented populations may exhibit unique adaptive strategies or trait-environment relationships that could modify general patterns observed across the broader range (Kawecki & Ebert, 2004; Sexton et al., 2009; 2024). Though we focus on marginal populations

in later chapters (Chps. 4-5), the same temporal documentation through long term studies would confirm our findings from two years of data of these marginal populations. Moreover, our sampling did not fully capture the northernmost (Canada) or easternmost (e.g., Pennsylvania US) extents of the species' range (USDA Plants Database, 2023), where environmental conditions and selective pressures may differ substantially from the core populations studied. The omission of these peripheral regions could mean that range-edge adaptations or locally unique trait-environment relationships are underrepresented in our dataset (Sexton et al., 2025).

Second, unmeasured biotic and abiotic factors could influence adaptive outcomes in ways not captured by the current design (Jiang et al., 2024). Soil microbial communities, including mycorrhizal fungi and nitrogen-fixing bacteria, can significantly affect nutrient uptake (Pattnaik et al., 2021), growth (Fincheira & Quiroz, 2018), and competitive interactions (Reynolds et al., 2003), yet their influence was not directly manipulated or quantified in this work. Similarly, interspecific interactions—including competition, herbivory, and facilitation (Huisman & Olff, 1998; Carroll & MacDougall, 2024)—can alter trait variation *in situ (*Luo et al., 2023), potentially modulating the strength of local adaptation. Nutrient availability (Funk et al., 2008; Volaire, 2018), disturbance regimes (e.g., fire or grazing; Smith & Knapp, 1999; Smith et al., 2009; Jentsch et al., 2022), and other abiotic stressors (Fay et al., 2008) may also interact with precipitation gradients (Knapp, 1985; Silletti & Knapp, 2002; Fay et al., 2003), leading to context-dependent responses not captured by our experimental treatments. Consequently, while the results provide strong evidence of rainfall-driven local adaptation, they may underestimate the complexity of all selective pressures operating in natural grassland ecosystems.

Third, the genomic and gene expression analyses are necessarily constrained by the ecotypes, populations, and experimental conditions included in this study. While SNP

genotyping, RNAseq, and co-expression networks provide powerful insights into mechanisms underlying drought tolerance and growth strategies (Ungerer et al., 2008; Savolainen et al., 2013; Upton et al., 2023), these findings may not fully represent the genetic and transcriptomic diversity present across the full species range. Rare alleles (Savolainen et al., 2013), epigenetic modifications (Dar et al., 2022), or gene-environment interactions (Des Marais et al., 2013) in unsampled populations may yield additional adaptive strategies not captured here. Moreover, focusing primarily on precipitation as the selective driver may overlook important interactions with temperature extremes, soil fertility gradients, or multi-year climatic variability, which could influence trait expression and adaptive potential (Song et al., 2023; Bernatchez et al., 2024).

Finally, methodological limitations inherent to both greenhouse and field experiments should be considered. Common garden and controlled drought experiments standardize environmental conditions to isolate specific drivers (Schwinning et al., 2022; Johnson et al., 2022), but they may simplify the complex environmental mosaic experienced by natural populations. Consequently, extrapolating results to landscape or continental scales requires caution. These limitations highlight opportunities for future research, including multi-factorial, multi-site experiments, broader ecotype sampling, and incorporation of additional genomic, epigenetic, and microbial data to fully capture the ecological and evolutionary dynamics shaping adaptation in *A. gerardi*.

Future Research Directions

Expanding the scope of abiotic variables beyond precipitation is a key avenue for future research. While this dissertation highlights precipitation as a primary driver of local adaptation (Chps 2-3) and ITV (Chp. 4-5), temperature extremes (Hatfield & Prueger, 2015), soil fertility

(Ahmad et al., 2016; Song et al., 2023), and disturbance regimes may interact with water availability to shape adaptive responses (Jentsch et al., 2022). Investigating these factors, and others, across spatial and temporal scales will provide a more comprehensive understanding of the environmental drivers influencing trait differentiation and population resilience in grasslands (Fay et al., 2011; Anderson et al., 2016; Song et al., 2023). Long-term monitoring under variable climatic conditions can further reveal temporal dynamics in adaptation that short-term experiments may miss (Cocciardi et al., 2024).

Community-level interactions are another important area for future exploration. Competition, facilitation, and mutualistic relationships, particularly with soil microbial communities, can significantly influence trait variation (Ma et al., 2025) and fitness outcomes (Rúa et al., 2016) among plants. Experimentally manipulating these biotic interactions alongside abiotic stressors would help clarify the relative contribution of biotic drivers (Briscoe Runquist et al., 2020) to local adaptation (Hartung et al., 2023; Kazarina et al., 2025). Understanding these interactions is essential for improving restoration strategies (Eviner & Hawkes, 2008) and predicting population persistence in complex, multi-species ecosystems (Garrote et al., 2022).

Cytotype variation represents a significant source of ITV in many perennial grasses (McAllister et al., 2015; Pavlikova et al., 2017; Martinez-Sagarra et al., 2021) and can influence their adaptive capacity (McIntyre & Strauss, 2017). Multiple cytotypes often coexist within populations (Chrtek et al., 2017), and these differences in genome size can shape phenotypic plasticity (Roop et al., 2025), stress tolerance (Pavlikova et al., 2017), and long-term evolutionary potential (Albert et al., 2010; Martinez-Sagarra et al., 2021). In *A. gerardi*, variation in ploidy levels has been documented across populations (McAllister et al., 2015), suggesting that both historical and environmental drivers contribute to cytotype diversity. Investigating the

role of cytotype variation in the patterns documented in this dissertation offers a promising avenue for understanding how genome size and genetic diversity together generate phenotypic diversity and influence drought response.

Stomatal architecture is a key functional trait that links plant form to environmental performance, influencing gas exchange, water-use efficiency, and drought tolerance (Caine et al., 2023). In *A. gerardi*, stomatal size, density, and distribution can vary across individuals and populations, shaping their physiological responses to environmental stress (Varvel et al., 2018; Sytsma & Ricker et al., in press). Studies have found that cytotype variation may be correlated with differences in stomatal size (Lattier et al., 2019; Marinho et al., 2021), suggesting that genome duplication may directly affect stomatal traits and, consequently, water use efficiency (Caine et al., 2023). Integrating studies of stomatal architecture with cytotype can therefore provide a more complete understanding of how populations respond to environmental challenges and identify ecotypes suited for restoration or climate-resilient management.

Finally, integrating genetic, trait, and environmental data into species distribution models (SDMs; Wittman et al., 2016; Benito Garzon et al., 2019; Chardon et al., 2020) can improve predictions of adaptive potential under future climate scenarios (Smith et al., 2017). Coupling molecular markers, functional trait measurements, and climate projections allows for identifying populations and ecotypes with the highest likelihood of persistence under changing conditions (Li et al., 2017; Chardon et al., 2020). SDMs informed by genomic and trait data can directly inform conservation planning and restoration efforts (Wittman et al., 2016), prioritizing areas and ecotypes that maximize ecosystem resilience. Such research would strengthen the connection between ecological genomics research and practical conservation outcomes (Vajana et al., 2022), ensuring grassland ecosystems remain functional and resilient in the Anthropocene.

Conclusions and takeaways

In conclusion, this dissertation demonstrates that climate adaptation of *Andropogon gerardi* arises from the dynamic interplay of climate, genetic variation, and phenotypic diversity. Reciprocal garden experiments and long-term field manipulations confirmed strong local adaptation (Chp. 2), with climate-matched ecotypes outperforming foreign ecotypes. Trait differentiation and gene expression analyses (Chp. 3) revealed that dry ecotypes prioritize drought tolerance while wet show trait assemblages involved in competitive growth and resource acquisition (Grime, 1988; Jardine et al., 2021), highlighting the mechanistic basis of adaptive strategies. These patterns of ITV extend to range-wide patterns (Chp. 4) which is strongly influenced by precipitation and genetic background (Chp. 5). This work reinforces the importance of preserving both genetic and functional diversity to sustain adaptive potential and ecosystem resilience under future climate change (Albert et al., 2010; Shaw et al., 2024).

In our work, we integrate field (Chps. 2-4), greenhouse (Chp. 5), and genomic approaches (Chps. 2-5). In doing so, we provide a multi-scale framework for understanding adaptation and drought tolerance in *A. gerardi*, offering insights into the genetic and ecological mechanisms that underpin its response to environmental change. By linking genetic variation, trait variation, and environmental gradients, this work demonstrates how predictive models for restoration and conservation can be strengthened (Smith et al., 2017). This includes the selection of climate-adapted ecotypes and the incorporation of molecular markers for drought tolerance (Anderson et al., 2016; Vitt et al., 2022). Beyond *A. gerardi*, these findings have broad implications for grassland ecosystem management, emphasizing the necessity of long-term, integrative approaches to safeguard ecosystems under rapid environmental change (IPCC, 2023;

King et al., 2024) and to translate ecological theory into practical, resilience-focused strategies (Grime, 1988; Kawecki & Ebert, 2004; Sagarin & Gaines, 2002; Li et al., 2017; Estarangue et al., 2023). Ultimately, the findings of this dissertation support adaptive, data-driven conservation strategies and highlight how combining ecological theory, genomics, and trait-based analyses can inform restoration practices (Clark et al., 2012; Breed et al., 2019; Prakash et al., 2024) to maintain resilient, biodiverse, and productive grasslands under future droughts.

References

Abdel-Ghany, S. E., Ullah, F., Ben-Hur, A., & Reddy, A. S. (2020). Transcriptome analysis of drought-resistant and drought-sensitive sorghum (Sorghum bicolor) genotypes in response to PEG-induced drought stress. *International Journal of Molecular Sciences*, *21*(3), 772.

Ahmad, A. A., Radovich, T. J., Nguyen, H. V., Uyeda, J., Arakaki, A., Cadby, J., ... & Teves, G. (2016). Use of organic fertilizers to enhance soil fertility, plant growth, and yield in a tropical environment. *Basic Concepts to Applied Outcomes*, 85–108.

Ahrens, C. W., Andrew, M. E., Mazanec, R. A., Ruthrof, K. X., Challis, A., Hardy, G., ... & Rymer, P. D. (2020). Plant functional traits differ in adaptability and are predicted to be differentially affected by climate change. *Ecology and evolution*, *10*(1), 232-248.

Ahrens, C. W., Rymer, P. D., & Tissue, D. T. (2021). Intra-specific trait variation remains hidden in the environment. *New phytologist*, 229(3), 1183-1185.

Aimar, P., Yang, S., & Kiani, S. (2014). The role of ABA in drought stress response and recovery. *Frontiers in Plant Science, 5*, 95.

Aitken, S. N., & Whitlock, M. C. (2013). Assisted gene flow to facilitate local adaptation to climate change. *Annual Review of Ecology, Evolution, and Systematics,* 44(1), 367–388.

Alam, I., Wu, X., Yu, Q., & Ge, L. (2022). Comprehensive genomic analysis of G2-like transcription factor genes and their role in development and abiotic stresses in Arabidopsis. *Diversity*, *14*(3), 228.

Albert, C. H., Grassein, F., Schurr, F. M., Vieilledent, G., & Violle, C. (2010). When and how should intraspecific variability be considered in trait-based plant ecology? *Perspectives in Plant Ecology, Evolution and Systematics,* 13(3), 217–225.

Aldea, J., Dahlgren, J., Holmström, E., & Löf, M. (2024). Current and future drought vulnerability for three dominant boreal tree species. *Global Change Biology*, *30*(1), e17079.

Anderegg, W. R., Wolf, A., Arango-Velez, A., Choat, B., Chmura, D. J., Jansen, S., ... & Pacala, S. (2017). Plant water potential improves prediction of empirical stomatal models. *PloS one*, *12*(10), e0185481.

Anderegg, W. R. L., Anderegg, L. D. L., Kerr, K. L., Trugman, A. T., & Huang, C. Y. (2018). Climate-driven risks to the climate mitigation potential of forests. *Science, 368*(6497), eaaz7005.

Anderson, J. T. (2016). Plant fitness in a rapidly changing world. *New Phytologist*, *210*(1), 81-87.

Anderegg, L. D., Skelton, R. P., Diaz, J., Papper, P., Ackerly, D. D., & Dawson, T. E. (2023). Plasticity drives geographic variation and trait coordination in blue oak drought physiology. *bioRxiv*, 2023-08.

Anderson, J. T. and Song, B. H. (2020) 'Plant adaptation to climate change—Where are we?', *Journal of Systematics and Evolution*, 58(5), pp. 533–545.

Anderson, J. T., Willis, J. H., & Mitchell-Olds, T. (2011). Evolutionary genetics of plant adaptation. *Trends in Genetics*, *27*(7), 258-266.

Anderson, J. T., Willis, J. H., & Mitchell-Olds, T. (2016). Evolutionary genetics of plant adaptation. *Trends in Genetics,* 32(7), 335–348.

Andrews S. (2010). FastQC: A Quality Control Tool for High Throughput Sequence Data.

Aoki, K., Ogata, Y., & Shibata, D. (2007). Approaches for extracting practical information from gene co-expression networks in plant biology. *Plant and cell physiology*, *48*(3), 381-390.

Aun, M. A., Farnese, F., Loram-Lourenço, L., de Abreu, I. M. P. G., Silva, B. R. A., Freitas, J. C. E., ... & Menezes-Silva, P. E. (2024). Evidence of combined flower thermal and drought

vulnerabilities portends reproductive failure under hotter-drought conditions. *Plant, Cell & Environment*, *47*(6), 1971-1986.

Avolio, M. L., Hoffman, A. M., & Smith, M. D. (2018). Linking gene regulation, physiology, and plant biomass in Andropogon gerardii in response to drought. *Plant Ecology*, *219*, 1-15.

Axelrod, D. I. (1985). Rise of the grassland biome, central North America. *The Botanical Review*, *51*, 163-201.

Bachle, S., Griffith, D. M., & Nippert, J. B. (2018). Intraspecific trait variability in Andropogon gerardii, a dominant grass species in Great Plains. *Frontiers in Ecology and Evolution*, *6*, 217.

Baer, S. G., J. M. Blair, S. L. Collins, and A. K. Knapp. (2003). Soil resources regulate productivity and diversity in newly established tallgrass prairie. *Ecology* **84**: 724–735.

Baer, S. G., Gibson, D. J., & Johnson, L. C., (2019). Restoring grassland in the context of climate change. In: Grasslands and climate change (Ed D.J. Gibson & J. A. Newman). *Cambridge University Press*, Cambridge, UK, 310-322.

Bai, Y., & Cotrufo, M. F. (2022). Grassland soil carbon sequestration: Current understanding, challenges, and solutions. *Science*, 377(6606), 603-608.

Baird, A. S., Taylor, S. H., Pasquet-Kok, J., Vuong, C., Zhang, Y., Watcharamongkol, T., ... & Sack, L. (2021). Developmental and biophysical determinants of grass leaf size worldwide. *Nature*, *592*(7853), 242-247.

Bandurska, H. (2022). Drought stress responses: coping strategy resistance. *Plants*, *11*(7), 922.

Bao, G., Chen, J., Chopping, M., Bao, Y., Bayarsaikhan, S., Dorjsuren, A., ... & Qin, Z. (2019). Dynamics of net primary productivity on the Mongolian Plateau: Joint regulations of phenology and drought. *International Journal of Applied Earth Observation and Geoinformation*, *81*, 85-97.

Bardgett, R. D., Bullock, J. M., Lavorel, S., Manning, P., Schaffner, U., Ostle, N., ... & Shi, H. (2021). Combatting global grassland degradation. *Nature Reviews Earth & Environment*, *2*(10), 720-735.

Barton, K. E., Jones, C., Edwards, K. F., Shiels, A. B., & Knight, T. (2020). Local adaptation constrains drought tolerance in a foundation tree. *Journal of Ecology*, *108*(4), 1540-1552.

Benfey, P. N., & Mitchell-Olds, T. (2008). From genotype to phenotype: systems biology meets natural variation. *Science*, *320*(5875), 495-497.

Benito Garzón, M., Robson, T. M., & Hampe, A. (2019). ΔTrait SDMs: SDMs that account for local adaptation and phenotypic plasticity. *New Phytologist*, 222(4), 1757–1765.

Bennett, J. A., Riibak, K., Tamme, R., Lewis, R. J., & Pärtel, M. (2016). The reciprocal relationship between competition and intraspecific trait variation. *Journal of Ecology*, *104*(5), 1410-1420.

Benning, J. W., Faulkner, A., & Moeller, D. A. (2023). Rapid evolution during climate change: demographic and genetic constraints on adaptation to severe drought. *Proceedings of the Royal Society B*, *290*(1998), 20230336.

Bernatchez, L., Ferchaud, A. L., Berger, C. S., Venney, C. J., & Xuereb, A. (2024). Genomics for monitoring and understanding species responses to global climate change. *Nature Reviews Genetics*, *25*(3), 165-183.

Bhaskara, G. B., Haque, T., Bonnette, J. E., Napier, J. D., Bauer, D., Schmutz, J., & Juenger, T. E. (2023). Evolutionary analyses of gene expression divergence in Panicum hallii: exploring constitutive and plastic responses using reciprocal transplants. *Molecular biology and evolution*, *40*(10), msad210.

Bhattacharya, A. (2022). Effect of low-temperature stress on germination, growth, and phenology of plants: A review. *Physiological processes in plants under low temperature*, 1-106.

Bita-Nicolae, C., & Dhyani, P. (2025). Plant diversity: the key to ecosystem resilience in a changing world. *Frontiers in Plant Science*, *15*, 1534119.

Blanco-Sánchez, M., Ramírez-Valiente, J. A., Ramos-Muñoz, M., Pías, B., Franks, S. J., Escudero, A., & Matesanz, S. (2024). Range-wide intraspecific variation reflects past adaptation to climate in a gypsophile Mediterranean shrub. *Journal of Ecology*, *112*(7), 1533-1549.

Blanquart, F., Kaltz, O., Nuismer, S. L., & Gandon, S. (2013). A practical guide to measuring local adaptation. *Ecology Letters*, 16(9), 1195–1205.

Blumenthal, D. M., Mueller, K. E., Kray, J. A., Ocheltree, T. W., Augustine, D. J., & Wilcox, K. R. (2020). Traits link drought resistance with herbivore defence and plant economics in semi-arid grasslands: The central roles of phenology and leaf dry matter content. *Journal of Ecology*, *108*(6), 2336-2351.

Blumenthal, D. M., LeCain, D. R., Porensky, L. M., Leger, E. A., Gaffney, R., Ocheltree, T. W., & Pilmanis, A. M. (2021). Local adaptation to precipitation in the perennial grass Elymus elymoides: Trade-offs between growth and drought resistance traits. *Evolutionary Applications*, *14*(2), 524-535.

Bohm, S., Kelly, N., Postuma, M., Wagemaker, N. C., ter Haar, S., Scheper, J., & Vergeer, P. (2025). Small populations, big challenges: Genetic, demographic, and landscape context collectively shape population performance of a perennial herb. *Biological Conservation*, *305*, 111044.

Bolger, A. M., Lohse, M., & Usadel, B. (2014). Trimmomatic: a flexible trimmer for Illumina sequence data. *Bioinformatics*, *30*(15), 2114-2120.

Bolnick, D. I., Amarasekare, P., Araújo, M. S., Bürger, R., Levine, J. M., Novak, M., ... & Vasseur, D. A. (2011). Why intraspecific trait variation matters in community ecology. *Trends in ecology & evolution*, *26*(4), 183-192.

Bomblies, K., & Peichel, C. L. (2022). Genetics of adaptation. *Proceedings of the National Academy of Sciences*, *119*(30), e2122152119.

Bonamour, S., Chevin, L. M., Charmantier, A. and Teplitsky, C. (2019) 'Phenotypic plasticity in response to climate change: The importance of cue variation', *Philosophical Transactions of the Royal Society B*, 374(1768), p. 20180178.

Breed, M. F., Stead, M. G., Ottewell, K. M., Gardner, M. G., & Lowe, A. J. (2013). Which provenance and where? Seed sourcing strategies for revegetation in a changing environment. *Conservation Genetics*, 14(1), 1–10.

Breed, M. F., Harrison, P. A., Blyth, C., Byrne, M., Gaget, V., Gellie, N. J., ... & Mohr, J. J. (2019). The potential of genomics for restoring ecosystems and biodiversity. *Nature Reviews Genetics,* 20(10), 615–628.

Briscoe Runquist, R. D., Gorton, A. J., Yoder, J. B., Deacon, N. J., Grossman, J. J., Kothari, S., ... & Moeller, D. A. (2020). Context dependence of local adaptation to abiotic and biotic environments. *The American Naturalist*, 195(3), 412–431.

Broadhurst, L. M., Lowe, A., Coates, D. J., Cunningham, S. A., McDonald, M., Vesk, P. A., & Yates, C. (2008). Seed supply for broadscale restoration: Maximizing evolutionary potential. *Evolutionary Applications,* 1(4), 587–597.

Brooker, R., Brown, L. K., George, T. S., Pakeman, R. J., Palmer, S., Ramsay, L., ... & Wilkinson, M. J. (2022). Active and adaptive plasticity in a changing climate. *Trends in Plant Science*, *27*(7), 717-728.

Brown, J. H. (1984) 'On the relationship between abundance and distribution of species', *The American Naturalist*, 124(2), pp. 255–279.

Bruelheide, H., Dengler, J., Purschke, O., Lenoir, J., Jiménez-Alfaro, B., Hennekens, S. M., ... & Jandt, U. (2018). Global trait–environment relationships of plant communities. *Nature ecology & evolution*, *2*(12), 1906-1917.

Brunet, J., Inouye, D. W., Wilson Rankin, E. E., & Giannini, T. C. (2025). Global change aggravates drought, with consequences for reproduction. *Annals of Botany*, *135*(1-2), 89-104.

Bucharova, A., Durka, W., Hölzel, N., Kollmann, J., Michalski, S., & Tischew, S. (2019). Are local plants the best for ecosystem restoration? It depends on the restoration target. *Basic and Applied Ecology,* 32, 25–33.

Buckley, L. B., Schoville, S. D., & Williams, C. M. (2021). Shifts in the relative fitness contributions of fecundity and survival in variable and changing environments. *Journal of Experimental Biology*, *224*(Suppl_1), jeb228031.

Caine, R. S., Harrison, E. L., Sloan, J., Flis, P. M., Fischer, S., Khan, M. S., ... & Croft, H. (2023). The influences of stomatal size and density on rice abiotic stress resilience. *New Phytologist*, *237*(6), 2180-2195.

Camacho, C., Coulouris, G., Avagyan, V., Ma, N., Papadopoulos, J., & Bealer, K. (2009). BLAST+: architecture and applications. *BMC Bioinformatics* 10:421.

Cardoso, J. A., Pineda, M., Jiménez, J. D. L. C., Vergara, M. F., & Rao, I. M. (2015). Contrasting strategies to cope with drought conditions by two tropical forage C4 grasses. *AoB Plants*, *7*, plv107.

Carroll, O., & MacDougall, A. S. (2024). Facilitation against herbivory more important than resource-based niche differences for plant coexistence in a field experiment. *Journal of Ecology,* 112(6), 1200–1209.

Castillioni, K., Newman, G. S., Souza, L., & Iler, A. M. (2022). Effects of drought on grassland phenology depend on functional types. *New Phytologist*, *236*(4), 1558-1571.

Castro-Camba, R., Sánchez, C., Vidal, N., & Vielba, J. M. (2022). Plant development and crop yield: The role of gibberellins. *Plants*, *11*(19), 2650.

Caudle, K. L., Johnson, L. C., Baer, S. G., & Maricle, B. R. (2014). A comparison of seasonal foliar chlorophyll change among ecotypes and cultivars of Andropogon gerardii (Poaceae) by using nondestructive and destructive methods. *Photosynthetica*, *52*, 511-518.

Chardon, N. I., Pironon, S., Peterson, M. L., & Doak, D. F. (2020). Incorporating intraspecific variation into species distribution models improves distribution predictions, but cannot predict species traits for a wide-spread plant species. *Ecography*, 43(1), 60–74.

Chen, M., Zhang, T. L., Hu, C. G., & Zhang, J. Z. (2023). The role of drought and temperature stress in the regulation of flowering time in annuals and perennials. *Agronomy*, *13*(12), 3034.

Chandanpurkar, H. A., Famiglietti, J. S., Gopalan, K., Wiese, D. N., Wada, Y., Kakinuma, K., ... & Zhang, F. (2025). Unprecedented continental drying, shrinking freshwater availability, and increasing land contributions to sea level rise. *Science Advances*, *11*(30), eadx0298.

Cherwin, K., & Knapp, A. (2012). Unexpected patterns of sensitivity to drought in three semi-arid grasslands. *Oecologia*, *169*(3), 845-852.

Chrtek, J., Herben, T., Rosenbaumová, R., Münzbergová, Z., Dočkalová, Z., Zahradníček, J., ... & Trávníček, P. (2017). Cytotype coexistence in the field cannot be explained by inter-cytotype

hybridization alone: Linking experiments and computer simulations in the sexual species Pilosella echioides (Asteraceae). *BMC Evolutionary Biology*, 17(1), 87.

Clark, D. L., Wilson, M., Roberts, R., Dunwiddie, P. W., Stanley, A., & Kaye, T. N. (2012). Plant traits–a tool for restoration? *Applied Vegetation Science,* 15(4), 449–458.

Clausen, J., Keck, D. D., & Hiesey, W. M. (1941). Regional differentiation in plant species. *The American Naturalist*, *75*(758), 231-250.

Cleland, E. E., Collins, S. L., Dickson, T. L., Farrer, E. C., Gross, K. L., Gherardi, L. A., ... & Suding, K. N. (2013). Sensitivity of grassland plant community composition to spatial vs. temporal variation in precipitation. *Ecology*, 94(8), 1687-1696.

Cocciardi, J. M., Hoffman, A. M., Alvarado-Serrano, D. F., Anderson, J., Blumstein, M., Boehm, E. L., ... & Avolio, M. L. (2024). The value of long-term ecological research for evolutionary insights. *Nature Ecology & Evolution*, *8*(9), 1584-1592.

Conesa, A., and Gotz, S. (2008). Blast2GO: A comprehensive suite for functional analysis in plant genomics. *Int. J. Plant Genomics* 2008:619832.

Cook, B. I., Ault, T. R., & Smerdon, J. E. (2015). Unprecedented 21st century drought risk in the American Southwest and Central Plains. *Science advances*, *1*(1), e1400082.

Craine, J. M., & Dybzinski, R. (2013). Mechanisms of plant competition for nutrients, water and light. *Functional Ecology*, *27*(4), 833-840.

Craine, J. M., Ocheltree, T. W., Nippert, J. B., Towne, E., Skibbe, A. M., Kembel, S. W., & Fargione, J. E. (2013). Global diversity of drought tolerance and grassland climate-change resilience. *Nature Climate Change*, *3*(1), 63-67.

Croft, H., Chen, J. M., Luo, X., Bartlett, P., Chen, B., & Staebler, R. M. (2017). Leaf chlorophyll content as a proxy for leaf photosynthetic capacity. *Global change biology*, *23*(9), 3513-3524.

CRP. (2023, December). Conservation Reserve Enrollments December 2023. Conservation Reserve Program Statistics 2023 *United States Department of Agriculture*.

CRP "Conservation Reserve Program Statistics." Conservation Reserve Programme, *USDA Department of Natural Resources*, Aug. 2024.

Csardi G, Nepusz T (2006). "The igraph software package for complex network research." *InterJournal Complex Systems* 1695.

Cyriac, D., Hofmann, R. W., Stewart, A., Sathish, P., Winefield, C. S., & Moot, D. J. (2018). Intraspecific differences in long-term drought tolerance in ryegrass. *PLoS One*, *13*(4), e0194977.

DaCosta, M., & Huang, B. (2009). Physiological adaptations of perennial grasses to drought stress. *Perspectives in biophysical plant ecophysiology*, 169-190.

Dallas, T.A., Santini, L., Decker, R. & Hastings, A. (2020) 'Weighing the evidence for the abundant-centre hypothesis', *Biodiversity Informatics*, 15(3), pp. 81-91.

Damgaard, C. (2015). Modelling pin-point cover data of complementary vegetation classes. *Ecological Informatics*, *30*, 179-184.

Dar, F. A., Mushtaq, N. U., Saleem, S., Rehman, R. U., Dar, T. U. H., & Hakeem, K. R. (2022). Role of epigenetics in modulating phenotypic plasticity against abiotic stresses in plants. *International Journal of Genomics*, 2022(1), 1092894.

De Kort, H., Prunier, J. G., Ducatez, S., Honnay, O., Baguette, M., Stevens, V. M., & Blanchet, S. (2021). Life history, climate and biogeography interactively affect worldwide genetic diversity of plant and animal populations. *Nature Communications*, *12*(1), 516.

De Kroon, H., Huber, H., Stuefer, J. F., & Van Groenendael, J. M. (2005). A modular concept of phenotypic plasticity in plants. *New phytologist*, *166*(1), 73-82.

Decena, M. A., Gálvez-Rojas, S., Agostini, F., Sancho, R., Contreras-Moreira, B., Des Marais, D. L., ... & Catalán, P. (2021). Comparative genomics, evolution, and drought-induced expression of dehydrin genes in model Brachypodium grasses. *Plants*, *10*(12), 2664.

Denelle, P., Violle, C., DivGrass Consortium, & Munoz, F. (2020). Generalist plants are more competitive and more functionally similar to each other than specialist plants: insights from network analyses. *Journal of Biogeography*, *47*(9), 1922-1933.

Des Marais, D. L., Hernandez, K. M., & Juenger, T. E. (2013). Genotype-by-environment interaction and plasticity: Exploring genomic responses of plants to the abiotic environment. *Annual Review of Ecology, Evolution, and Systematics,* 44, 5–29.

Des Roches, S., Post, D. M., Turley, N. E., Bailey, J. K., Hendry, A. P., Kinnison, M. T., ... & Palkovacs, E. P. (2018). The ecological importance of intraspecific variation. *Nature ecology & evolution*, *2*(1), 57-64.

Des Roches, S., Pendleton, L. H., Shapiro, B., & Palkovacs, E. P. (2021). Conserving intraspecific variation for nature's contributions to people. *Nature ecology & evolution*, *5*(5), 574-582.

DeWoody, J.A., Harder, A.M., Mathur, S. & Willoughby, J.R. (2021) 'The long-standing significance of genetic diversity in conservation', *Molecular Ecology*, 30(17), pp. 4147-4154.

Díaz, S., Kattge, J., Cornelissen, J. H., Wright, I. J., Lavorel, S., Dray, S., ... & Gorné, L. D. (2016). The global spectrum of plant form and function. *Nature*, *529*(7585), 167-171.

Dietrich, J. D., & Smith, M. D. (2016). The effect of timing of growing season drought on flowering of a dominant C 4 grass. *Oecologia*, *181*, 391-399.

Dietz, K. J., Zörb, C., & Geilfus, C. M. (2021). Drought and crop yield. *Plant Biology*, *23*(6), 881-893.

Dixon, A.L., Herlihy, C.R. & Busch, J.W. (2013) 'Demographic and population-genetic tests provide mixed support for the abundant centre hypothesis in the endemic plant *Leavenworthia stylosa*', *Molecular Ecology*, 22(7), pp. 1777-1791.

Dobin, A., Davis, C. A., Schlesinger, F., Drenkow, J., Zaleski, C., Jha, S., ... & Gingeras, T. R. (2013). STAR: ultrafast universal RNA-seq aligner. *Bioinformatics*, *29*(1), 15-21.

Doherty, K. D., Butterfield, B. J., & Wood, T. E. (2017). Matching seed to site by climate similarity: techniques to prioritize plant materials development and use in restoration. *Ecological Applications*, *27*(3), 1010-1023.

Dolezal, J., Jandova, V., Macek, M., & Liancourt, P. (2021). Contrasting biomass allocation responses across ontogeny and stress gradients reveal plant adaptations to drought and cold. *Functional Ecology*, *35*(1), 32-42.

Dong, N., Prentice, I. C., Wright, I. J., Evans, B. J., Togashi, H. F., Caddy-Retalic, S., ... & Lowe, A. J. (2020). Components of leaf-trait variation along environmental gradients. *New Phytologist*, *228*(1), 82-94.

Doyle, J. J., & Dickson, E. E. (1987). Preservation of plant samples for DNA restriction endonuclease analysis. *Taxon*, *36*(4), 715-722.

Doyle, J. J., & Doyle, J. L. (1987). A rapid DNA isolation procedure for small quantities of fresh leaf tissue. *Phytochemical bulletin*.

Eckert, C.G., Samis, K.E. & Lougheed, S.C. (2008) 'Genetic variation across species ' geographical ranges: the central–marginal hypothesis and beyond', *Molecular Ecology*, 17(5), pp. 1170-1188.

Ellegren, H., & Galtier, N. (2016). Determinants of genetic diversity. *Nature Reviews Genetics*, 17(7), 422–433.

Ellstrand, N. C., & Rieseberg, L. H. (2016). When gene flow really matters: gene flow in applied evolutionary biology. *Evolutionary applications*, *9*(7), 833.

Ellsworth, P. Z., & Cousins, A. B. (2016). Carbon isotopes and water use efficiency in C_4 plants. *Current Opinion in Plant Biology*, 31, 155–161.

Epstein, H. E., Lauenroth, W. K., Burke, I. C., & Coffin, D. P. (1998). Regional productivities of plant species in the Great Plains of the United States. *Plant Ecology*, 134(2), 173-195.

Estarague, A., Vasseur, F., Sartori, K., Bastias, C. C., Cornet, D., Rouan, L., ... & Violle, C. (2023). Into the range: a latitudinal gradient or a center-margins differentiation of ecological strategies in Arabidopsis thaliana?. *Annals of Botany*, *129*(3), 343-356.

Etterson, J.R. (2004) 'Evolutionary potential of *Chamaecrista fasciculata* in relation to climate change. I. Clinal patterns of selection along an environmental gradient in the Great Plains', *Evolution*, 58(7), pp. 1446-1456.

Eviner, V. T., & Hawkes, C. V. (2008). Embracing variability in the application of plant–soil interactions to the restoration of communities. *Restoration Ecology*, 16(4), 713–729.

Exposito-Alonso, M., Booker, T. R., Czech, L., Gillespie, L., Hateley, S., Kyriazis, C. C., ... & Zess, E. (2022). Genetic diversity loss in the Anthropocene. *Science*, *377*(6613), 1431-1435.

Eziz, A., Yan, Z., Tian, D., Han, W., Tang, Z., & Fang, J. (2017). Drought effect on plant biomass allocation: A meta-analysis. *Ecology and evolution*, *7*(24), 11002-11010.

Fahad, S., Sonmez, O., Saud, S., Wang, D., Wu, C., Adnan, M., & Turan, V. (Eds.). (2021). *Climate change and plants: biodiversity, growth and interactions*. CRC press.

Faralli, M., Williams, K., Corke, F., Li, M., Doonan, J. H., & Varotto, C. (2021). Interspecific and intraspecific phenotypic diversity for drought adaptation in bioenergy Arundo species. *GCB Bioenergy*, *13*(4), 753-769.

Farquhar, G., O'Leary, M. & Berry, J. (1982) 'On the relationship between carbon isotope discrimination and the intercellular carbon dioxide concentration in leaves', *Functional Plant Biology*, 9, p. 121.

Farquhar, G. D., Ehleringer, J. R., & Hubick, K. T. (1989). Carbon isotope discrimination and photosynthesis. *Annual Review of Plant Physiology and Plant Molecular Biology*, 40, 503–537.

Fay, P. A., Carlisle, J. D., Knapp, A. K., Blair, J. M., & Collins, S. L. (2000). Altering rainfall timing and quantity in a mesic grassland ecosystem: design and performance of rainfall manipulation shelters. *Ecosystems*, *3*(3), 308-319.

Fay, P. A., Carlisle, J. D., Danner, B. T., Lett, M. S., McCarron, J. K., Stewart, C., ... & Collins, S. L. (2002). Altered rainfall patterns, gas exchange, and growth in grasses and forbs. *International Journal of Plant Sciences*, *163*(4), 549-557.

Fay, P. A., Carlisle, J. D., Knapp, A. K., Blair, J. M., & Collins, S. L. (2003). Productivity responses to altered rainfall patterns in a C 4-dominated grassland. *Oecologia*, *137*, 245-251.

Fay, P. A., Kaufman, D. M., Nippert, J. B., Carlisle, J. D., & Harper, C. W. (2008). Changes in grassland ecosystem function due to extreme rainfall events: implications for responses to climate change. *Global Change Biology*, *14*(7), 1600-1608.

Fay, P. A., Carlisle, J. D., Knapp, A. K., Blair, J. M., & Collins, S. L. (2011). Productivity responses to altered rainfall patterns in a C_4-dominated grassland. *Oecologia*, 168(3), 791–802.

Feldman, A. F., Feng, X., Felton, A. J., Konings, A. G., Knapp, A. K., Biederman, J. A., & Poulter, B. (2024). Plant responses to changing rainfall frequency and intensity. *Nature Reviews Earth & Environment*, *5*(4), 276-294.

Felton, A. J., Slette, I. J., Smith, M. D., & Knapp, A. K. (2020). Precipitation amount and event size interact to reduce ecosystem functioning during dry years in a mesic grassland. *Global Change Biology*, 26(2), 658-668.

Ferguson, L., Upton, H. E., Pimentel, S. C., Jeans, C., Ingolia, N. T., & Collins, K. (2025). Improved precision, sensitivity, and adaptability of ordered two-template relay cDNA library preparation for RNA sequencing. *RNA*, *31*(2), 224-244.

Fernández-de-Uña, L., Martínez-Vilalta, J., Poyatos, R., Mencuccini, M., & McDowell, N. G. (2023). The role of height-driven constraints and compensations on tree vulnerability to drought. *New Phytologist*, *239*(6), 2083-2098.

Figueroa-Macías, J. P., García, Y. C., Núñez, M., Díaz, K., Olea, A. F., & Espinoza, L. (2021). Plant growth-defense trade-offs: molecular processes leading to physiological changes. *International journal of molecular sciences*, *22*(2), 693.

Fincheira, P., & Quiroz, A. (2018). Microbial volatiles as plant growth inducers. *Microbiological Research*, 208, 63–75.

Fitzpatrick, M. C., & Keller, S. R. (2015). Ecological genomics meets community-level modelling of biodiversity: Mapping the genomic landscape of current and future environmental adaptation. *Ecology Letters,* 18(1), 1–16.

Foll, M., & Gaggiotti, O. (2006). Identifying the environmental factors that determine the genetic structure of populations. *Genetics*, *174*(2), 875-891.

Fortunato, A. E., & Pires, A. S. (2020). Plant functional traits in the context of abiotic stress: A review. *Environmental and Experimental Botany*, 179, 104182.

Foti, S., Cosentino, S., Patanè, C., Copani, V., & Sanzone, E. (2003). Plant indicators of available soil water in the perennial herbaceous crop Miscanthus giganteus Greef et Deu. *Agronomie*, *23*(1), 29-36.

Franks, S. J., Sim, S., & Weis, A. E. (2007). Rapid evolution of flowering time by an annual plant in response to a climate fluctuation. *Proceedings of the National Academy of Sciences*, 104(4), 1278–1282.

Fréjaville, T., Vizcaíno-Palomar, N., Fady, B., Kremer, A., & Benito Garzón, M. (2020). Range margin populations show high climate adaptation lags in European trees. *Global Change Biology*, *26*(2), 484-495.

Funk, J. L., Cleland, E. E., Suding, K. N., & Zavaleta, E. S. (2008). Restoration through reassembly: Plant traits and invasion resistance. *Trends in Ecology & Evolution*, 23(12), 695–703.

Gagnaire, P. A. (2020). Comparative genomics approach to evolutionary process connectivity. *Evolutionary Applications*, *13*(6), 1320-1334.

Galliart Matthew, Nora Bello, Mary Knapp, Jesse Poland, Paul St Amand, Sara Baer, Brian Maricle, Adam B. Smith, Loretta Johnson (2019). Local Adaptation, Genetic Divergence, and Experimental Natural Selection in a Foundation Grass across the US Great Plains' Climate Gradient. *Global Change Biology*. 25(3):850-868.

Galliart, M., Sabates, S., Tetreault, H., DeLaCruz, A., Bryant, J., Alsdurf, J., ... & Johnson, L. (2020). Adaptive genetic potential and plasticity of trait variation in the foundation prairie grass Andropogon gerardi across the US Great Plains' climate gradient: Implications for climate change and restoration. *Evolutionary applications*, 13(9), 2333-2356.

Galmés, J., Flexas, J., Savé, R., & Medrano, H. (2007). Water relations and stomatal characteristics of Mediterranean plants with different growth forms and leaf habits: Responses to water stress and recovery. *Plant and Soil, 290*(1–2), 139–155.

Garrote, P. J., Castilla, A. R., & Fedriani, J. M. (2022). Coping with changing plant–plant interactions in restoration ecology: Effect of species, site, and individual variation. *Applied Vegetation Science*, 25(1), e12644.

Gaskin, J. F., Espeland, E., Johnson, C. D., Larson, D. L., Mangold, J. M., McGee, R. A., Milner, C., Paudel, S., Pearson, D. E., Perkins, L. B., Prosser, C. W., Runyon, J. B., Sing, S. E., Sylvain, Z. A., Symstad, A. J., & Tekiela, D. R. (2021). Managing invasive plants on Great Plains grasslands: A discussion of current challenges. *Rangeland Ecology & Management,* 78, 235–249.

Gaudinier, A., & Blackman, B. K. (2020). Evolutionary processes from the perspective of flowering time diversity. *New Phytologist*, *225*(5), 1883-1898.

Gazol, A., Fajardo, A., & Camarero, J. J. (2023). Contributions of intraspecific variation to drought tolerance in trees. *Current Forestry Reports*, *9*(6), 461-472.

Geber, M. A., & Griffen, L. R. (2003). Inheritance and natural selection on functional traits. *International journal of plant sciences*, *164*(S3), S21-S42.

Germain, S.J. & Lutz, J.A. (2020) 'Climate extremes may be more important than climate means when predicting species range shifts', *Climatic Change*, 163(1), pp. 579-598.

Glaubitz, J. C., Casstevens, T. M., Lu, F., Harriman, J., Elshire, R. J., Sun, Q., & Buckler, E. S. (2014). TASSEL-GBS: a high capacity genotyping by sequencing analysis pipeline. *PloS one*, *9*(2), e90346.

Gibson, D. J. (2009). Community Ecology. *Grasses and Grassland Ecology*. Oxford University Press. 110-128.

Gibson, D.J., Donatelli, J.M., AbuGhazaleh, A., Baer, S.G. & Johnson, L.C. (2017) 'Ecotypic variation in forage nutrient value of a dominant prairie grass across a precipitation gradient', *Grassland Science*, 62(4), pp. 233-242.

Gibson, D.J., Barfknecht, D.F., Baer, S.G., Galliart, M., Sytsma, J., Ren, Z., & Johnson, L. (2024). Diversity-productivity relationships are dependent upon location and ecotypes of the dominant species growing across a precipitation gradient.

Gilbert, S. L., Broadley, K., Doran-Myers, D., Droghini, A., Haines, J. A., Hämäläinen, A., ... & Boutin, S. (2020) 'Conservation triage at the trailing edge of climate envelopes', *Conservation Biology*, 34(1), pp. 289-292.

Götz, S., García-Gómez, J. M., Terol, J., Williams, T. D., Nagaraj, S. H., Nueda, M. J., ... & Conesa, A. (2008). High-throughput functional annotation and data mining with the Blast2GO suite. *Nucleic acids research*, *36*(10), 3420-3435.

Goudet, J., Jombart, T., & Goudet, M. J. (2015). Package 'hierfstat'. *Estimation and Tests of Hierarchical F-Statistics*.

Gould, B. A., Palacio-Mejia, J. D., Jenkins, J., Mamidi, S., Barry, K., Schmutz, J., ... & Lowry, D. B. (2018). Population genomics and climate adaptation of a C4 perennial grass, Panicum hallii (Poaceae). *BMC genomics*, *19*(1), 792.

Grabherr, M. G., Haas, B. J., Yassour, M., Levin, J. Z., Thompson, D. A., Amit, I., ... & Regev, A. (2011). Full-length transcriptome assembly from RNA-Seq data without a reference genome. *Nature biotechnology*, *29*(7), 644-652.

Grant, P. R., Grant, B. R., Huey, R. B., Johnson, M. T., Knoll, A. H., & Schmitt, J. (2017). Evolution caused by extreme events. *Philosophical Transactions of the Royal Society B: Biological Sciences*, *372*(1723), 20160146.

Gray, M. M., St. Amand, P., Bello, N. M., Galliart, M. B., Knapp, M., Garrett, K. A., ... & Johnson, L. C. (2014). Ecotypes of an ecologically dominant prairie grass (Andropogon gerardi) exhibit genetic divergence across the US Midwest grasslands' environmental gradient. *Molecular Ecology*, 23(24), 6011-6028.

Greig-Smith, P. (1983) Quantitative plant ecology. 4th edn. *Oxford: Blackwell Scientific.*

Griffin-Nolan, R. J., Slette, I. J., & Knapp, A. K. (2021). Deconstructing precipitation variability: Rainfall event size and timing uniquely alter ecosystem dynamics. *Journal of Ecology*, *109*(9), 3356-3369.

Grime, J. P. (1988). The CSR model of primary plant strategies—origins, implications and tests. In *Plant evolutionary biology* (pp. 371-393). Dordrecht: Springer Netherlands.

Grossiord, C., Buckley, T. N., Cernusak, L. A., Novick, K. A., Poulter, B., Siegwolf, R. T. W., ... & McDowell, N. G. (2020). Plant responses to rising vapor pressure deficit. *New Phytologist, 226*(6), 1550–1566.

Guasconi, D., Manzoni, S., & Hugelius, G. (2023). Climate-dependent responses of root and shoot biomass to drought duration and intensity in grasslands–a meta-analysis. *Science of the Total Environment*, *903*, 166209.

Gupta, S., Ranjan, R., Bijlwan, A., Jha, A., & Jena, R. K. (2024). Enhancing Water Use Efficiency Through Trait-Based Approaches. In *Plant Functional Traits for Improving Productivity* (pp. 133-147). Singapore: Springer Nature Singapore.

Gustafson, D. J., Major, C., Jones, D., Synovec, J., Baer, S. G., & Gibson, D. J. (2014). Genetic sorting of subordinate species in grassland modulated by intraspecific variation in dominant species. *PLoS One,* 9(3), e91511.

Habte, E., Teshome, A., Muktar, M. S., Assefa, Y., Negawo, A. T., Machado, J. C., ... & Jones, C. S. (2022). Productivity and feed quality performance of Napier grass (*Cenchrus purpureus*) genotypes growing under different soil moisture levels. *Plants*, *11*(19), 2549.

Hamerlynck, E. P., Scott, R. L., Moran, M. S., Keefer, T. O., & Huxman, T. E. (2010). Growing season ecosystem and leaf-level gas exchange of an exotic and native semiarid bunchgrass. *Oecologia*, *163*, 561-570.

Hampe, A. and Petit, R. J. (2005) 'Conserving biodiversity under climate change: the rear edge matters', *Ecology Letters*, 8(5), pp. 461-467.

Hamann, E., Pauli, C. S., Joly-Lopez, Z., Groen, S. C., Rest, J. S., Kane, N. C., ... & Franks, S. J. (2021). Rapid evolutionary changes in gene expression in response to climate fluctuations. *Molecular Ecology*, *30*(1), 193-206.

Hanisch, M., Schweiger, O., Cord, A. F., Volk, M., & Knapp, S. (2020). Plant functional traits shape multiple ecosystem services, their trade-offs and synergies in grasslands. *Journal of Applied Ecology*, *57*(8), 1535-1550.

Hargreaves, A. L., Samis, K. E., & Eckert, C. G. (2014). Are species' range limits simply niche limits writ large? A review of transplant experiments beyond the range. *The American Naturalist,* 183(2), 157–173.

Hartung, E. (2023). Perennial grass ecotype ecological and genetic response to local and non-local microbial inoculum is ecotype-specific. Master's Thesis. *KREX Kansas State University*.

Hatfield, J. L., & Prueger, J. H. (2015). Temperature extremes: Effect on plant growth and development. *Weather and Climate Extremes*, 10(Part A), 4–10.

Hayford, R. K., Serba, D. D., Xie, S., Ayyappan, V., Thimmapuram, J., Saha, M. C., ... & Kalavacharla, V. K. (2022). Global analysis of switchgrass (Panicum virgatum L.) transcriptomes in response to interactive effects of drought and heat stresses. *BMC Plant Biology*, *22*(1), 107.

He, N., Li, Y., Liu, C., Xu, L., Li, M., Zhang, J., ... & Yu, G. (2020). Plant trait networks: improved resolution of the dimensionality of adaptation. *Trends in Ecology & Evolution*, *35*(10), 908-918.

Heckman, R. W., Aspinwall, M. J., Taylor, S. H., Lowry, D. B., Khasanova, A., Bonnette, J. E., ... & Juenger, T. E. (2025). Changes in leaf economic trait relationships across a precipitation gradient are related to differential gene expression in a C4 perennial grass. *New Phytologist*, *246*(4), 1583-1596.

Hefley, T. J., Hooten, M. B., Russell, R. E., Walsh, D. P., & Powell, J. A. (2017). When mechanism matters: Bayesian forecasting using models of ecological diffusion. *Ecology Letters*, *20*(5), 640-650.

Henn, J. J., Buzzard, V., Enquist, B. J., Halbritter, A. H., Klanderud, K., Maitner, B. S., ... & Vandvik, V. (2018). Intraspecific trait variation and phenotypic plasticity mediate alpine plant species response to climate change. *Frontiers in Plant Science*, *9*, 1548.

Hereford, J. (2009). A quantitative survey of local adaptation and fitness trade-offs. *The American Naturalist,* 173(5), 579–588.

Hevroy, T. H., Moody, M. L., & Krauss, S. L. (2018). Population genetic analysis reveals barriers and corridors for gene flow within and among riparian populations of a rare plant. *AoB Plants*, *10*(1), plx065.

Hilty, J., Muller, B., Pantin, F., & Leuzinger, S. (2021). Plant growth: the what, the how, and the why. *New Phytologist*, *232*(1), 25-41.

Hoban, S., Kelley, J. L., Lotterhos, K. E., Antolin, M. F., Bradburd, G., Lowry, D. B., Poss, M. L., Reed, L. K., Storfer, A., & Whitlock, M. C. (2016). Finding the genomic basis of local adaptation: Pitfalls, practical solutions, and future directions. *American Naturalist*, 188(4), 379–397.

Hoekstra, J. M., Boucher, T. M., Ricketts, T. H., & Roberts, C. (2005). Confronting a biome crisis: global disparities of habitat loss and protection. *Ecology letters*, *8*(1), 23-29.

Hoffmann, W. A., & Poorter, H. (2002). Avoiding bias in calculations of relative growth rate. *Annals of Botany*, 90(1), 37–42.

Hoffman AM, Smith MD. (2018). Gene expression differs in codominant prairie grasses under drought. *Mol Ecol Resour*.; 18: 334–346.

Hoffman, A. M., & Smith, M. D. (2021). Nonlinear drought plasticity reveals intraspecific diversity in a dominant grass species. *Functional Ecology*, *35*(2), 463-474.

Hord, A. M., Fischer, D. G., Schweitzer, J. A., LeRoy, C. J., Whitham, T. G., & Bailey, J. K. (2025). Hybrid introgression as a mechanism of rapid evolution and resilience to climate change in a riparian tree species. *Communications Biology*, *8*(1), 1173.

Howard, T. G., & Goldberg, D. E. (2001). Competitive response hierarchies for germination, growth, and survival and their influence on abundance. *Ecology*, *82*(4), 979-990.

Hrmova, M., & Hussain, S. S. (2021). Plant transcription factors involved in drought and associated stresses. *International journal of molecular sciences*, *22*(11), 5662.

Hufford, K. M., & Mazer, S. J. (2003). Plant ecotypes: Genetic differentiation in the age of ecological restoration. *Trends in Ecology & Evolution*, 18(3), 147–155.

Huisman, J., & Olff, H. (1998). Competition and facilitation in multispecies plant-herbivore systems of productive environments. *Ecology Letters*, 1(1), 25–29.

Hungate, B. A., Barbier, E. B., Ando, A. W., Marks, S. P., Reich, P. B., Van Gestel, N., ... & Cardinale, B. J. (2017). The economic value of grassland species for carbon storage. *Science Advances*, *3*(4), e1601880.

Hussain, T., Hussain, N., Tahir, M., Raina, A., Ikram, S., Maqbool, S., ... & Duangpan, S. (2022). Impacts of drought stress on water use efficiency and grain productivity of rice and utilization of genotypic variability to combat climate change. *Agronomy*, *12*(10), 2518.

Invasive Species in Forests and Rangelands of the United States [Chapter on ecosystem impacts of invasives]. (2021). In *Invasive Species in Forests and Rangelands of the United States* (pp. 41–55). Springer.

IPCC, 2023: Climate Change 2023: The Physical Science Basis. Contribution of Working Group I to the Sixth Assessment Report of the Intergovernmental Panel on Climate Change[Masson-Delmotte, V., P. Zhai, A. Pirani, S.L. Connors, C. Péan, S. Berger, N. Caud, Y. Chen, L. Goldfarb, M.I. Gomis, M. Huang, K. Leitzell, E. Lonnoy, J.B.R. Matthews, T.K. Maycock, T. Waterfield, O. Yelekçi, R. Yu, and B. Zhou (eds.)]. *Cambridge University Press*, Cambridge, United Kingdom and New York, NY, USA, doi:10.1017/9781009157896.

Jardine, E. C., Thomas, G. H., & Osborne, C. P. (2021). Traits explain sorting of C4 grasses along a global precipitation gradient. *Ecology and Evolution*, *11*(6), 2669-2680.

Jauregui, I., Rothwell, S. A., Taylor, S. H., Parry, M. A., Carmo-Silva, E., & Dodd, I. C. (2018). Whole plant chamber to examine sensitivity of cereal gas exchange to changes in evaporative demand. *Plant Methods*, *14*, 1-13.

Jenkins TL (2024). "mapmixture: an R package and web app for spatial visualisation of admixture and population structure." *Molecular Ecology Resources*, 24(4), e13943.

Jentsch, A., Seidl, R., Wohlgemuth, T., Burton, P. J., ... & White, P. S. (2022). Disturbances and disturbance regimes. In *Disturbance Ecology* (pp. 11–40). Cham: Springer Publishing.

Ji, W., Koh, J., Li, S., Zhu, N., Dufresne, C. P., Zhao, X., ... & Li, J. (2016). Quantitative proteomics reveals an important role of GsCBRLK in salt stress response of soybean. *Plant and Soil*, *402*, 159-178.

Jiang, F., Bennett, J. A., Crawford, K. M., Heinze, J., Pu, X., Luo, A., & Wang, Z. (2024). Global patterns and drivers of plant–microbe interactions. *Ecology Letters*, 27(1), e14364.

Jin, Y., Hao, G., Hammond, W. M., Yu, K., Liu, X., Ye, Q., ... & Wang, C. (2023). Aridity-dependent sequence of water potentials for stomatal closure and hydraulic dysfunctions in woody plants. *Global Change Biology*, *29*(7), 2030-2040.

Johansson, J., Bolmgren, K., & Jonzén, N. (2013). Climate change and the optimal flowering time of annual plants in seasonal environments. *Global change biology*, *19*(1), 197-207.

Johnson, L. A. and Tausch, R. J. (2009) 'Reproductive biology and dispersal mechanisms of *Andropogon gerardii* in the Great Plains', *Journal of Range Management*, 62(5), pp. 482-489.

Johnson, R., Stritch, L., Olwell, P., Lambert, S., Horning, M. E., & Cronn, R. (2010a). What are the best seed sources for ecosystem restoration on BLM and USFS lands? *Native Plants Journal,* 11(2), 117–131.

Johnson, N. C., Rowland, D. L., Corkidi, L., Egerton-Warburton, L. M., Allen, E. B., & Allen, M. F. (2010b). Soil communities alter comparisons of native and exotic plant growth. *Ecology*, 91(3), 703–711.

Johnson, L. C., Olsen, J. T., Tetreault, H., DeLaCruz, A., Bryant, J., Morgan, T. J., ... & Maricle, B. R. (2015). Intraspecific variation of a dominant grass and local adaptation in reciprocal garden communities along a US Great Plains' precipitation gradient: implications for grassland restoration with climate change. *Evolutionary Applications*, 8(7), 705-723.

Johnson, L. C., Galliart, M. B., Alsdurf, J. D., Maricle, B. R., Baer, S. G., Bello, N. M., ... & Smith, A. B. (2022). Reciprocal transplant gardens as gold standard to detect local adaptation in grassland species: New opportunities moving into the 21st century. *Journal of Ecology*, 110(5), 1054-1071.

Joint Genomics Institute (2023*). Andropogon gerardi* v1.1 DOE-JGI, https://phytozome-next.jgi.doe.gov/info/AgerardiHAP2_v1_1".

Jombart T (2008). "adegenet: a R package for the multivariate analysis of genetic markers." *Bioinformatics*, 24, 1403-1405.

Joshi, J., Schmid, B., Caldeira, M. C., Dimitrakopoulos, P. G., Good, J., Harris, R., ... & Lawton, J. H. (2001). Local adaptation enhances performance of common plant species. *Ecology letters*, 4(6), 536-544.

Joswig, J. S., Wirth, C., Schuman, M. C., Kattge, J., Reu, B., Wright, I. J., ... & Mahecha, M. D. (2022). Climatic and soil factors explain the two-dimensional spectrum of global plant trait variation. *Nature ecology & evolution*, *6*(1), 36-50.

Jump, A. S. and Peñuelas, J. (2005) 'Running to stand still: adaptation and the response of plants to rapid climate change', *Ecology Letters*, 8(9), pp. 1010–1020.

Jump, A. S., Marchant, R., & Peñuelas, J. (2009). Environmental change and the option value of genetic diversity. *Trends in plant science*, *14*(1), 51-58.

Kang, M., Wu, H., Liu, H., Liu, W., Zhu, M., Han, Y., ... & Liu, J. (2023). The pan-genome and local adaptation of Arabidopsis thaliana. *Nature Communications*, *14*(1), 6259.

Kawecki, T. J., & Ebert, D. (2004). Conceptual issues in local adaptation. *Ecology Letters*, 7(12), 1225–1241.

Kazarina, A., Sarkar, S., Adams, B., Vogt, B., Rodela, L., Pogranichny, S., ... & Lee, S. T. (2025). Interaction of plant-derived metabolites and rhizobiome functions enhances drought stress tolerance. *Genome Biology,* 26(1), 310.

Keeler, K., Williams, C., and Vescio, L. (2002) 'Clone size of *Andropogon gerardii* Vitman (big bluestem) at Konza Prairie, Kansas', *American Midland Naturalist*, 147(2), pp. 295–304.

Keep, T., Sampoux, J.P., Barre, P., Blanco-Pastor, J.L., Dehmer, K.J., Durand, J.L. and Volaire, F., (2021). To grow or survive: which are the strategies of a perennial grass to face severe seasonal stress?. *Functional Ecology*, 35(5), pp.1145-1158.

Kichenin, E., Wardle, D. A., Peltzer, D. A., Morse, C. W., & Freschet, G. T. (2013). Contrasting effects of plant inter-and intraspecific variation on community-level trait measures along an environmental gradient. *Functional Ecology*, 27(5), 1254-1261.

King, K. E., Cook, E. R., Anchukaitis, K. J., Cook, B. I., Smerdon, J. E., Seager, R., ... & Spei, B. (2024). Increasing prevalence of hot drought across western North America since the 16th century. *Science Advances*, *10*(4), eadj4289.

Kirwa, E. C., Njoroge, K., Cheminingâ, G. N., & Mnene, W. N. (2016). Ecological effects on the flowering phenology of Cenchrus ciliaris L. collections from the arid and semiarid lands of Kenya. *African Journal of Agricultural Research*, *11*(12), 1008-1018.

Kleyer, M., Trinogga, J., Cebrián-Piqueras, M. A., Trenkamp, A., Fløjgaard, C., Ejrnæs, R., ... & Blasius, B. (2019). Trait correlation network analysis identifies biomass allocation traits and stem specific length as hub traits in herbaceous perennial plants. *Journal of Ecology*, *107*(2), 829-842.

Knapp, A. K. (1985). Effect of fire and drought on the ecophysiology of Andropogon gerardii and Panicum virgatum in a tallgrass prairie. *Ecology*, *66*(4), 1309-1320.

Knapp, A. K., Briggs, J. M., Blair, J. M., & Turner, C. L. (1998). Patterns and controls of aboveground net primary production in tallgrass prairie. In A. K. Knapp, J. M. Briggs, D. C. Hartnett, & S. L. Collins (Eds.), Grassland dynamics: Long-term ecological research in tallgrass prairie (pp. 193–221). *Oxford University Press.*

Knapp, A. K., Fay, P. A., Blair, J. M., Collins, S. L., Smith, M. D., Carlisle, J. D., ... & McCarron, J. K. (1999). Increased rainfall variability reduces productivity and alters stability in a mesic grassland. *Science*, 298(5601), 2202–2205.

Knapp, A. K., Briggs, J. M., & Koelliker, J. K. (2001). Frequency and extent of water limitation to primary production in a mesic temperate grassland. *Ecosystems*, *4*, 19-28.

Knapp, A. K., Beier, C., Briske, D. D., Classen, A. T., Luo, Y., Reichstein, M., ... & Weng, E. (2008a). Consequences of more extreme precipitation regimes for terrestrial ecosystems. *Bioscience*, 58(9), 811-821.

Knapp, A. K., Briggs, J. M., Collins, S. L., Archer, S. R., Bret-Harte, M. S., Ewers, B. E., Peters, D. P. C., Young, D. R., Shaver, G. R., Pendall, E., & Cleary, M. B. (2008b). Shrub encroachment in North American grasslands: Shifts in growth form dominance rapidly alters control of ecosystem carbon inputs. *Global Change Biology*, 14(3), 615–623.

Knapp, A. K., Carroll, C. J., Denton, E. M., La Pierre, K. J., Collins, S. L., & Smith, M. D. (2015). Differential sensitivity to regional-scale drought in six central US grasslands. *Oecologia*, *177*, 949-957.

Knipfer, T., Bambach, N., Hernandez, M. I., Bartlett, M. K., Sinclair, G., Duong, F., ... & McElrone, A. J. (2020). Predicting stomatal closure and turgor loss in woody plants using predawn and midday water potential. *Plant Physiology*, *184*(2), 881-894.

Kolde R. (2019) Package 'pheatmap' version 1.0.12. CRAN repository R.

Konings, A. G., Williams, A. P., & Gentine, P. (2017). Sensitivity of grassland productivity to aridity controlled by stomatal and xylem regulation. *Nature Geoscience*, *10*(4), 284-288.

Kramer, D. L., Maricle, K. L., Hilt, C. J., Martin, N. M., Urban, A. D., Smart, C. M., ... & Maricle, B. R. (2018). Drought tolerance in ecotypes of big bluestem (Andropogon gerardii) relates to above-ground surface area: Results from a common garden experiment. *Flora*, *246*, 52-60.

Krishnadas, M., Sankaran, M., Page, N., Joshi, J., Machado, S., Nataraj, N., ... & Krishnamani, R. (2021). Seasonal drought regulates species distributions and assembly of tree communities across a tropical wet forest region. *Global Ecology and Biogeography*, *30*(9), 1847-1862.

Kuppler, J., Albert, C. H., Ames, G. M., Armbruster, W. S., Boenisch, G., Boucher, F. C., ... & Junker, R. R. (2020). Global gradients in intraspecific variation in vegetative and floral traits are partially associated with climate and species richness. *Global Ecology and Biogeography*, *29*(6), 992-1007.

Lait, L. A., Graham, B. A., Galbraith, D. A., Burg, T. M., & McCune, J. L. (2025). Conservation genetics of Stylophorum diphyllum (Papaveraceae): investigating the genetic diversity and

differentiation of peripheral and core populations across the range. *Conservation Genetics*, *26*(2), 249-262.

Lambert, A. M., Baer, S. G., & Gibson, D. J. (2011). Intraspecific variation in ecophysiology of three dominant prairie grasses used in restoration: cultivar versus non-cultivar population sources. *Restoration Ecology*, *19*(101), 43-52.

Langfelder P, Horvath S. (2008). WGCNA: An R Package for Weighted Correlation Network Analysis. *BMC Bioinf* 9:559.

Lasky, J. R., Josephs, E. B., & Morris, G. P. (2023). Genotype–environment associations to reveal the molecular basis of environmental adaptation. *The Plant Cell*, *35*(1), 125-138.

Lattier, J. D., Chen, H., & Contreras, R. N. (2019). Variation in genome size, ploidy, stomata, and rDNA signals in Althea. *Journal of the American Society for Horticultural Science*, 144(2), 130–140.

Lauenroth, W.K. and Adler, P.B., (2008). Demography of perennial grassland plants: survival, life expectancy and life span. *Journal of Ecology*, 96(5), pp.1023–1032.

Laughlin, D. C., Knight, T. M., & St. Clair, J. B. (2020a). Plant functional traits and the management of vegetation in a changing world. *Plant Ecology, 221*(1), 55–65.

Laughlin, D. C., Gremer, J. R., Adler, P. B., Mitchell, R. M., & Moore, M. M. (2020b). The net effect of functional traits on fitness. *Trends in Ecology & Evolution, 35*(12), 1037–1047.

Le, V. H., Collins, S. L., & Vargas, R. (2025). Long-term ecological studies must continue: insights from a dryland transition zone. *Oecologia*, *207*(11), 1-12.

Le Corre, V., & Kremer, A. (2012). The genetic differentiation at quantitative trait loci under local adaptation. *Molecular ecology*, *21*(7), 1548-1566.

Ledo, A., Trnka, M., & Hlavinka, P. (2018). Impacts of drought on biomass production and water-use efficiency in different grassland ecosystems. *Agricultural and Forest Meteorology, 250*, 235-245.

Leimu, R., & Fischer, M. (2008). A meta-analysis of local adaptation in plants. *PLoS ONE,* 3(12), e4010.

Lesica, P. and Allendorf, F.W., (1995). When are peripheral populations valuable for conservation? *Conservation Biology*, 9, pp.753–760.

Less, H., Angelovici, R., Tzin, V., & Galili, G. (2011). Coordinated gene networks regulating Arabidopsis plant metabolism in response to various stresses and nutritional cues. *The Plant Cell*, *23*(4), 1264-1271.

Li, W., & Godzik, A. (2006). Cd-hit: a fast program for clustering and comparing large sets of protein or nucleotide sequences. *Bioinformatics*, *22*(13), 1658-1659.

Li, Y., Wang, R., & Zhang, X. (2017). Climate-driven clines in plant functional traits across spatial gradients. *Ecography*, 40(10), 1189–1199.

Li, D., Wu, S., Liu, L., Zhang, Y., & Li, S. (2018). Vulnerability of the global terrestrial ecosystems to climate change. *Global change biology*, *24*(9), 4095-4106.

Linhart, Y. B., & Grant, M. C. (1996). Evolutionary significance of local genetic differentiation in plants. *Annual review of ecology and systematics*, *27*(1), 237-277.

Liu, Y., Fan, B., Gong, Z., He, L., Chen, L., Ren, A., ... & Gao, Y. (2023). Intraspecific trait variation and adaptability of Stipa krylovii: Insight from a common garden experiment with two soil moisture treatments. *Ecology and Evolution*, *13*(9).

López, A. S., López, D. R., Caballé, G., Siffredi, G. L., & Marchelli, P. (2020). Local adaptation along a sharp rainfall gradient occurs in a native Patagonian grass, Festuca pallescens, regardless of extensive gene flow. *Environmental and Experimental Botany*, *171*, 103933.

López-Goldar, X., & Agrawal, A. A. (2021). Ecological interactions, environmental gradients, and gene flow in local adaptation. *Trends in Plant Science*, *26*(8), 796-809.

Lortie, C. J., & Hierro, J. L. (2022). A synthesis of local adaptation to climate through reciprocal common gardens. *Journal of Ecology*, *110*(5), 1015-1021.

Love, M. I., Huber, W., & Anders, S. (2014). Moderated estimation of fold change and dispersion for RNA-seq data with DESeq2. *Genome biology*, *15*(12), 550.

Loveless, M. D., & Hamrick, J. L. (1984). Ecological determinants of genetic structure in plant populations. *Annual review of ecology and systematics*, 65-95.

Lovell, J. T., Mullen, J. L., Lowry, D. B., Awole, K., Richards, J. H., Sen, S., ... & McKay, J. K. (2015). Exploiting differential gene expression and epistasis to discover candidate genes for drought-associated QTLs in Arabidopsis thaliana. *The Plant Cell*, *27*(4), 969-983.

Lovell, J. T., Schwartz, S., Lowry, D. B., Shakirov, E. V., Bonnette, J. E., Weng, X., ... & Juenger, T. E. (2016). Drought responsive gene expression regulatory divergence between upland and lowland ecotypes of a perennial C4 grass. *Genome research*, *26*(4), 510-518.

Lovell, J. T., Jenkins, J., Lowry, D. B., Mamidi, S., Sreedasyam, A., Weng, X., ... & Juenger, T. E. (2018). The genomic landscape of molecular responses to natural drought stress in Panicum hallii. *Nature communications*, *9*(1), 5213.

Lovell, J. T., MacQueen, A. H., Mamidi, S., Bonnette, J., Jenkins, J., Napier, J. D., ... & Juenger, T. E. (2021). Genomic mechanisms of climate adaptation in polyploid bioenergy switchgrass. *Nature*, 590(7846), 438–444.

Lowry, D. B., Behrman, K. D., Grabowski, P., Morris, G. P., Kiniry, J. R., & Juenger, T. E. (2014). Adaptations between ecotypes and along environmental gradients in Panicum virgatum. *The American Naturalist*, *183*(5), 682-692.

Lowry, D. B., Hernandez, K., Taylor, S. H., Meyer, E., Logan, T. L., Barry, K. W., ... & Juenger, T. E. (2015). The genetics of divergence and reproductive isolation between ecotypes of Panicum hallii. *New Phytologist*, *205*(1), 402-414.

Lowry, D. B., ., Hernandez, K., Taylor, S. H., Meyer, E., Logan, T. L., Barry, K. W., ... & Juenger, T. E. (2019). QTL × environment interactions underlie adaptive divergence in switchgrass across 17° latitude. *PNAS*, 116(21), 9095–9100.

Luo, W., Griffin-Nolan, R. J., Song, L., Te, N., Chen, J., Shi, Y., ... & Collins, S. L. (2023). Interspecific and intraspecific trait variability differentially affect community-weighted trait responses to and recovery from long-term drought. *Functional Ecology*, *37*(3), 504-512.

Lynn, J. S., Kazenel, M. R., Kivlin, S. N., & Rudgers, J. A. (2019). Context-dependent biotic interactions control plant abundance across altitudinal environmental gradients. *Ecography*, *42*(9), 1600-1612.

Ma, J. G., Yu, J. F., & Wang, X. B. (2025). Relationships between plant trait and environment and microbe vary across plant resource strategies. *Plant and Soil*, 1-16.

Maitner, B., & Maitner, M. B. (2020). Package 'BIEN'.

Makishima, D., Sutou, R., Goto, A., Kawai, Y., Ishii, N., Taniguchi, H., ... & Sasaki, T. (2021). Potential extinction debt due to habitat loss and fragmentation in subalpine moorland ecosystems. *Plant Ecology*, *222*, 445-457.

Marinho, R. C., Mendes-Rodrigues, C., Bonetti, A. M., & Oliveira, P. E. (2021). Stomatal size, ploidy and polyembryony in Eriotheca Stellate Trichome Species Complex (Bombacoideae–Malvaceae) in the Cerrados of Brazil. *Plant Biology*, 23(1), 91–99.

Marks, C. O., & Lechowicz, M. J. (2006). Alternative designs and the evolution of functional diversity. *The American Naturalist, 167*(1), 55–66.

Martínez-Sagarra, G., Castro, S., Mota, L., Loureiro, J., & Devesa, J. A. (2021). Genome size, chromosome number and morphological data reveal unexpected infraspecific variability in Festuca (Poaceae). *Genes*, 12(6), 906.

Matesanz, S., & Ramírez-Valiente, J. A. (2019). A review and meta-analysis of intraspecific differences in phenotypic plasticity: Implications to forecast plant responses to climate change. *Global Ecology and Biogeography*, *28*(11), 1682-1694.

Matos, I. S., Eller, C. B., Oliveras, I., Mantuano, D., & Rosado, B. H. (2021). Three eco-physiological strategies of response to drought maintain the form and function of a tropical montane grassland. *Journal of Ecology*, *109*(1), 327-341.

McAllister, C., Blaine, R., Kron, P., Bennett, B., Garrett, H., Kidson, J., ... & Miller, A. J. (2015). Environmental correlates of cytotype distribution in Andropogon gerardii (Poaceae). *American Journal of Botany*, 102(1), 92–102.

McCain, K. N., Baer, S. G., Blair, J. M., & Wilson, G. W. (2010). Dominant grasses suppress local diversity in restored tallgrass prairie. *Restoration Ecology*, *18*, 40-49.

McGill, B. J., Enquist, B. J., Weiher, E., & Westoby, M. (2006). Rebuilding community ecology from functional traits. *Trends in Ecology & Evolution, 21*(4), 178–185.

McIntyre, P. J., & Strauss, S. (2017). An experimental test of local adaptation among cytotypes within a polyploid complex. *Evolution*, 71(8), 1960–1969.

McMillan, C. (1956). Nature of the plant community. II. Variation in flowering behavior within populations of Andropogon scoparius. *American Journal of Botany*, 429-436.

McMillan, C. (1961). Nature of the plant community. VI. Texas grassland communities under transplanted conditions. *American Journal of Botany*, *48*(9), 778-785.

McMillan, C. (1965). Ecotypic differentiation within four North American prairie grasses. II. Behavioral variation within transplanted community fractions. *American Journal of Botany*, *52*(1), 55-65.

McMillan, C. (1969). Ecotypes and ecosystem function. *BioScience*, 19(2), 131-134.

Mendola, M. L., Baer, S. G., Johnson, L. C., & Maricle, B. R. (2015). The role of ecotypic variation and the environment on biomass and nitrogen in a dominant prairie grass. *Ecology*, *96*(9), 2433-2445.

Meier, I. C., & Leuschner, C. (2008). Belowground drought response of European beech: fine root biomass and carbon partitioning in 14 mature stands across a precipitation gradient. *Global Change Biology*, *14*(9), 2081-2095.

Messier, J., Lechowicz, M. J., McGill, B. J., Violle, C., & Enquist, B. J. (2017). Interspecific integration of trait dimensions at local scales: The plant phenotype as an integrated network. *Journal of Ecology, 105*(6), 1775–1790.

Metz, J., & Tielbörger, K. (2023). A drought year favored drier-adapted origins over local origins in a reciprocal transplant experiment along a rainfall gradient. *Oikos*, *2023*(11), e09806.

Meyer, E., Aspinwall, M. J., Lowry, D. B., Palacio-Mejía, J. D., Logan, T. L., Fay, P. A., & Juenger, T. E. (2014). Integrating transcriptional, metabolomic, and physiological responses to drought stress and recovery in switchgrass (Panicum virgatum L.). *BMC genomics*, *15*(1), 527.

Mganga, K. Z., Kuhla, J., Carminati, A., Pausch, J., & Ahmed, M. A. (2023). Leaf gas exchange characteristics, biomass partitioning, and water use efficiencies of two C4 African grasses under simulated drought. *Grassland Research*, *2*(1), 37-45.

Mijangos, J. L., & Koo, H. (2021). Population size and connectivity affect genetic diversity and structure in fragmented plant populations. *Molecular Ecology*, 30(5), 1195–1210

Mitchell-Olds, T., Willis, J. H., & Goldstein, D. B. (2007). Which evolutionary processes influence natural genetic variation for phenotypic traits?. *Nature Reviews Genetics*, 8(11), 845-856.

Moran, E. V., Hartig, F., & Bell, D. M. (2016). Intraspecific trait variation across scales: implications for understanding global change responses. *Global Change Biology*, *22*(1), 137-150.

Moore, K. J., Collins, M., Nelson, C. J., & Redfearn, D. D. (Eds.). (2020). *Forages, Volume 2: The science of grassland agriculture*. John Wiley & Sons.

Moles, A. T., Warton, D. I., Warman, L., Swenson, N. G., Laffan, S. W., Zanne, A. E., ... & Leishman, M. R. (2009). Global patterns in plant height. *Journal of ecology*, *97*(5), 923-932.

Moran, E. V., Hartig, F., & Bell, D. M. (2016). Intraspecific trait variation across scales: implications for understanding global change responses. *Global Change Biology*, 22(1), 137-150.

Munson, S. M., & Long, A. L. (2017). Climate drives shifts in grass reproductive phenology across the western USA. *New Phytologist, 213*(4), 1945–1955.

Münzbergová, Z., Hadincová, V., Skálová, H., & Vandvik, V. (2017). Genetic differentiation and plasticity interact along temperature and precipitation gradients to determine plant performance under climate change. *Journal of Ecology*, *105*(5), 1358-1373.

Nadeau, C. P., & Urban, M. C. (2019). Eco-evolution on the edge during climate change. *Ecography*, *42*(7), 1280-1297.

Napier, J. D., Heckman, R. W., & Juenger, T. E. (2023). Gene-by-environment interactions in plants: Molecular mechanisms, environmental drivers, and adaptive plasticity. *The Plant Cell*, *35*(1), 109-124.

Ni, Z., Liu, N., Yu, Y., Bi, C., Chen, Q., & Qu, Y. (2021). The cotton 70-kDa heat shock protein GhHSP70-26 plays a positive role in the drought stress response. *Environmental and Experimental Botany*, *191*, 104628.

Nicotra, A. B., Atkin, O. K., Bonser, S. P., Davidson, A. M., Finnegan, E. J., Mathesius, U., ... & van Kleunen, M. (2010). Plant phenotypic plasticity in a changing climate. *Trends in plant science*, *15*(12), 684-692.

Niinemets, Ü. (2007). Photosynthesis and resource distribution through plant canopies. *Plant, Cell & Environment, 30*(3), 105–125.

Nilsson, O. (2013). A pathway to flowering—why staying cool matters. *Science*, *342*(6158), 566-567.

Nippert, J. B., Knapp, A. K., & Briggs, J. M. (2006). Intra-annual rainfall variability and grassland productivity: can the past predict the future?. *Plant Ecology*, *184*, 65-74.

Nomoto, H. A., & Alexander, J. M. (2021). Drivers of local extinction risk in alpine plants under warming climate. *Ecology Letters*, *24*(6), 1157-1166.

Nunes, T. D., Slawinska, M. W., Lindner, H., & Raissig, M. T. (2022). Quantitative effects of environmental variation on stomatal anatomy and gas exchange in a grass model. *Quantitative Plant Biology*, *3*, e6.

Ochola, C. A., Ngugi, M. P., Nyaboga, E. N., & Njarui, D. M. (2024). Morpho-physiological and yield traits for selection of drought tolerant Urochloa grass ecotypes. *AoB Plants*, *16*(3), plae034.

Ohdo, T., & Takahashi, K. (2020). Plant species richness and community assembly along gradients of elevation and soil nitrogen availability. *AoB Plants*, *12*(3), plaa014.

Oksanen, J., Blanchet, F.G., Kindt, R., Legendre, P., O'Hara, R.B., Simpson, G.L., Solymos, P., Henry, M., Stevens, H. and Wagner, H., (2010). Package 'vegan'. Community ecology package. *Sustainability.*

Oppido, S., Ragozino, S., & Esposito De Vita, G. (2023). Peripheral, Marginal, or Non-Core Areas? Setting the Context to Deal with Territorial Inequalities through a Systematic Literature Review. *Sustainability*, *15*(13), 10401.

Osborne, O. G., Kafle, T., Brewer, T., Dobreva, M. P., Hutton, I., & Savolainen, V. (2020). Sympatric speciation in mountain roses (Metrosideros) on an oceanic island. *Philosophical Transactions of the Royal Society B*, *375*(1806), 20190542.

Osmolovsky, I., Shifrin, M., Gamliel, I., Belmaker, J., & Sapir, Y. (2022). Eco-geography and phenology are the major drivers of reproductive isolation in the royal irises, a species complex in the course of speciation. *Plants*, *11*(23), 3306.

Osnato, M., Cota, I., Nebhnani, P., Cereijo, U., & Pelaz, S. (2022). Photoperiod control of plant growth: flowering time genes beyond flowering. *Frontiers in plant science*, *12*, 805635.

Parker, T. C., Unger, S. L., Moody, M. L., Tang, J., & Fetcher, N. (2021). Intraspecific variation in phenology offers resilience to climate change for Eriophorum vaginatum. *Arctic Science*, *8*(3), 935-951.

Parmesan, C., & Hanley, M. E. (2015). Plants and climate change: complexities and surprises. *Annals of botany*, *116*(6), 849-864.

Panter, C. T., Kambach, S., Bachman, S. P., Baines, O., Bruelheide, H., Sporbert, M., ... & Schrodt, F. (2025). Plants with higher dispersal capabilities follow ‘abundant-centre’distributions but such patterns remain rare in animals. *Nature Communications*, *16*(1), 8205.

Pardo, J., Man Wai, C., Chay, H., Madden, C. F., Hilhorst, H. W., Farrant, J. M., & VanBuren, R. (2020). Intertwined signatures of desiccation and drought tolerance in grasses. *Proceedings of the National Academy of Sciences*, *117*(18), 10079-10088.

Pattnaik, S., Mohapatra, B., & Gupta, A. (2021). Plant growth-promoting microbe mediated uptake of essential nutrients (Fe, P, K) for crop stress management: Microbe–soil–plant continuum. *Frontiers in Agronomy*, 3, 689972.

Pavlíková, Z., Holá, D., Vlasáková, B., Procházka, T., & Münzbergová, Z. (2017). Physiological and fitness differences between cytotypes vary with stress in a grassland perennial herb. *PLoS ONE*, 12(11), e0188795.

Penfield, S., & MacGregor, D. R. (2017). Effects of environmental variation during seed production on seed dormancy and germination. *Journal of Experimental Botany, 68*(4), 819–825.

Pennington, L. K., Slatyer, R. A., Ruiz-Ramos, D. V., Veloz, S. D., & Sexton, J. P. (2021). How is adaptive potential distributed within species ranges?. *Evolution*, *75*(9), 2152-2166.

Perret, D.L. and Sax, D.F. (2022). Evaluating a study design for optimal sampling of species' climatic niches. *Ecography* 2022:e06014.

Petermann, J. S., & Buzhdygan, O. Y. (2021). Grassland biodiversity. *Current Biology*, 31(19), R1195-R1201.

Piao, S., Liu, Q., Chen, A., Janssens, I. A., Fu, Y., Dai, J., ... & Zhu, X. (2019). Plant phenology and global climate change: Current progresses and challenges. *Global change biology*, *25*(6), 1922-1940.

Pierce, S., Brusa, G. and Dainese, M. (2019) 'Microclimatic drivers of trait variability in alpine plant species', *Functional Ecology*, 33(9), pp. 1653–1664.

Pironon, S., Papuga, G., Villellas, J., Angert, A. L., García, M. B., & Thompson, J. D. (2017). Geographic variation in genetic and demographic performance: new insights from an old biogeographical paradigm. *Biological Reviews*, *92*(4), 1877-1909.

Pfeifer, B., Wittelsbürger, U., Ramos-Onsins, S. E., & Lercher, M. J. (2014). PopGenome: an efficient Swiss army knife for population genomic analyses in R. *Molecular biology and evolution*, *31*(7), 1929-1936.

Poland, J. A., & Rife, T. W. (2012). Genotyping-by-sequencing for plant breeding and genetics. *The plant genome*, *5*(3).

Prakash, A., Capblancq, T., Shallows, K., Saville, D., Landau, D., Landress, C., ... & Keller, S. (2024). Bringing genomics to the field: An integrative approach to seed sourcing for forest restoration. *Applications in Plant Sciences*, 12(3), e11600.

Prober, S. M., Byrne, M., McLean, E. H., Steane, D. A., Potts, B. M., Vaillancourt, R. E., & Stock, W. D. (2015). Climate-adjusted provenancing: A strategy for climate-resilient ecological restoration. *Frontiers in Ecology and Evolution*, 3, 65.

Puglielli, G., Laanisto, L., Poorter, H., & Niinemets, Ü. (2021). Global patterns of biomass allocation in woody species with different tolerances of shade and drought: evidence for multiple strategies. *New Phytologist*, *229*(1), 308-322.

R Core Team (2024) *R*: A language and environment for statistical computing. Vienna, Austria: R *Foundation for Statistical Computing.*

Raffard, A., Lecerf, A., Cote, J., Buoro, M., Lassus, R., & Cucherousset, J. (2017). The functional syndrome: linking individual trait variability to ecosystem functioning. *Proceedings of the Royal Society B: Biological Sciences*, *284*(1868), 20171893.

Rahman, M. A., Woo, J. H., Song, Y., Lee, S. H., Hasan, M. M., Azad, M. A. K., & Lee, K. W. (2022). Heat shock proteins and antioxidant genes involved in heat combined with drought stress responses in perennial rye grass. *Life*, *12*(9), 1426.

Räikkönen, J. Jones, E., & Mayer, l. (2017) 'Adaptive potential of peripheral populations in the face of climate change', *Ecology and Evolution*, 7(12), pp. 4361–4374.

Ramírez-Valiente, J. A., Santos del Blanco, L., Alía, R., Robledo-Arnuncio, J. J., & Climent, J. (2022). Adaptation of Mediterranean forest species to climate: Lessons from common garden experiments. *Journal of Ecology*, *110*(5), 1022-1042.

Recommended chemical soil test procedures for the North Central Region, University of Missouri Agricultural Experiment Station (1998) *Recommended chemical soil test procedures for the North Central Region*, North Central Regional Publication No. 221 (Revised). Columbia, MO: University of Missouri.

Rellstab, C., Dauphin, B., & Exposito-Alonso, M. (2021). Prospects and limitations of genomic offset in conservation management. *Evolutionary Applications*, *14*(5), 1202-1212.

Ren, Z., Gibson, D. F., Baer, S. G., Johnson, L., & Wilson, L. E. (2021). Grassland restoration reveals the importance of ecotypic variation on community assembly along a longitudinal aridity gradient. *ScienceOpen Posters*.

Ren, Z., Baer, S. G., Johnson, L. C., Galliart, M. B., Wilson, L. R., & Gibson, D. J. (2023). The role of dominant prairie species ecotypes on plant diversity patterns of restored grasslands across a rainfall gradient in the US Great Plains. *Applied Vegetation Science*, *26*(2), e12725.

Ren, Z., Baer, S. G., Johnson, L. C., Galliart, M. B., & Gibson, D. J. (2024). Effects of Manipulated Rainfall and Intraspecific Variation Within Dominant Species on Community Assembly: Insights From a Long-Term Grassland Restoration Experiment. *Ecology and Evolution*, *14*(11), e70571.

Reynolds, H. L., Packer, A., Bever, J. D., & Clay, K. (2003). Grassroots ecology: Plant–microbe–soil interactions as drivers of plant community structure and dynamics. *Ecology*, 84(9), 2281–2291.

Riesch, R., Plath, M., & Bierbach, D. (2018). Ecology and evolution along environmental gradients. *Current Zoology*, *64*(2), 193-196.

Rippey, B. R. (2015). The US drought of 2012. *Weather and climate extremes*, *10*, 57-64.

Robinson, A., Lehmann, J., Barriopedro, D., Rahmstorf, S., & Coumou, D. (2021). Increasing heat and rainfall extremes now far outside the historical climate. *NPJ Climate and Atmospheric Science*, *4*(1), 45.

Rogler, G. A. (1944). Relative payabilities of grasses under cultivation on the northern Great Plains. *Journal of the American Society of Agronomy*. 35, 547-559.

Roop, S. R., Reinhardt, K., Aho, K., Germino, M. J., & Richardson, B. A. (2025). Cytotype and local adaptation drive phenotypic variation in two subspecies of big sagebrush (Artemisia tridentata). *Ecosphere*, 16(3), e70206.

Rosbakh, S., Hartig, F., Sandanov, D. V., Bukharova, E. V., Miller, T. K., & Primack, R. B. (2021). Siberian plants shift their phenology in response to climate change. *Global Change Biology*, *27*(18), 4435-4448.

Rúa, M. A., Godoy, O., & Hawkins, B. A. (2016). Home-field advantage? Evidence of local adaptation among mycorrhizal symbioses. *BMC Evolutionary Biology*, 16(1), 1–11.

Rueda, M., Godoy, O., & Hawkins, B. A. (2018). Trait syndromes among North American trees are evolutionarily conserved and show adaptive value over broad geographic scales. *Ecography*, *41*(3), 540-550.

Sagarin, R. D., & Gaines, S. D. (2002). The "abundant center" distribution: To what extent is it a biogeographical rule? *Ecology Letters*, 5(1), 137–147.

Sagarin, R.D., Gaines, S.D. and Gaylord, B. (2006) 'Moving beyond assumptions to understand abundance distributions across the ranges of species', *Trends in Ecology & Evolution*, 21(9), pp. 524–530.

Samson, F., & Knopf, F. (1994). Prairie conservation in north america. *BioScience*, *44*(6), 418-421.

Savolainen, O., Pyhäjärvi, T., & Knürr, T. (2007). Gene flow and local adaptation in trees. *Annu. Rev. Ecol. Evol. Syst.*, *38*(1), 595-619.

Savolainen, O., Lascoux, M., & Merilä, J. (2013). Ecological genomics of local adaptation. *Nature Reviews Genetics,* 14(11), 807–820.

Sayols S (2023). "rrvgo: a Bioconductor package to reduce and visualize Gene Ontology terms." *Micropublication Biology*.

Schuchardt, M. A., Berauer, B. J., von Heßberg, A., Wilfahrt, P., & Jentsch, A. (2021). Drought effects on montane grasslands nullify benefits of advanced flowering phenology due to warming. *Ecosphere*, *12*(7), e03661.

Schwinning, S., Lortie, C. J., Esque, T. C., & DeFalco, L. A. (2022). What common-garden experiments tell us about climate responses in plants. *Journal of Ecology*, *110*(5), 986-996.

Seleiman, M. F., Al-Suhaibani, N., Ali, N., Akmal, M., Alotaibi, M., Refay, Y., ... & Battaglia, M. L. (2021). Drought stress impacts on plants and different approaches to alleviate its adverse effects. *Plants*, *10*(2), 259.

Serin, E. A., Nijveen, H., Hilhorst, H. W., & Ligterink, W. (2016). Learning from co-expression networks: possibilities and challenges. *Frontiers in plant science*, *7*, 185898.

Sexton, J. P., McIntyre, P. J., Angert, A. L., & Rice, K. J. (2009). Evolution and ecology of species range limits. Annual Review of Ecology, Evolution, and Systematics, 40, 415–436.

Sexton, J.P., Strauss, S.Y. and Rice, K.J. (2011) 'Gene flow increases fitness at the warm edge of a species 'range', *Proceedings of the National Academy of Sciences*, 108(28), pp. 11704–11709.

Sexton, J. P., Hufford, M. B., C. Bateman, A., Lowry, D. B., Meimberg, H., Strauss, S. Y., & Rice, K. J. (2016). Climate structures genetic variation across a species' elevation range: A test of range limits hypotheses. *Molecular ecology*, *25*(4), 911-928.

Shah, S. H., Islam, S., Mohammad, F., & Siddiqui, M. H. (2023). Gibberellic acid: A versatile regulator of plant growth, development and stress responses. *Journal of Plant Growth Regulation*, *42*(12), 7352-7373.

Shi, J., Joshi, J., Tielbörger, K., Verhoeven, K. J., & Macel, M. (2018). Costs and benefits of admixture between foreign genotypes and local populations in the field. *Ecology and Evolution*, *8*(7), 3675-3684.

Shavrukov, Y., Kurishbayev, A., Jatayev, S., Shvidchenko, V., Zotova, L., Koekemoer, F., ... & Langridge, P. (2017). Early flowering as a drought escape mechanism in plants: how can it aid wheat production?. *Frontiers in plant science*, *8*, 1950.

Shaw, R.E., Farquharson, K.A., Bruford, M.W., Coates, D.J., Elliott, C.P., Mergeay, J., (2025). Global meta-analysis shows action is needed to halt genetic diversity loss. *Nature*, pp.1-7.

Sheth, S.N., Morueta-Holme, N. & Angert, A.L., (2020). Determinants of geographic range size in plants. *New Phytologist*, 226(3), pp.650-665.

Shrestha, N., Hu, H., Shrestha, K., & Doust, A. N. (2023). Pearl millet response to drought: A review. *Frontiers in Plant Science*, *14*, 1059574.

Siefert, A., Violle, C., Chalmandrier, L., Albert, C. H., Taudiere, A., Fajardo, A., … Wardle, D. A. (2015). A global meta-analysis of the relative extent of intraspecific trait variation in plant communities. *Ecology Letters*, 18(12), 1406–1419.

Siepielski, A. M., Morrissey, M. B., Buoro, M., Carlson, S. M., Caruso, C. M., Clegg, S. M., ... & MacColl, A. D. (2017). Precipitation drives global variation in natural selection. *Science*, 355(6328), 959-962.

Silletti, A., & Knapp, A. (2002). Long-term responses of the grassland co-dominants Andropogon gerardii and Sorghastrum nutans to changes in climate and management. *Plant Ecology,* 163(1), 15-22.

Simão, F. A., Waterhouse, R. M., Ioannidis, P., Kriventseva, E. V., & Zdobnov, E. M. (2015). BUSCO: assessing genome assembly and annotation completeness with single-copy orthologs. *Bioinformatics*, *31*(19), 3210-3212.

Sinnott-Armstrong, M. A., Deanna, R., Pretz, C., Liu, S., Harris, J. C., Dunbar-Wallis, A., ... & Wheeler, L. C. (2022). How to approach the study of syndromes in macroevolution and ecology. *Ecology and Evolution*, *12*(3), e8583.

Slette, I. J., Hoover, D. L., Smith, M. D., & Knapp, A. K. (2023). Repeated extreme droughts decrease root production, but not the potential for post-drought recovery of root production, in a mesic grassland. *Oikos*, *2023*(1), e08899.

Smith, A. B., Alsdurf, J., Knapp, M., Baer, S. G., & Johnson, L. C. (2017). Phenotypic distribution models corroborate species distribution models: A shift in the role and prevalence of a dominant prairie grass in response to climate change. *Global Change Biology*, 23(10), 4365-4375.

Smith, M. D., & Knapp, A. K. (1999). Exotic plant species in a C4-dominated grassland: invasibility, disturbance, and community structure. *Oecologia*, *120*(4), 605-612.

Smith, M. D., Knapp, A. K., & Collins, S. L. (2009). A framework for assessing ecosystem dynamics in response to chronic resource alterations induced by global change. *Ecology*, *90*(12), 3279-3289.

Smith, M. D., Wilkins, K. D., Holdrege, M. C., Wilfahrt, P., Collins, S. L., Knapp, A. K., ... & Sun, W. (2024). Extreme drought impacts have been underestimated in grasslands and shrublands globally. *Proceedings of the National Academy of Sciences*, *121*(4), e2309881120.

Smith, N. E., Kooijmans, L. M., Koren, G., Van Schaik, E., van Der Woude, A. M., Wanders, N., ... & Peters, W. (2020). Spring enhancement and summer reduction in carbon uptake during the 2018 drought in northwestern Europe. *Philosophical Transactions of the Royal Society B*, *375*(1810), 20190509.

Solarik, K. A., Messier, C., Ouimet, R., Bergeron, Y., & Gravel, D. (2018). Local adaptation of trees at the range margins impacts range shifts in the face of climate change. *Global Ecology and Biogeography*, *27*(12), 1507-1519.

Soliani, C., Azpilicueta, M.M., Arana, M.V. & Marchelli, P., (2020). Clinal variation along precipitation gradients in Patagonian temperate forests: unravelling demographic and selection signatures in three *Nothofagus* spp. *Annals of Forest Science*, 77, pp.1-17.

Soliani, C., Mattera, M. G., Marchelli, P., Azpilicueta, M. M., & Dalla-Salda, G. (2021). Different drought-adaptive capacity of a native Patagonian tree species (Nothofagus pumilio) resulting from local adaptation. *European Journal of Forest Research*, *140*(5), 1147-1161.

Soma, F., Takahashi, F., Yamaguchi-Shinozaki, K., & Shinozaki, K. (2021). Cellular phosphorylation signaling and gene expression in drought stress responses: ABA-dependent and ABA-independent regulatory systems. *Plants*, *10*(4), 756.

Song, W. H., & Li, J. J. (2023). The effects of intraspecific variation on forecasts of species range shifts under climate change. *Science of The Total Environment*, *857*, 159513.

Song, B., Ning, W., Wei, D., Jiang, M., Zhu, K., Wang, X., ... & Cheng, S. (2023). Plant genome resequencing and population genomics: Current status and future prospects. *Molecular Plant*, *16*(8), 1252-1268.

Song, J., Henry, H. A., & Tian, L. (2019). Brachypodium histone deacetylase BdHD1 positively regulates ABA and drought stress responses. *Plant science*, *283*, 355-365.

Sork, V. L. (2018). Genomic studies of local adaptation in natural plant populations. *Journal of Heredity*, *109*(1), 3-15.

Sporbert, M., Keil, P., Seidler, G., Bruelheide, H., Jandt, U., Aćić, S., et al., (2020). Testing macroecological abundance patterns: The relationship between local abundance and range size, range position and climatic suitability among European vascular plants. *Journal of Biogeography*, 47(10), pp.2210-2222.

Stevens, N., Bond, W., Feurdean, A., & Lehmann, C. E. R. (2022). Grassy ecosystems in the Anthropocene. *Annual Review of Environment and Resources,* 47, 261–289.

Stotz, G.C., Salgado-Luarte, C., Escobedo, V.M., Valladares, F. & Gianoli, E., (2021). Global trends in phenotypic plasticity of plants. *Ecology Letters*, 24(10), pp.2267-2281.

Stronen, A. V., Norman, A. J., Vander Wal, E., & Paquet, P. C. (2022). The relevance of genetic structure in ecotype designation and conservation management. *Evolutionary applications*, *15*(2), 185-202.

Stroud, J. T., & Ratcliff, W. C. (2025). Long-term studies provide unique insights into evolution. *Nature*, *639*(8055), 589-601.

Sun, W. (2024). Extreme drought impacts have been underestimated in grasslands and shrublands globally. *Proceedings of the National Academy of Sciences*, *121*(4), e2309881120.

Supek, F., Bošnjak, M., Škunca, N., & Šmuc, T. (2011). REVIGO summarizes and visualizes long lists of gene ontology terms. *PLOS ONE, 6*(7), e21800.

Swaminathan, K., Alabady, M. S., Varala, K., De Paoli, E., Ho, I., Rokhsar, D. S., ... & Hudson, M. E. (2010). Genomic and small RNA sequencing of Miscanthus× giganteus shows the utility of sorghum as a reference genome sequence for Andropogoneae grasses. *Genome biology*, *11*, 1-18.

Swemmer, A. M., Knapp, A. K., & Smith, M. D. (2006). Growth responses of two dominant C4 grass species to altered water availability. *International Journal of Plant Sciences,* 167(5), 1001-1010.

Sytsma, J., & Ricker, R., Winters, H., Maricle, B., Patterson, R., Fogarty, K., & Johnson, L., (in press). Stomatal Architecture and Gas Exchange in a Dominant Prairie Grass *Andropogon gerardi* Sourced from Across Broad Climatic Gradients: Intraspecific Variation of Populations and Adaptive Responses to Drought. *American Journal of Botany.*

Sytsma, J., Galliart, M., Gibson, D.J., Hartung, E., Maricle, B., & Johnson, L., (in press). Adaptive Alleles on the Prairie: Genomic Insights for a Warming World. *The Routledge Handbook of Grasslands.*

Sytsma, J., Galliart, M., Fogarty. K., Howe, K., Olson, B., Baer, S., Gibson, D.J., Hartung, E., & Johnson, L., (in review). Taking genomics outdoors in the Great Plains: Linking trait variation and gene expression of perennial grass ecotypes in prairies across a precipitation gradient. *Molecular Ecology.*

Sytsma, J., Winters, H., Galliart, M., Smith, A., Louthan, A. M., Newmann, E., & Johnson, L., (in review). Abundance, functional traits, and genetic patterns of a dominant grass across its wide native range: A case study testing core vs. margin paradigms to identify potential sources of climate adaptation. *Ecography.*

Taleb, M. H., Majidi, M. M., Pirnajmedin, F., & Maibody, S. A. M. M. (2023). Plant functional trait responses to cope with drought in seven cool-season grasses. *Scientific Reports*, *13*(1), 5285.

Tamayo, P.R., Weiss, O. & Sánchez-Moreiras, A.M., (2001). Gas exchange techniques in photosynthesis and respiration infrared gas analyser. In: *Handbook of Plant Ecophysiology Techniques*, pp.113-139. Dordrecht: Springer Netherlands.

Tardella, F. M., Piermarteri, K., Malatesta, L., & Catorci, A. (2016). Environmental gradients and grassland trait variation: insight into the effects of climate change. *Acta Oecologica*, *76*, 47-60.

Tardieu F., (2022). "Different avenues for progress apply to drought tolerance, water use efficiency and yield in dry areas." *Current Opinion in Biotechnology* 73: 128-134.

Taylor, S. H., Ripley, B. S., Martin, T., De-Wet, L. A., Woodward, F. I., & Osborne, C. P. (2014). Physiological advantages of C_4 grasses in the field: A comparative experiment demonstrating the importance of drought. Global Change Biology, 20(6), 1992–2003.

Tero, N., Aspi, J., Siikamäki, P., Jäkäläniemi, A., & Tuomi, J. (2003). Genetic structure and gene flow in a metapopulation of an endangered plant species, Silene tatarica. *Molecular ecology*, *12*(8), 2073-2085.

Thomas, H. (2022). Drought resistance in plants. In *Mechanisms of environmental stress resistance in plants* (pp. 1-42). Routledge.

Tian, J., Guo, S., Deng, L., Yin, J., Pan, Z., He, S., & Li, Q. (2021). Adaptive optimal allocation of water resources response to future water availability and water demand in the Han River basin, China. *Scientific Reports*, *11*(1), 7879.

Tilman, D., & El Haddi, A. (1992). Drought and biodiversity in grasslands. *Oecologia*, 89(2), 257-264.

Török, K., Valkó, O., & Deák, B. (2024). Ecosystem restoration with local or broad seed provenancing: Debates and perceptions in science and practice. *Biological Conservation*, *293*, 110535.

Trono, D., & Pecchioni, N. (2022). Candidate genes associated with abiotic stress response in plants as tools to engineer tolerance to drought, salinity and extreme temperatures in wheat: an overview. *Plants*, *11*(23), 3358.

Turesson, G. (1922). The genotypical response of the plant species to the habitat. *Hereditas*, 3, 211– 350.

Turesson, G. (1925). The plant species in relation to habitat and climate: contributions to the knowledge of genecological units. *Hereditas*, *6*(2), 147-236.

Ungerer, M. C., Johnson, L. C., & Herman, M. A. (2008). Ecological genomics: Understanding gene and genome function in the natural environment. Heredity, 100(2), 178–183.

Upton, R. N., Correr, F. H., Lile, J., Reynolds, G. L., Falaschi, K., Cook, J. P., & Lachowiec, J. (2023). Design, execution, and interpretation of plant RNA-seq analyses. *Frontiers in plant science*, *14*, 1135455.

USA National Phenology Network USA, (2023). Daily Temperature Accumulations - 32 Base Temp as of 2017-08-02. Region: USA, *National. USA-NPN. USA.*

USDA, National Agricultural Statistics Service (NASS). (2023). Meat Animals Production, Disposition, and Income. 2022 Summary. Washington DC.

USDA, National Agricultural Statistics Service (NASS). (2024). Meat Animals Production, Disposition, and Income. 2023 Summary. Washington DC.

USDA Plants Database (2022). Andropogon gerardi Vitman Big Bluestem. *United States Department of Agriculture.* 2022.

USDA Plants Database (2023). Andropogon gerardi Vitman Big Bluestem. *United States Department of Agriculture.* 2023.

Valladares, F., Matesanz, S., Guilhaumon, F., Araújo, M.B., Balaguer, L., Benito-Garzón, M., Cornwell, W., Gianoli, E., van Kleunen, M., Naya, D.E., Nicoreta, A.B., Poorter, H., and Zavala, M.A. 2014. The effects of phenotypic plasticity and local adaptation on forecasts of species range shifts under climate change. *Ecology Letters* 17:1351-1364.

Vajana, E., Bozzano, M., Marchi, M., & Piotti, A. (2022). On the inclusion of adaptive potential in species distribution models: Towards a genomic-informed approach to forest management and conservation. *Environments*, 10(1), 3.

de Valpine, P., Turek, D., Paciorek, C.J., Anderson-Bergman, C., Lang, D.T. and Bodik, R. (2017). Programming with models: Writing statistical algorithms for general model structures with NIMBLE. *Journal of Computational and Graphical Statistics*, 26, pp. 403-413.

Van der Meer, P., & Jansen, L. A. (2019). Local adaptation in plants and its implications for ecosystem responses to climate change. *Ecology Letters*, 22(5), 898-906.

VanWallendael, A., Lowry, D. B., & Hamilton, J. A. (2022). One hundred years into the study of ecotypes, new advances are being made through large-scale field experiments in perennial plant systems. *Current opinion in plant biology*, 66, 102152.

Vekemans, X., & Hardy, O. J. (2004). New insights from fine-scale spatial genetic structure analyses in plant populations. *Molecular ecology*, *13*(4), 921-935.

Verelst, W., Bertolini, E., De Bodt, S., Vandepoele, K., Demeulenaere, M., Pè, M. E., & Inzé, D. (2013). Molecular and physiological analysis of growth-limiting drought stress in Brachypodium distachyon leaves. *Molecular Plant*, *6*(2), 311-322.

Verma, K. K., Song, X. P., Kumari, A., Jagadesh, M., Singh, S. K., Bhatt, R., ... & Li, Y. R. (2025). Climate change adaptation: Challenges for agricultural sustainability. *Plant, Cell & Environment*, *48*(4), 2522-2533.

de Villemereuil, P., Gaggiotti, O. E., Mouterde, M., & Till-Bottraud, I. (2016). Common garden experiments in the genomic era: new perspectives and opportunities. *Heredity*, *116*(3), 249-254.

Violle, C., Navas, M.-L., Vile, D., Kazakou, E., Fortunel, C., Hummel, I., & Garnier, E. (2007). Let the concept of trait be functional! *Oikos, 116*(5), 882–892.

Vitt, P., Finch, J., Barak, R. S., Braum, A., Frischie, S., & Redlinski, I. (2022). Seed sourcing strategies for ecological restoration under climate change: A review of the current literature. *Frontiers in Conservation Science*, *3*, 938110.

Vogt, B., Kazarina, A., Sytsma, J., Adams, B., Rodela, L., Clouse, D., ... & Lee, S. T. (2025). Plant host identity drives Andropogon gerardii rhizobiome assembly strategies under increasing abiotic stress. *bioRxiv*, 2025-04.

Volaire, F. (2018). A unified framework of plant adaptive strategies to drought: Crossing scales and disciplines. *Global Change Biology*, 24(2), 1–16.

Wadgymar, S. M., DeMarche, M. L., Josephs, E. B., Sheth, S. N., & Anderson, J. T. (2022). Local adaptation: Causal agents of selection and adaptive trait divergence. *Annual Review of Ecology, Evolution, and Systematics*, *53*(1), 87-111.

Wang, S.Q. (2020). Genetic diversity and population structure of the endangered species *Paeonia decomposita* endemic to China and implications for its conservation. *BMC Plant Biology*, 20, pp. 1-14.

Wang, T., Hamann, A., Spittlehouse, D., and Carroll, C. (2016). Locally downscaled and spatially customizable climate data for historical and future periods for North America. *Public Library of Science ONE* 11:e0156720.

Wang, H., Wang, R., Harrison, S. P., & Prentice, I. C. (2022a). Leaf morphological traits as adaptations to multiple climate gradients. *Journal of Ecology*, *110*(6), 1344-1355.

Wang, Z., Zhao, X., Ren, Z., Abou-Elwafa, S. F., Pu, X., Zhu, Y., ... & Ku, L. (2022b). ZmERF21 directly regulates hormone signaling and stress-responsive gene expression to influence drought tolerance in maize seedlings. *Plant, Cell & Environment*, *45*(2), 312-328.

Wang, Y., Tao, Z., Wang, W., Filiault, D., Qiu, C., Wang, C., ... & Li, P. (2020). Molecular variation in a functionally divergent homolog of FCA regulates flowering time in Arabidopsis thaliana. *Nature communications*, *11*(1), 5830.

Wang, G. L., An, Y. H., Zhou, C. L., Hu, Z. Z., Ren, X. Q., & Xiong, A. S. (2022). Transcriptome-wide identification of NAC (no apical meristem/Arabidopsis transcription activation factor/cup-shaped cotyledon) transcription factors potentially involved in salt stress response in garlic. *PeerJ*, *10*, e14602.

Wang, Y., Chen, G., Zeng, F., Deng, F., Yang, Z., Han, Z., ... & Chen, Z. H. (2025). Genomic and evolutionary evidence for drought adaptation of grass allopolyploid Brachypodium hybridum. *Journal of Experimental Botany*, eraf128.

Weaver, J. E. (1968). *Prairie Plants and their Environment: a fifty-year study in the Midwest*. *University of Nebraska Press*, Lincoln, Nebraska, USA.

Webb, W. P. (2022). *The great plains*. U of Nebraska Press.

Welles, S. R., & Funk, J. L. (2021). Patterns of intraspecific trait variation along an aridity gradient suggest both drought escape and drought tolerance strategies in an invasive herb. *Annals of Botany*, *127*(4), 461-471.

Werling, B. P., Dickson, T. L., Isaacs, R., Gaines, H., Gratton, C., Gross, K. L., Liere, H., Malmstrom, C. M., Meehan, T. D., Ruan, L., Robertson, B. A., Robertson, G. P., Schmidt, T. M., Schrotenboer, A. C., Teal, T. K., Wilson, J. K., & Landis, D. A. (2014). Perennial grasslands enhance biodiversity and multiple ecosystem services in bioenergy landscapes. *Proceedings of the National Academy of Sciences of the United States of America,* 111(4), 1652–1657.

Westerband, A. C., Funk, J. L., & Barton, K. E. (2021a). Intraspecific trait variation in plants: a renewed focus on its role in ecological processes. *Annals of botany*, *127*(4), 397-410.

Westerband, A. C., Knight, T. M., & Barton, K. E. (2021b). Intraspecific trait variation and reversals of trait strategies across key climate gradients in native Hawaiian plants and non-native invaders. *Annals of botany*, *127*(4), 553-564.

White, R. P., Murray, S., Rohweder, M., Prince, S. D., & Thompson, K. M. (2000). Grassland ecosystems.

Whitham, T. G., Young, W. P., Martinsen, G. D., Gehring, C. A., Schweitzer, J. A., Shuster, S. M., ... & Kuske, C. R. (2003). Community and ecosystem genetics: a consequence of the extended phenotype. *Ecology*, 84(3), 559-573.

Whitham, T. G., Lonsdorf, E., Schweitzer, J. A., Bailey, J. K., Fischer, D. G., Shuster, S. M., ... & Woolbright, S. (2005). " All effects of a gene on the world": Extended phenotypes, feedbacks, and multi-level selection. *Ecoscience*, 12(1), 5-7.

Whitham, T. G., Allan, G. J., Cooper, H. F., & Shuster, S. M. (2020). Intraspecific genetic variation and species interactions contribute to community evolution. *Annual Review of Ecology, Evolution, and Systematics*, *51*(1), 587-612.

Wilcox, K. R., Shi, Z., Gherardi, L. A., Lemoine, N. P., Koerner, S. E., Hoover, D. L., Bork, E., Byrne, K. M., Cahill, J., Collins, S. L., Evans, S., Gilgen, A. K., Holub, P., Jiang, L., Knapp, A. K., LeCain, D., Liang, J., Garcia-Palacios, P., Peñuelas, J., … Luo, Y. (2017). Asymmetric responses of primary productivity to precipitation extremes: A synthesis of grassland precipitation manipulation experiments. *Global Change Biology*, 23(10), 4376–4385.

Wilsey, B. J. (2010). Productivity and subordinate species response to dominant grass species and seed source during restoration. *Restoration Ecology*, *18*(5), 628-637.

Wilson, J. B. (2011). Cover plus: ways of measuring plant canopies and the terms used for them. *Journal of Vegetation Science*, *22*(2), 197-206.

Wilson, L. R., Gibson, D. J., Baer, S. G., & Johnson, L. C. (2016). Plant community response to regional sources of dominant grasses in grasslands restored across a longitudinal gradient. *Ecosphere*, 7(4), e01329.

Wittmann, M. E., Barnes, M. A., Jerde, C. L., Jones, L. A., & Lodge, D. M. (2016). Confronting species distribution model predictions with species functional traits. *Ecology and Evolution,* 6(4), 873–879.

Wood, S. N. (2017). Generalized additive models: an introduction with R. chapman and hall/CRC.

Woods, E.C., Hastings, A.P., Turley, N.E., Heard, S.B. and Agrawal, A.A. (2012). Adaptive geographical clines in the growth and defense of a native plant. *Ecological Monographs*, 82(2), pp. 149-168.

Woods, H. A., Pincebourde, S., Dillon, M. E., & Terblanche, J. S. (2021). Extended phenotypes: buffers or amplifiers of climate change?. *Trends in Ecology & Evolution*, *36*(10), 889-898.

Wright, I. J., Reich, P. B., & Westoby, M. (2001). Strategy shifts in leaf physiology, structure and nutrient content between species of high- and low-rainfall and high- and low-nutrient habitats. *Functional Ecology*, 15(4), 423–434.

Wright, I. J., Reich, P. B., Westoby, M., Ackerly, D. D., Baruch, Z., Bongers, F., ... & Villar, R. (2004). The worldwide leaf economics spectrum. *Nature, 428*(6985), 821–827.

Wright, C. K., & Wimberly, M. C. (2013). Reply to Kline et al.: Cropland data layer provides a valid assessment of recent grassland conversion in the Western Corn Belt. *Proceedings of the National Academy of Sciences*, *110*(31), E2864-E2864.

Wu, J., Wang, J., Hui, W., Zhao, F., Wang, P., Su, C., & Gong, W. (2022). Physiology of plant responses to water stress and related genes: A review. *Forests*, *13*(2), 324

Wu, Q., Dong, S., Zhao, Y., Yang, L., Qi, X., Ren, Z., ... & Cheng, J. (2023). Genetic diversity, population genetic structure and gene flow in the rare and endangered wild plant Cypripedium macranthos revealed by genotyping-by-sequencing. *BMC Plant Biology*, *23*(1), 254.

Xu, X., Liu, H., Wang, W., Hu, G., Wu, X., & Song, Z. (2021). Effects of manipulated precipitation on aboveground net primary productivity of grassland fields: Controlled rainfall experiments in Inner Mongolia, China. *Land Degradation & Development*, *32*(5), 1981-1992.

Xu, Y. Y., Zeng, R. F., Zhou, H., Qiu, M. Q., Gan, Z. M., Yang, Y. L., ... & Zhang, J. Z. (2022). Citrus FRIGIDA cooperates with its interaction partner dehydrin to regulate drought tolerance. *The Plant Journal*, *111*(1), 164-182.

Yahdjian, L., & Sala, O. E. (2002). A rainout shelter design for intercepting different amounts of rainfall. *Oecologia*, *133*(2), 95-101.

Yan, P., He, N., Fernández-Martínez, M., & Jiang, L. (2025). Plant Acquisitive Strategies Promote Resistance and Temporal Stability of Grasslands. *Ecology Letters*, *28*(4), e70110.

Yang, T., Chen, J., Zhong, X., Yang, X., Wang, G., Yao, Y., ... & Sun, W. (2022). Divergent responses of plant biomass and its allocation to the altered precipitation regimes among different degraded grasslands in China. *Plant and Soil*, *473*(1), 149-166.

Ying, S., Scheible, W. R., & Lundquist, P. K. (2023). A stress-inducible protein regulates drought tolerance and flowering time in Brachypodium and Arabidopsis. *Plant Physiology*, *191*(1), 643-659.

Yu, Y., Peñuelas, J., Sardans, J., Pei, J. Y., Li, G., Liu, G. L., & Ye, J. S. (2024). Water addition but not reduction alters plant biomass–diversity relationship. *Global Change Biology*, *30*(7), e17430.

Zeiter, M., Schärrer, S., Zweifel, R., Newbery, D. M., & Stampfli, A. (2016). Timing of extreme drought modifies reproductive output in semi-natural grassland. *Journal of Vegetation Science*, *27*(2), 238-248.

Zellmer, A. J., & Knowles, L. L. (2009). Disentangling the effects of historic vs. contemporary landscape structure on population genetic divergence. *Molecular Ecology*, *18*(17), 3593-3602.

Zhang, K., Johnson, L. C., Prasad, P. V., Pei, Z., Yuan, W., & Wang, D. (2015). The potential of big bluestem and other native grasses for bioethanol production. In *2015 ASABE Annual International Meeting* (p. 1). American Society of Agricultural and Biological Engineers.

Zhang, R., & Tielbörger, K. (2019). Facilitation from an intraspecific perspective–stress tolerance determines facilitative effect and response in plants. *New Phytologist*, *221*(4), 2212.

Zhang, L., Wang, J., Zhao, R., Guo, Y., & Hao, L. (2022). Aboveground net primary productivity and soil respiration display different responses to precipitation changes in desert grassland. *Journal of Plant Ecology*, *15*(1), 57-70.

Zhang, P., Seabloom, E. W., Foo, J., MacDougall, A. S., Harpole, W. S., Adler, P. B., ... & Borer, E. T. (2025a). Dominant species predict plant richness and biomass in global grasslands. *Nature ecology & evolution*, 1-13.

Zhang, Y., Zhang, L., Chen, M., Wang, J., Dong, S., Yuan, X., & Li, X. (2025b). Genome-wide identification and expression analysis of the DREB gene family in foxtail millet (Setaria Italica L.). *BMC Plant Biology*, *25*(1), 1-14.

Zheng X, Levine D, Shen J, Gogarten S, Laurie C, Weir B (2012). "A High-performance Computing Toolset for Relatedness and Principal Component Analysis of SNP Data." *Bioinformatics*, 28(24), 3326-3328.

Zheng, H., Gao, Y., Sui, Y., Dang, Y., Wu, F., Wang, X., ... & Sui, N. (2023). R2R3 MYB transcription factor SbMYBHv33 negatively regulates sorghum biomass accumulation and salt tolerance. *Theoretical and Applied Genetics*, *136*(1), 5.